THE TRANSACTIONS OF

The Royal Institution of Naval Architects

Vol 159 Part A4 2017

International Journal of Maritime Engineering

The Transactions of The Royal Institution of Naval Architects – Part A

International Journal of Maritime Engineering

The International Journal of Maritime Engineering (IJME) provides a forum for the reporting and discussion on technical and scientific issues associated with the design and construction of marine vessels and offshore structures. The IJME is published four times a year as Part A of the Transactions of The Royal Institution of Naval Architects. Contributions in the form of scientific and technical papers and notes on all aspects of maritime engineering, together with comment on published papers are welcomed.

PAPERS

Papers may introduce new theory or evaluate existing theory, or describe experimental or novel practical work, Papers presenting case histories will report on new or existing techniques, including design and production. Papers may also provide literary reviews which appraise and evaluate published work. All papers are refereed.

TECHNICAL NOTES

Technical notes will provide early announcement of new ideas, findings, procedures, applications, interim results, etc., which might later on form part of a full paper. Technical notes are refereed as for papers, but due allowance will be made for their immediate nature.

DISCUSSION

Comments on papers and technical notes will normally be published in the first available issue of the *IJME* following that in which the paper was published. Discussion may be continued in subsequent issues, at the discretion of the Editor. Authors will be invited to respond to published comment.

ISSN 1479-8751

The Transactions of The Royal Institution of Naval Architects

Vol 159 Part A4 2017 **ISSN 1479-8751**

International Journal of Maritime Engineering

CONTENTS

PAPERS

TECHNICAL NOTES

There are no Technical Notes published in this issue of IJME

DISCUSSION

HULLFORM & HYDRODYNAMIC CONSIDERATIONS IN THE DESIGN OF THE UK FUTURE AIRCRAFT CARRIER (CVF)

(DOI No: 10.3940/rina.ijme.2017.a4.403)

M E Campbell-Roddis, British Aerospace & BAE SYSTEMS Future Carrier Project Team Member (1996-2003)
Glasgow & Filton (Bristol), UK

SUMMARY

An overview is provided of the manner in which hydrodynamic and hullform-related design considerations were addressed in the development of the BAE SYSTEMS team's design proposal for the UK Future Aircraft Carrier (CVF). It also outlines how broader design considerations such as aviation, survivability and supportability requirements influenced these aspects of the design. A summary is also provided of some of the more detailed requirements development, option assessment and performance evaluation work that has been undertaken. The aircraft carrier designs discussed in this paper correspond to the BAE SYSTEMS team's final design submission as it stood in January 2003, at the time it was discontinued by the UK Ministry of Defence, in favour of the rival Thales / BMT team design that has since been developed into the UK Royal Navy's new 'Queen Elizabeth' class aircraft carrier. This final BAE SYSTEMS design submission consisted of two distinct design variants - one configured to operate a CTOL-based air group, the other configured to accommodate a STOVL air group. Both variants were based on a common 'core' ship design. The discussion presented in this paper is applicable to both variants.

This paper was originally written for presentation at the June 2003 Royal Institution of Naval Architects 'Warships 2003 - Air Power at Sea' Conference. However, it was withheld from publication at the request of the UK Ministry of Defence, due to sensitivity surrounding the UK Aircraft Carrier project at that time. Following re-appraisal in June 2016, the UK Ministry of Defence has now authorised publication of this paper in full. The paper is presented here in its original (2003) form, with Section 2 added to provide historical perspective (given the passage of time).

NOMENCLATURE

AEW	Airborne Early Warning
ANEP	Allied Naval Engineering Publication (a type of naval design standard)
AR&M	Availability, Reliability & Maintainability
CTOL	Conventional Take-Off and Landing. The traditional 'Cats & Traps' mode of fixed wing carrier aircraft operation, whereby launch catapults are used for aircraft launch and the aircraft recovers by rolling landing using arrestor wires. Sometimes also referred to as 'CATOBAR' (Catapult Assisted Take-Off But Arrested Recovery)
CFD	Computational Fluid Dynamics
COEIA	Combined Operational Effectiveness and Investment Appraisal
CPP	Controllable Pitch Propeller
CVF	The Royal Navy's new 'Queen Elizabeth' class aircraft carrier, as it was referred to at the design study stage
CVSG(R)	The initial UK MoD name for the 'Invincible' Class Replacement
FCBA	Future Carrier-borne Aircraft. The generic term for the alternative fixed wing aircraft types originally considered for CVF (most notably JSF, F/A-18 E/F Super Hornet, navalised Eurofighter Typhoon, Rafale)
FPP	Fixed Pitch Propeller
GM	Metacentric Height
IAT	UK MoD-Industry Integrated Alliance Team for the CVF Future Aircraft Carrier
IFEP	Integrated Full Electric Propulsion
IMO	The International Maritime Organisation
JSF	The F-35 Lightning II Joint Strike Fighter aircraft
MIIs	Motion-Induced Interruptions (a statistical measure used to assess the effect of ship motion on human performance)
MoD	The UK Ministry of Defence
MSI	Motion Sickness Incidence (another statistical measure used to assess the effect of ship motion on human performance)
NATO	The North Atlantic Treaty Organisation
PTO	Percentage Time Operable (in representative sea conditions)
PV	Private Venture (funding)
RAOs	Response Amplitude Operators
RAS	Replenishment at Sea
RMS	Root Mean Square
SAWE	International Society of Allied Weight Engineers, Los Angeles, USA (www.sawe.org)
SDR	Strategic Defence Review
SLEP	Ship Life Extension Project
SRD	The industry team's Systems Requirements Document, that decomposes the MoD customer's high level URD requirements into a series of detailed and specific design requirements

STANAG	A NATO Standardization Agreement (defining common technical procedures between the member countries of the alliance)
STOBAR	Short Take-Off but Arrested Recovery. The mode of fixed wing carrier aircraft operation whereby the aircraft launches unassisted via a 'Ski Jump' ramp and recovers by rolling landing using arrestor wires
STOVL	Short Take-Off and Vertical Landing. The mode of fixed wing carrier aircraft operation whereby the aircraft launches unassisted via a 'Ski Jump' ramp and recovers by hovering and then landing vertically on deck
STUFT	Ship Taken Up from Trade
URD	User Requirements Document, detailing the MoD customer's high level requirements for the ship
WOD	Wind Over Deck

1. INTRODUCTION

This paper outlines the manner in which hydrodynamic and hullform-related design considerations were addressed in the development of the BAE SYSTEMS team's design proposal for the UK Future Aircraft Carrier (CVF).

The work presented is based on the final BAE SYSTEMS design proposal for CVF, as it stood at the end of 2002. It was subsequently announced in January 2003 that CVF will progressed through an Integrated Alliance Team formed of representatives from the UK MoD and the former BAE SYSTEMS and Thales-led industry teams for CVF, using a Thales CVF design concept as a basis. Consequently, references to design features contained in this paper do not reflect the current design configuration for CVF. Nevertheless, it is hoped the paper will provide an interesting overview of some of the key hydrodynamic design issues and options pertinent both to CVF specifically, and aircraft carriers generally, and provide an insight into design deliberations of the former-BAE SYSTEMS team.

2. PROJECT ORIGINS

The origins of the UK Future Aircraft Carrier (CVF) programme can be traced back at least as far as the 'Invincible' class replacement ('CVSG(R)') feasibility studies, commissioned by the UK MoD Procurement Executive in the mid-1990s (see Eddison & Groom, 1997). These studies, conducted with industry support from BAeSEMA (YARD) (Glasgow) and BMT Defence Services (Bath), included consideration of the following design concepts:

- **'CVSG(R) STUFT':** This was an aircraft carrier concept based on conversion of a container ship taken up from trade (i.e. following on from previous mercantile conversions of RFA Reliant and RFA ARGUS in the 1980s). Factors weighing against this concept were the limited availability of suitably sized twin shaft merchant ship hulls, the extent of the conversion required, and the compromises in naval standards and warship functionality that would result.

Figure 1: The BAE SYSTEMS Team's Final Design Proposal for CVF (STOVL Design Variant)

- **'CVSG(R) SLEP':** This was a concept for major upgrade and life extension of the existing 'Invincible' class hulls for a further 30 years of service, into the late 2030s and early 2040s (see Eddison & Groom, 1997). Several different SLEP options were considered, all of which would have involved cutting the existing hull at its maximum section to lengthen it *(by around 20m or approximately 10% of the waterline length, as the author recalls)* while retaining the existing main machinery.

  This lengthening of the ship would have resulted in the existing (unusually long) superstructure of the 'Invincible' class being split (between the funnels) into two separate Islands, which (at that time) was considered potentially sub-optimal for flight deck operations. In addition, the configuration of the 'Invincible' class, with its narrow hangar centre section ('bow tie'-shaped hangar deck plan) and aircraft lifts impinging onto the runway, was less than ideal for larger scale fixed wing aircraft operations and stowage (see Honnor & Andrews (1982) and Eddison & Groom (1997)).

  Consequently, the final SLEP option considered extensive re-work of the hull down to hangar deck level, to achieve a more usable (near-rectangular) hangar shape. It also relocated the axial runway to port (partially onto sponsons) in order to clear the aircraft lifts, with the after aircraft lift being moved inboard to assist in this. It also replaced the split Island superstructure with a single, entirely new (comparatively short) Island into which the existing main engine uptakes would be routed. All-in-all an extensive (and potentially expensive) undertaking!

  The relatively light structural scantlings of the 'Invincible' class and concerns regarding support and obsolescence of shipboard machinery and equipment 60+ years after the first-of-class entered service, were significant concerns with the CVSG(R) SLEP concept. At the time these 'Invincible' SLEP studies were being conducted, the hull lengthening and ship life extension refit of the landing ship RFA SIR BEDIVERE was running into some difficulty, in terms of emergent growth in cost and scope of the SLEP refit (due to age of the hull and equipment). This highlighted the potential risks and pitfalls of undertaking a SLEP refit on the 'Invincible' class. Irrespective, the option of performing a 'SLEP' life extension refit on the 'Invincible' class was never progressed beyond initial feasibility study.
- **Newbuild Carrier Concepts:** Initial newbuild carrier concept studies, conducted by the UK MoD with industry support from 1996 onwards, informed the 1998 UK Strategic Defence Review (SDR) decision to proceed with a newbuild aircraft carrier design, with the intent to build two larger carrier hulls to replace the existing three smaller 'Invincible' class ships.

From 1997 British Aerospace (now BAE SYSTEMS) undertook self-funded (PV) studies to prepare for the carrier project, partly in recognition that a large aircraft carrier had not been designed in the UK since the Royal Navy's 'CVA01' carrier was cancelled (at the design stage) some 30 years previously. The highlight of this PV-funded work was a 1998 British Aerospace concept design for a STOBAR-based aircraft carrier, capable of accommodating a 40-strong air group based around a 'navalised' variant of Eurofighter Typhoon. This work, included simulated STOBAR-type deck landings of Eurofighter on a carrier deck using the flight simulator at BAe (Warton), to demonstrate the feasibility of launching the aircraft via 'Ski Jump' and recovering it onboard using arrestor wires.

MoD-funded Industry studies for the newbuild carrier commenced in late 1999, under two rival teams headed by BAE SYSTEMS (newly-formed from the merger of British Aerospace and Marconi Electronic Systems) and Thales UK. Participants in the BAE SYSTEMS' team included Rolls Royce and Vosper Thornycroft. Thales were teamed with BMT Defence Services, Babcock and Lockheed-Martin.

The initial phase of these funded industry studies, which completed in May 2000, provided preliminary ship sizing, general arrangements and cost estimates for a range of different aircraft carrier sizes and capabilities. This fed into the MoD 'FCBA COEIA' studies on the choice of fixed wing aircraft for the carrier. High level carrier concept designs generated at this early stage included STOVL, STOBAR and CTOL modes of fixed wing aircraft operation, and a range of different air group sizes (with 'surge' capacity for additional aircraft in an emergency).

BAE SYSTEMS followed this up in mid-2000 by proposing a novel 'hybrid' carrier concept (never progressed) that was equipped primarily for STOVL operation, but with limited provision for CTOL aircraft operation. The primary motivation for this was to allow operation of fixed wing AEW aircraft (with their superior performance compared to helicopter-borne AEW) and also to provide scope for 'cross-decking' conventional CTOL fighter aircraft with allies.

In early 2001 the decision was taken by the UK government to discount the STOBAR mode of aircraft operation and instead progress solely with carrier design options based upon STOVL and CTOL variants of the F-35 joint Strike Fighter (JSF). At this time, the MoD also narrowed focus towards carrier options sized for larger air groups.

This led to the BAE SYSTEMS team progressing just two (larger) carrier design options, based around STOVL and CTOL F-35 air groups respectively. These two distinct variants were re-baselined around a common 'core' carrier design during 2002, leading to the final

STOVL and CTOL carrier design variants discussed in this paper (see Figure 1 and Table 1 respectively).

Final carrier design submissions by the two rival industry teams in November 2002 led to the UK government decision in January 2003 to discontinue the BAE SYSTEMS carrier designs and proceed instead with the rival 'adaptable' carrier design offered by the Thales / BMT team. The political decision was also taken at this point to progress CVF through a joint Alliance Team formed of representatives from the UK MoD and the former BAE SYSTEMS and Thales teams. Effectively absorption of selected representatives from the 'losing' BAE SYSTEMS team into the 'winning' Thales team, to create a MoD-industry 'rainbow team' (the Aircraft Carrier Alliance) to progress the Thales / BMT carrier design into detail and build.

14½ years on, in June 2017, the end result of this process is the aircraft carrier QUEEN ELIZABETH, which has just left Rosyth on builder's sea trials, and its sister ship, PRINCE OF WALES, which is still in build.

This paper is based on the discontinued (rival) BAE SYSTEMS team's aircraft carrier design submission to the UK Ministry of Defence, as it stood in January 2003, at the time it was discontinued in favour of the Thales / BMT carrier design. As such, this paper relates to discounted design proposals for the carrier, rather than the final design proposal taken forward into build.

Table 1: Ship Particulars for the Final BAE SYSTEMS CVF Design Proposal (CTOL Variant)

Displacement	62,300 tonnes ****
Length Overall	296 m
Waterline Length	270 m
Beam Overall	74.0 m
Beam at waterline	40.0 m
Depth to Flight Deck	28.5 m
Draught	9.1 m ****
Maximum Speed	In excess of 25 knots
Total Accommodation	1,400-1,700 ++
Nominal Air Group Size	40 Fixed & Rotary Wing Aircraft ^^
Hangar Capacity	Hangar stowage for approximately two thirds of the nominal air group.
Aircraft Lifts	3 x Deck Edge Lifts ##

**** CTOL variant, in the start-of-life Deep Condition.
++ Including 'austere' accommodation.
^^ With capacity to embark and operate additional 'Surge' (overload) aircraft.
Each lift sized to accommodate a single F-35 aircraft.

3. BACKGROUND ON THE UK FUTURE CARRIER (CVF) PROJECT

The UK Future Carrier (CVF) programme aims to provide a new class of aircraft carrier for the Royal Navy. The requirement is for a class of two ships to replace the Royal Navy's three current 'Invincible' class STOVL aircraft carriers (see Honnor & Andrews (1982) for an overview of the design and development of the 'Invincible' class). Unlike the ships that they will replace, which were originally designed primarily[1] to satisfy a Rotary Wing anti-submarine scenario (Friedman, 1988), the emphasis in the design of the new ships is on power projection capability and through-life flexibility.

To these ends CVF is to be larger, more capable and more flexible than its predecessors, and, as only two ships are planned, the emphasis is on increased Availability and rapid re-roling. Current requirements (as of May 2003) are for an 'adaptable' CVF initially designed to operate an air group configured around the STOVL variant of the F-35 joint Strike Fighter (JSF), but with the capability for conversion to operate a CTOL-based air group if necessary at a later stage in the vessel's life.

Key customer-imposed constraints (imposed at the outset of the MoD-funded industry design studies in 1999) were that CVF will not be nuclear powered, must be of conventional monohull design and should be capable of operating for extended periods without docking (e.g. by making use of 'in-water' maintenance/repair techniques where appropriate).

As of May 2003, plans envisaged the award of the contract for the detailed design and manufacture of the ships in 2004, with the first vessel to enter service in 2012 and the second in 2015.

4. REQUIREMENTS DEVELOPMENT

4.1 OVERALL APPROACH

In accordance with the UK MoD's Smart Procurement Initiative, CVF is a requirements-led design. Essentially, this means that the capabilities and features of the ship design, and associated costs, can be traced back to (and justified against) the high-level requirements for the ship, specified in the customer's User Requirements Document (URD). This approach aims to avoid the unnecessary design cost, risk and complexity, or indeed design under-performance, that can result from inappropriate specification of design features and capabilities, for example based on preceding classes of vessel.

A key focus of the industry teams during the Assessment Phase studies was to produce a draft Systems Requirements Document (SRD) for CVF that decomposes these high level URD requirements into a more detailed and quantifiable form. The resulting SRD will ultimately form the contractual basis for the detailed design, construction and acceptance of the vessel.

[1] The referee for this paper advises that the design of the 'Invincible' class included provision for the (subsequently cancelled) P1154 supersonic STOVL aircraft. Significantly, this governed the design of the aircraft lifts (size and strength) and the strength limit of the flight deck.

Requirements decomposition work of this type, conducted as part of the hullform and hydrodynamics studies reported in this paper, are given in the following subsections:-

4.2 SHIP SPEED REQUIREMENTS & ASSOCIATED MARGINS

Particular emphasis was placed on the decomposition and analysis of requirements relating to maximum ship speed because of the impact this has on the resultant installed power, initial/through-life cost, and on broader aspects of the ship design (e.g. ship dimensions, hullform shape, shaftline arrangement and internal layout). To these ends, analysis of required maximum speed was based on the following four URD scenarios, which were considered to represent the fundamental drivers of required maximum ship speed for CVF:-

Scenario 1: Maintaining Speed of Advance During Transit. Under this scenario the vessel must be capable of maintaining a prescribed average speed of advance, allowing for the time lost when the vessel turns off course to launch/recover aircraft and the subsequent time taken for the ship to 'catch up the fleet'.

- Scenario 2: Launch of Aircraft in Conditions of Low Ambient Wind. This scenario requires that the maximum speed of the vessel must be such that it can generate sufficient wind-over-deck to allow launch/recovery of aircraft (with a prescribed payload) in conditions of low ambient wind, allowing a small margin to ensure that the ship can accelerate up to this speed in a timely manner.
- Scenario 3: Conduct of Aircraft Operations in a Fixed Geographic 'Box'. Under this scenario the vessel must be capable of sufficient speed to allow a specified level of flying operations to be sustained within a limited size of sea area.
- Scenario 4: Turning and Accelerating into Wind to Launch Deck Alert Aircraft. This scenario requires that, to obtain maximum operational flexibility, the ship should be capable of being turned into wind and accelerated to a minimum aircraft launch speed within Deck Alert time limits. This is an important requirement, for it maximises the scope for defensive air cover to be maintained using shipborne alert aircraft, minimising the need for Combat Air Patrol. It represents something of an implicit ship speed requirement, in that it influences maximum achievable ship speed indirectly through its impact on installed power.

In the case of a CTOL-based air group, the key driver of required maximum ship speed was found to be launch of fully laden CTOL aircraft in conditions of low ambient wind (i.e. Scenario 2). For a STOVL-based air group the principal drivers were found to be the launching of fully laden Rotary Wing aircraft and, to a lesser extent, speed of advance requirements.

It is important to note, however, that these findings are sensitive to detailed analysis assumptions, most notably those regarding aircraft payload, length of take-off run, Wind Over Deck requirements, intensity of flying operations, and assumptions regarding wind and sea conditions. Moreover, survivability/redundancy considerations, such as the desire to launch/recover aircraft at some reduced-capacity following loss or damage to a shaft, can *implicitly* tend to result in a higher required ship speed than that implied from the above. For the design studies reported in this paper, survivability assessments were conducted for a range of damage scenarios, although the sensitive nature of this work prevents details being presented here.

Table 2: Proposed Margins on CVF Powering & Ship Speed

	Margin	Description
Margins on Resistance & Powering Estimates	Fouling Allowance	To allow for increased resistance due to the deterioration of the hull surface finish in service due to such issues as biological fouling and corrosion. Dependent on assumed hull coatings and maintenance policy, operating area and intervals between hull cleaning and painting.
	Confidence Margin	To allow for uncertainties in the accuracy and reliability of resistance and powering predictions, and detailed issues (e.g. the effect of minor hull openings) that cannot easily be explicitly modelled as part of powering assessment.
	Appendage Form Factor	Factor applied in the calculation of appendage resistance.
	Ship-Model Correlation Allowance	Correction applied to achieve correlation of estimates with empirical data for full scale ships.
Margins on Maximum Ship Speed	Sea Margin	To allow for increased shaft power requirements to maintain a given speed in a seaway (i.e. in wind and waves).
	Allowance for Uncertainties in Maximum Ship Speed Requirements	The purpose of this margin is to:- • Allow for uncertainties associated with CVF ship speed requirements (e.g. required WoD); • Provide operational flexibility; • Ensure that the ship can accelerate up to maximum required Wind Over Deck speed in a timely manner. • Make allowance for redundancy/survivability issues pending the outcome of more detailed survivability analysis.
	Other Margins	Maximum ship speed (including margins) to be achieved in the End-of-Life Deep Condition, in specified sea water and air temperatures.

A range of supporting margins were formulated for application to the resulting requirement for maximum ship speed and in the powering assessment of the ship design, as indicated in Table 2. A key point to note is that CVF is required to achieve its required maximum speed under quite onerous conditions. For a significant proportion of its service life the vessel will therefore be able to achieve a higher ship speed.

4.3 SEAKEEPING REQUIREMENTS

4.3(a) General

There are two key sets of seakeeping performance requirements that need to be addressed within the design of an aircraft carrier, such as CVF:-

- Requirements for Normal Shipboard Activity (i.e. those specifying the limiting sea conditions in which routine shipboard and aviation activity is possible, without appreciable hazard to either personnel or equipment);
- Requirements for Extreme Weather Survival (i.e. those specifying the performance and integrity required of the ship and shipboard equipment in extreme seas, in order to ensure the safety of the ship, its equipment, personnel and payload).

Requirements for extreme weather survival are generally addressed through the adoption of appropriate design standards, such as established standards for ship stability, structural design, aircraft lashing point specification and equipment design limits, which are not considered further here.

4.3(b) Requirements for Normal Shipboard Activity

There is a range of openly published guidance on design criteria for use in evaluating the safe limit of operation of aircraft carriers in a seaway[2]. This guidance, supplemented where appropriate by criteria adopted for previous UK MoD ship designs, formed the basis of the decomposed seakeeping requirements/criteria proposed for CVF. The resulting measures of seakeeping performance, as adopted in the assessment of the CVF design proposal, are summarised in Table 3.

An important point to note is that whilst the ship motion criteria for launch/recovery of Rotary Wing and STOVL aircraft are essentially identical to each other, the criteria for launch/recovery of CTOL aircraft are fundamentally more onerous, with particular regard to acceptable levels of Pitch and Pitch-related motion. This (i.e. operability in higher sea states) represents a key advantage of STOVL aircraft over conventional (CTOL) fixed wing carrier aircraft.

Table 3: Summary of Key Measures of Seakeeping Performance for CVF

Activity	Limiting Parameters
Launch/Recovery of STOVL & Rotary Wing Aircraft	RMS pitch
	RMS roll
	RMS vertical velocity at landing spot
Launch/Recovery of CTOL Aircraft	RMS pitch
	RMS roll
	RMS lateral displacement at round-down
	RMS vertical displacement at round-down
	RMS vertical velocity at touch-down point
Aircraft Handling	RMS pitch
	RMS roll
	RMS lateral acceleration at aircraft location
	RMS vertical acceleration at aircraft location
Aircraft Lift Operability - Side Lifts	Wetnesses per hour on underside of lift structure
Aircraft Lift Operability - Inboard Lifts	As for aircraft handling (above).
General Flight Deck & Hangar Operations	Natural roll period
Overall Hull Performance	Green seas per hour on flight deck
	Bow slamming incidences per hour
	Incidences of sponson immersion per hour
	Observations of stern slamming during tank tests
	Propeller emergences per hour
Crew Comfort, Safety & Effectiveness	Motion sickness incidences (MSIs) at key points around vessel
	Motion-induced interruptions (MIIs) at key points around vessel

4.3 (c) Consideration of the Need for Explicit Limits on Natural Roll Period

A seakeeping parameter that assumes particular importance in the design of an aircraft carrier is that of natural roll period, due to its significant impact on flight deck and hangar operability. Moreover, it represents a parameter that the ship designer has an inherent ability to specify and control provided that it is addressed at a sufficiently early stage of design, for example through the judicious choice of hull parameters and through-life stability management (e.g. ballasting) strategies.

In general, to optimise flight deck and hangar operability for a large carrier such as CVF, it is beneficial to achieve the longest practicable natural roll period as this will tend to:

- Minimise both roll amplitudes and associated levels of deck velocity/acceleration (i.e. by moving the resonant roll frequency of the ship away from the spectral peak of the seaway, and by also reducing the roll "stiffness" of the vessel);

[2] See: Comstock *et al* (1982), Ricketts & Gale (1989), Pattison & Bushway (1991), Crossland et al (1998) and also STANAG 4154 (2000).

- Maximise the quarter-cycle of roll motion - something that is regarded as key to facilitating movement of aircraft in limiting sea states (Pattison & Bushway, 1991);

Maximising natural roll period in this manner is achieved by minimising the metacentric height of the vessel within the constraints imposed by broader ship design considerations, most notably those associated with ship stability and heel-in-turn performance (see Section 6). Of particular note in this regard were the difficulties encountered following the second blistering refit of USS MIDWAY in the mid-1980's (Ricketts & Gale, 1989)[3]. In this instance fitting substantial blisters to the hull, to improve ship stability, resulted in a marked reduction in the vessel's natural roll period and consequentially a significantly adverse impact on flight deck operability.

For the purposes of the CVF design studies reported in this paper, it was assumed that the minimum natural roll period for CVF should not be less than 18.5s, and should ideally exceed 20.0s. The former (18.5s) value approximates to the natural roll period of USS MIDWAY prior to her unsuccessful (2nd) blister addition (see Table 4 and Ricketts & Gale (1989)), while the latter (20.0s) limit corresponds to the somewhat higher value indicated by the trends in fixed wing aircraft handling characteristics proposed by Pattison & Bushway (1991) and in STANAG 4154 (2000).

Although similar issues of flight deck operability resulted in some consideration also being given to the need for equivalent limits on natural pitch period for CVF, the following factors mitigated against this:

- The effect of forward speed means that it is Encounter Period rather than natural pitch period *per se* that is importance to determining pitch-related motions in a seaway.
- Once the length of the ship has been set, the designer has very little practical control over natural pitch period and the key parameters that determine it (i.e. pitch radius of gyration and longitudinal metacentric height). Rather these parameters tend to be constrained by fundamental higher-level design considerations (e.g. internal arrangement issues and broader hullform design considerations).
- For those activities where the quarter-cycle of pitch motion is likely to be of principal importance (e.g. launch/recovery of CTOL aircraft), the proposed limits on pitch amplitude are so onerous that natural pitch period is unlikely to represent a significant additional driving constraint.

[3] An earlier (first) blistering refit on USS MIDWAY, conducted 30 years earlier in the mid-1950s, had been a success (Ricketts & Gale, 1989).

Table 4: Quoted Values of Natural Roll Period for US NAVY Warships & Other Vessels (Ricketts & Gale (1989) and Sims (1989))

Ship Type	Ship	Natural Roll Period (s)
Aircraft Carriers	USS MIDWAY (CV 41) *prior* to unsuccessful 1986 blister refit	18.6
	USS KITTY HAWK (CV 63)	22.2
	WWII Fleet Aircraft Carrier	14-16
Other Warships	Battleship	14-16
	Cruiser	11-12
	Destroyer	7.5-9
Commercial Vessels	Liner *(designed to commercial ship stability standards)*	20-24

4.4 MANOEUVRING & COURSE-KEEPING REQUIREMENTS

There is only limited established guidance on desirable levels of manoeuvring and course-keeping performance for aircraft carriers, and indeed warships generally. Standards of manoeuvring performance for new classes of warship appear generally to have been based largely upon the achieved performance of existing similar vessels, and desired improvements relative to such established benchmarks. Looking to the future, ongoing NATO studies are currently (2003) addressing the issue of common (role-dependent) standards for warship manoeuvring performance, with a view to compiling a NATO standard ('ANEP') on the issue.

As regards commercial standards of manoeuvring and course-keeping performance, these are laid down in IMO Resolution A751(18) (1993) *(now superseded by IMO Resolution MSC 137(76) (2002))*. Being based on fundamental ship safety considerations (e.g. directional stability, collision avoidance, stopping performance), and being intended to encompass very large commercial vessels (e.g. VLCCs), they may be regarded as bare minimum standards of manoeuvring performance that must be achieved by any warship. The IMO requirements clearly do not explicitly address either aircraft operating requirements nor the broader military operational issues of relevance to aircraft carriers, for example:

- Manoeuvring and maintaining station in proximity to other vessels (e.g. during RAS);
- Survivability requirements (e.g. maintaining steerage after damage, emergency evasive manoeuvres, optimisation of countermeasures performance, positioning for self-defence).

Given the foregoing, the approach adopted for the CVF studies reported here was to define a set of minimum (safety-related) criteria for CVF manoeuvrability based on IMO Requirements, and then supplement these with CVF-specific manoeuvring criteria derived from the customer's high level User Requirements, and, where appropriate, manoeuvring criteria for previous UK MoD vessels. The resulting measures of manoeuvring and course-keeping

performance, as adopted in the assessment the CVF design proposal, are summarised in Table 5. Pending further investigation, and in the absence of substantive evidence to the contrary, the levels of course-keeping performance required for CTOL, STOVL and Rotary Wing aircraft operations were assumed to be identical.

5. KEY DRIVERS OF SHIP DIMENSIONS & PROPORTIONS

An important prerequisite to the commencement of design development, and one in which hydrodynamic considerations play a key part, is the selection of dimension and proportions for the ship - an activity that is naturally somewhat iterative and subject to refinement as the design of the ship evolves.

For the CVF design proposal covered in this paper, overall length and overall beam were, understandably, governed by the flight deck outline, as determined from sortie generation requirements and aircraft launch/recovery considerations (e.g. aircraft, 'ski jump', catapult and arrester gear characteristics). While CTOL launch/recovery requirements were found to be the dominant factor in this area, overall sortie generation requirements meant that movement to a wholly STOVL/Rotary Wing-based air group would only allow a modest reduction in ship length.

Waterline length was, in the first instance, found to be driven simply by flight deck length. However, the desire to best utilise the resulting surplus space within the hull subsequently led to the adoption of enhanced standards of crew accommodation, modularised/containerised stores facilities and more spacious aviation facilities, resulting in a more volume-critical design. As weight estimates and supporting margins were refined, the freeboard of the damage control deck, and to a lesser extent extreme draught and side lift freeboard became more of a concern. These issues, allied with a desire to avoid the powering penalties associated with further increases in block coefficient, meant that any further displacement growth would have been better accommodated by a further increase in waterline length. In this regard the final CVF design proposal covered by this paper may be considered to be weight, volume and flight deck driven. Hangar size was not found to represent a primary driver of waterline length, due to the inherently good spatial characteristics of the selected above and below water form, and the assumed size of hangar required. Analysis clearly showed the powering benefits of maximising waterline length, and consequently the option of adopting a significant stern overhang (a so-called 'counter stern') was rapidly discounted.

Having fixed waterline length, waterline beam was based on achieving an appropriate operating metacentric height (see Section 6), with account also being taken of available build and support infrastructure (e.g. dry docks).

There are clear limits on extreme draught for CVF imposed by base port, build and through-life docking considerations. Other constraints include the need to achieve an acceptable freeboard for the damage control deck, deck edge lifts and hangar deck, and the need to achieve a reasonably fine underwater form consistent with near-optimal powering performance. These factors drove the choice of moulded design draught, block coefficient, propeller tip projection and the projection of other hull appendages below the keel line.

Hull depth was evaluated as the sum of the following constituents:

- The design draught of the ship;
- The design freeboard of the damage control deck (i.e. the deck beneath the hangar deck), as determined from damaged stability considerations;

Table 5: Summary of Key Measures of Manoeuvring Performance for CVF (evaluated for specified ship speeds, wind/sea/tidal conditions and ship loading conditions)

Requirement	Functional Description	Manoeuvre	Performance Parameter
Basic Ship Safety-Related Criteria	Turning Ability	Turning Circle Manoeuvre	Tactical Diameter
			Advance
	Initial Turning Ability	IMO 10° - 10° Zig-Zag Manoeuvre	Distance Travelled to First Rudder Execute
	Yaw-Checking & Course-Keeping Ability	IMO 10° - 10° Zig-Zag Manoeuvre	Value of the First Overshoot Angle
			Value of the Second Overshoot Angle
		IMO 20° - 20° Zig-Zag Manoeuvre	Value of the First Overshoot Angle
	Stopping Ability	IMO Full Astern Stopping Test	Track Reach
	Directional Stability	Spiral Test or Pull-Out Manoeuvre	Directional stability
General Operational Tasking	Accuracy of Heading Control	Straight Line Course at Constant Ship Speed	Error bound to within which heading can be maintained in prescribed wind and sea conditions
Low Speed Manoeuvring	Berthing	Maintaining Position Against a Beam Wind/Current while Stationary	Vessel at zero forward speed to be capable of generating sufficient lateral thrust at the bow and stern to allow it to maintain position and heading unaided against specified combinations of wind, tidal current and clear water depth under the keel.
Survivability	Emergency Evasive Manoeuvres	Turning Circle Manoeuvre	Rate of Turn average over first 180° of the turn
Accessibility & Navigability	Canal Transit	Transit of International Canals	Ship Length, Waterline Beam, Overall Beam, Draught and Air Draught
	Passage Under Bridges	Passage Under Specified Bridges	Overall Beam, Draught and Air Draught.

- The required 'tween deck height of the damage control deck, as determined by clear headroom requirements, deckhead services and larger items of equipment sited on this deck level (e.g. switchboards).
- The required hangar height, determined by aircraft maintenance requirements and structural allowances/clearances;
- The tween deck height of the gallery deck above the hangar, as determined by flight deck structural considerations and the decision to use this deck to accommodate containerised stores.

Consideration was also given to the freeboard of the hangar deck, which represents a key determinant of the operability of the ship's deck edge lifts in a seaway.

A level keel design trim was selected, noting the tight limits on static trim for CTOL operations (Pattison & Bushway, 1991).

Finally air draught (i.e. mast top height) was constrained by an assumed requirement to pass beneath the Forth Bridges, in order to facilitate access to proposed build and support facilities located at Rosyth.

6. CHOICE OF METACENTRIC HEIGHT

As alluded to elsewhere in this paper, the choice of operating metacentric height (GM) for an aircraft carrier, such as the CVF, is effectively constrained by the following principal considerations:-

- Ship stability requirements (intact and damaged), heel-in-turn considerations, and the need to limit the heel induced by aircraft movements, all of which tend to prescribe minimum acceptable operating GM;
- Minimum acceptable natural roll period, as determined from ship motions considerations, which tends to determine maximum acceptable operating GM.

The result is that there tends to be a well-defined 'window' of acceptable operating GM which needs to be satisfied in all through-life ship operating conditions, if ship safety and operational effectiveness is to be maintained. In the case of CVF, these limits on acceptable through-life operating GM prove particularly challenging to satisfy, for the following reasons:-

- The highly variable load and onerous through-life growth requirements for the ship, which tend to accentuate through-life variations in metacentric height;
- The strong desire for benign flight deck motions in order to facilitate intensive aircraft operations in higher sea states;
- The high lower bound limits on metacentric height imposed by warship intact and damaged stability standards, heel-in-turn considerations, and to a lesser extent the desire to minimise heel induced by aircraft movements;
- Any scope to relax the constraints imposed on metacentric height by damaged stability considerations tends to be limited by internal layout considerations specific to CVF (e.g. aircraft lift, magazine and machinery space sizes), which effectively constrain bulkhead spacing.

The first step in achieving acceptable operating metacentric height for the carrier lay in the judicious choice of waterline beam for the design (see Section 5) - something which in turn required reliable weight and centroid estimation from the earliest stages of design. Thereafter, as the design progressed in detail, appropriate layout of tanks, careful weight and centroid management and appropriate weight margins policy were all key to ensuring that metacentic height remained within reasonable bounds in the start-of-life ship condition.

It was also necessary to consider appropriate through-life stability management strategies for the design (e.g. through-life ballasting, weight management and weight margins policy) in order to ensure that GM would be maintained within acceptable bounds across all likely through-life operating conditions. Allied to this was the necessity to establish a reliable estimate of roll radius of gyration to allow the upper bound limit on operating GM, as determined from natural roll period considerations, to be confirmed (see Section 13.5).

7. HULLFORM DESIGN

7.1 DESIGN OF THE UNDERWATER FORM

The choice of parent underwater form was based on a review of three alternative parent forms that were collectively considered to cover the likely range of desired CVF hullform characteristics, viz:-

- A resistance-optimised parent form, based on practice for previous Royal Navy aircraft carriers;
- A parent form representative of design practice for modern cruise liners;
- A 'low pitch' concept hullform, constructed around established guidance for minimising pitching motion[4], noting (see Section 4.3(b)) that pitch-related motion represents a key factor in limiting the operability of aircraft (specifically CTOL aircraft) from aircraft carriers in a seaway.

Key characteristics of each of the three candidate forms are summarised in Table 6.

[4] See: Lewis (1989), Purvis (1974), Kehoe et al (1980), Kiss (1990), Smitke et al (1979), Walden & Grundmann (1985), Bales & Cieslowski (1981), Comstock & Keane (1980) and Kehoe et al (1987).

Table 6: Key Characteristics of Each of the Three Candidate Underwater Forms

Option 1: 'Resistance-Optimised' Warship Form	**Option 2: 'Cruise Liner' Form**	**Option 3: 'Low Pitch' Form**
Narrow after lines and a correspondingly fine design waterplane aft.	Broad, relatively flat after lines and correspondingly full design waterplane aft.	Very full after waterplane.
Zero transom immersion.	Zero transom immersion.	Wide, shallow transom immersion
A relatively full forward waterplane and a correspondingly high angle of entrance.	Fine design waterplane forward and correspondingly low angle of entrance forward. Comparatively pronounced shoulder forward.	A relatively long, fine entry and very smooth shoulder forward.
Fullest midships section of the three options.	Full midships section.	Low midships section coefficient (i.e. well-rounded bilges, flared sides and Rise of Floor).
Minimal Flat-of-Side below the waterline.	Significant vertical Flat-of-Side below the waterline.	Flared sides below the waterline.
Design Waterline maintains its maximum breadth for only a short length close to midships.	Design waterline maintains its maximum breadth for a significant proportion (i.e. in excess of 40%) of ship length.	Design waterline maintains its maximum breadth for a significant proportion of ship length, but less than cruise liner form.
Zero Rise of Floor.	Zero Rise of Floor.	Modest Rise of Floor.
No Parallel Middle Body.	No Parallel Middle Body.	No Parallel Middle Body.
No Bulbous Bow. **	Resistance-Optimised Bulbous Bow.	Large seakeeping-optimised bulbous bow.
		Low vertical prismatic coefficient.
		Large separation between the LCB and LCF.
		A relatively long, shallow, cut-up.

****** The presence or otherwise of a bulbous bow was neglected in the comparative assessment of the three candidate underwater forms, on the basis that the potential benefits and required configuration of a bulbous bow for CVF were the subject of separate study, and that a bulbous bow could in any case be readily applied to whichever parent form was selected.

It was readily apparent that CVF would likely to require a skeg of some form for structural/docking reasons and also to achieve an appropriate balance between manoeuvrability and course-keeping characteristics. Accordingly a single centreline skeg was applied to the design. An alternative arrangement based upon twin skegs was also considered, ostensibly on grounds of the potential supportability benefits of enclosing the two conventional shaftlines, and potential resistance/powering benefits (Watson, 1998). However, more detailed consideration, taking into account specialist hydrodynamic advice and the likely weight penalties led to this option being discounted.

To provide a fair basis for comparison, the three candidate forms were scaled to a common set of underwater dimensions and a displacement representative of CVF, and then subjected to both qualitative and quantitative (computational) assessment in terms of a range of hydrodynamic and broader CVF design considerations. Key discriminators identified were as follows:

- Of the three candidates, the resistance-optimised warship form appeared to offer markedly superior resistance characteristics across the entire speed range, while the low pitch form displayed the poorest resistance characteristics of all three candidates (i.e. of the order 10%-15% higher than the resistance-optimised form at maximum speed). However, the inherently lower metacentric height of the resistance-optimised warship form (see below) will be likely to result in the need for increased waterline beam, thereby tending to erode (at least partially) its apparently superior resistance characteristics.
- Analysis (Section 13.3(b)) indicated that adoption of the low pitch form might typically reduce pitch amplitudes by 10% - slightly more if pitch damping mechanisms, that cannot be adequately modelled by strip theory, are accounted for (e.g. viscous damping associated with its large seakeeping-optimised bulbous bow). While certainly not insignificant, this level of pitch reduction is unlikely to offer any significant scope for extending aircraft operations into higher sea states. Meanwhile, the improvements in pitching performance must be weighed against the form's inherently inferior roll motion characteristics, associated with its more rounded bilges (analysis indicated roll amplitudes around 50% higher than for the other forms).
- There was some evidence from strip theory analysis that the full after waterplane of the cruise liner and low pitch hullform might result in much "stiffer" pitching motions (i.e. higher pitch-induced accelerations), and hence a less benign flight deck motions than the resistance-optimised warship form.
- For a given set of ship particulars, the cruise liner and low pitch forms, with their full after waterplanes, provide an inherently higher value of metacentric height than the resistance-optimised form, with its narrow after lines. By the same virtue, these forms will also tend to result in a greater proportion of the reserve of initial stability being invested in their after lines.
- The resistance-optimised warship form, with is full forward lines, comparatively full midships section and relatively short cut-up, tends to result in very good ship layout characteristics, in spite of its narrower after lines. Its full forward lines tend to maximise tank top width forward, and, when extrapolated to the above water form, also maximise side shell clearance at the forward end of the hangar (Figure 2), easing the routing of access routes and services around the outside of the hangar. By contrast the flared sides, rounded bilges and

correspondingly low Midships Section Coefficient of the 'low pitch' form tend to minimise space available low in the hull, and its relatively long, shallow cut-up potentially increases required shaft lengths and limits space available low in the hull around the aft end.

- Given that significant amounts of curvature are required in the underwater form to ensure acceptable hydrodynamic performance, the relative proportion of flat *vs* single-curvature *vs* double-curvature surfaces is not considered to represent a fundamental discriminator between the producibility characteristics of the three candidate forms. Nonetheless, the cruise liner form appeared to offer the best producibility characteristics, for it maximises the extent of flat of side and flat of bottom, minimises the length of the after cut-up, provides a full midships section, and maximises the proportion of ship length over which the design waterline remains parallel to the ship's centreline. All these features tend to improve the scope for adopting modular build and outfit principles.

On balance, the resistance-optimised warship form was considered to offer the best all-round characteristics for CVF, and accordingly was adopted as the basis underwater form for the CVF design proposal covered in this paper.

As part of the subsequent refinement activity, a bulbous bow was applied to the form, shaped and sized so as to optimise resistance characteristics at maximum speed. It was anticipated that the bulb would reduce resistance by around 5%-10% at maximum speed, and that it would remain broadly beneficial for ship speeds down to about 11 knots. Although consideration was given to reshaping/resizing the bulb to bias its performance more towards cruise speeds, analysis based on empirical data and an assumed CVF operating profile indicated that this would increase installed power by a small (but not insignificant) margin, whilst being roughly neutral in terms of overall fuel burn. The separate option of substituting a seakeeping-optimised bulb (see Lewis (1989) and Schneekluth & Bertram (1998)) in order to minimise pitching motion for CTOL operations was rejected, as any reduction in pitching motion was likely to be small and unjustified in the context of the likely resistance penalties.

In accordance with established (Froude number-based) guidance on resistance optimisation, the transom was configured to give zero immersion at the nominal design draught of the vessel. Although consideration was given to introducing a stern wedge or flap, this was rejected given the significant variations in operating draught of the vessel, and in light of expert advice that any resistance benefit was likely at best to be limited.

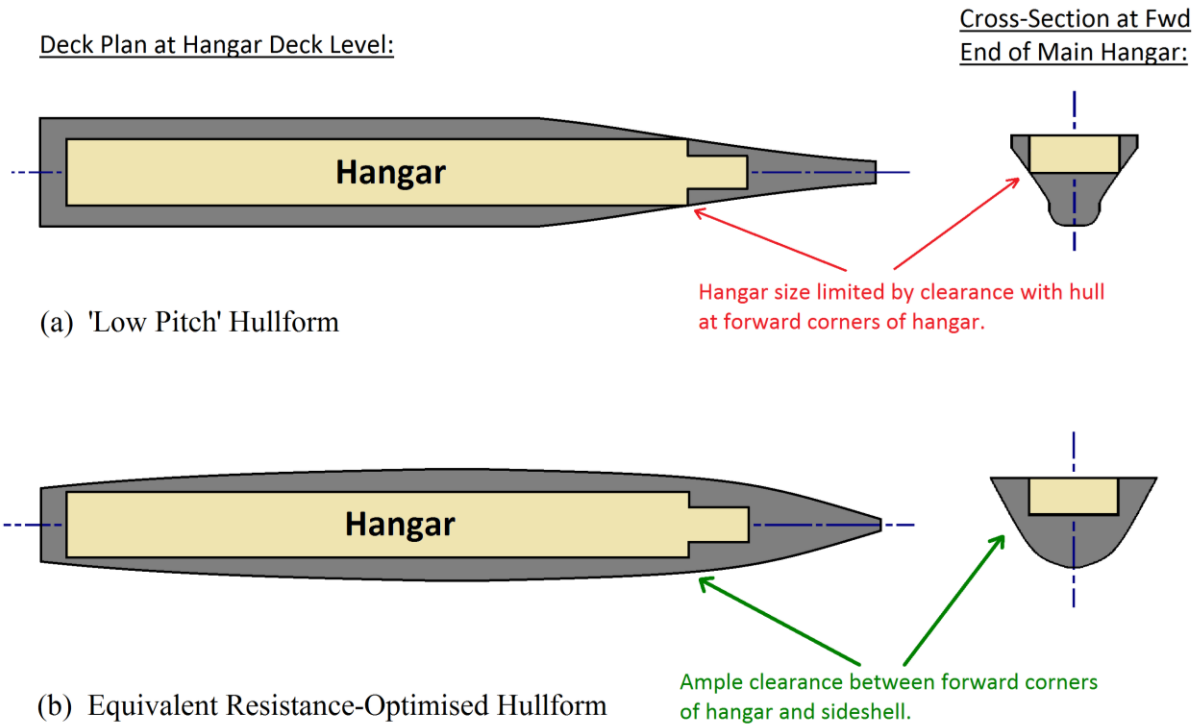

Figure 2: Comparison of the Spatial Characteristics of a Low Pitch Parent Form with an Equivalent Resistance-Optimised Hullform - note how the latter is more readily able to accommodate a large hangar

Other detailed refinements applied to the selected underwater form included: adjustment of longitudinal centre of buoyancy; refinement of the entrance to optimise resistance characteristics; refinement of afterbody lines to reflect shaftline, powering and noise/vibration considerations; and application of modest flare to the midships section beneath the waterline to reduce target echo strength.

Although not incorporated within the baseline design proposal, established empirical 'design lanes' (Saunders, 1957) indicate that there is at least limited scope for incorporating parallel middle body on CVF without incurring marked resistance penalties. Possible reasons for introducing parallel middle body include potential improvements to producibility and ship layout, minor adjustments to ship length at the design stage, or to facilitate possible lengthening of the vessel through-life.

7.2 DESIGN OF THE ABOVE WATER FORM

Given the fundamental disparity between overall ship dimensions for CVF (which are driven principally by aircraft operating/stowage requirements) and waterline dimensions (which are determined by broader ship design considerations), two fundamental alternative styles were identified for the above water form, viz:

- A traditional style of carrier above water form, employing a wall-sided form and sponsons;
- A novel 'highly flared' style of above-water form, employing above water flare as a means of minimising the need for sponsons.

With the traditional style of above water form (Figure 3) the basic envelope of the above water form is wall-sided (or near wall-sided), and sponsons are appended to this basic envelope to achieve the required flight deck plan. The origins of the approach can be traced at least as far back as the early 1950s to the retrofit of angled runways to existing (axial-runway) CTOL carriers, where appending a sponson onto the existing wall-sided form proved to be the simplest and most practical way of achieving the required local change in flight deck outline. Since then, this approach has been adopted universally on new-build carriers where there is a fundamental mismatch between waterline dimensions and desired flight deck outline.

In practice there is considerable variation in the depth and shape of the sponsons adopted on a given design, both along the length of the ship and between the port and starboard sides of the hull. Along the starboard side of the hull, where space is at a premium (and there is often an offset Island superstructure to support), the sponsons tend to be deeper and more box-shaped, to maximise the amount of utilisable internal space within the sponson. Down the port side of the hull, where internal space is at much less of a premium, and the overhang of the flight deck tends to be greatest, the sponsons tend to have steeply sloped sides, presumably to minimise steel weight and associated weight centroid implications. Additional, smaller, shallower sponsons tend to be appended around the above water form of the ship as required, to meet specific localised requirements (e. g. to provide platforms for sensors or self-defence/decoy systems). Major sponsons (i.e. those supporting flight deck extensions on both sides of the hull) tend to extend over the full depth of the hangar.

By contrast, the fundamental feature of the 'highly flared' style of above water form (Figure 4) is its use of straight line flare extending down to, or close to, the waterline[5], in order to minimise or avoid the need for the large sponsons traditionally associated with aircraft carriers. To these ends, the basic angle of side flare is maintained from the transom to a point as far forward on the hull as practicable.

Direct comparison between the two styles of above water form is somewhat subjective, for in the case of the traditional style of above water form there is considerable flexibility in the configuration (e.g. shape, location, extent) of the sponsons. Nonetheless, potentially key discriminators identified in the course of the CVF studies were as follows:

- The highly flared approach offers a number of features that are attractive from the point of view of producibility, ship layout and modular construction/outfit. Specifically, it ensures symmetry of the above water form up to the highest possible deck level, simplifies internal structural arrangement (e.g. by eliminating of the need for a longitudinal bulkhead at the interface between the sponson and the main hull, to maintain structural continuity), and tends to maximise the amount of flat/single curvature plating and parallel side in the above water form. It also tends to maximise the breadth of hull at hangar deck level, easing the routing of access/service routes, uptakes/downtakes and stores/weapons lifts around the outside of the hangar.
- The highly flared approach offers an inherently spacious above water form for a given set of ship dimensions.
- The highly flared approach potentially offers enhanced levels of intact and damaged stability performance, in terms of large angle stability and increased metacentric height at damaged draughts.
- There are a range of potential discriminators between the two styles of above water form in terms of structural characteristics (e.g. longitudinal, torsional and shear strength characteristics, global

[5] Although the side flare can, in principle, be initiated at the turn of bilge, the implications for metacentric height at lighter draughts, together with hydrodynamic concerns, meant that this sub-option was not explored as part of the present studies.

and local wave loading, residual strength characteristics). On balance, it was considered that the highly flared style of above water form offers scope for achieving a simpler, lighter, more efficient and more produceable hull structure than would otherwise be the case.

- The highly flared style of above water form is likely to place additional constraints on the berthing and docking of the vessel due to the high angles of flare close to the waterline (i.e. at around the level of the quayside or dockside).

Provided that due attention is paid in the design of the above water form, radar cross-section and air wake characteristics should not represent significant discriminators between the two styles of above water form.

The seakeeping characteristics of the highly flared above water form were initially deemed a potential area of concern, due to risks associated with immersion/re-emergence of the side flare in a seaway, although subsequent seakeeping experiments (see Section 13.3) alleviated these concerns. At this point it should be noted that the seakeeping characteristics of the traditional style of carrier above water form are also not without risk. Specifically, careful attention must be paid to the design of the sponsons, particularly their freeboard relative to the still water line, their outreach, and the shape of their undersides, if the risk of flare slamming, local freeboard exceedance and undesirable interaction effects (e.g. spray generation around side lift openings) are to be minimised.

Having taken the above factors into account, the decision was made to proceed with the highly flared style of form for the CVF design proposal covered in this paper. In line with the findings of de-risking experiments (Section 13.3(d)), this was implemented based on a basic flare angle of 35° and initiation of the flare approximately 3.0m above the deepest operating waterline. To reflect structural and producibility considerations, the principal knuckle lines of the above water form were sited so as to lie slightly above the deck lines.

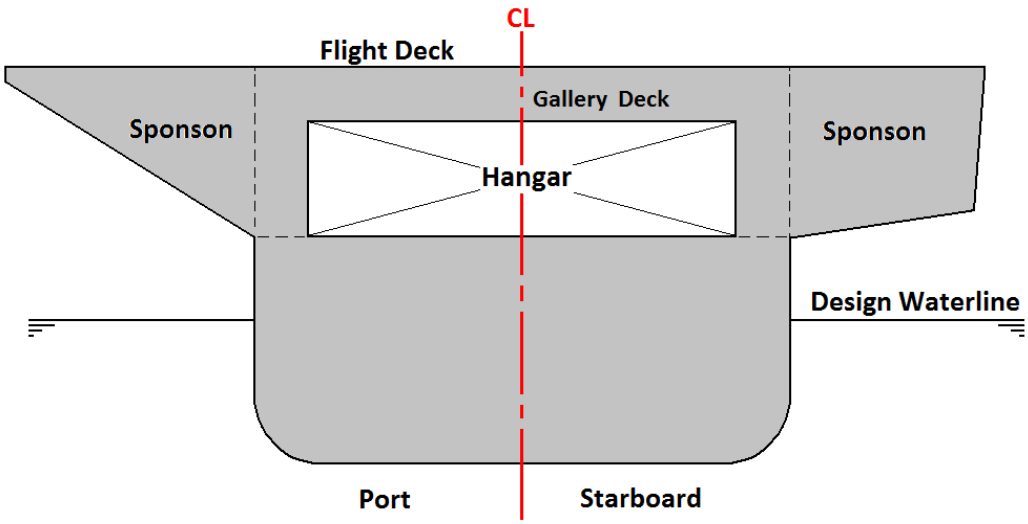

Figure 3: Traditional (Sponson) Style of Carrier Above Water Form for a representative midships section

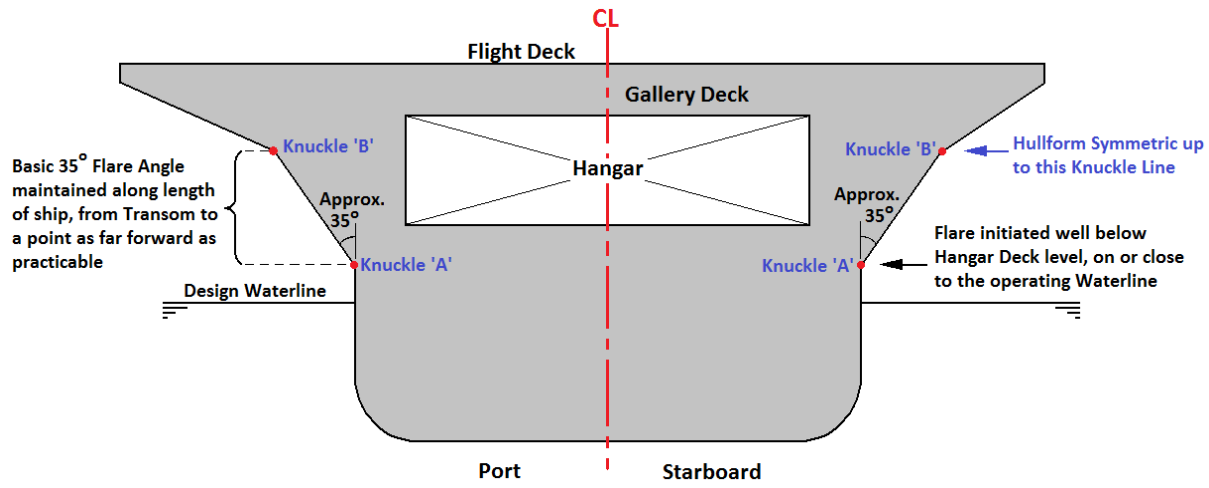

Figure 4: 'Highly Flared' Style of Carrier Above Water Form for a representative midships section

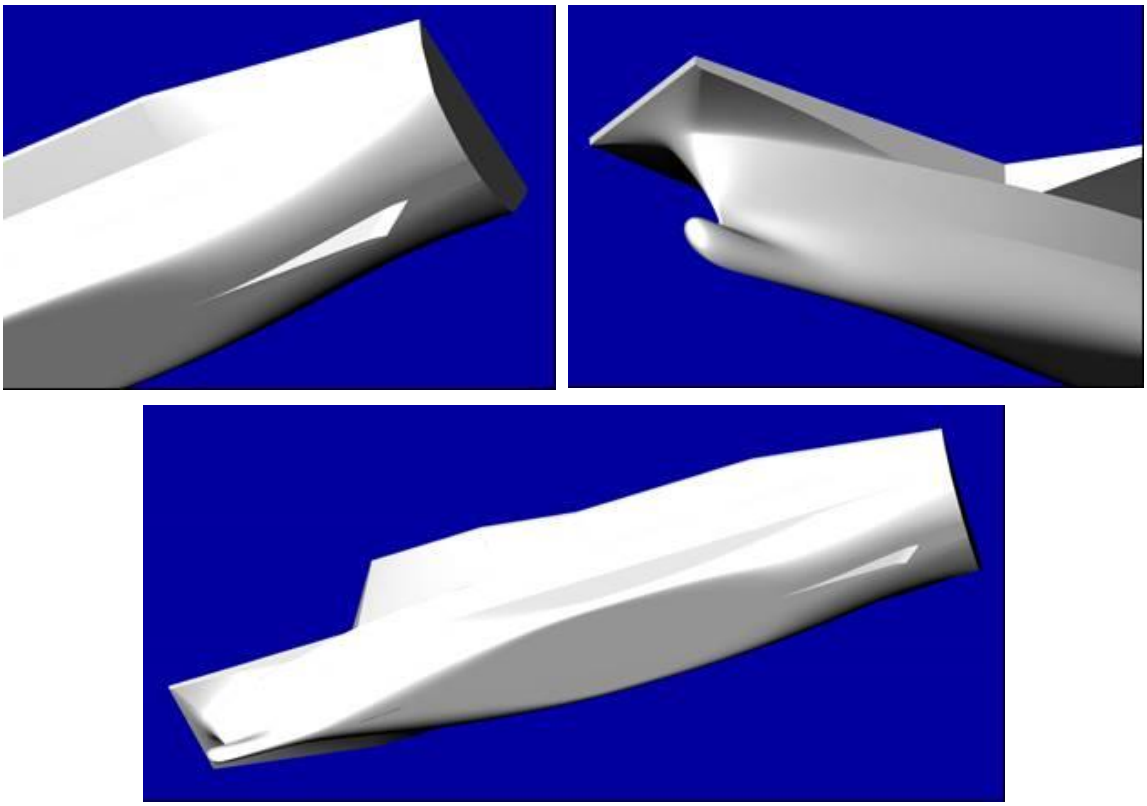

Figure 5: Hullform Definition for the CVF Design Proposal covered in this paper

In terms of the shaping of the above water form around the bow, efforts initially focussed on developing a simplified bow shape composed predominantly of flat and single curvature surfaces, in a bid to improve producibility (Figure 12). Subsequently, consideration of seakeeping performance in extreme seas (e.g. mitigation of the effects of immersion/re-emergence of the upper region of the bow, deflection of spray/green water clear of the flight deck), supported by observations during seakeeping experiments, led to a decision to adopt a more traditional rounded bow shape.

The resulting hullform arrangement is shown in Figure 5.

8. SHAFTLINE & PROPULSOR CONSIDERATIONS

8.1 DELIBERATIONS ON SHAFTLINE CONFIGURATION

The choice of shaftline arrangement was the subject of some deliberation during the CVF design studies, due to its fundamental impact on broader ship design considerations (e.g. cost, ship layout, producibility, vulnerability and signatures), and the potential offered by more novel propulsor types. Ability to sustain flying operations (at least in some reduced capacity) following loss of a shaftline to damage/flooding/failure was a particularly key consideration for CVF, as an aircraft carrier. Given the Integrated Full Electric Propulsion (IFEP) power system proposed there were a range of possible shaftline configurations for CVF, employing conventional shaftlines, azimuthing podded propulsors, waterjets, and combinations thereof.

For the purposes of the CVF studies outlined in this paper, options employing triple or quadruple conventional shaftlines were discounted due to the relatively low shaft power levels anticipated for CVF, and because of the likely implications for the cost and ship layout. Single shaft solutions were also discounted, on grounds of lack of redundancy, survivability, and achievable shaftline rating. Solutions based wholly around waterjets were rejected due to the perceived risks associated with applying such novel propulsors to a large warship, such as CVF. Specific concerns with waterjets included shock performance, likely degradation in performance in a seaway due to inlet aeration, likely impact on ship layout (i.e. around the aft end), and inherently low propulsive efficiency except at the highest CVF operating speeds. The acoustic characteristics of waterjets are also a concern, although there is some evidence (Källman, & Li (2001)) to suggest that the potential drawbacks in this area may not be as great as might at first be thought.

Other shaftline configurations identified as being of potential interest for CVF included:-

- The twin conventional shaftline option;

- Options based wholly around fixed/azimuthing podded propulsors (Warship Technology, 2003);
- Hybrid shaftline arrangements employing one or two conventional shaftlines, in conjunction with one or two azimuthing podded propulsors;
- Hybrid shaftline arrangements employing twin conventional shaftlines in conjunction with one or two waterjets. Here the conventional shaftlines would power the vessel at low-intermediate speeds and in extreme seas, with the waterjets providing 'boost' for higher speeds and in calmer seas where their performance penalties are less marked. The waterjets would also offer potential for improvements in manoeuvring and stopping performance (i.e. using steerable nozzles and/or reversing buckets).

The key options were assessed in terms of a broad range of design issues, including vulnerability, noise and vibration, manoeuvrability, ship layout, propulsive efficiency, supportability characteristics, cost, risk, required shaftline rating, and the scope for modularisation of the entire propulsion train for build purposes.

This led to the shaftline arrangement of the final design proposal, shown in Figure 6, which is a hybrid arrangement employing twin conventional shaftlines and a single 'tractor' ('pull-mode') azimuthing podded propulsor. To avoid manoeuvring ability being invested wholly in the pod, this arrangement includes a rudder sited downstream of both conventional shaftlines.

Given the degree of redundancy inferred by the presence of the pod, it was deemed acceptable for the motors of the two conventional shaftlines to be collocated in the same longitudinal compartment, rather than longitudinally staggered for survivability reasons (i.e. as would have normally been required in applying a twin shaft configuration to a front line warship design). This feature greatly reduces the ship layout implications of adopting twin conventional shaftlines on CVF, by minimising the amount of internal space consumed low in the hull and forward of the cut-up, where space is at a premium (i.e. due to the demands imposed by power generation machinery and weapons magazines). By reducing the proportion of ship's length over which the shaftline components are distributed, it also greatly improves the scope for the adoption of modular build practices, and it also results in a shaftline arrangement that is wholly symmetric about the ship's centreline.

The design included provision for a watertight cofferdam (double bulkhead) on the centreline of this compartment, to segregate the two conventional shaftline motors into separate (port and starboard) motor rooms, and thereby minimise the risk of both being put out of action simultaneously in the event of flooding or action damage.

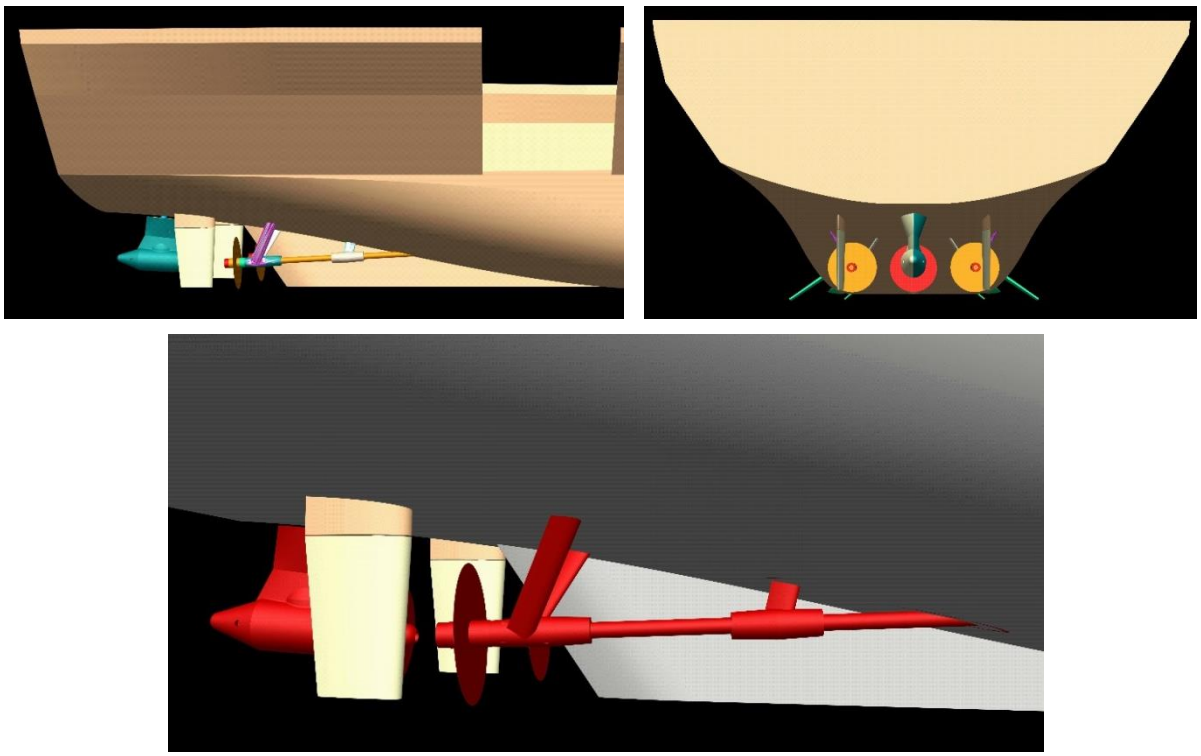

Figure 6: Final Shaftline and Hull Afterbody Arrangement for the CVF Design Proposal covered in this paper (Conventional Twin Shaftlines/Rudders, Single Azimuthing Podded Propulsor, Centreline Skeg)

In terms of manoeuvring characteristics, simulation work (see Section 13.4) based on this hybrid shaftline arrangement indicated little appreciable difference in manoeuvring performance at ocean going speeds compared to an equivalent twin conventional shaftline design without a pod. Nonetheless, the ability of the pod to generate lateral thrust during low speed manoeuvring is clearly beneficial.

In general it is expected that the pod would be operated in parallel with the conventional shaftlines over the entire range of forward ship speeds. However, for quiet operation at low-intermediate ocean-going speeds, it was anticipated that the pod's propeller would be 'windmilled'/idled to eliminate (or at least minimise) pod machinery noise.

8.2 PROPULSOR CONFIGURATION

Following a high level review of alternative propulsor types (including novel propulsor types) conventional Fixed Pitch Propellers (FPPs) were adopted as the baseline for the CVF design proposal covered in this paper, on grounds of proven performance, relatively low technical risk, simplicity and low through-life cost. Although Controllable Pitch Propellers (CPPs) can offer improvements in efficiency at off-design conditions and improved stopping performance, considerations of design point efficiency, likely acoustic performance, mechanical complexity and through-life cost led to their provisionally being discounted. The baseline assumption of IFEP propulsion for CVF, where shaft rotation can be readily reversed, also weakened the case for CPPs.

The preliminary choice of directions of rotation for the propellers (Figure 7) was based on specialist advice and took high level account of the likely impact on manoeuvring and directional stability characteristics, propulsive efficiency (i.e. inflow swirl), and, of particular importance for CVF, propeller-induced vibration and cavitation performance. In the case of the conventional shaftlines, cavitation and vibration considerations were the dominant consideration, and, taking into account cruise liner experience (Kinns & Bloor (2000)) and the alignment of the shafts, led to a provisional decision to adopt inward turning propellers - a choice that was provisionally confirmed by unpowered (nominal) wake field experiments. In the case of the centreline (podded) propeller, the clean inflow characteristics arising from the 'pull-mode' pod configuration and the location of the pod on the centreline meant that the direction of this rotation for this propeller was based on steering bias considerations and utilisation of the paddle wheel effect during normal berthing (i.e. starboard side to) - issues that led to the adoption of a left-handed propeller.

It will be noted that the choice of shaftline arrangement effectively precludes full shaft synchronisation (i.e. to minimise underwater signature and noise and vibration), although it would be possible to synchronise the two conventional shaftlines.

9. MANOEUVRING DEVICE FIT

9.1 GENERAL

The fit of primary manoeuvring devices is highly dependent on the shaftline arrangement. Given the hybrid shaftline arrangement proposed in Section 8 (Figure 5), twin conventional rudders were proposed, supplemented by the manoeuvring capabilities of the podded propulsor, with twin tunnel-type bow thrusters provided for low speed manoeuvring.

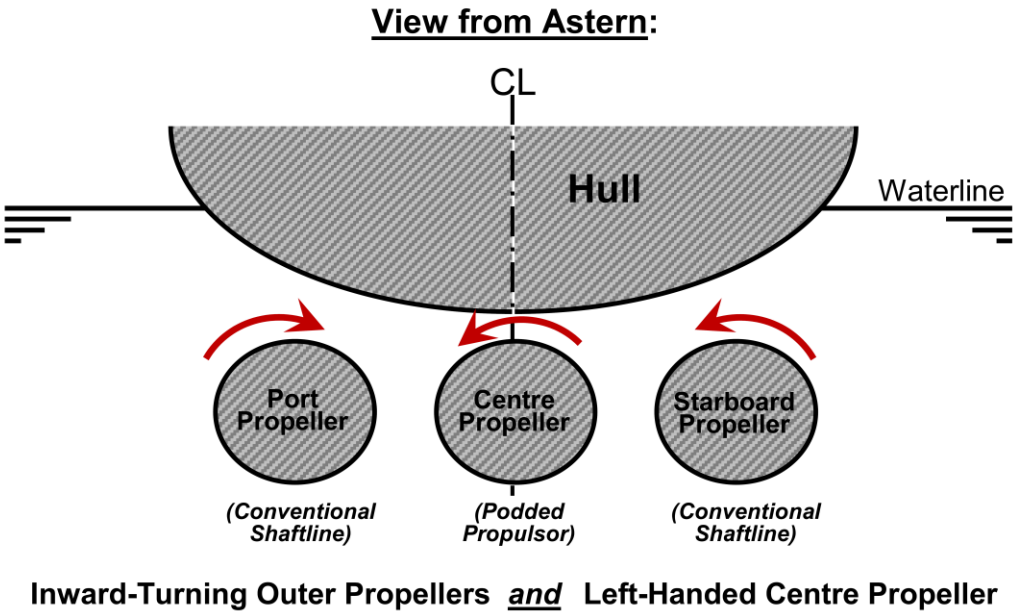

Figure 7: Proposed Propeller Directions of Rotation

As noted in Section 8, it was considered prudent to include two conventional rudders, to supplement the manoeuvring and course-keeping capabilities of the pod, both for survivability/redundancy reasons and to avoid the need to use the pod for routine course-keeping (e.g. during long transits). As a starting point, rudders of the all-movable (balanced spade) type, fitted with a fixed headbox to avoid mechanical interference with the hull, were proposed on grounds of simplicity, maintenance considerations and minimisation of rudder torque. Subsequent calculations indicated that the required diameter of rudder stock could prove prohibitive (e.g. in terms of weight and required rudder thickness), and consequently it is likely that horn-type rudders would have been substituted as part of the next stage of design development.

The azimuthing podded propulsor was configured so that it could be azimuthed to ±90° during low speed manoeuvring (e.g. berthing operations), thereby allowing significant amounts of purely lateral thrust to be developed at the stern, without the need for dedicated stern thrusters. At higher forward speeds the azimuth of the pod was to be limited to ±35° to minimise the hydrodynamic forces on the pod, limit the cross flow at the pod propeller, and reduce the risk of undesirable hydrodynamic interactions with the races of the conventional shaftlines. It was anticipated that during long transits the pod would be locked, to avoid wear on the pod azimuthing mechanism, and the conventional rudders used for course-keeping.

The principal area of concern relating to the final shaftline arrangement shown in Figure 5 is that, for certain combinations of rudder incidence and pod azimuth during manoeuvring, the rudders might deflect the races of the conventional shaftlines onto the podded propeller, resulting in cavitation and adverse levels of noise and vibration. A four-stage approach was proposed for de-risking this issue, based around:-

- Refining the siting of the conventional shaftlines and the hull afterbody appendages, to minimise the risk of undesirable hydrodynamic interactions occurring;
- Use of Computational Fluid Dynamics (CFD) analysis to assess the likelihood of undesirable interactions;
- Cavitation tunnel testing to evaluation the implications of undesirable interactions occurring;
- Consideration of the need for limitations on allowable combinations of rudder incidence and/or pod azimuth.

9.2 DELIBERATIONS ON THE CHOICE OF BOW THRUSTER

The potential need for bow thrusters onboard CVF stems from a desire that, in order to minimise the need for tug support, the vessel should ideally be capable of berthing unassisted (i.e. without tugs) in various conditions of cross wind and tidal cross-flow. To these ends, three principal types of bow thruster were considered (Figures 8, 9 & 10).

Of these, the azimuthing ‘drop-down’ type of thruster is attractive in that it remains effective at forward speed, offers an inherently high efficiency, and because it offers considerable scope for use as a means of emergency propulsion. However, as this type of thruster projects below the keel line when in use, its suitability for adoption on a draught-limited vessel, such as CVF, was considered questionable.

Pump-type thrusters offer similar advantages to ‘drop down’ thrusters in terms of their ability to provide an emergency means of propulsion through directable thrust. Additional advantages arise from the fact that the installation does not project significantly below the keel line. However, the efficiency of this type of thruster is markedly lower than for the other types of thruster, with implications for installed weight, space and power requirements, and cost. For CVF the need for pump thrusters to be sited low in the hull on a reasonably wide and flat part of the hull underside means that they tend to occupy a large amount of relatively high value space that could be used for a range of other purposes (e.g. aviation fuel stowage).

Tunnel Thrusters represent low risk, low cost technology, and are arguably mechanically simpler and require less maintenance than other types of thruster. They can be located wholly within the lines of the hull and therefore do not impose additional draught constraints on the vessel. Additionally, they can be located well forward in the narrow portion of the hull, where internal hull space is at less of a premium and where their effectiveness at countering wind/current-induced hull moments is maximised. In terms of drawbacks, their performance deteriorates sharply with rising forward speed due to cross flow effects, and they can only generate lateral thrust, thereby offer no prospect of providing emergency propulsion. Additionally, there is a small (but not insignificant) drag penalty and potential flow noise concerns unless closures are fitted.

From the point of view of hydrodynamics and propulsion, a bow thruster fit based around pump thrusters was considered to represent an attractive option, principally because of the emergency propulsion capability offered. However, pending clarification of the need for such an emergency propulsion capability, broader considerations of cost, weight, required power and ship layout led to the decision to proceed with a baseline bow thruster fit based around tunnel thrusters. Two such thrusters were provided on grounds of required rating and redundancy in the event of one failing during operation.

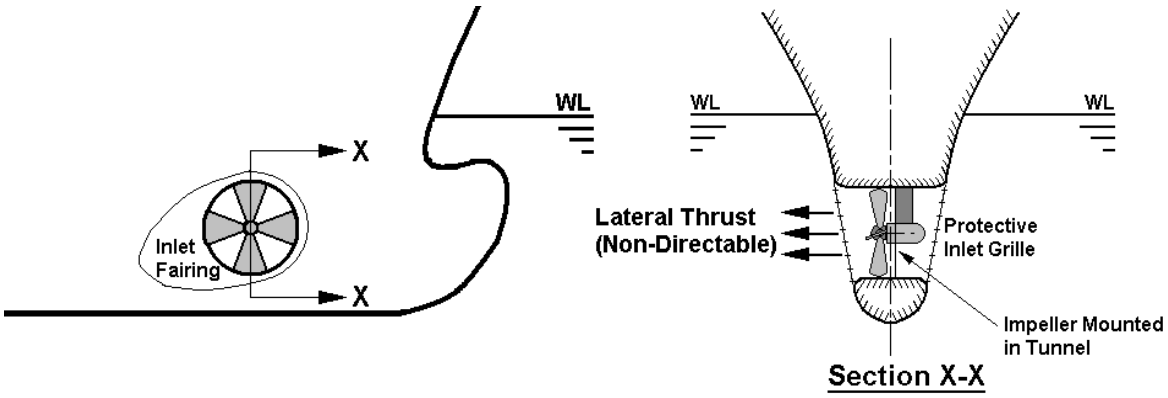

Figure 8: Transverse Tunnel-Type Bow Thruster

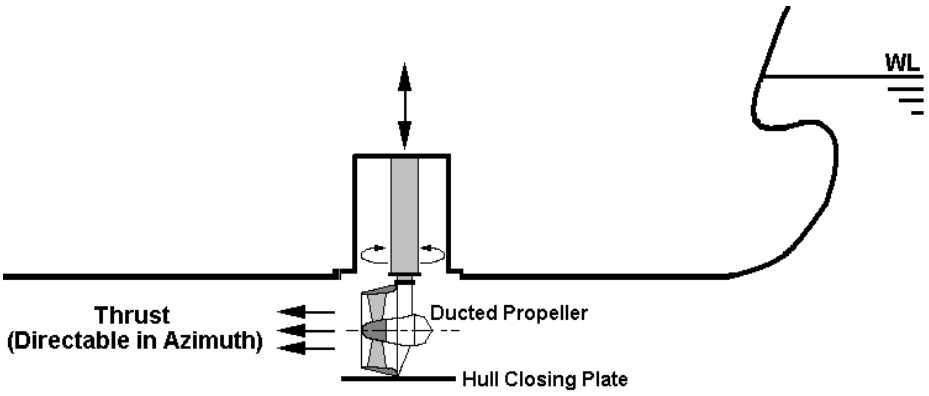

Figure 9: "Drop-Down" (Retractable) Azimuthing Bow Thruster

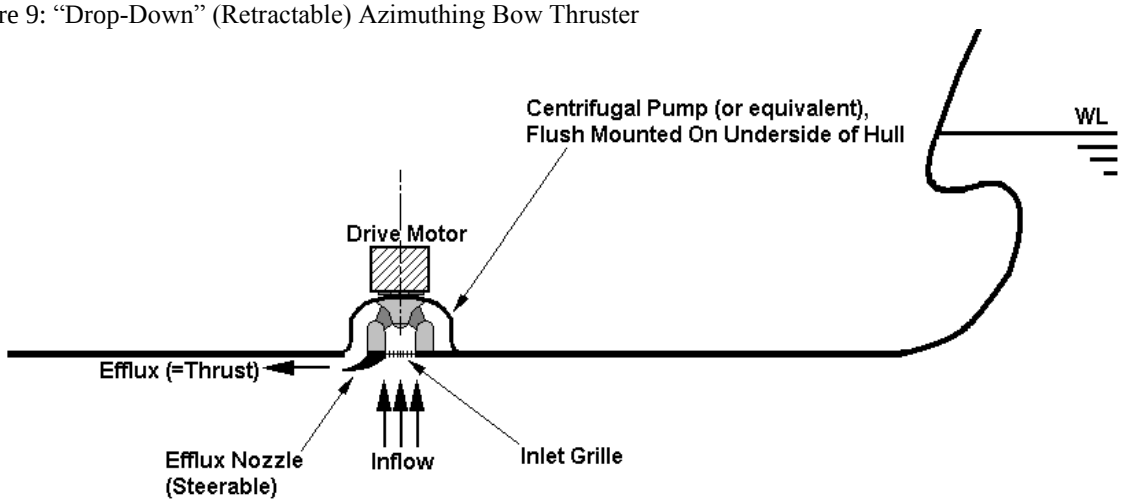

Figure 10: Pump-Type Thruster (Flush-Mounted with Underside of Hull) (see: www.schottel.de/marine-propulsion/spj-pump-jet)

10. MOTION-REDUCTION FIT

Noting that pitch-related motion represents a key factor limiting the operability of CTOL aircraft in a seaway, the initial review of motion-reduction measures for CVF considered not only means for reducing roll, as is common practice in ship design, but also those for reducing pitch.

Whilst there are a number of specific measures which could be applied to the CVF in order to minimise its pitching motion, these have generally not been widely adopted on either warships or merchant ships. This is essentially because they tend to impose significant penalty in terms of either broader aspects of ship performance (e.g. the 'low pitch' parent form and a seakeeping-optimised bulb considered in Section 7.1),

ship size (i.e. tank-based pitch stabilisation) and/or risk and development cost (e.g. anti-pitch fins[6]). Consequently, explicit measures for minimising pitch motion were discounted.

As regards roll-reduction measures for CVF, these are principally intended to maximise the range of headings and ship speeds on which unrestrained aircraft handling is possible, and ensure general ship habitability (i.e. crew comfort, safety and effectiveness) in a seaway. However, they do not tend to significantly influence the range of sea states in which aircraft launch and recovery is possible, at least for Fixed Wing operations, because wind-over-deck considerations generally dictate that launch/recovery is conducted into the principal wave direction where rolling motion is generally minimised. It will be further noted that the specification of roll reduction measures for CVF is somewhat subjective, given:

- The random nature of a seaway, which could make unrestrained aircraft handling in beam seas a hazardous operation even in moderate seaways;
- The subjective issue as to which scenarios to meet when sizing the stabilisers for a given sea state (e.g. parametric roll in head/following seas, resonant roll in beam seas, or simply statistically-averaged conditions which are likely to be significantly less onerous);
- Difficulties in accurately modelling fin stabiliser performance and their effect on ship roll motion, computationally or at model scale;
- The potential secondary role of the fin stabilisers in correcting heel-in-turn (see Section 12.3 (below).

For the CVF design proposal covered in this paper, the decision was taken to proceed with a baseline roll reduction fit based around one pair of bilge keels sited between two pairs of high-outreach retractable fin stabilisers.

Bilge keels essentially represent standard fit for a warship, such as CVF, as they represent a simple, effective and low-cost means of reducing roll at all ship speeds. Although they result in a slight increase in ship resistance and flow noise, this can be minimised through correct flow alignment. In the case of the CVF design proposal covered in this paper, 'V'-section bilge keels were adopted, to allow outreach (and hence bilge keel effectiveness) to be maximised within the turn-of-bilge of the ship.

As regards the active fin stabilisers, these were adopted as they represent established low-risk technology and readily lend themselves to higher speed, volume-critical ships, such as CVF. They are very effective at higher forward speeds, although their performance deteriorates markedly at lower forward speeds. The choice of fin stabiliser configuration (i.e. retractable vs non-retractable) essentially represented a trade-off between survivability considerations (i.e. shock performance) versus fin performance during normal operation (i.e. fin outreach), with cost and internal space requirements being additional considerations. Ultimately retractable fins were selected because of the much higher outreach that can be achieved, which considerably enhances performance during normal operation[7]. Concerns associated with the increased vulnerability of retractable systems have been mitigated, at least in part, by the adoption of two well-separated pairs of fins per ship, which provides some degree of redundancy.

In terms of other potential roll-reduction measures, while tank stabilisation offers the benefit of being effective at lower ship speeds, where fin stabilisers are rendered ineffective, likely weight and internal space requirements led to this option being discounted. Likewise, whilst rudder roll stabilisation (Baitis et al, 1983) represents a potentially a low cost approach, that makes beneficial use of the increased flow velocities within the propeller races, it has only appears to have been applied to a limited number of vessels, most notably onboard the French aircraft carrier CHARLES DE GAULLE (Kummer et al (1998) and Autret & Deybach (1997)). Concerns regarding the development costs and risks, together with the complexity it could add to the ship's safety-critical manoeuvring system, led to this option being considered more as a candidate for possible substitution at a later date rather than as a baseline solution for CVF.

11. AIRCRAFT LIFT CONFIGURATION

The three basic aircraft lift configurations generally adopted for aircraft carriers are shown in Figure 11. Of these stern lifts are generally restricted to vessels operating solely Rotary Wing and STOVL Fixed Wing aircraft.

The choice of aircraft lift configuration impacts on a range of ship design issues, including flight deck/hangar layout and operability, structural design, hydrodynamics, damaged stability characteristics, internal ship layout, availability, reliability & maintainability (AR&M), vulnerability, storing/replenishment routes, and radar cross section. In the case of an aircraft carrier designed for intensive air operations, such as CVF, issues of flight deck/hangar layout and operability tend to predominate.

[6] For discussion of anti-pitch fins, see: Abkowitz (1959), Conolly & Goodrich (1970), Ferreiro et al (1994) and Ochi (1961).

[7] The outreach of non-retractable fins tends to be limited by the local beam and draught of the hull, in order to afford them some degree of protection from damage during berthing and docking.

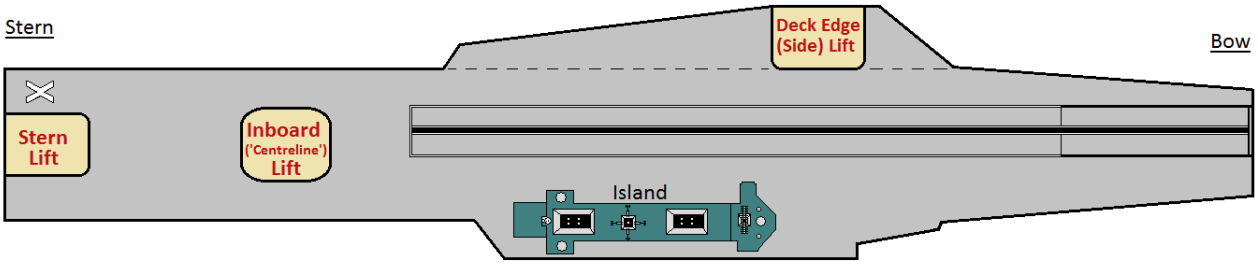

Figure 11: Alternative Aircraft Lift Configurations, shown on a Generic Aircraft Carrier Deck Plan

(Note: As indicated by Figure 1, the final BAE SYSTEMS aircraft carrier design proposals (both CTOL and STOVL variants) employed three (3) deck edge aircraft lifts, one of which emerged into an opening in the Island superstructure. Preceding design variants (from 2001) were based on just two (2) larger deck edge lifts, capable of accommodating two aircraft simultaneously.)

Specific advantages of deck edge lifts in this context include:

- Location of the aircraft lifts well away from the main operating areas (e.g. runways and taxiing routes) of the flight deck;
- Minimal encroachment into hangar stowage space;
- Increased flexibility in terms of the ability to accommodate large aircraft, in that the physical size of aircraft that can be accommodated is not so rigidly constrained by the size of lift platform (e.g. aircraft tails can overhang the edge of the lift platform);
- Improved scope for adopting larger lift platforms (e.g. to allow two aircraft to be accommodated simultaneously).

Notwithstanding this, there are a number of hydrodynamic issues associated with deck edge lifts that are worthy of further comment.

The key point is that deck edge lifts are inherently much more exposed to the elements than comparable inboard lifts, which places limits on their operability in a seaway. Specifically, under the influence of ocean waves, ship motion and the ship's running wave pattern, the lowered platform of a deck edge lift is subject to wave slamming loads, green seas and spray in relatively low sea states - factors that will tend to prevent safe aircraft movement between the hangar and flight deck in comparatively low sea states. Indeed, the work of Comstock et al (1982) suggests that for large US carriers operability of deck edge lifts is limited above Sea State 5.

Key factors determining the operability of deck edge lifts in this regard are:

- The freeboard of the hangar deck in the deepest through-life loading condition. This represents a fundamental geometric constraint on the design of an aircraft carrier, in that once deck heights have been fixed early in the design process, the likelihood of lift platform immersion is largely prescribed, and any deficiency in this regard is difficult to subsequently correct. Moreover, it tends to preclude the adoption of side lifts on smaller aircraft carriers;
- Metacentric height. For the reasons outlined in Section 4.3, adopting a relatively low operation metacentric height consistent with maximising natural roll period will tend to reduce roll amplitude and therefore reduce the incidence of lift platform wetness in a seaway. The down side of this is that angles of turning-induced heel will tend to be inherently higher, resulting in increased risk of the lowered lift platform immersing during manoeuvring (see below);
- The depth of supporting structure beneath the lift platform, noting that the spray generated by waves impinging on the lift platform structure can limit aircraft lift operability (e.g. due to the risk of aircraft skidding as they are manoeuvred on/off the lift platform (Comstock et al, 1982);
- The longitudinal position of the lift platform, noting that the operability of side lift platforms mounted significantly further forward than midships will tend to be particularly poor;
- The presence and configuration of flight deck sponsons immediately adjacent to the lift platform, which on one hand might afford some degree of shelter from green seas and wind, but on the other hand might generate unfavourable interactions and exacerbate the incidence of wetness and spray on the lift.

The minimum freeboard of the hangar deck was of the order of 6.5m (21 feet), which after allowing for the depth of lift platform structure, is comparable to figures quoted for larger US carriers (Comstock et al, 1982).

In terms of the evaluation of the likelihood of deck edge lift wetness in a seaway, two specific points are worthy of note. Firstly, seakeeping experiments conducted as part of the CVF studies (see Section 13.3) indicated a

clear tendency for strip theory, such as that commonly embodied in seakeeping assessment software, to markedly underestimate the occurrence of side lift wetness compared to experimental measurements. This, together with operability issues that cannot be modelled using strip theory (e.g. the occurrence of undesirable hydrodynamic interactions around side lift openings) strongly suggests that reliable assessment of deck edge lift wetness is best achieved through model testing. Secondly, it will be noted that the established criteria for assessing the deck edge lift wetness at the design stage (e.g. the commonly quoted limit of 5 wetnesses per hour presented by Comstock et al (1982)) is essentially concerned with minimising the occurrence of lift wetness based on statistically-averaged performance, rather than minimising its consequences. Clearly lift wetness is a safety issue, in terms of the risk to aircraft and personnel, and moreover, its occurrence in a given seaway will tend to be random. It is therefore important that appropriate consideration is given to minimising the consequences of lift wetness in the design and location of the lift platforms, and in the design of the surrounding above water hullform (e.g. through the judicious location and sizing of sponsons).

A separate issue influencing the operability of deck edge lifts, even in calm conditions, is the risk of a lowered lift platform becoming immersed as the vessel heels while manoeuvring, resulting in noise, spray, vibration, and risk to personnel and equipment. Analysis of the CVF design proposal covered in this paper indicated that, at least in flat calm conditions, such immersion only occur at heel angles of greater than around 10° - something that was considered acceptable, given that likely heel limits for unrestrained aircraft handling are much lower (i.e. around 3.5°), and because of the scope for raising the lift platform to avoid this type of immersion. Adoption of a suitably high operating metacentric height is key to minimising manoeuvring-induced heel, and hence immersion of this type.

It will be noted that inboard lifts, such as those traditionally fitted to Royal Navy carriers, are sheltered from the elements and are not prone to immersion in a seaway or under the influence of manoeuvring-induced heel. As such they might be expected to remain operable in all sea states in which aircraft handling is possible. Consequently, there are strong arguments in favour of the adoption of inboard lifts on aircraft carriers where the air group is based solely around STOVL and Rotary Wing aircraft, as this ensures that the enhanced operability offered by these aircraft types in a seaway (i.e. compared to CTOL aircraft) will be maximised. Likewise, for smaller aircraft carriers, the adoption of inboard lifts (or at least a stern lift) is likely to be a necessity if air group operability is sought in anything other than relatively calm conditions.

12. HEEL-IN-TURN CONSIDERATIONS

12.1 THE SIGNIFICANCE OF HEEL-IN-TURN FOR AN AIRCRAFT CARRIER

Turning-induced heel assumes special significance in the design of an aircraft carrier, for it fundamentally affects the operational flexibility and responsiveness of the ship, in terms of:-

- Allowing flight deck preparations (e.g. aircraft movements) to be undertaken whilst manoeuvring the ship into wind to launch or recover aircraft;
- Ensuring that Deck Alert requirements (i.e. the ability to launch defensive aircraft at short notice) can be satisfied from the widest range of initial headings, ship speeds and wind/sea conditions, without the need to constrain routine flight deck activity (e.g. aircraft movements) before or during the manoeuvre.

In pursuit of the above objectives, it is highly desirable that combined angles of heel/roll that develop in the turn (i.e. under the combined influence of wind, waves, ship turning and aircraft movement) do not exceed established limits for unrestrained aircraft handling. In addition it is desirable that the lowered platforms of deck edge lifts (where fitted) do not become immersed - see Section 11 for discussion of this latter issue.

12.2 MEASURES TO LIMIT HEEL-IN-TURN

For a given ship speed and helm angle, the fundamental parameter determining angles of turning-induced heel is metacentric height. Accordingly, the aim of the ship designer in the first instance should be to minimise turning-induced heel by maximising the metacentric height of the vessel within the constraints imposed by broader design considerations (see Section 6). Allied to this, appropriate strategies should be adopted (e.g. through-life ballasting strategies) to ensure that adequate metacentric height is maintained across all through-life loading conditions.

If further improvements on heel-in-turn characteristics are sought there are a range of alternative heel correction systems that can be installed onboard the ship, each of differing performance potential and ship impact. Options of this type considered as part of the CVF studies covered in this paper are summarised in Table 7.

Of these, dedicated (tank-based) fluid transfer systems were discounted due to inherent weight and space penalties, and the general feasibility and associated power levels required to transfer the working fluid at a rate sufficient for effective heel correction. Circular movement of solid weights in a horizontal plane was also

discounted on grounds of general ship impact and feasibility. Of the remaining options it was concluded that none would be capable of fully meeting CVF heel correction requirements for all 'loiter' speeds and rates of turn, although:

- A system based around use of the ship's fin stabilisers would provide a partial heel correction capability at low cost, risk and ship impact;
- A dedicated transverse moving weight system (i.e. similar to that fitted onboard the French aircraft carrier CHARLES DE GAULLE)[8], used in conjunction with the ship's fin stabilisers, would maximise the range of turn rates, ship speeds and sea states over which unrestrained aircraft handling would be possible in the turn. However, the moving weight component of the system would adversely impact on ship weight/centroids and on internal layout (e.g. on fore-aft access and the layout of modular stores facilities located on the gallery deck) and impose additional cost, risk and maintenance requirements.

Table 7: Heel Correction Options Considered for CVF

Type	Option
Fluid (Tank)-Based Systems	Transfer of Fluid from One Side to Another by Pumping
	Transfer of Fluid from One Side to Another by Compressed Air
	Discharge of Fluid Overboard from One Side or Other of the Ship
	Use of the Ship's Main Ballast System
Moving Solid Mass Heel Control System	Transverse Movement of Solid Weights
	Circular Movement of Solid Weights in a Horizontal Plane
Hydrofoil-Based Systems	Use of Active Fin Heel/Roll Stabilisers

12.3 ANALYSIS & CONCLUSIONS ON THE NEED FOR A HEEL CORRECTION SYSTEM ONBOARD CVF

Analysis of turning-induced heel was based on empirically-based simulations of manoeuvring performance under Deck Alert scenarios, obtained as part of the work described in Section 13.4. This analysis of heel-in-turn, which considered a range of initial speeds, helm angles and wind conditions, was based on a 'turn and accelerate' manoeuvre, whereby the ship turns through 180° into wind, applying power (to maximise rate of turn and speed on exit from the turn), before accelerating and steadying on the new course to reach aircraft launch speed. This assumed a limiting combined angle of heel/roll in the turn of 3.5°, which corresponds to the limiting significant single roll amplitude value quoted by Comstock et al (1982) for aircraft handling in a seaway. Conclusions were:

- Given appropriate management of metacentric height there was adequate scope for CVF to satisfy aviation-related heel-in-turn limits in calmer seas, without the need for a dedicated heel correction system;
- In intermediate and higher sea states dynamic roll, rather than turning-induced heel, would represent the key factor preventing unrestrained aircraft handling during the turn;
- There are various 'work arounds' that could be employed by the ship's command to mitigate or avoid those scenarios where unrestrained aircraft handling in the turn is not possible (e.g. placing limitations on ship heading, restrictions routine aircraft movements, or unlashing aircraft after the point of maximum heel has passed in the turn).

This led to the overall conclusion that the broader ship design penalties of adopting a dedicated heel correction system, such as a transverse moving weight system, were not warranted for CVF, but that the potential use of the ship's fin stabilisers to provide a heel correction capability should be explored further.

12.4 OTHER POTENTIAL HEEL CORRECTION REQUIREMENTS

Minimisation of the heel induced by aircraft movements on/off the ship represents a potentially key consideration for an aircraft carrier, such as CVF, where intensive flying operations are required. Indeed, the limits on heel (typically 0.5°-1.0°, see Pattison & Bushway (1991)) are potentially much lower than those associated with turning-induced heel (typically 3.5° - see above). This is because the determining factor is likely to be requirements for ongoing aircraft launch/recovery operations, rather just unrestrained aircraft handling.

Nonetheless, measures to limit heel-in-turn (see above) will also tend to minimise or offer scope for counteracting the heel induced by aircraft movements.

The CVF studies covered by this paper indicated that, provided operating metacentric height is sufficient to satisfy heel-in-turn requirements, there is generally adequate scope to counteract the heel induced by aircraft movements in a timely manner using the ship's main ballast system, without the need for a dedicated heel correction system. However, this conclusion is clearly sensitive to such issues as metacentric height, flight deck dimensions/configuration, aircraft weights, assumed flying programme and ballast system design, and therefore requires confirmation through analysis in the context of a given ship design.

[8] See Kummer et al (1998) and Autret & Deybach (1997) for an overview of the moving weight heel correction system onboard the CHARLES DE GAULLE.

13. HYDRODYNAMIC PERFORMANCE EVALUATION

13.1 HYDRODYNAMIC TANK TESTING

Two phases of hydrodynamic tank testing work were conducted as part of the CVF studies covered in this paper, both conducted at SSPA, Gothenburg (Sweden) during 2002.

The first phase of tank tests, which were conducted at 1/60 scale (Figure 12), focussed on addressing the key areas of hydrodynamic risk and uncertainty, namely:-

- Preliminary confirmation and hydrodynamic de-risking of the characteristics of the above/below water hullform;
- Validation of powering characteristics to allow the power system, shaftline configuration and fuel capacity to be confirmed.

The scope of this initial testing included expert review/refinement of the hullform and appendage arrangement, followed by seakeeping and naked hull resistance experiments, and supporting estimation of powering characteristics using empirically-based estimates of propulsive efficiency.

The second phase of tank tests were conducted late in 2002, at larger scale than the initial tests (i.e. 1/35 scale, see Figure 13) and to an updated set of design particulars. The scope of work consisted of a more detailed expert review/refinement of the hullform/appendage arrangement, naked hull resistance measurements and empirical estimation of propulsive efficiency, and nominal (unpowered) wake surveys on both the podded and conventional shaftline propellers.

13.2 EVALUATION OF RESISTANCE & POWERING CHARACTERISTICS

The fundamental approach adopted in the assessment of CVF powering characteristics centred around the use of commercially available regression-based powering prediction software.

Having produced initial estimates on this basis, the resulting predictions were compared against towing tank predictions for the design as they became available. The output from this validation activity was a set of revised empirical correction factors (e.g. revised values of ship-model correlation allowance, appendage form factor and propulsive efficiency elements) for use in future runs of the regression software.

This approach of calibrating the regression software against the tank test predictions allowed the tank test results to be extrapolated with a good degree of confidence to revised ship particulars and loading conditions as the design of the ship developed.

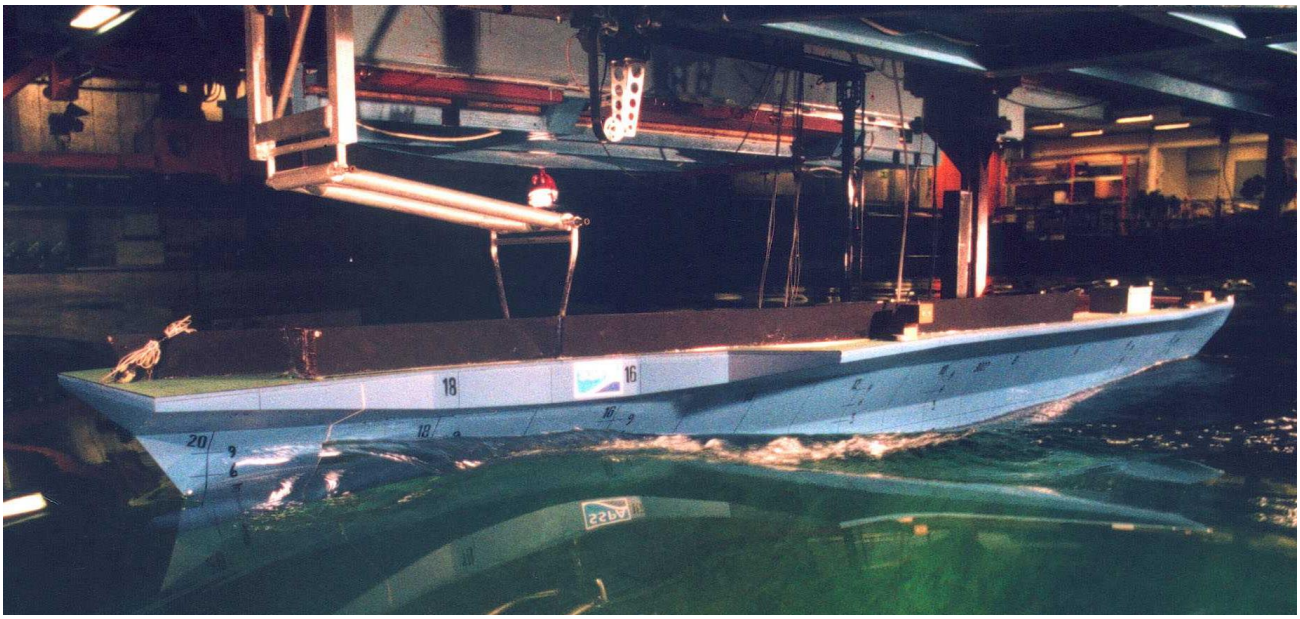

Figure 12: Initial 1/60 Scale Seakeeping Tests on the BAE SYSTEMS CVF Design Proposal (CTOL Variant) (Source: SSPA, June 2002)


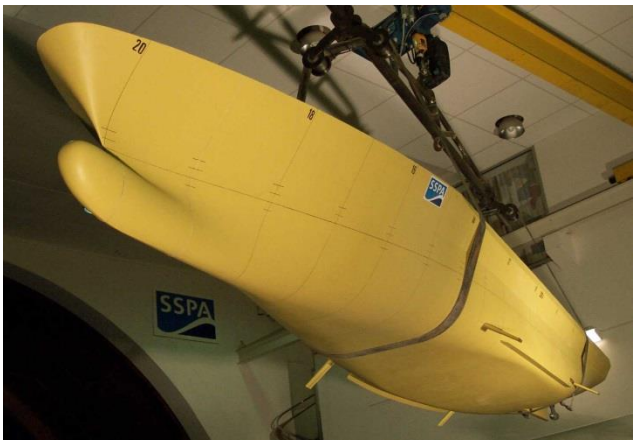

Figure 13: 1/35 Scale Model of the Final BAE SYSTEMS CVF Design (CTOL Variant), Rigged in Preparation for Propeller Wake Survey Measurements (Source: SSPA, December 2002)

(Note: The upper portion of above water form and side lift recesses were not modelled in these final 1/35 scale tests, as seakeeping tests were not part of the itinerary. Also, note the revised (fuller) above water bow shape compared to earlier tests of Figure 12 - see Section 7.2 for discussion of this.)

13.3 SEAKEEPING ASSESSMENT

13.3 (a) Approach

The detailed seakeeping assessment of the CVF design proposal was based on commercially available strip theory analysis software. This approach readily lent itself to the rapid and low cost evaluation of the relative large number of metrics and assessment locations required to assess compliance with the derived seakeeping criteria for CVF (see Section 4.3). It also generated data required to perform follow-up assessment of percentage time operable (PTO) of the CVF air group in different worldwide ocean areas, and readily allowed sensitivity studies into such issues as the effect of sea spectra, wave directionality, metacentric height and roll radius of gyration on seakeeping performance.

Separately, a set of 1/60 scale seakeeping experiments were conducted (see Section 13.1) to assess phenomena that could not be adequately assessed using strip theory, namely parametric roll and phenomena pertaining to the above water form. In addition, the experiments generated seakeeping data for a representative CVF design against which the strip theory predictions could be validated.

13.3 (b) Strip Theory Results

The findings of the strip theory analysis of CVF were broadly in line with the findings of Comstock et al (1982), clearly demonstrating the inherent benefits of STOVL and Rotary Wing aircraft over CTOL aircraft in terms of operability in higher sea states.

In terms of the operability of CTOL aircraft in a seaway, the key limiting factor is pitch-related motion, specifically pitch amplitude and limitations on absolute vertical displacement at the round-down (i.e. at the aft end of the angled runway). While increasing ship length within practicable bounds will tend to reduce pitch amplitude, its effect on vertical displacement at the round-down is much less marked. Meanwhile, although such measures as adopting a large (seakeeping-optimised) bulbous bow and 'low pitch' underwater form may reduce pitching motion (see Section 7.1), the effect is unlikely to be so marked as to allow any appreciable extension of the operating envelope of CTOL aircraft into higher sea states. On this basis it was concluded that there is a well-defined safe sea state for the operation of CTOL aircraft from CVF, that is inherently lower than for STOVL and Rotary Wing aircraft.

With STOVL and Rotary Wing aircraft, the constraints on acceptable ship motions are inherently less onerous. Accordingly, broader factors will tend to represent more of a limiting factor in the operability of these aircraft types in higher sea states, specifically the operability of deck edge lifts (where adopted), or maximum safe Wind Over Deck as determined such issues as:-

- The ability of flight deck personnel to stay upright under the combined influences of wind and ship motions;
- The risks to pilots who may need to eject during a failed launch/recovery;
- The risk of damage to aircraft (e.g. damage to opened aircraft canopies);
- For Rotary Wing operations, rotor spread, fold and engage operations.

The guidance of Crossland et al (1998) and STANAG 4154 indicates a safe wind over deck limit of 35 knots. For the typical ocean conditions of STANAG 4194 and zero ship speed, this corresponds to around Upper Sea State 5.

13.3 (c) Validation Results

One key use of the results from the 1/60 scale seakeeping experiments was validation of the computational (strip theory) predictions that underpinned the detailed seakeeping assessment of the design proposal. Parameters compared in this validation work included Response Amplitude Operators (RAOs) (i.e. regular seas predictions), RMS motions amplitudes in irregular seas, zero speed Relative Motions predictions at the deck edge lifts, and natural roll period.

This validation exercise showed that, at least for zero ship speed, experimental predictions of Relative Motion at the deck edge lift locations were significantly (i.e. up to 50%) greater than those predicted by strip theory. Given the potential implications for lift operability in a seaway, a more thorough assessment of deck edge lift wetness was planned for subsequent phases of seakeeping experiments. Additionally, in accordance with the established limitations of strip theory, roll RAO predictions were somewhat lower than those indicated by the seakeeping experiments. Other than this, the validation work showed a good degree of correlation between the strip theory and experimental seakeeping predictions (i.e. in terms of pitch and heave motion, irregular seas roll, and natural roll period).

13.3 (d) De-Risking of the Above Water Form

Another key aspect of the 1/60 scale seakeeping experiments was the de-risking of the seakeeping characteristics of the proposed 'highly flared' above water form. These de-risking tests were conducted both for a representative normal operating sea state and for a representative extreme sea state (i.e. Sea State 9), and considered both head seas at zero and forward ship speed and beam seas at zero ship speed. The results indicated that, provided the lowest knuckle of the highly flared form is sited well above (i.e. around 3.0m above) the deepest operating draught of the vessel and a flare angle of no more than 35° is adopted, as was the case with the design proposal, the potential risks associated with immersion of the flare should be avoided. The latter risks were considered to be excessive motions, sudden accelerations/decelerations and parametric roll.

These findings went a considerable way to alleviating concerns associated the seakeeping implications of the highly flared style of above water form, pending more detailed de-risking proposed for subsequent stages of testing (e.g. oblique seas tests and measurement of hydrodynamic loading on specific areas of the highly flared form).

13.3 (e) Parametric Roll

As part of the 1/60 scale experimental tests to de-risk the above water form, head seas tests were conducted to assess the occurrence of parametric roll in head seas. This work concluded that, provided that the flare is initiated sufficiently high above the deepest operating waterline (i.e. in line with the design proposal), the occurrence and severity of parametric roll for the 'highly flared' form was likely to be no worse for than for an equivalent traditional (i.e. sponson) style of above water form. Nonetheless, the tests provided an apt demonstration of the consequences of parametric roll occurring on a large aircraft carrier and so are worthy of description here.

Firstly, it should be noted that, at least for the long-crested head seas case tested, parametric roll is an instability-related phenomena triggered by slight disturbances - for example small angles of yaw, list or roll. As such it is not detected by off-the-shelf computational (e.g. strip theory-based) seakeeping assessment software. Given the presence of such disturbances, a succession of waves of exactly the right encounter period (i.e. half the natural roll period of the ship) can cause a resonant roll motion to develop. For the head seas case tested, the results indicated that large angles of resonant roll motion of between ±10° and ±15° could develop. The effects of this are exacerbated by the very short period of motion (i.e. half the natural roll period of the ship), which would result in high levels of deck velocity and acceleration. Clearly this would preclude safe aircraft launch/recovery and would place any unlashed aircraft and ground support equipment on the flight deck (or in the hangar) in jeopardy, while additionally placing personnel at risk.

In mitigation, the probability of a succession of waves of exactly the right frequency being encountered is small, and the resonant motion will take a period of time to develop. Moreover, the occurrence of parametric roll is sensitive to encounter frequency, and so simply adjusting ship speed by a knot or two will tend to cause the motion to subside.

Nonetheless, parametric roll represents a phenomena that can occur on a range of headings (i.e. head, following or oblique seas) and can place personnel, support equipment and aircraft at risk, and so is worthy of note.

13.4 MANOEUVRING ASSESSMENT

During early CVF design studies, which assumed a conventional shaftline arrangements, and where the scope of the analysis was more limited, manoeuvring

performance was assessed using a commercially-available manoeuvring simulation software package based upon empirical data. This allowed evaluation of manoeuvring performance in a range of standard IMO-type manoeuvres (e.g. Turning Circle, Zig-Zag and acceleration/stopping manoeuvres).

As design work progressed, a hybrid shaftline arrangement was substituted for the more conventional arrangement, employing an azimuthing podded propulsor (Figure 6). The latter effect could not be reliably modelled using readily available commercial packages. Moreover, with progress towards increasing design maturity, there was a pressing need to model manoeuvres and phenomena of specific importance to aircraft carrier operations, but which are not typically provided for in commercial software. These carrier operations specifically need to address heel-in-turn characteristics, the effects of applying power in the turn, and Deck Alert 'turn-and-accelerate' type manoeuvres.

Accordingly later phases of manoeuvring assessment were sub-contracted to MARIN, who undertook bespoke simulation of manoeuvring performance based on empirical data for vessels of similar size, windage and hydrodynamic characteristics to CVF. This specialist simulation work considered a range of IMO-type and Deck Alert-type manoeuvres, for a range of wind speeds, helm angles and ship speeds. In addition, the work package included limited validation against historical data, expert review of the rudder/skeg arrangement, and independent (empirically-based) evaluation of lateral wind and current forces to support confirmation of the proposed bow thruster fit. The work was conducted in two phases, the first phase evaluated an early shaftline concept based around twin podded propulsors and a single conventional shaftline. The second phase investigated the final hybrid shaftline proposal shown in Figure 6. In both instances equivalent ship designs employing a twin conventional shaftline arrangement (without pods) were also evaluated, to provide a benchmark against which the likely manoeuvring benefits/drawbacks of the hybrid shaftline arrangements could be assessed.

This manoeuvring simulation work required a number of key supporting assumptions to be made regarding the characteristics of the ship's IFEP power system, steering gear and propulsion train. The required assumptions included assumed rudder/pod azimuth rates, shaftline torque limitations, control of power during crash-stop and acceleration manoeuvres, and whether dynamic braking resistors should be fitted to assist in decelerating the vessel.

A key benefit of basing the manoeuvring assessment on computational simulation was that it allowed rapid evaluation of a wide range of scenarios and comparison of alternative shaftline configurations at significantly lower cost than would have been possible through tank testing. It also generated detailed histories of manoeuvring parameters during the turn (e.g. position, yaw rate, turning-induced heel) for use in future studies, and quality computer animations of the results (Figure 14), which proved a useful means of interpreting and disseminating the results. In terms of drawbacks, the simulations were limited in that they took no account of wave action, and were based on empirically-derived windage/hydrodynamic coefficients, rather than design-specific data. As the latter issue clearly places limits on the degree of confidence that can be placed in the predictions, follow-up phases of hydrodynamic experiments were scheduled to include:

- Captive manoeuvring experiments and wind tunnel tests to generate hydrodynamic and windage coefficients for use in place of empirical data in future manoeuvring simulations;
- Self-propulsion manoeuvring experiments for a limited range of key manoeuvring scenarios, to validate overall manoeuvring characteristics predicted by the simulations, and assess the effect of ocean waves on manoeuvring performance;
- Assessment of lateral current forces and moments on the hull;
- Wind tunnel tests to confirm air wake characteristics.

Relevant findings from the manoeuvring simulation work are included in the discussion of shaftline arrangement in Section 8.1.

13.5 EVALUATION OF ROLL RADIUS OF GYRATION

Roll radius of gyration represents a key parameter determining the natural roll period of the vessel, and by virtue of this, the upper bound limit on an acceptable operating metacentric height for an aircraft carrier, such as CVF (see Section 6). Given initial indications that the limits on operating metacentric height for CVF would be particularly onerous, particular importance was therefore attached to establishing a reliable estimate of roll radius of gyration for CVF.

For most ship designs similarities with preceding vessels mean that roll radius of gyration can be estimated with reasonable accuracy, for example from established 'rule of thumb' guidance, such as that presented by Lloyd (1998), the International Society of Allied Weight Engineers (SAWE Recommended Practice No. 14, (2001)) and Cimino & Redmond (1991). For CVF, however, the availability of such type specific ship data is at best limited, particularly once the bespoke nature of the above water form (e.g. the effect of flight deck overhangs) is taken into account, as this tends to distort trends between roll radius of gyration and waterline beam.

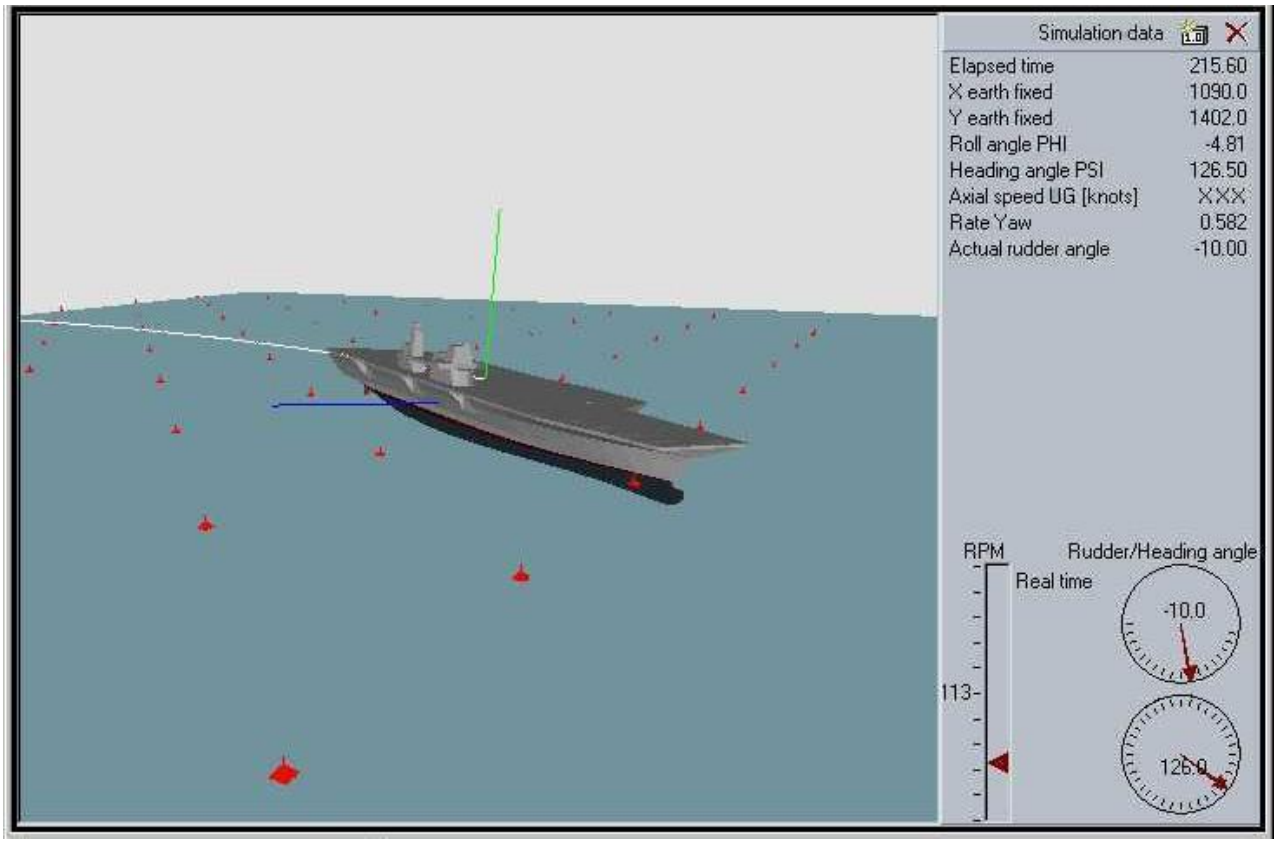

Figure 14: Snapshot from one of the Computer Animations Output from the Manoeuvring Simulation Work (Source: MARIN)

Accordingly, it was considered appropriate to construct a "bottom up" spreadsheet estimate of roll radius of gyration for CVF from weight breakdown data. The procedure adopted was based on that presented in SAWE Recommended Practice No. 14 (2001) and Cimino & Redmond (1991). These split the component moments of inertia down into the 'self-inertia' of each item, about its own centre of gravity, and the 'transference inertia' of each item, due to the separation of its centre of gravity, from that of the whole ship. The level of effort required was greatly reduced by the availability of a NAPA STEEL[9] model of the primary hull structure, which allowed a reliable radius of gyration estimate for the majority of the steel weight to be downloaded and input into the calculation as a single line item.

The calculations indicated a 'dry' radius of gyration value of around 43.0% to 44.5% of waterline beam, depending on loading condition and through-life growth. This is slightly higher than the figure of 40.9% waterline beam quoted by the International Society of Allied Weight Engineers (2001) for a US 'Nimitz' class Carrier employing a more traditional style of above water form. To this 'dry' radius of gyration must be applied a correction to allow for the effects of entrained water. Roll decay tests conducted as part of 1/60 scale seakeeping tests (see Section 13.1) indicated that such entrained water effects could be allowed for by multiplying the 'dry' radius of gyration by a correction factor of around 1.056. This is in close agreement with the generic correction factor of 1.05 presented by Rawson & Tupper (1984).

[9] See: www.napa.fi/Design-Solutions/NAPA-Steel

13.6 PROPULSOR WAKE FIELD SURVEYS

As noted in Section 13.1 (above) the final stage of tank tests for the design proposal included nominal (unpowered) wake surveys at the propeller discs of both the conventional shaftlines and the podded propulsor of the proposed hybrid shaftline arrangement (Figure 6).

These tests were aimed predominantly at providing a library of wake field data (e.g. circumferential wake field variations) to support underwater signatures and noise & vibration studies. However, they also allowed preliminary confirmation of the choice of optimum propeller direction of rotation based on noise and vibration considerations, provided nominal wake figures for use in estimating propulsive efficiency, and also gave an indication of the hull afterbody flow pattern for consideration in further hullform refinement work.

14. CONCLUDING COMMENTS

This paper has provided an overview of hullform and hydrodynamics-related design experience accumulated in the course of BAE SYSTEMS team's design studies for CVF, in terms of:

- Hydrodynamics design requirements;
- Hullform and hydrodynamics-related design options, including some of the more innovative proposals considered;
- The manner in which hydrodynamic performance was evaluated, the balance achieved between computational and experimental approaches, and how the level of performance evaluation has been matched to the level of design maturity;
- Other key hydrodynamic design issues of relevance to CVF.

As stated earlier, CVF is now (2003) being progressed to a different design under a joint UK MoD-Industry Integrated Alliance Team (IAT). Nonetheless, it is hoped that the work presented here serves a useful purpose in highlighting some of the key design issues of importance in aircraft carrier hydrodynamic design, identifying readily available sources of design guidance available to the designer, and highlighting appropriate design methodology and design options.

15. ACKNOWLEDGEMENTS

The work presented in this paper represents the outcome of team effort, and the author is therefore indebted to a number of individuals for their contribution to what is presented.

Firstly, thanks are due to James Swan of BAE SYSTEMS Land & Sea Systems, and Ralph Bonfield and Richard Irvine of VT Shipbuilding, who together undertook the bulk of the detailed studies that underpin the findings presented here. Thanks are also due to representatives from BAE SYSTEMS, VT Group and Rolls Royce - unfortunately too numerous to list here - whose specialist advice provided substance to the work presented, and whose spirit of teamwork and collaboration as part of the BAE SYSTEMS CVF proposal sets an example for others to follow.

Proposals for the 'highly flared' style of above water form are attributable to original concepts by the late Professor Louis Rydill, who also provided a range of other guidance on the BAE SYSTEMS design proposal. Likewise, much of the discussion pertaining to propulsor-induced noise and vibration is attributable to specialist advice received from Dr. Roger Kinns of RKAcoustics.

The work presented draws heavily on hydrodynamic tank testing and supporting specialist advice received from SSPA of Sweden, and specialist manoeuvring simulation work undertaken by MARIN of the Netherlands. In this regard thanks are due to Lennart Byström of SSPA and Frans Quadvlieg and Giedo Loeff of MARIN.

Finally, the author would like to thank the MoD CVF IPT, then under Mr. Ali Baghei, for kind permission to publish this paper and Mr. J. Scott Whiteford, Chief Engineer of the CVF Integrated Alliance Team, for encouragement in publishing this paper and providing guidance on structuring it for publication.

The opinions expressed in this paper are solely those of the author, and do not necessarily represent those of BAE SYSTEMS or its partners.

The author would like to thank Mr Philip Dunne MP (then UK Minister of State for Defence Procurement) and his team at the Ministry of Defence for authorising publication of this paper in June 2016, and Mr Steven Paterson MP, Member of Parliament for Stirling (2015-2017), for assisting on this matter.

16. REFERENCES

1. ABKOWITZ, M.A. *'The Effect of Anti-Pitching Fins on Ship Motions'*, Trans. SNAME, Vol. 69, 1959
2. AUTRET, G., DEYBACH, F. *'Nuclear Aircraft Carrier CHARLES DE GAULLE'*, Paper No. 5, Warship '97 International Symposium on Air Power at Sea, RINA, 1997
3. BAITIS, E., WOOLAVER, D.A., BECK, T.A. *'Rudder Roll Stabilisation for Coast Guard Cutters and Frigates'*, Naval Engineers Journal, ASNE, May 1983
4. BALES, N.K., CIESLOWSKI, D.S. *'A Guide to Generic Seakeeping Performance Assessment'*, Naval Engineers Journal, ASNE, April 1981
5. CIMINO, D., REDMOND, M., *'Naval Ships Weight Moment of Inertia - A Comparative Analysis'*, SAWE Paper No. 2013 (Category No. 13), International Society of Allied Weight Engineers, Los Angeles, USA, May 1991
6. COMSTOCK, E.N., BALES, S.L., GENTILE, D.M. *'Seakeeping Performance Comparison of Air Capable Ships'*, Naval Engineers Journal, April 1982
7. COMSTOCK, E.N., KEANE, R.G. *'Seakeeping by Design'*, Naval Engineers Journal, ASNE, April 1980
8. CONOLLY, J.E., GOODRICH, G.J. *'Sea Trials of Anti-Pitching Fins'*, Trans. RINA, Vol. 112, 1970
9. CROSSLAND, P., et al, *'A Rational Approach To Specifying Seakeeping Performance In The Ship Design Process'*, RINA Warship '98 Conference ('Surface Warships - the Next Generation'), RINA, 1998

10. EDDISON, J.F.P., GROOM, J.P., '*Innovation in the CV(F) - An Aircraft Carrier for the 21st Century*', RINA Warship '97 Conference ('Air Power at Sea'), RINA, 1997
11. FERREIRO, L.D. SMITH, T.C., THOMAS, W.L. MACEDO, R. *'Pitch Stabilisation for Surface Combatants'*, Naval Engineering Journal, Vol. 106, July 1994
12. FRIEDMAN, N. *'British Carrier Aviation – The Evolution of the Ships and their Aircraft'*, pp. 349-355, ISBN 0-85177-488-1, Conway Maritime Press, London, UK, 1988
13. HONNOR, A F, ANDREWS, D J: - *'HMS INVINCIBLE - The First of a New Genus of Aircraft Carrying Ships'*, Trans RINA, Vol 124, 1982.
14. 'IMO Resolution A751(18) - Interim Standards for Ship Manoeuvrability', International Maritime Organisation, November 1993 *(now superseded by IMO Resolution MSC 137(76) (2002))*
15. 'IMO Resolution MSC 137(76) - Standards for Ship Manoeuvrability', International Maritime Organisation, December 2002
16. KÄLLMAN, M., LI, D. *'Waterjet Propulsion Noise'*, RINA Waterjet Propulsion III Conference, Gothenburg, Sweden, 20th-21st February 2001
17. KEHOE, J.W., BROWE, K.S., SERTER, E.H. *'The Deep-Vee Hullform - Improves Seakeeping and Combat System Performance'*, Naval Engineers Journal, ASNE, May 1987
18. KEHOE, J.W., GRAHAM, C., BROWER, K.S., MEIER, H.A. *'Comparative Naval Architecture Analysis of NATO and Soviet Frigates - Part II'*, Naval Engineers Journal, ASNE, December 1980
19. KINNS, R., BLOOR, C.D. *'The effect of shaft rotation direction on cavitation-induced vibration in twin-screw ships'*, Proceedings of NCT'50, Newcastle-upon-Tyne, 3rd-5th April 2000
20. KISS, T.K., *'The Effects of Transom Beam on the Seakeeping Qualities of Large Surface Ships'*, Naval Engineers Journal, ASNE, November 1990
21. KUMMER, S., HARDIER, G., LAMBERT, C. *'Heel Compensation for the CHARLES DE GAULLE Aircraft Carrier: Principles and Control Structure'*, Paper no. 14 (RTO MP-15), NATO RTO/AVT Symposium on Fluid Dynamic Problems of Vehicles Operating Near or In the Air-Sea Interface, Amsterdam, 5th-8th October 1998
22. LEWIS, E.V. (Editor) *'Principles of Naval Architecture'*, Vol. III, Second Revision, SNAME, 1989
23. LLOYD, A.R.J.M. *'Seakeeping: Ship Behaviour In Rough Weather'*, Revised Edition, Published by the Author, 1998
24. OCHI, K.M. *'Hydroelastic Study of a Ship Fitted with an Anti-Pitching Fin'*, Trans. SNAME, Vol. 69, 1961
25. PATTISON, J.H., BUSHWAY, R.R. *'Deck Motion Criteria For Carrier Aircraft Operations'*, NATO AGARD Conference Proceedings 509, November 1991
26. RAWSON, K.J., TUPPER, E.C. *'Basic Ship Theory'*, Vol. 2, Third Edition, Longman Scientific & Technical, 1984
27. RICKETTS, R.V., GALE, P.A. *'On Motions, Wetness, and Such: The USS MIDWAY Blister Story'*, SNAME Transactions, Vol. 97, 1989
28. PURVIS, M.K. *'Post War RN Frigate and Guided Missile Destroyer Design 1944-1969'*, Trans RINA, 1974
29. SAUNDERS, H.E *'Hydrodynamics in Ship Design'*, Vols. I-III, SNAME, 1957
30. *'SAWE Recommended Practice No. 14 - 'Weight Estimating and Margin Manual for Marine Vehicles'*, International Society of Allied Weight Engineers (SAWE), Los Angeles, USA, 22nd May 2001
31. SCHNEEKLUTH, H., BERTRAM, V. *'Ship Design for Efficiency & Economy'*, 2nd Edition, Butterworth Heinemann, 1998
32. SIMS, P. *'Bulging Warships'*, Naval Engineers Journal, November 1989
33. SMITKE, R.T., GLEN, I.F., MURDEY, D.C. *'Development of a Frigate Hullform for Superior Seakeeping'*, Eastern Canadian Section, SNAME, April 1979
34. *'STANAG 4154 - Common Procedures for Seakeeping in the Ship Design Process'*, Edition 3, NATO, 2000 *(see also Crossland et al (1998), which provides an overview of this standard)*
35. *'STANAG 4194 - Standardized Wave and Wind Environments, and Shipboard Reporting of Sea Conditions'*, Edition 1 (Including Amendments 1-5), NATO, April 1983
36. Warship Technology, *'Podded Propulsors: A Viable Option for Future Warships'*, p.21, January 2003
37. WALDEN, D.A., GRUNDMANN, P. *'Methods for Designing Hullforms with Reduced Motions and Dry Decks'*, Naval Engineers Journal, ASNE, May 1985
38. WATSON, D.G.M *'Practical Ship Design'*, Elsevier Publishing, 1998
39. www.napa.fi/Design-Solutions/NAPA-Steel (Accessed 8th April 2017)
40. www.sawe.org (Accessed 8th April 2017)
41. www.schottel.de/marine-propulsion/spj-pump-jet (Accessed 8th April 2017)

NON-DIMENSIONALISATION OF LATERAL DISTANCES BETWEEN VESSELS OF DISSIMILAR SIZES FOR INTERACTION EFFECT STUDIES

(DOI No: 10.3940/rina.ijme.2017.a4.429)

N Jayarathne, **D Ranmuthugala**, **Z Leong** and **J Fei**, Australian Maritime College, University of Tasmania, Australia

SUMMARY

To date, most of the hydrodynamic interaction studies between a tug and a ship during ship assist manoeuvers have been carried out using model scale investigations. It is however difficult to establish how well results from these studies represent full scale interaction behaviour. This is further exacerbated by the lack of proven methodologies to non-dimensionalise the relative distances between the two vessels, enabling the comparison of model and full scale interaction effect data, as well as between vessels of dissimilar size ratios. This study investigates a suitable correlation technique to non-dimensionalise the lateral distance between vessels of dissimilar sizes, and a scaling option for interaction effect studies. It focuses on the interaction effects on a tug operating around the forward shoulder of a tanker at different lateral distances during ship assist operations. The findings and the non-dimensioning method presented in this paper enable the interaction effects determined for a given ship-to-tug ratio to be used to predict the safe operational distances for other ship-to-tug ratios.

NOMENCLATURE

BR	Breadth Ratio, $BR = B_S/B_t$
B_s	Breadth of the tanker (m)
B_t	Breadth of the tug (m)
C_N	Yaw moment coefficient
C_X	Surge force coefficient
C_Y	Sway force coefficient
DR	Displacement Ratio, $(\nabla_s / \nabla_t)^{1/3}$
F_r	Length Froude Number, $F_r = u/\sqrt{g\ L_{WL}}$
g	Acceleration due to gravity (9.81 m s^{-2})
L_{OA}	Length overall of the tanker/tug (m)
L_s	Length waterline of the tanker (m)
L_t	Length waterline of the tug (m)
N	Yaw moment acting on tug (N m)
R_G	Mesh convergence ratio
T	Draft of the tanker/tug (m)
u	Fluid flow velocity (m s^{-1})
X	Surge force acting on tug (N)
Y	Sway force acting on tug (N)
y^+	Non-dimensional wall distance of first inflation layer
ΔX	Non-dimensionalised longitudinal-distance between vessels
δx	Longitudinal distance between vessels (m)
ΔY	Non-dimensionalised lateral distance between vessels
δy_{cl}	Lateral distance between vessels' centrelines (m)
δy_m	Lateral distance between vessels' midship (m)
ρ	Density of water (kg m^{-3})
∇_s	Volumetric displacement of the tanker (m^3)
∇_t	Volumetric displacement of the tug (m^3)

1. INTRODUCTION

Large ships operating at low speeds generally suffer from limited manoeuvrability, which can lead to dangerous situations in restricted or congested waters. Thus, in such situations, they are usually assisted by attending tugs, which exposes the smaller tugs to dangers such as collision, grounding, girting, and run-overs due to the hydrodynamic interaction effects between the two vessels (Hensen, 2012). The influence of hydrodynamic interaction is prominent when the comparative sizes of the two ships differ significantly, for example, when a tug operates near a large ship such as a large tanker or bulk carrier (Hensen, 2003). Furthermore, the effects of the interaction can change with the hull shapes of the ship and the tug, the width of the navigable channel in the river or harbour, the tug's location relative to the ship, the relative and absolute speeds of the two vessels, and the drift angle between them (Hensen, 2012).

When a ship is moving forward in calm water, it generates a pressure field around the hull. This results in a higher pressure around the bow region due to the retarded flow around the stagnation region in that area. The pressure reduces significantly around the mid-body section as the flow accelerates, which is followed by partial pressure recovery around the stern region. In the latter region, the adverse pressure gradient causes flow separation that results in a wake region around the stern and immediately aft of the hull. When vessels are operating in proximity to each other, the flow between the adjacent hulls can accelerate due to the limited space between them. This causes a low pressure region between the hulls (relative to the rest of the pressure field around the vessels) resulting in an attraction force between them, which in the case of a smaller tug can result in the tug colliding with, or being run over by, the larger ship. Conversely in the higher pressure regions such as the bow region of the ship, the smaller tug will experience a strong repulsive force that can adversely affect the tug's motion and orientation. Therefore, it is clear that the pressure field of the larger ship has a significant influence on the smaller ship when operating in close quarters, which needs to be investigated in order to

provide operators with information to avoid dangerous situations during ship assist operations.

To date, most of the interaction studies between vessels have been carried out for similar sized vessels (Chen & Fang, 2001, Falter, 2010, Fortson, 1974, Lataire et al., 2012, Lu et al., 2009, Newton, 1960, Pinkster & Bhawsinka, 2013, Tuck & Newman, 1974, Zou & Larsson, 2013), with only a small number targeting dissimilar sized vessels operating in close proximity (Dand, 1975, Fonfach *et al.*, 2011, Geerts *et al.*, 2011, Simonsen *et al.*, 2011, Vantorre *et al.*, 2002). Among them Dand (1975) conducted the pioneering Experimental Fluid Dynamics (EFD) based model scale study to investigate the dangers tug operators faced due to interaction effects while working in close proximity to large ships. The study used two different ship models and a single screw tug model at two different lateral distances between the ship and the tug. Dand (1975) concluded that if a tug can operate near the midship region of a larger ship, it experiences minimal interaction effects induced by the latter. Although his model scale findings provide tug operators with safe locations relative to the ship during ship assist manoeuvres, it is prudent to correlate it to full-scale scenarios and broaden the investigation to include various tug manoeuvres that occur during ship assist operations.

Vantorre *et al.* (2002) conducted model scale experiments to determine ship interaction effects for head-on and overtaking encounters of similar and dissimilar size ships and used the results to create a mathematical model to improve the realism of the interaction effects modelled within ship manoeuvring simulators. However, their model was unable to accurately represent the interaction effects generated between vessels of significant size difference, such as between a ship and a tug. Geerts *et al.* (2011) assessed the hydrodynamic interaction forces acting on a tug sailing freely in the vicinity of the bow of a larger ship through a series of model tests. The results were incorporated into a simulation program to assess the steering action of the tug required to counteract the ship's hydrodynamic effects in order to keep station relative to the ship. The authors do not provide any explanation on the extrapolation methodology employed to correlate the model scale results to full-scale vessel operations in order to represent actual ship-tug interaction manoeuvres. Simonsen *et al.* (2011) carried out a Computational Fluid Dynamics (CFD) study validated through model scale experiments to investigate quasi-steady interaction effects on a tug located at a number of positions parallel to a large tanker. Although they concluded that Reynolds Averaged Navier Stokes (RANS) based CFD simulations offer a promising tool for ship interaction studies, no information on the scaling effects on the interaction between the vessels were presented.

Among the literature available in the public domain, the study by Fonfach *et al.* (2011) is a notable contribution utilising full-scale CFD simulations to predict tug interaction effects. They used Froude scaling to compare full-scale CFD interaction effect coefficients with model scale EFD interaction effect coefficients for a tug located at various stations alongside a larger ship, with both vessels travelling at the same speed on parallel courses. The results revealed a relatively weak influence of viscosity on the interaction effects. Nevertheless, they expect the viscosity effects to be more pronounced in non-parallel operations, and when the tug is located within the ship's wake. They observed large discrepancies between their CFD and EFD results at small lateral clearances, especially for the sway force, although the cause of the discrepancies was not discussed. These discrepancies were possibly due to the lack of a comprehensive mesh independence study and the lack of a proven correlation technique to non-dimensionalise the vessel locations for comparison and scaling. The authors give no information on how the scaling issues between the model scale EFD and the full scale CFD were reconciled, which may have contributed to the differences between their results.

Most research studies available in the public domain (Dand, 1975, Fonfach *et al.*, 2011, Geerts *et al.*, 2011, Simonsen *et al.*, 2011, Vantorre *et al.*, 2002) do not explicitly describe or evoke a method to compare the interaction behaviour between a tug and a ship for different scales (for example to compare model scale results with full scale operations). With the exception of Fonfach *et al.* (2011), these studies utilised only model scale EFD investigations or model scale CFD simulations to investigate the interaction effects. Therefore, it is difficult to establish how well these model scale results represent full-scale interaction behaviours. This is further exacerbated by the lack of proven methodologies that can scale the relative model scale distances between the two vessels to full scale.

The work presented in this paper outlines an approach to non-dimensionalise lateral distances between vessels of dissimilar sizes to predict the interaction effects acting on a tug operating near large ships of different sizes or to correlate model scale and full scale interaction effects. It involves verification of the non-dimensionalising approaches for the lateral distances between vessels of different sizes and ratios. Previous work by the authors (Jayarathne *et al.*, 2014) compared different numerical approaches (RANS based CFD vs Potential Flow) against experimental measurements to identify an accurate method to model the interaction effects between a tug and a ship. It was found that the CFD was the most accurate simulation technique to analyse non-streamlined bodies, although modelling and solution times can be significantly higher. This led to all future work being conducted with RANS based CFD, using StarCCM+®. CFD models were verified and validated at model scale using experimental measurements. Throughout the

analysis the tug was maintained within the forward shoulder of the ships, which according to Dand (1975) is the most hazardous region for a tug to operate. The findings enable tug operators to familiarise themselves with the relationship between the hydrodynamic interaction effects and the lateral distances between dissimilar sized vessels.

2. CASE STUDY

Figure 1 shows the four cases including the model scale investigations used in this study to identify a suitable approach to non-dimensionalise the lateral distances between two vessels of dissimilar size. The dimensions of the smaller vessel geometry, i.e. the stern drive tug, was kept fixed, while the larger ship geometry, i.e. the MARAD-F series tanker, was scaled to obtain the different breadth ratios (*BR*), defined as the tanker breadth (B_s) to the tug breadth (B_t) as shown in eqn. 1.

$$BR = \frac{B_S}{B_t} \tag{1}$$

Full scale CFD simulations were carried out for all the breadth ratios, while model scale CFD simulations were carried at a breadth ration of 1.14 to enable validation against experimental data. The tanker and tug particulars for the different scales and breath ratios are outlined in Table 1. These breadth ratios were selected based on the most common dimensions of the small to medium size ships and tugs currently operational in international waters (Artyszuk, 2013).

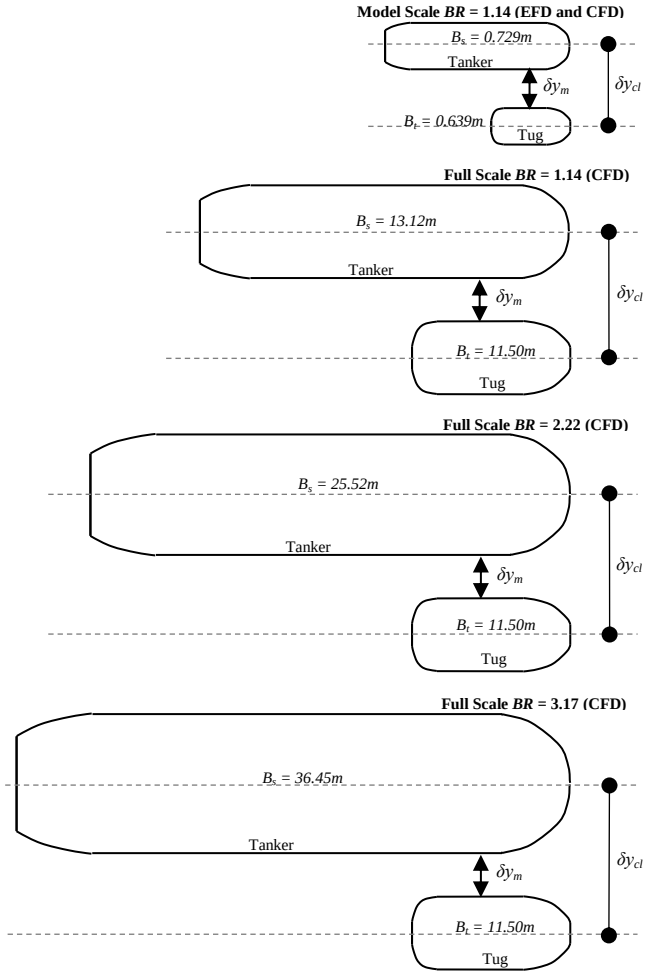

Figure 1: Different Ship Breadth Ratios (*BR*) investigated within the study showing the distance between ships' centrelines (δy_{cl}) and the distance between ships' midship (δy_m). *Not to scale.*

Table 1. Principal particulars of the selected hull forms.

Scale type		Model Scale		Full Scale		Full Scale		Full Scale	
Breadth Ratio (*BR*)		1.14		1.14		2.22		3.17	
Displacement Ratio (*DR*)		1.12		2.42		4.70		6.72	
Analysis type		EFD and CFD		CFD		CFD		CFD	
Main Particulars	Unit	Tanker	Tug	Tanker	Tug	Tanker	Tug	Tanker	Tug
Length Overall (L_{OA})	m	4.200	1.732	75.60	31.16	147.00	31.16	210.00	31.16
Length Waterline (L_s *or* L_t)	m	4.000	1.581	72.00	28.46	140.00	28.46	200.00	28.46
Breadth (B_s *or* B_t)	m	0.729	0.639	13.12	11.50	25.52	11.50	36.45	11.50
Draft (*T*)	m	0.246	0.197	4.42	4.50	8.61	4.50	12.30	4.50
Scale	-	1	1	18	18	35	18	50	18
Froude number (Length) $u/(\sqrt{gL_{wl}})$	-	0.065	0.104	0.065	0.104	0.047	0.104	0.039	0.104
Froude number (Depth) $u/(\sqrt{gD})$	-	0.146		0.146		0.146		0.146	
Speed (u)	m/s	0.41		1.74		1.74		1.74	

Figure 2 shows the local (tug) and global coordinate systems used for the spatial, force, and moment references. Throughout the analysis the tug was located on the port side of the tanker. The approaches used to non-dimensionalise the lateral distance and that for the longitudinal distances are given in eqns. 2, 3, and 4 respectively.

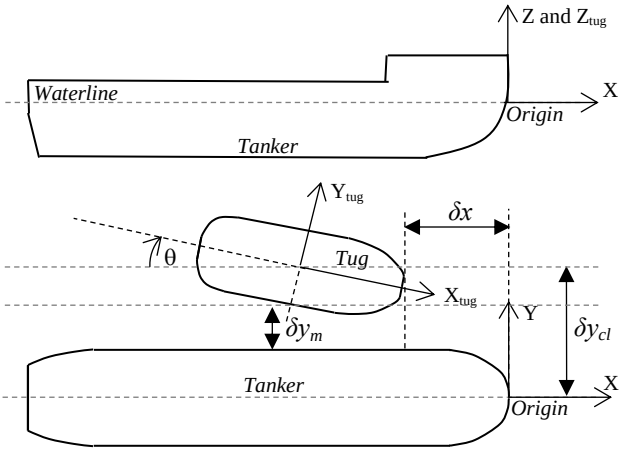

Figure 2: Local (tug) and global coordinate systems and vessel locations.

$$\Delta Y_{ship} = \frac{\delta y_{cl}}{B_s} \quad (2)$$

$$\Delta Y_{tug} = \frac{\delta y_{cl}}{B_t} \quad (3)$$

$$\Delta X = \frac{2\delta x}{L_s} \quad (4)$$

The ratio ΔY_{ship} is the non-dimensionalised lateral distance between the vessels calculated as a ratio of the tanker breadth (i.e. large ship breadth). ΔY_{tug} is the same however, calculated as a ratio of the tug breadth. ΔX is the non-dimensionalised longitudinal distance between two ship bows.

The tug was located at the forward shoulder of the tanker throughout the analysis, maintaining $\delta x = 0$, and therefore the non-dimensionalised longitudinal distance was zero, i.e. $\Delta X = 0$. The tug drift angle (θ) was maintained as zero degrees throughout the analysis representing parallel vessel operations.

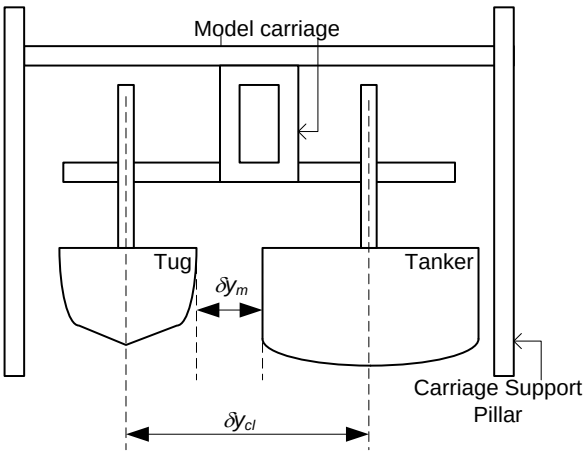

Figure 3: Schematic of the experimental setup in AMC's Model Test Basin.

As seen in Figure 3, due to the limited distance between the carriage support pillars in the experiment, only two cases representing different lateral distances between the midship of hull models (δy_{m_1} and δy_{m_2}) of 0.913m and 0.975m were used in the study. For each of the above cases, the lateral distances between ship centrelines (δy_{cl}) were measured as δy_{cl_1}= 1.597m and δy_{cl_2}= 1.659m respectively.

Table 2. Lateral distances between vessel centrelines (δy_{cl}).

Lateral distances between vessel centrelines (δy_{cl}) calculated based on;		Model Scale *BR* = 1.14	Full Scale *BR* = 1.14	Full Scale *BR* = 2.22	Full Scale *BR* = 3.17
		δy_{cl} (m)	δy_{cl} (m)	δy_{cl} (m)	δy_{cl} (m)
		EFD and CFD	CFD	CFD	CFD
1	δy_{m_1} = 0.913m	1.597	13.22	19.42	24.89
2	ΔY_{ship_1} = 2.190	1.597	28.75	55.89	79.85
3	ΔY_{tug_1} = 2.499	1.597	28.74	28.74	28.74
4	δy_{m_2}= 0.975m	1.659	13.27	19.48	24.95
5	ΔY_{ship_2}= 2.276	1.659	29.86	58.06	82.95
6	ΔY_{tug_2}= 2.596	1.659	29.86	29.86	29.86

The first of the approaches to represent lateral distance between ship and tug used the absolute distance between the two hulls (δy_m) that was maintained as per the experimental distances at δy_{m_1}= 0.913m and δy_{m_2}= 0.975m. This enabled a comparison between the approaches using the absolute distance and the two non-dimensional distances given in eqns. 2 and 3. For the second approach, the lateral distance between the vessel centrelines (δy_{cl}) was calculated by eqn. 2 using the same non-dimensionalised distance (ΔY_{ship}), which was determined from the model scale vessel dimensions and set-up. The last approach was similar, except for the use of eqn. 3 for non-dimensioning the lateral distances. A summary of the distances calculated for the three approaches is given in Table 2.

The surge force (X), sway force (Y), and yaw moment (N) acting on the tug for different cases were measured and non-dimensionalised using volumetric displacements according to eqns. 5 to 7 (Fonfach *et al.*, 2011, Simonsen *et al.*, 2011) respectively.

$$C_X = \frac{2X}{u^2 \nabla_t^{1/3} \nabla_s^{1/3} \rho} \tag{5}$$

$$C_Y = \frac{2Y}{u^2 \nabla_t^{1/3} \nabla_s^{1/3} \rho} \tag{6}$$

$$C_N = \frac{2N}{u^2 \nabla_t^{1/3} \nabla_s^{1/3} L_t \rho} \tag{7}$$

where;

C_N	Yaw moment coefficient
C_X	Surge force coefficient
C_Y	Sway force coefficient
L_t	Length waterline of the tug (m)
u	Fluid flow velocity (m s^{-1})
ρ	Density of water (kg m^{-3})
∇_s	Volumetric displacement of the tanker (m^3)
∇_t	Volumetric displacement of the tug (m^3)

3. CFD SETUP

The commercial CFD code, Star-CCM+® was used to investigate the test scenarios outlined in Table 2 via Reynolds Averaged Navier-Stokes (RANS)-based simulations. Model scale CFD simulations replicated the experimental captive model test conditions to enable the validation of the CFD models. The validated model was then scaled up to full scale using Froude scaling technique to create the full scale CFD simulation domains (see Figure 4). Local mesh refinements were carried out to maintain the y^+ value and to improve the quality and the stability of the simulations. Both the tanker and tug geometries were fixed within the domain, i.e. with zero degrees of freedom.

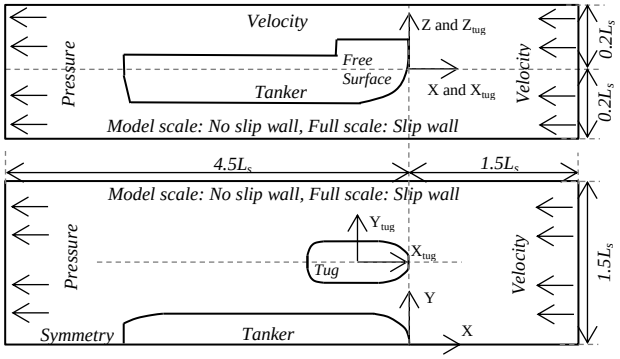

Figure 4: Computational domain used in Star-CCM+® simulations.

The upstream end and top boundaries of the domain were kept as inlet boundaries, while the downstream end was maintained as a pressure outlet. The velocity inlet at the top boundary was used in preference to a slip wall boundary to reduce the simulation convergence time without affecting the accuracy of results (CD-Adapco, 2015). A symmetry boundary along the longitudinal mid-plane of the tanker, as used by Fonfach (2010), was employed in this study to significantly reduce the computational effort by reducing the size of the mesh domain. As the domain is not symmetric about the x-y plane due to the placement of the tug on the Port bow of the tanker, it was required to verify that the use of a symmetry plane resulted in minimum errors on the forces and moments calculated. This was carried out by comparing the results between a domain utilising the symmetry plane geometry as shown in Figure 4 against a compatible full domain simulation. The maximum difference between the forces and moments obtained for the two simulation domains were within 0.5% of each other and were thus deemed negligible for the current study. The free surface in the CFD simulation was modelled as an Euler Multiphase using the volume of fluid (VOF) technique. The turbulence was modelled with a Shear Stress Transport (SST) turbulence model, which enabled the closure of the RANS equations.

4. EFD SETUP

Experimental captive model testing was conducted in the AMC's 35m (length) x 12m (width) x 1.0m (depth) Model Test basin to validate the CFD model. It was equipped with a multi model carriage mechanism (Figure 5). Tanker and tug models of 1:18 scale were attached to the carriage by keeping them fixed in all degrees of freedom and without allowing relative motion at their fully loaded drafts. The tug model was connected using two strain gauges to measure the surge and sway forces and to calculate the yaw moment. The tanker model was attached to the carriage without strain gauges, since this study focused on the interaction effects on the smaller tug hull due to the relative size difference in typical tug assist operations. Experimental uncertainty limits were calculated in accordance with the ITTC (2002) giving 7%, 9.4%, and 7% for the interaction surge force, sway force, and yaw moment respectively (Jayarathne *et al.*, 2017).

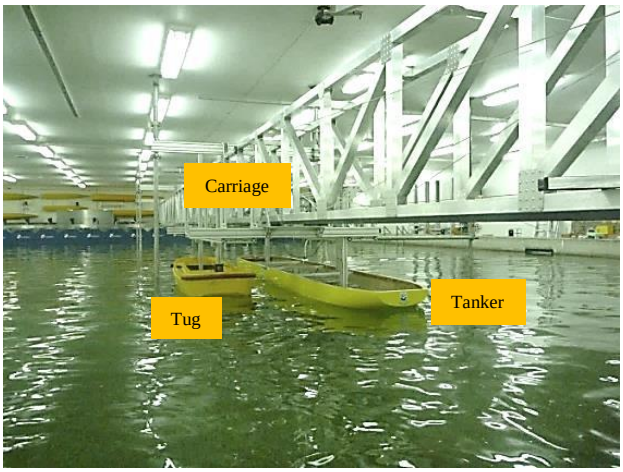

Figure 5: Experimental setup to measure the interaction effects between vessels in AMC's Model Test Basin.

5. CFD VERIFICATION AND VALIDATION

5.1 MESH SENSITIVITY STUDY

A suitable mesh for simulation was identified by evaluating the effects of the mesh resolution. As stated by Fonfach *et al.* (2011), the study carried out by the authors in Jayarathne *et al.* (2017) showed that it is required to resolve the boundary layer in order to accurately model the hydrodynamic interaction effects on a tug that is operating in close proximity to a larger vessel and at an angle of drift to the latter. Therefore, the initial (base) mesh setting had a nominal total inflation layer thickness of two times Prandtl's 1/7th power law turbulent boundary layer thickness estimate ($2x0.16L_t/Re_{Lt}^{1/7}$), while a first layer y^+ of 1 were applied around the vessels. The authors provide more information on these selections and mesh refinement in Jayarathne *et al.*, (2017) and Leong *et al.*, (2014). In order to determine the uncertainty of the mesh resolution selected, mesh sensitivity studies for the model and full scale mesh domains were conducted using the Richardson Extrapolation method (Stern *et al.*, 2001).

The mesh models were generated by Star-CCM+®'s built in mesh generator using an unstructured hexahedral mesh approach. For each model and full scale breadth ratio, three mesh models: fine, medium and coarse were created with an approximate refinement ratio of $\sqrt{2}$ (see Table 3). The relevant mesh refinements were carried out on the vessel surfaces and in the pressure regions around the vessels.

Table 3. Mesh resolution of the simulations used for the sensitivity study (M – Millions).

Mesh (Number)	Fine (1)	Medium (2)	Coarse (3)
Model Scale *BR* = 1.14	7.2M	4.8M	3.5M
Full Scale *BR* = 1.14	12.3M	8.7M	6.0M
Full Scale *BR* = 2.22	13.2M	9.2M	6.8M
Full Scale *BR* = 3.17	14.6M	10.9M	7.6M

Mesh convergence ratios (R_G, given in eqn. 8) for the surge force, sway force, and yaw moment for all the conditions were within $0<R_G<1$, and thus monotonic convergence was deemed to be achieved (Stern *et al.*, 2001).

$$R_G = \frac{\epsilon_{21}}{\epsilon_{32}} \tag{8}$$

where ϵ_{21} is the change in the results between the fine and medium mesh while ϵ_{32} is the change between the medium and coarse mesh.

Numerical errors for the selected mesh models were calculated in accordance with the procedure described by Stern *et al.* (2001), with errors calculated for the surge and sway forces and the yaw moment presented in Table 4. The error percentage estimates in comparison to the Richardson extrapolated values (Stern *et al.*, 2001) for the fine mesh models were below the experimental uncertainties, thus providing sufficient accuracy for the cases investigated in the current study. As mentioned previously, the y^+ value was maintained below 1, with information on the y^+ study given in Jayarathne *et al.* (2017). The fine mesh models selected for the remainder of this study are shown in Figure 6.

Table 4. Relative error percentage estimates of the surge and sway forces and the yaw moment with respect to the Richardson extrapolated values.

Interaction Effect	Percentages (%) of the relative error estimates								
	Surge Force			Sway Force			Yaw Moment		
Mesh Number	1	2	3	1	2	3	1	2	3
Model scale *BR* = 1.14	0.43	1.44	4.78	1.96	3.89	7.55	1.21	2.53	5.24
Full Scale *BR* = 1.14	0.81	4.99	10.38	5.08	9.83	13.34	2.09	4.51	12.26
Full Scale *BR* = 2.22	0.98	3.25	8.73	5.12	8.41	14.09	5.35	7.88	14.44
Full Scale *BR* = 3.17	0.41	2.10	6.87	2.09	5.99	9.12	3.56	6.64	13.25

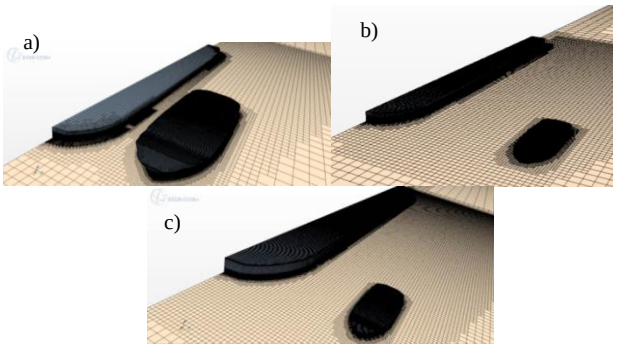

Figure 6: Selected mesh models a) Full Scale *BR* = 1.14, b) Full Scale *BR* = 2.22, Full Scale *BR* = 3.17.

5.2 CFD VALIDATION AGAINST EFD MEASUREMENTS

Figure 7 shows the comparison of model scale EFD, model scale CFD, and full scale CFD interaction effects on a tug for *BR* = 1.14 at two non-dimensioned lateral distances, i.e. ΔY_{ship}= 2.190 and ΔY_{ship}= 2.276. It compares the CFD predicted interaction surge and sway forces and yaw moment acting on the tug at different lateral distances against the EFD measurements.

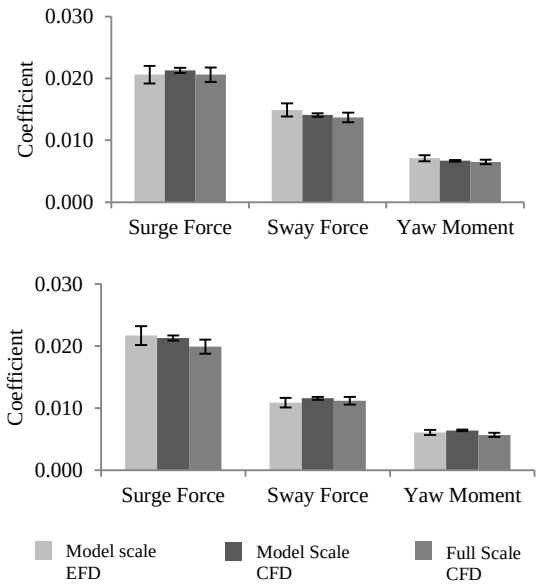

Figure 7: Interaction effect coefficients obtained through model scale EFD, model scale CFD and full scale CFD for the tug for *BR* = 1.14, a) ΔY_{ship} = 2.190 and b) ΔY_{ship} = 2.276. Error bars represent the respective CFD and EFD uncertainties.

The model scale CFD and model scale EFD results are in good agreement, with the difference being less than the experimental uncertainty, i.e. 7%, 9.4%, and 7% for the surge force, sway force, and yaw moment respectively. The model scale and full-scale predictions were in good agreement (within 8%) thus providing confidence for the CFD model to be extended to full scale conditions. However, it is important to note that the agreement between these results was not validated using full scale experimental results. This was due to the absence of such data or studies conducted to investigate full scale interaction effects.

6. RESULTS DISCUSSION

This section discusses the surge and sway forces and yaw moment coefficients on the tug when positioned alongside three different tankers at different lateral distances, as explained in Section 2. It compares the methods used to scale lateral distances between vessels of dissimilar sizes. This is followed by the characterisations of the flow field around the vessels using pressure visualisation.

6.1 COMPARISON OF METHODS USED TO CALCULATE LATERAL DISTANCES

Figure 8 illustrates the interaction effect coefficients (eqns. 5 to 7) of the tug. These were determined through different lateral distance calculation methods (δy_m, ΔY_{ship} and ΔY_{tug}, i.e. the absolute distance and the non-dimensional distances given in eqns. 2 and 3) with the different full scale breadth ratios (i.e. *BR* = 1.14, 2.22, 3.17) investigated in this study. Two lateral distances are presented for each of the methods to verify the behaviour on the interaction effects between different sized vessels.

When using absolute lateral distance (δy_m) to represent the distance between vessels, the forces and moment coefficients changed substantially with changing breath ratios (Figure 8). As seen in the figure, the sway force showed a significant decline in contrast to the yaw moment, which showed a rapid increase with the increasing breadth ratio. The discrepancies of the results between the breadth ratios were 268%, 44%, and 13% for the yaw moment, sway force, and surge force coefficients respectively. These discrepancies were far beyond the experimental and numerical uncertainties, and thus using the absolute distance is unsuitable for scaling and comparing the hydrodynamic interaction effects between vessels of different sizes. This would be expected, as the absolute distance disregards the size of the vessels.

Next consider the results using the non-dimensionalised lateral distance based on the tug breadth, i.e. ΔY_{tug}. At a $\Delta Y_{tug_1}$of 2.499, the discrepancies were up to 9%, 41%, and, 11% for surge force, sway force and yaw moment coefficients respectively between the three breadth ratios. At ΔY_{tug_2}= 2.596, the discrepancies were also found to be substantial with 23%, 35%, and, 2% differences for surge force, sway force and yaw moment respectively between the breadth ratios. As seen in Figure 8, except for the sway force at $\Delta Y_{tug_2}$and yaw moment at ΔY_{tug_1}, the rest of the cases showed that the maximum discrepancies were at the breadth ratio of 3.17. Although it is hard to define

an exact pattern in the results, it is apparent that the discrepancies were mainly affected by the increase in the breadth ratio. Thus, the non-dimensionalising method using the ΔY_{tug} is also unsuitable as the discrepancies in the results is not consistent between the two lateral distances and still exceeds EFD and CFD uncertainties. The weakness of the ΔY_{tug} approach is that it uses only the tug's breadth (B_t) to non-dimensionalise the lateral distance, thus neglecting dimensions of the larger ship. Thus, a scaling that solely uses the tug's breadth is deemed insufficient to represent the required lateral distances for the tug to experience similar interaction effects when operating in close proximity to ships of different sizes.

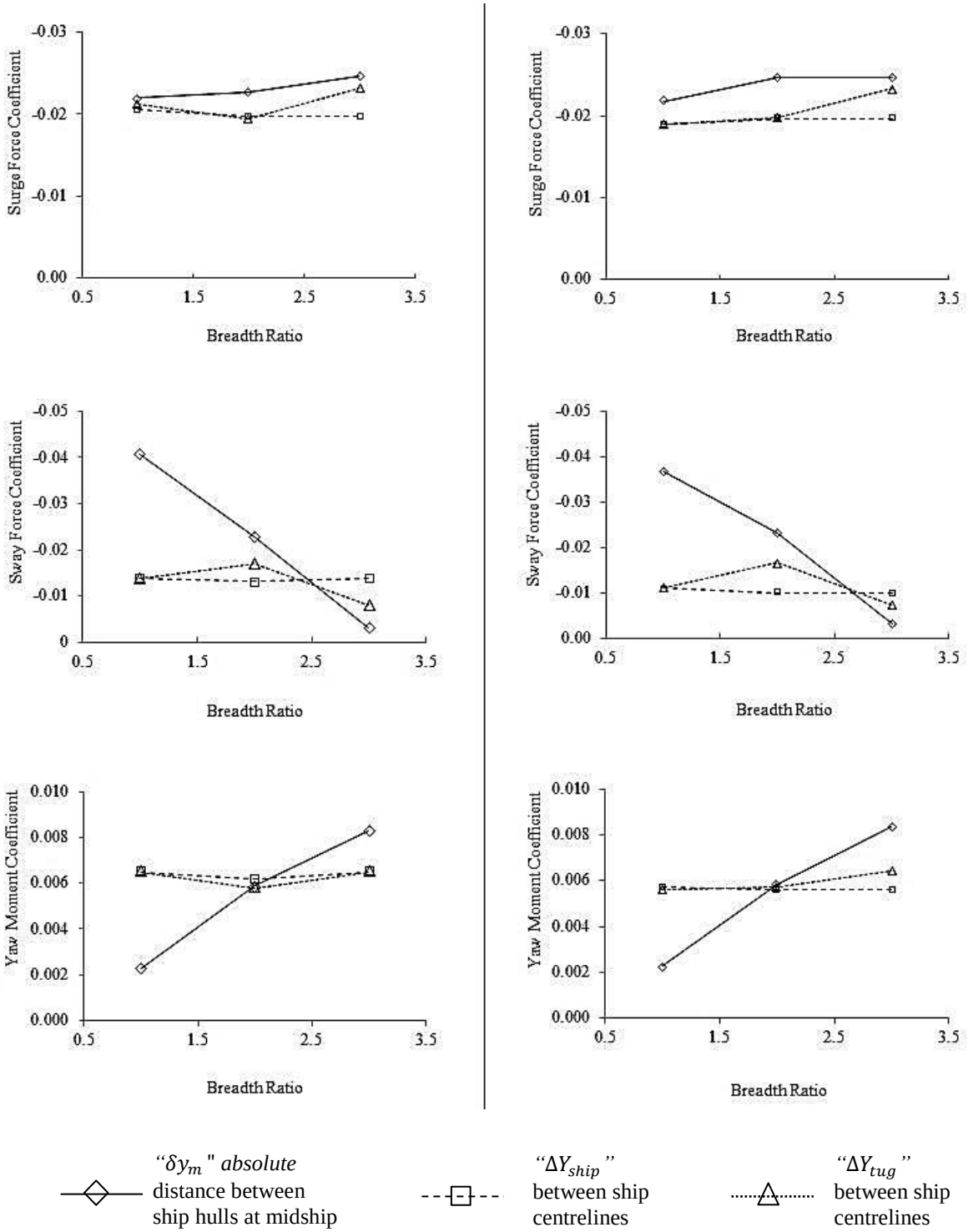

Figure 8: Surge force, sway force, and yaw moment coefficients of the tug determined for different δy_m, ΔY_{ship} and ΔY_{tug} for three full scale breadth ratios; *BR* = 1.14, 2.22, 3.17

As illustrated in Figure 8, the results determined using the ship's breadth to non-dimensionalise the lateral distance, i.e. ΔY_{ship}, showed good agreement in the interaction effects predicted for the three breadth ratios. The maximum discrepancies between the coefficients calculated were found to be 4%, 4%, and, 5% for surge force, sway force and yaw moment respectively for a ΔY_{ship_1} of 2.190 and up to 4%, 9% and 2% for a ΔY_{ship_2} of 2.276 respectively.

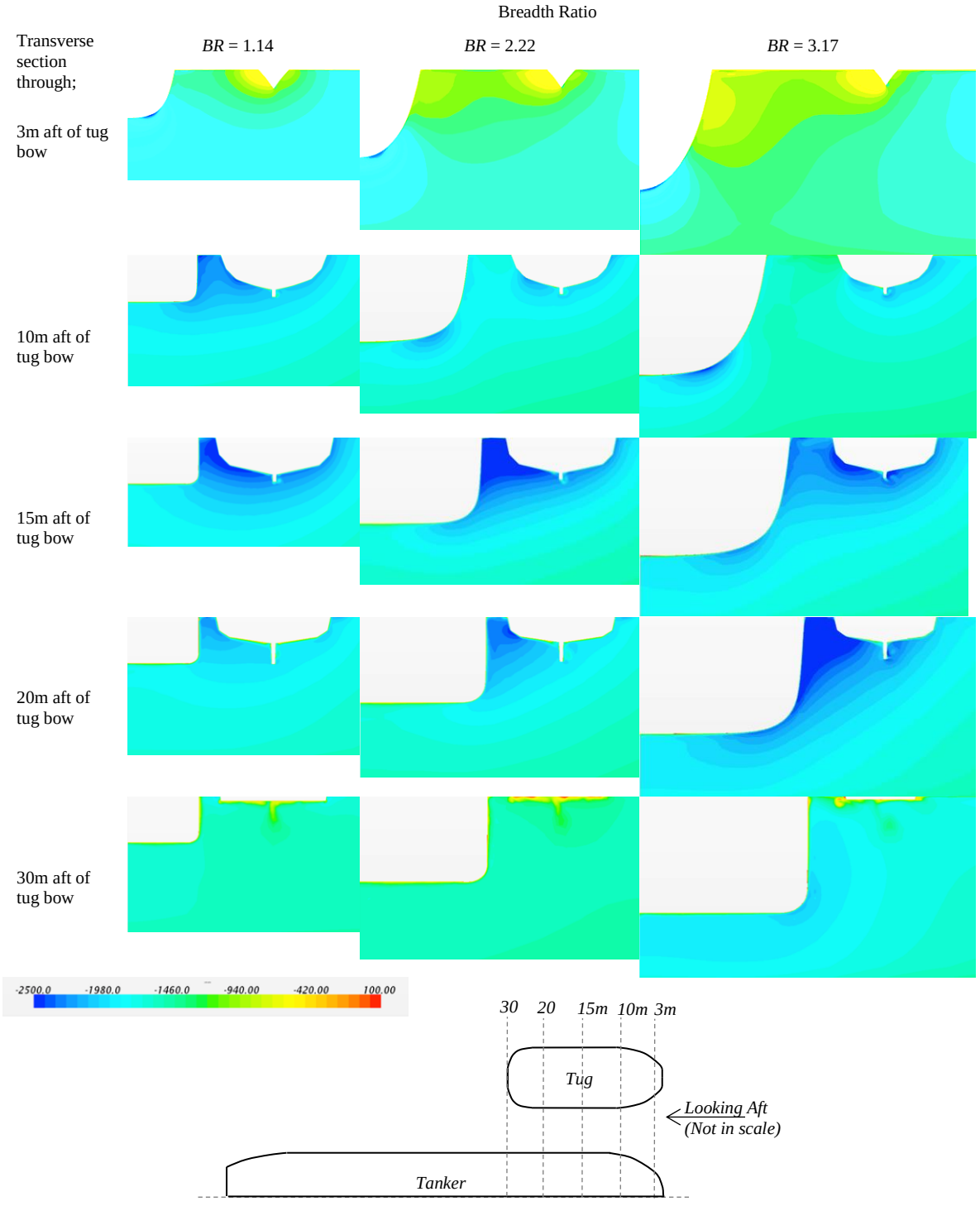

Figure 9: Pressure distribution plots on the transverse sections along the length of the tug at 3m, 10m, 15m, 20m, and 30m aft of the tug's bow for *BR* = 1.14, *BR* = 2.22, and *BR* = 3.17 when the lateral distance between vessel' hulls was maintained at δy_{m_1} = 0.913m.

These discrepancies were within the EFD and CFD uncertainties discussed in Section 5.2. In summary therefore, among the three lateral distance scaling methods investigated, the non-dimensioning method used with larger ship breadth, i.e. ΔY_{ship} was the most appropriate for interaction effect predictions. That is, it was the best for widely used ship-tug combinations that lie within and above the tested breadth ratio range. If it is required to use ΔY_{ship} for breadth ratios below this threshold where tugs are used to manoeuver with smaller ships, it is advisable to carry out further investigations to test its applicability.

6.2 PRESSURE PLOT VISUALISATION

CFD generated pressure plots are illustrated and discussed in the following two subsections. This is to highlight the significance of using non-dimensionalised values to predict the interaction effects of dissimilar sized vessels.

6.2 (a) Absolute lateral distance for scaling

Due to similar patterns in the results for the lateral distances (δy_m) of 0.913m and 0.975m (see Figure 8), only the results predicted for δy_m of 0.913m are discussed in this section. Figure 9 illustrates the full scale CFD pressure plots due to the interaction between the two hulls along transverse planes at tug lengths of 3m, 10m, 15m, 20m, and 30m aft of the tug's bow for *BR* of 1.14, 2.22, and, 3.17. As shown in Figure 9, near the tug bow (i.e. 3m aft of the bow), the pressure between the hulls increased significantly with the breadth ratio as a result of the increased tanker bow pressure region. For a *BR* of 3.17, the tanker bow pressure effect remains high up to the tug's midship (i.e. around 15m aft of the bow). This caused relatively high pressure between the hulls in comparison to the lesser breadth ratios.

Beyond midship however, pressure between the hulls reduced as the breadth ratio increased, as seen in Figure 9. At 20m aft of the tug's bow, a *BR* of 3.17 showed the least pressure between the hulls compared to the smaller breadth ratios due to the amplified venturi effect by the highly accelerated flow passing between the hulls. At the lower breadth ratio of 1.14, the low pressure region between the hulls was adversely affected due to a reduction in the accelerated flow between the hulls. This was influenced by the pressure around the tug's stern region as shown in the pressure plot at 20m aft of the tug's bow.

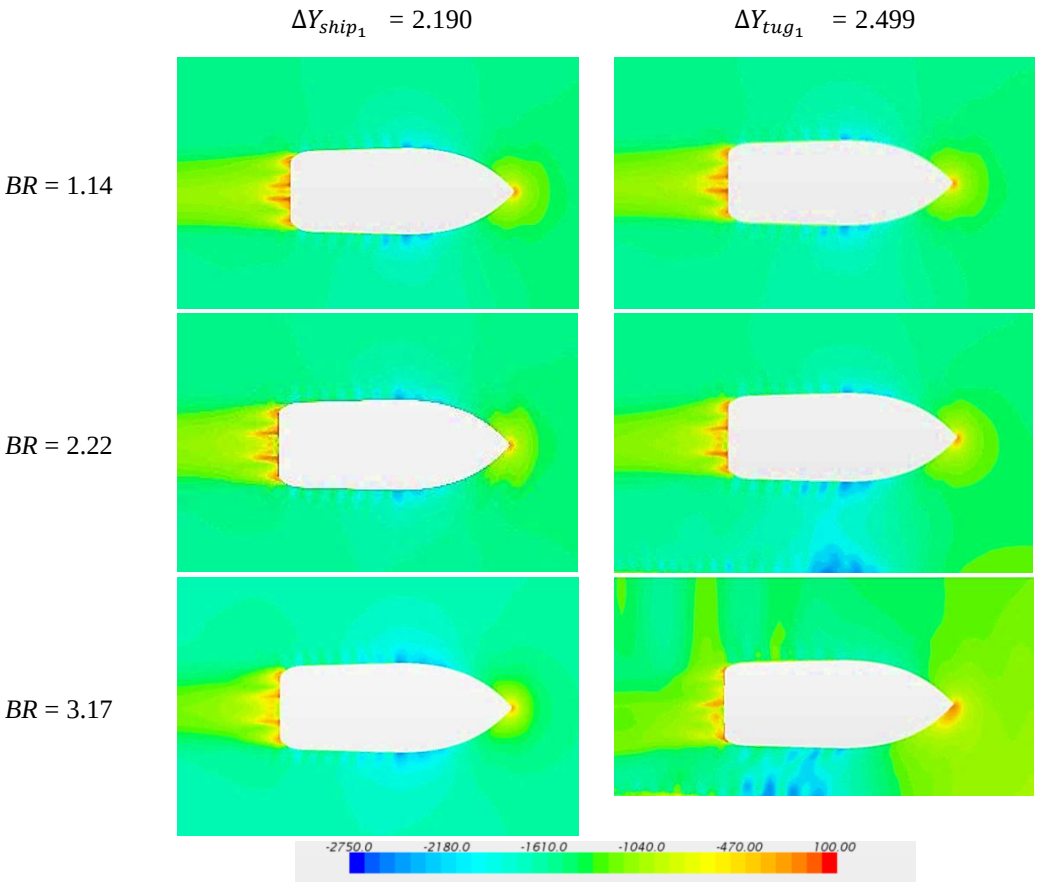

Figure 10: Pressure distribution plots on the tug for *BR* = 1.14, *BR* = 2.22, and *BR* = 3.17 for non-dimensionalised lateral distances of ΔY_{ship_1} = 2.190 and ΔY_{tug_1} = 2.499.

The results presented in Figure 9, at the aft-most point of the tug (i.e. 30m aft of the bow), show a decrease in pressure between the hulls with an increasing breadth ratio. It is therefore clear that the interaction effects predicted by using the absolute lateral distance for scaling were dominated by the larger ship size. This stresses the importance of having a suitable non-dimensioning method, as discussed in the previous section.

6.2 (b) Non-dimensionalised lateral distances for scaling

Figure 10 illustrates the pressure distribution around the tug when placed at different lateral distances to the tanker, as calculated by the two lateral distance non-dimensioning formula used in this study (eqns. 2 and 3). As seen in Figure 10, lateral distances calculated using the ΔY_{ship} formula (i.e. non-dimensionalised using the tanker breadth) showed similar pressure fields around the tug for all breadth ratios. This complimented the behaviour observed in the quantified interaction surge and sway forces and yawing moment coefficients presented in Figure 8, which displayed good agreement between different breadth ratios. For the ΔY_{tug} method, the pressure plots showed increasing pressure distribution differences as the breadth ratio increased. This supported the earlier quantitative findings in Figure 8, where larger discrepancies in the force coefficients between the different breadth ratios were observed.

These findings confirm that the non-dimensionalised lateral distance calculated using the breadth of the larger ship (i.e. ΔY_{ship}) was the most suitable method for comparing interaction effects acting on a tug during ship-assist manoeuvres. In other words it provided good scaling between different breadth ratios for the investigation of interaction effects between two dissimilar sized vessels.

7. CONCLUSION

Hydrodynamic interaction effects between two vessels operating in close proximity can affect the operational safety of those vessels. This is especially the case if the vessels are significantly different in size, for example when tugs assist large ships. The work presented here focused on the interaction effects on a tug operating around the forward shoulder of a tanker at different lateral distances during ship assist operations. It outlined an approach to non-dimensionalise lateral distances between vessels of dissimilar sizes. This is useful for predicting the interaction effects acting on the tug operating near ships of varying sizes and for correlating model scale and full scale interaction effects. This involved the verification of the approaches for non-dimensionalising lateral distances between the vessels for different full scale size vessels using validated CFD simulations.

The following are the key findings of this study:

- In order to compare the interaction effects between model scale and full scale data or to extrapolate model scale interaction effects to full scale, the lateral distance between the vessel centrelines should be non-dimensionalised using the large ship's breadth. The results obtained using this approach revealed a good agreement between the different breadth ratios investigated, i.e. 1.14 to 3.17, with the maximum differences for surge force, sway force, and yaw moment being 4%, 9%, and 5% respectively, which was within the calculated uncertainties. Thus, it is possible to use the interaction effects results from one ship-to-tug ratio to predict the safe operational distances for other ship-to-tug ratios when using the large ship breadth as the reference for the non-dimensioning method.
- Lateral distances calculated as a ratio of the tug's breadth did not provide satisfactory agreement between results for different breadth ratios. Rather, there was discrepancy of the forces as large as 41%. In the same way, using the absolute distance between the vessels was unsatisfactory as it doesn't account for vessel dimensions. This resulted in force and moment deviations of up to 268% across the breadth ratios considered in this study.
- When the tug was operating in close proximity to the forward quarter of the larger ship, interaction sway forces and yaw moments exhibited notable changes. As the breath ratio increased, the sway force declined, whereas the yaw moment rapidly increased. It is important that tug operators are aware of variations to the interaction effects when they operate in close proximity to ships of varying sizes, as it can lead to dangerous situations such as collisions or run-overs.

In future work, the location of a tug near a tanker will be extended to different lateral and longitudinal locations as well as different tug drift angles across a range of Froude numbers to develop comprehensive interaction effect plots for varying breadth ratios. These plots, together with the non-dimensioning method described here will enable tug operators to identify safe operational envelopes for a range of ship assist manoeuvers when they operate in close proximity to ships of varying sizes.

8. ACKNOWLEDGEMENTS

The authors would like to acknowledge the extensive support given by the AMC Model Test Basin staff during the experimental phase of this programme and DST Group for the use of the model carriage.

9. REFERENCES

1. ARTYSZUK, J. (2013). Types and Power of Harbour Tugs - The Latest Trends. Prace Naukowe Politechniki Warszawskiej - Transport, z.98. 1230-9265.

2. CD-ADAPCO (2015). User Manual of StarCCM+ Version 10.02.
3. CHEN, G. R. & FANG, M. C. (2001). Hydrodynamic Interactions Between Two Ships Advancing in Waves. Ocean Engineering, 28, 1053-1078. 0029-8018. http://dx.doi.org/10.1016/s0029-8018(00)00042-1
4. DAND, I. W. (1975). Some Aspects of Tug-Ship Interaction. The Fourth International Tug Convention, 1975 New Orleans, Louisiana, USA.
5. FALTER, J. (2010). Validation of a Potential Flow Code for Computation of Ship-Ship Interaction Forces with Captive Model Test Results. Ghent University, Belgium.
6. FONFACH, J. M. A. (2010). Numerical Study of the Hydrodynamic Interaction Between Ships in Viscous and Inviscid Flow. Instituto Superior Tecnico, Portugal.
7. FONFACH, J. M. A., SUTULO, S. & SOARES, C. G. (2011). Numerical Study of Ship to Ship Interaction Forces on the Basis of Various Flow Models. 2nd International Conference on Ship Manoeuvring in Shallow and Confined Water: Ship to Ship Interaction, 2011 Trondheim, Norway. RINA, 137-146
8. FORTSON, R. M. (1974). Interaction Force Between Ships. Massachusetts Institute of Technology, USA.
9. GEERTS, S., VANTORRE, M., ELOOT, K., HUIJSMANS, R. & FIERENS, N. (2011). Interaction Forces in Tug Operation. 2nd International Conference on Ship Manoeuvring in Shallow and Confined Water: Ship to Ship Interaction, 2011 Trondheim, Norway.
10. HENSEN, H. (2003). Tug Use in Port: A Practical Guide, Nautical Institute. 9781870077392.
11. HENSEN, H. (2012). Safe Tug Operation: Who Takes the Lead? International Tug & OSV, 2012, 70-76.
12. ITTC (2002). Testing and Extrapolation Methods - Resistance Uncertainty Analysis. International Towing Tank Conference.
13. JAYARATHNE, B. N., RANMUTHUGALA, D., CHAI, S. & FEI, G. (2014). Accuracy of Potential Flow Methods to Solve Real-time Ship-Tug Interaction Effects within Ship Handling Simulators. International Journal on Marine Navigation and Safety of Sea Transportation, 8, 497-504. 2083-6473. http://dx.doi.org/10.12716/1001.08.04.03
14. JAYARATHNE, B. N., RANMUTHUGALA, D., LEONG, Z. Q., CHAI, S. & FEI, G. (2017). Numerical and Experimental Prediction of Hydrodynamic Interaction Effects Acting on Tugs during Ship Manoeuvres. Journal of Marine Science and Technology (Accepted for publication). 1023-2796.
15. LATAIRE, E., VANTORRE, M., DELEFORTRIE, G. & CANDRIES, M. (2012). Mathematical Modelling of Forces Acting on Ships During Lightering Operations. Ocean Engineering, 55, 101-115. 0029-8018. https://doi.org/10.1016/j.oceaneng.2012.07.029
16. LEONG, Z. Q., RANMUTHUGALA, D., PENESIS, I. & NGUYEN, H. (2014). RANS-Based CFD Prediction of the Hydrodynamic Coefficients of DARPA SUBOFF Geometry in Straight-Line and Rotating Arm Manoeuvres. Transactions RINA: Part A1- International Journal Maritime Engineering. 1479-8751.
17. LU, H., YANG, C. & LOHNER, R. (2009). Numerical Studies of Ship-Ship Interactions in Extreme Waves. Grand Challenges in Modeling & Simulation 2009 USA. 43-55
18. NEWTON, R. N. (1960). Some Notes on Interaction Effects Between Ships Close Aboard in Deep Water. First Symposium on Ship Maneuverability, 1960 Washington D. C.: U.S. Government Printing Office,
19. PINKSTER, J. A. & BHAWSINKA, K. (2013). A Real-time Simulation Technique for Ship-Ship and Ship-Port Interactions. 28th International Workshop on Water Waves and Floating Bodies (IWWWFB 2013), 2013 L'Isle sur la Sorgue, France.
20. SIMONSEN, C. D., NIELSEN, C. K., OTZEN, J. F. & AGDRUP, K. (2011). CFD Based Prediction of Ship-Ship Interaction Forces on a Tug Beside a Tanker. 2nd International Conference on Ship Manoeuvring in Shallow and Confined Water: Ship to Ship Interaction, 2011 Trondheim, Norway.
21. STERN, F., WILSON, R. V., COLEMAN, H. W. & PETERSON, E. G. (2001). Comprehensive Approach to Verification and Validation of CFD Simulations - Part 1: Methodology and Procedures. Journal of Fluids Engineering, 123, 793-802. 0098-2202. https://doi.org/10.1115/1.1412235
22. TUCK, E. O. & NEWMAN, J. N. (1974). Hydrodynamic Interactions Between Ships. 10th Symposium on Naval Hydrodynamics, 1974 USA. 35-69
23. VANTORRE, M., VERZHBITSKAYA, E. & LAFORCE, E. (2002). Model Test Based Formulations of Ship-Ship Interaction Forces. Ship Technology Research, 49, 124-141. 0937-7255.
24. ZOU, L. & LARSSON, L. (2013). Numerical Predictions of Ship-to-Ship Interaction in Shallow Water. Ocean Engineering, 72, 386–402. 0029-8018.

ANALYSIS OF A WWII T2-TANKER USING A VIRTUAL 3D MODEL AND CONTEMPORARY CRITERIA

(DOI No: 10.3940/rina.ijme.2017.a4.430)

C Bonnici, **C De Marco Muscat-Fenech**, and **R Ghirlando**, Department of Mechanical Engineering, Faculty of Engineering, University of Malta, Malta

SUMMARY

The S.S. Ohio that saved the Maltese from capitulation during WWII made it to Malta barely afloat on the 15th of August 1942. Historical literature provides three main hypotheses as to why the tanker did not sink under heavy attack, namely: the use of water pumps partially restored buoyancy, the cargo density and a strong fully welded hull. A stability, floodable length and residual strength analysis was conducted to confirm or disprove the hypotheses. The results indicated that the vessel was stable, the water pumps partially restored buoyancy and was sinking despite her welded structure and cargo on-board. A challenge was to draw a comparison between the results and applicable criteria. At the time, criteria only governed the ship's scantlings and did not focus on stability, floodable length and residual strength. The research provided engineering evidence on how the S.S. Ohio survived, whilst contemporary criteria were identified to assess the tanker's characteristics.

NOMENCLATURE

ABS	American Bureau of Shipping
AP	Aft Perpendicular
AVS	Angle of Vanishing Stability (^{o})
B	Moulded beam (m)
C_1	LR section modulus coefficient
C_2	0.01 as per ABS rules
C_B	Block coefficient
CoG	Centre of Gravity
D	Depth (m)
f_1	Ship service factor
f_p	Nominal permissible bending stress (N/m^2)
GM	Metacentric Height (m)
GZ	Righting Lever (m)
I	Moment of inertia (m^4)
k_L	Tank dimensionless coefficient
L_{BP}	Length between perpendiculars (m)
LCB	Longitudinal Centre of Buoyancy (m)
LCG	Longitudinal Centre of Gravity (m)
L_{OA}	Length Overall (m)
LR	Lloyd's Register
MARPOL	International Convention for the Prevention of Pollution from Ships
$\overline{M_S}$	Permissible still water bending moment (Nm)
M_w	Wave induced bending moment (Nm)
RINA	Registro Italiano Navale SpA
SOLAS	International Convention for the Safety of Life At Sea
TCG	Transverse Centre of Gravity (m)
USCG	United States Coast Guard
VCG/KG	Vertical Centre of Gravity (m)
WPA	Waterplane Area (m^2)
Z	Ship section modulus with respect to either keel or freeboard deck (m^3)
Δ_{LIGHT}	Lightship displacement (t)

1. INTRODUCTION

The 15th of August 1942, a date enshrined in Maltese history, is fondly remembered by the population as the day Malta was saved from capitulation during WWII. On that day, the T2-tanker S.S. Ohio was towed into Grand Harbour, Valletta, Malta carrying vital oil replenishments without which the islands would have surrendered to the Axis Powers (Pearson, 2004). However, those witnessing the arrival of the tanker were astonished how, despite the heavy damage inflicted en-route to Malta, she remained afloat.

This historic event provided a research opportunity to analyse the tanker's damage and understand the factors that kept her afloat. A major challenge was to draw a comparison between the results obtained and applicable standards. At the time of construction of the S.S. Ohio, any rules and criteria governed only the ship's scantlings without providing any specific requirements on stability, floodable length and residual strength.

Thus the main aim of this work is to:

- Provide an engineering explanation on how the S.S. Ohio survived her ordeal
- Compare the stability, floodable length and residual strength characteristics of the WWII tanker with contemporary standards and analyse the results obtained.

2. HISTORICAL BACKGROUND

2.1 THE S.S. OHIO

The S.S. Ohio (Figure 1) was an American T2-tanker, built by the Sun Shipbuilding and Drydock and owned by the Texas Company (later transformed into Chevron Corporation). Her keel was laid on the 7th of September 1939 and seven months later, on the 20th of April 1940, the

S.S. Ohio was launched (Pearson, 2004), (The Texas Company, 1940(a)). Initially, the tanker was registered under the American flag, but on the 29th of June 1942, the ship was bareboat registered under the British flag to take part of the convoy mission, code- named Operation Pedestal (Bogart, 1994), (UK Ministry of War Transport, 1942).

Figure 1: S.S. Ohio (Bogart, 1994)

The overall length (L_{OA}) of the S.S. Ohio was 156.7m, whilst the length between perpendiculars (L_{BP}) was equal to 147.8m. Her moulded depth (D) and moulded beam (B) were equal to 11.0m and 20.7m respectively (The Texas Company. 1940(a)), (Lloyd's Register, 1940), (Lloyd's Register, 1939). The tanker had a total deadweight of 14377t, whilst her lightship displacement (Δ_{LIGHT}) was equal to 5253t (The Texas Company, 1940(a)), Lloyd's Register, 1940), (Lloyd's Register, 1939). Her ship side was riveted, whilst her internal structure, bottom shell and deck plating were welded. The tanker was divided by two longitudinal bulkheads and a series of transverse bulkheads, forming 18 watertight compartments with a total cargo capacity of 1705m^3 (The Texas Company. 1940(a)), (Lloyd's Register, 1940), (Lloyd's Register, 1939).

The S.S. Ohio was classed by Lloyd's Register (LR) and American Bureau of Shipping (ABS) and assigned the following class notation:

✠*100A1, Carry Petroleum in Bulk, LMC* (Lloyd's Register, 1940)

Such a class notation meant (Lloyd's Register, Marine, 2014(a)):

- ✠: the tanker was constructed under the survey of a classification society
- *100*: the tanker was considered suitable for sea going service
- *A*: the tanker was maintained in a good and efficient manner
- *1*: the tanker had good and efficient anchoring and mooring equipment
- *Carry Petroleum in Bulk*: ships intended to transport petroleum products
- *LMC*: propulsion and auxiliary machinery were constructed, installed and tested under class survey

The S.S. Ohio's main machinery consisted of two Westinghouse Steam Turbines and Babcock and Wilcox steam boilers, which generated a total of 9000shp at 90rpm, which propelled the ship at 17 knots (The Texas Company, 1940(b)).

2.2 OPERATION PEDESTAL

The S.S. Ohio was acquired under the British Flag to form part of Operation Pedestal, the last convoy mission undertaken by the allies to supply the besieged islands of Malta in August 1942. Had it not been for Operation Pedestal, Malta would have surrendered to the Axis Powers in September 1942 (Pearson, 2004), (Lucas, 1993), (Holland, 2003).

The T2-tanker was joined by 13 other merchant ships and naval escort and approached the Strait of Gibraltar under the cover of darkness on the 10th of August 1942 (Pearson, 2004), (Lucas, 1993), (Holland, 2003). The 13 merchant ships were carrying a variety of cargo replenishments required by the islands, but as the sole oil tanker, only the S.S. Ohio was capable of delivering the required oil supplies to keep the country fighting against the enemy (Pearson, 2004), (Lucas, 1993), (Holland, 2003). So important was the S.S. Ohio that if all the other merchant ships reached Malta, except for the S.S. Ohio, the convoy mission would have been considered a failure (Pearson, 2004), (Lucas, 1993), (Holland, 2003). Knowing how important the tanker was to the Maltese islands, the Axis Powers attacked her relentlessly. So large was the damage inflicted that she was left dead in the water with her freeboard at 0.76m (Figure 2) and only reached Grand Harbour under tow by the escorting destroyers (Pearson, 2004), (Lucas, 1993), (Holland, 2003).

Figure 2: S.S. Freeboard of the S.S. Ohio at 0.76m (Cook, 1942)

As the years passed by, several hypotheses were put forward as to how the S.S. Ohio survived mainly being:

- Auxiliary water pumps supplied by the escorting destroyers decreased the flooding rate and partially restored the tanker's buoyancy (Shankland & Hunter, 1983). Historical literature says that additional water pumps from the escorting destroyers decreased the flooding rate and bought ample time for the tanker to reach Malta and discharge her cargo before she sunk (Caruana, 1992)

- The oil cargo being less dense than water prevented the ship from reaching Davy Jones' Locker (Caruana, 1992)
- The strong fully welded hull was able to withstand such an ordeal that the welded structure prevented the ship from collapsing (Shankland & Hunter, 1983)

However, tangible engineering evidence providing a clear understanding on how the S.S. Ohio survived her ordeal, whilst proving or disproving the hypotheses does not exist. Thus the main scope of this work is to establish such facts, whilst comparing the attained results to contemporary rules and criteria.

3. METHODOLOGY

The following methodology was adopted for the research.

- First a historical literature review of both primary and secondary sources was undertaken to determine the chain of events surrounding the ordeal of the S.S. Ohio. Such accounts shed light on the inflicted damage as the tanker proceeded onwards to Malta.
- An information gathering process followed to determine the main characteristics and dimensions of the S.S. Ohio. Several sources were consulted including but not limited to the company which owned the tanker, the ship's classification societies and the flag registers.
- The main characteristics and principal dimensions were then utilised to create a 3D virtual model of the S.S. Ohio using *Bentley Maxsurf 20.04 V8i Suite Software* which includes *Maxsurf Modeller Advanced* and *Maxsurf Stability Enterprise* (Bentley Systems, 2014).
- Using design formulae, the lightship Centre of Gravity (CoG) was located.
- Stability, floodable length and residual strength analyses were carried out using manual calculations, results of which were verified using *Maxsurf Stability Enterprise*.
- Afterwards, contemporary rules and criteria were analysed to determine applicability as if the S.S. Ohio was built recently.
- Finally the results were compared to the 'applicable' rules and criteria to assess the stability, floodable length and residual strength results.

Through the adopted methodology and results obtained, valuable insight was shed on how the S.S. Ohio remained afloat.

4. VIRTUAL MODEL CREATION

A virtual 3D model of the S.S. Ohio was essential for the research, especially when a physical model suitable for testing was not available. The foundation of the tanker's 3D model is the table of offsets. Unfortunately no such table was available for the S.S. Ohio. Instead a table of offsets of a similar ship was utilised (Bailey, 1976) and Bailey's method implemented to modify the offsets table and recreate that of the S.S. Ohio (Bentley Systems, 2014). Afterwards the modified table was inputted in *Maxsurf Modeller Advanced* to create the virtual model of the tanker's hull. Using a general arrangement plan (Lloyd's Register, 1939), the tanks and compartments were modelled (Figure 3) and the margin line placed 76mm beneath the freeboard deck of the 3D hull.

The virtual model was then ready for analysis after it was loaded with crew weight, defensive armament to protect the ship against air attacks, required ammunition and full complement of cargo as per quantities listed below (Pearson, 2004):

- Fuel oil – 8334.6t
- Diesel oil – 1733.0t
- Kerosene – 1924.4t
- Bunker fuel – 1320.9t
- Lubricating oil – 15.3t.

5. CENTRE OF GRAVITY LOCATION

A vessel's lightship CoG is the fulcrum of the stability, floodable length and residual strength calculations. Unfortunately reliable information or direct calculations indicating the location of the CoG of the S.S. Ohio in the lightship condition were not available. As a result, design methods and formulae implemented during the rudimentary stages of ship design were adopted to locate the lightship CoG of the S.S. Ohio, which was then inputted in the virtual model. The CoG is divided into three components being:

- Vertical Centre of Gravity (VCG)
- Longitudinal Centre of Gravity (LCG)
- Transverse Centre of Gravity (TCG)

5.1 THE VERTICAL CENTRE OF GRAVITY

The design formulae put forward by Schneekluth and Bertram (Schneekkluth & Bertram, 1998), Ganesan (Ganesan, 1999) and Benford (Benford, 1967) were utilised to reverse engineer the VCG of the S.S. Ohio. The theory put forward by Schneekluth and Bertram (Schneekluth and Bertram, 1998), Ganesan (Ganesan, 1999) and Benford (Benford, 1967) divided the lightship weight and VCG into three components being:

- Steel structure
- Hull equipment and outfit
- Machinery

The VCG and the weight of each component were located using the design formulae, results of which were

included in the Principle of Moments method used to locate the lightship VCG. The latter was located at 7.7m above the baseline.

5.2 THE LONGITUDINAL CENTRE OF GRAVITY

The lightship LCG of the S.S. Ohio was evaluated at 70.8m from the AP. Knowing that for equilibrium the LCG and the LCB lie on the same vertical plane and that the LCB position is the centroid of the underwater volume along the ship's longitudinal centreline, Approximate Integration Methods were utilised to locate LCB in the fully loaded condition. Afterwards, considering the loaded and lightship mass displacement of the S.S. Ohio, the LCB (the LCG in the loaded condition), the mass displacement and LCG of the individual cargo on-board were identified; the lightship LCG was calculated using the Principle of Moments.

5.3 THE TRANSVERSE CENTRE OF GRAVITY

The S.S. Ohio was symmetrical about the ship's centreline (Bogart, 1994), (US Maritime Administration, 2006), therefore the TCG lay on the ship's centreline.

6. DAMAGE SUSTAINED

During Operation Pedestal heavy damage was inflicted on the S.S. Ohio. Yet for the scope of the research only the damage scenarios which caused flooding were analysed. Any other damage was not included in the research.

6.1 FIRST DAMAGE SCENARIO – 12th OF AUGUST 1942, 19.56HRS

On the evening of the 12th of August 1942, at 19.56hrs, the Italian submarine, Axum fired a 21 inch torpedo and hit the S.S. Ohio in her port side midship pumproom, blowing a 24 foot (7.32m) wide by a 27 foot (8.23m) hole (Pearson, 2004), (Bogart, 1994), (Caruana, 1992) (Figure 3). The force of the explosion damaged the pump room bulkhead whilst two centre tanks and four wing tanks were also damaged (Pearson, 2004), (Bogart, 1994), (Caruana, 1992). Fortunately no further damage was reported for the remainder of the day.

6.2 SECOND DAMAGE SCENARIO – 13th OF AUGUST 1942, 08.10HRS

The following morning, August 13th 1942, at 08.10hrs, the S.S. Ohio was near missed by a 500lbs bomb at the ship's bow (Figure 3). According to the damage report by Captain Mason and Chief Engineer Wyld the near miss flooded the forepeak tank (Pearson, 2004), (Bogart, 1994), (Caruana, 1992), (Smith, 1970), (Wyld, 1942), (Barton, 1942), (Mason, 1942).

6.3 THIRD DAMAGE SCENARIO – 13th OF AUGUST 1942, 18.30HRS

Major damage was reported when in the evening of the same day at 18.30hrs, the S.S. Ohio was hit in the engine room (Figure 3). A 500lbs bomb pierced the boat deck forward of the ship's funnel, destroyed the engineer's accommodation on the upper deck and exploded in the boiler room (Pearson, 2004), (Bogart, 1994), (Admiralty, 1942-46), (Wyld, 1942), (Mason, 1942), (Jerome, 1942). The boilers were destroyed, the boiler room aft bulkhead was blasted and the rest of the engine room was flooded (Bogart, 1994).

6.4 FOURTH DAMAGE SCENARIO – 14th OF AUGUST 1942, 10.50HRS

Further damage was inflicted on the 14th of August 1942. At 10.50hrs, an air attack formed over the S.S. Ohio (Pearson, 2004). A 1000lbs bomb exploded in the vicinity of the vessel's stern (Figure 3), misaligning the ship's propeller and blowing off her rudder. In addition, the aft peak tank and steering gear room were flooded (Pearson, 2004), (Caruana, 1992), (Smith, 1970), (Jerome, 1942).

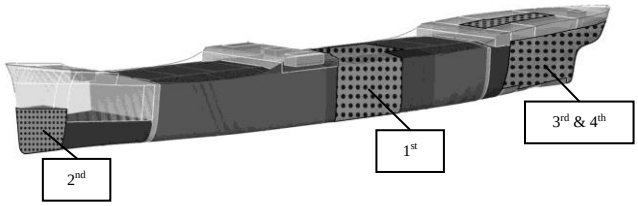

Figure 3: S.S. Ohio 3D virtual model using *Maxsurf Modeller Advanced* (Bentley Systems, 2014) and showing damaged scenarios (dotted compartments)

7. STABILITY ASSESSMENT

7.1 INTACT STABILITY

A stability analysis was undertaken to examine the intact stability of the S.S. Ohio. Consumable items such as bunker fuel, whose quantities varied during the voyage, were accounted for in the intact stability assessment. Using manual calculations, an equilibrium condition and a Righting Lever (GZ) Curve (Graph 1) were established at the instant prior to the first damage scenario. The results were verified using *Maxsurf Stability Enterprise* and compared to the 2008 Intact Stability Code (IMO, 2011) and the stability requirements set in MARPOL Annex I, Regulation 27 (IMO, 2011) (Table 1). Whilst noting that the S.S. Ohio was built well before the stability criteria entered into force, thus not applicable, the same were used as a means to obtain a clearer picture of the tanker's stability in light of today's requirements.

The analysis presented here indicated that the S.S. Ohio exhibited adequate stability when loaded. Furthermore

the intact stability assessment showed that the S.S. Ohio satisfied and exceeded the stability criteria set by today's codes and conventions. Therefore one can state that the stability characteristics of the tanker when built in 1940 have been proved to even surpass today's criteria.

Table 1: 2008 Intact Stability Code (IMO, 2009) and MARPOL Annex I, Regulation 27 (IMO, 2011) intact stability criteria as on the 12th of August 1942

2008 Intact Stability Code	**Results**	**Criterion Met?**
The area under the righting lever curve shall not be less than 3.151mdeg up to a 30° angle of heel	37.6mdeg	Yes
The area under the righting lever curve shall not be less than 5.157mdeg up to a 40° angle of heel	55.2mdeg	Yes
Additionally , the area under the righting lever curve between the angles of heel of 30° and 40° shall not be less than 1.719mdeg	17.6mdeg	Yes
The righting lever shall be at least 0.2m at an angle of heel equal to or greater than 30°	1.8m	Yes
The maximum righting lever shall occur at an angle of heel not less than 25°	26.4°	Yes
The initial metacentric height shall not be less than 0.15m	5.9m	Yes
MARPOL Annex I, Regulation 27	**Results**	**Criterion Met?**
At sea the area under the righting lever curve shall not be less than 3.151mdeg up to a 30° angle of heel	16.2mdeg	Yes
At sea the area under the righting lever curve shall not be less than 5.157mdeg up to a 40° angle of heel	27.1mdeg	Yes
At sea the area under the righting lever curve between the angles of heel of 30° and 40° shall not be less than 1.719mdeg	10.9mdeg	Yes
At sea the righting lever shall be at least 0.2m at an angle of heel equal to or greater than 30°	1.2m	Yes
At sea the maximum righting arm shall occur at an angle of heel preferably exceeding 30° but not less than 25°	47.3°	Yes
In port, the initial metacentric height *GM*, corrected for the free surface measured at 0°, shall not be less than 0.15m	2.0m	Yes

7.2 DAMAGE STABILITY

The Lost Buoyancy Method was utilised to establish the equilibrium condition of each damage scenario. Using *Maxsurf Stability Enterprise*, the GZ curve of each damaged condition was plotted (Graph 1).

The GZ curves plotted for the first and second damage scenarios indicated that the stability of the S.S. Ohio was improved when compared with the intact condition. The maximum GZ of the first and second damage scenarios was equal to 1.3m, whilst that for the intact condition was equal to 1.2m. In addition, the Angle of Vanishing Stability (AVS) for both the first and second damage scenarios was equal to 100° whilst the AVS of the intact condition was equal to 98°. Thus a larger maximum GZ and AVS in the first two damage scenarios resulted in a larger area under the graph when compared with the intact condition, meaning that the S.S. Ohio could absorb higher heeling forces before she capsized. According to Patterson and Ridley (Ridley & Patterson, 2014), such a scenario occurs when there's either a reduction in displacement or an increase in freeboard. However, as shown in Graph 2, the S.S. Ohio experienced both a reduction in displacement, due to cargo loss from damaged tanks and a freeboard reduction, due to buoyancy loss from damaged compartments. Despite of this anomaly, stability was improved when the S.S. Ohio was damaged because for the first two damage scenarios, the reduction in displacement had a far more superior effect than the freeboard loss. Such a scenario was consolidated further, as despite the enhancement in the ship's stability when damaged, the Water Plane Area (WPA) decreased for each damage scenario (Graph 2). Such a scenario should have impaired the ship's stability, yet as shown in Graph 1, the ship's initial stability was also increased.

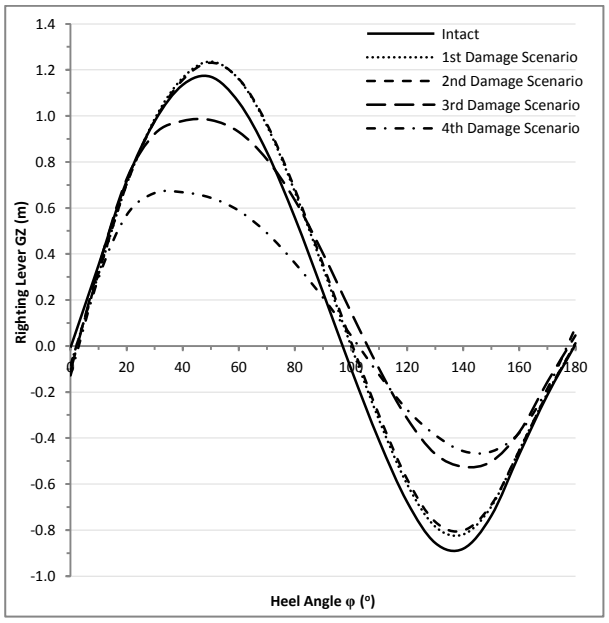

Graph 1: GZ curves for both intact and damage scenarios

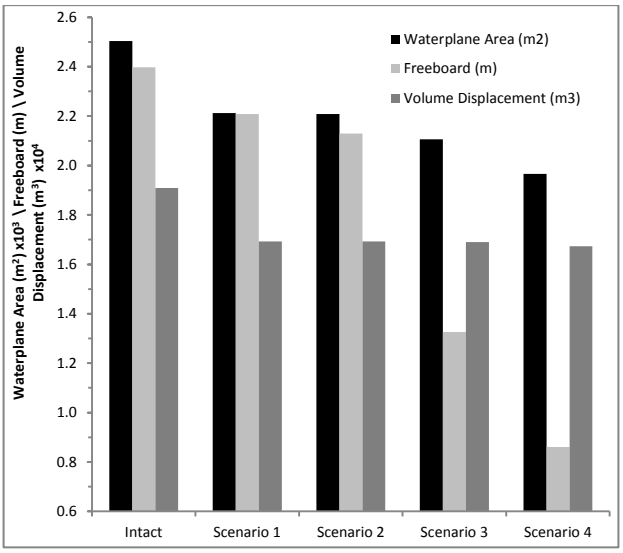

Graph 2: Column chart of waterplane area, volume displacement and freeboard variation between each intact and damage scenario

On the contrary, for the third and fourth damage scenarios, a reduction in stability was observed when compared to both the intact condition and the preceding damage cases. The maximum GZ for third and fourth damage scenarios was equal to 1.0m and 0.7m respectively, smaller than that obtained in the intact and first two damage scenarios. As a result, the area under the GZ curves of the last two damage scenarios was smaller than the intact and first two damage scenarios.

As shown in Graph 2, a reduction in both displacement and freeboard was also observed for the third and fourth damage scenarios. However the freeboard reduction was considerable when compared to the previous scenarios, whilst the displacement in each scenario remained almost constant. Hence the decline in stability for the last two damage scenarios was attributed to the freeboard reduction being more significant than the displacement loss. Even though a reduction in WPA was observed, the initial stability for the third and fourth damage scenarios was better than the intact condition.

The GZ curves of the S.S. Ohio also indicated that at neither instant of damage was the tanker at risk of capsizing, as the angle of final equilibrium of each damaged condition was less than 3^{o}. Despite the reduction in stability, the S.S. Ohio was never exposed to a capsizing risk. In fact, the late Allan Shaw, the last living crew member who was on-board the S.S. Ohio, confirmed that any list due to damage went unnoticed (Shaw, 2014).

8. FLOODABLE LENGTH CALCULATIONS

A ship is divided into several watertight divisions to ensure that when a compartment is breached, flooding will remain contained within the compromised subdivision. The adequate subdivision lengths are determined from the floodable length calculations. For the S.S. Ohio the calculations were based on the method put forward by Shirokauer in (Shirokauer, 1928) as cited by Nickum in (Nickum, 1988), results of which were verified using *Maxsurf Stability Enterprise*.

The floodable length calculations indicate the maximum length which could be flooded without immersing the margin line below the waterline and assuming the ship as lost (Nickum, 1988). The maximum length which could be flooded without immersing the margin line is determined from the floodable length curve, as shown in Graph 3.

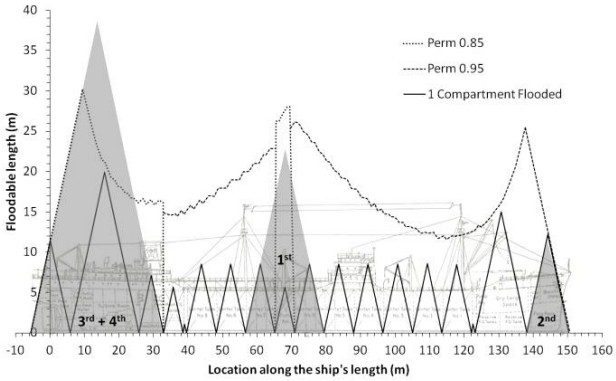

Graph 3: Floodable length curve of the S.S. Ohio with the flooded length of each damage scenario

Thus the length of each watertight compartment should be smaller than the allowable floodable length as indicated by the height of the apex of each triangle (Nickum, 1988). Graph 3 indicates that a single flooded compartment of the S.S. Ohio would not immerse her margin line below the waterline (Bogart, 1994), (Lloyd's Register, 1939) as per SOLAS 1948, Chapter II, Part B, Regulation 7 which states:

"Sufficient intact stability shall be provided in all service conditions so as to ensure the ship to withstand the final stage of flooding of one main compartment which is required to be within the floodable length" (International Community, 1948)

One shall note that such a requirement was first introduced in SOLAS 1948. Therefore it could be stated that the S.S. Ohio was a one compartment ship and satisfied criteria implemented well after her date of build. Furthermore SOLAS 1974 as amended, Chapter II-1, Regulation 4.3 states:

"Ships shall be as efficiently subdivided as is possible having regard to the nature of the service for which they are intended" (IMO, 2014(a))

Graph 3 indicated that the S.S. Ohio was divided into 18 watertight compartments, efficiently subdividing as much as possible her length, as per today's requirements.

On the other hand, if two adjacent compartments were breached and flooded, at certain instances along the tanker's length, the flooded length would be greater than the allowable floodable length. At such instances of damage the S.S. Ohio would be assumed lost. Yet despite being a one compartment ship, when the S.S. Ohio was torpedoed (first damage scenario), three compartments at her midship were flooded but was not assumed lost. The floodable length of the breached compartments within the midship region did not exceed the allowable floodable length and the margin line was not immersed beneath the waterline as shown in Graph 3. In reality, the damaged compartments were not fully breached because the starboard longitudinal bulkhead of the damaged region held despite the torpedo explosion (Wyld, 1942), (Mason, 1942), (Shaw, 2014), (Gray, 1942). Thus an unaccounted reserve of buoyancy was still present in the damaged compartments. In fact, after the torpedo damage, she continued with her voyage under her own steam (Pearson, 2004), (Caruana, 1992), (Smith, 1970). The floodable length calculations showed that despite the considerable structural damage, the torpedo was not the blow which crippled the tanker. Similarly, in the second damage scenario, the margin line was not immersed beneath the waterline because the flooded length was still smaller than the allowable floodable length.

It was not the case for the third damage scenario. The S.S. Ohio received a direct hit aft, which flooded her engine room. According to the floodable length curve, the length of the flooded compartment within this region was larger than the allowable floodable length with the margin line possibly immersed beneath the waterline. The flooded length was increased further in the fourth damage scenario, as shown in Graph 3. Compartments adjacent to the engine room were also flooded because of a near miss aft, which could have immersed the margin line further beneath the waterline. At this stage the S.S. Ohio was assumed lost and on the brink of sinking. The direct hit in the engine room and the near miss aft were the blows which could have crippled the tanker. History says that the S.S. Ohio was only saved due to the auxiliary water pumps brought onboard from the escorting destroyers to decrease the flooding rate (Shankland & Hunter, 1983), (Caruana, 1992). The floodable length calculations show that had it not been for these auxiliary pumps, the S.S. Ohio may have sunk before she reached harbour and discharge her valuable cargo (Shankland & Hunter, 1983), (Caruana, 1992).

9. RESIDUAL STRENGTH ASSESSMENT

9.1 INTACT CONDITION

A residual strength assessment of the S.S. Ohio was undertaken to understand her strength characteristics in her fully loaded and intact condition. The induced shear forces and bending moments were analysed using Simple Beam Theory, results of which are presented in Graph 4. The latter was verified using *Maxsurf Stability Enterprise*.

The results indicated that in still water, fully loaded and intact, the vessel was sagging. Thus the S.S. Ohio experienced the largest bending moment when sailing through sagging waves.

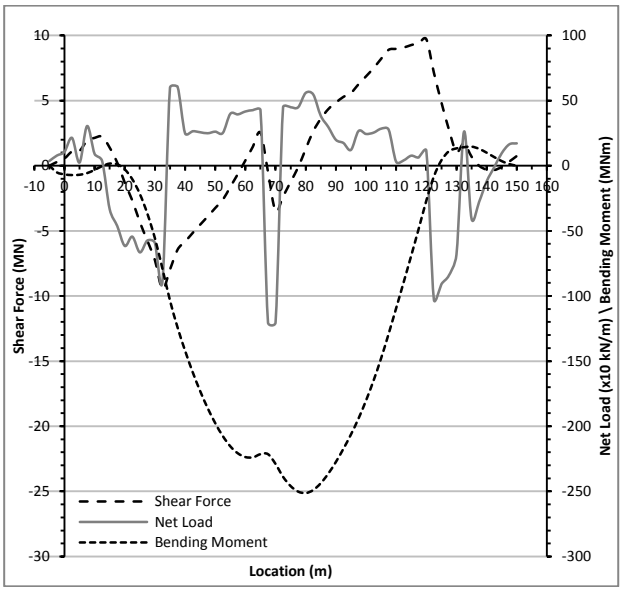

Graph 4: Still water net load, shear force and bending moment diagrams of the S.S. Ohio in the intact condition

Using the bending moment obtained from Graph 4 and the ship's midship section (Lloyd's Register, 1939), the moment of inertia and the section modulus of the tanker's midship were calculated and found equal to $38.7m^4$ and $6.3m^3$ respectively. Class criteria were used to analyse the strength characteristics because in 1940, the year the T2-tanker was constructed, international regulations and class rules governed only the required scantlings, without providing any specific residual strength requirements (International Community, 1929), (ABS, 1938), (Lloyd's Register, 1938). Therefore contemporary regulations and criteria were used for guidance purposes only to analyse the S.S. Ohio's residual strength. In fact SOLAS Chapter II-1, Part A-1, Regulation 3-1 states:

"...ships shall be designed, constructed and maintained in compliance with the structural, mechanical and electrical requirements of a classification society..." (IMO, 2014(b))

As such the residual strength criteria set forth by LR and ABS for single hull oil tankers were applied to the S.S. Ohio, as shown in Table 2 (Lloyd's Register, 2014(b)), (ABS, 2015).

Table 2: Residual Strength Criteria according to LR and ABS

LR Residual Strength Criteria	
Criterion	*Rules and Regulations for the Classification of Ships Part 3, Chapter 4, Section 5.4.1: Minimum Hull Section Modulus:* The hull midship section modulus about the transverse neutral axis, at the deck or the keel, is to be not less than $Z_{min} = f_1 k_L C_1 L^2 B(C_B + 0.7) \times 10^{-6}$
Results	**Required Z_{min} = 5.6m^3** Z_{keel} of S.S. Ohio: 6.3m^3
Criterion met?	Yes
Criterion	*Rules and Regulations for the Classification of Ships Part 3, Chapter 4, Section 5.8.1:* The hull midship section moment of inertia about the transverse neutral axis is to be not less than the following using the maximum total bending moment, sagging or hogging, $I_{min} = \frac{3L\lvert\bar{M}_s + M_w\rvert}{k_L f_p} \times 10^{-5}$
Results	**Required I = 21.4m^4** I of the S.S. Ohio: 38.7m^4
Criterion met?	Yes
ABS Residual Strength Criteria	
Criterion	*Part 3, Chapter 2, Section 1, Regulation 3.7.1: Hull Girder Section Modulus3.7.1a: The required hull girder section modulus for 0.4L amidships is to be the greater of the values obtained from the equation* $Z = \frac{M_t}{f_p}$ *or 3.7.1.b: Minimum Section Modulus. The minimum hull girder section modulus amidships is not to be less than obtained from the equation* $Z = C_1 C_2 L^2 B(C_B + 0.7)$
Results	3.7.1a: Z = 4.73m^3 3.7.1b: Z = 5.63m^3 **Required Z: 5.63m^3** Z_{keel} of S.S. Ohio: 6.28m^3
Criterion met?	Yes
Criterion	*Part 3, Chapter 2, Section 1, Regulation 3.7.2: Hull Girder Moment of Inertia. The hull girder moment of inertia amidships, is to be not less than* $I = \frac{LZ}{33.3}$
Results	**Required I = 24.99m^4** I of the S.S. Ohio: 38.68m^4
Criterion met?	Yes

The class criteria served as a mean to assess the S.S. Ohio's strength in light of today's requirements. Table 2 indicates that the S.S. Ohio was capable of meeting requirements applicable to ships built well after her time. Furthermore compliance with class criteria showed that the S.S. Ohio was built to high residual strength standards.

9.2 DAMAGE CONDITION

Using *Maxsurf Stability Enterprise* the still and wave induced shear forces and bending moments were compiled for each damage scenario. The method put forward by Paik, Thayamballi and Hong Yang in (Paik, Thayamballi and Hong Yang, 1998), was adopted to analyse the vessel's strength when damaged. The method determined the ultimate bending moment a damaged ship in either hogging or sagging condition could withstand before the hull collapsed (Paik, Thayamballi and Hong Yang, 1998).

The results showed that the S.S. Ohio experienced the largest bending moment when the tanker was torpedoed (Graph 5). From the analysis, the maximum bending moment imparted to the S.S. Ohio in her first damage scenario was equal to 588.4MNm, higher than that obtained in the intact condition and 16% higher than the ultimate bending moment of 509.2MNm, as predicted by Paik et al's method for the first damage scenario (Graph 5). As such it was concluded that when the S.S. Ohio was torpedoed (first damage scenario) she was at the greatest risk of hull collapse, even though her internal structure was welded.

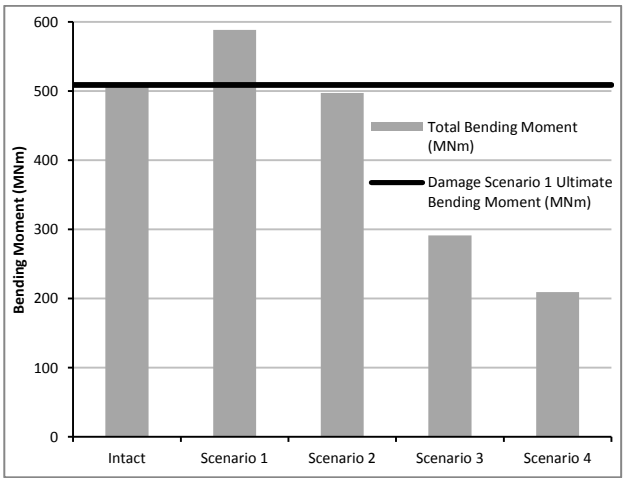

Graph 5: Bending moment for the intact and damage conditions

As further damage was inflicted elsewhere along the ship's length, the maximum bending moment decreased as shown in Graph 5. Such a scenario was also observed in separate studies carried out by Teixeira and Guedes Soares (Teixeira, Guedes Soares, 2009) and Horte, Skjong, Friis-Hansen, Teixeira and Viejo de Franciso (Horte, Skjong, Friis-Hansen, Teixeira and Viejo de

Franciso, 2007). A plausible explanation to such a scenario is that the remaining buoyant sections in her aft and forward regions were also flooded, sinking the ship deeper into the water, whilst decreasing the tanker's bending moment. The damage itself, served as a life saver, since despite the S.S. Ohio sinking further, the ship's sagged condition decreased.

However even though the maximum bending moment amidship was decreasing with each damage scenario, this does not imply that the tanker's strength was improved. On the contrary, with every damage scenario, cross-sectional area was being lost from the ship's length, thus reducing the moment of inertia and the ability to withstand bending. Furthermore, between the first and third damage scenarios, almost 24 hours had elapsed when the total bending moment was considerably reduced. As a result, the S.S. Ohio was at a high risk of collapse for an elongated period of time, amplifying the risk of breaking in half. Such a risk could have been mitigated by the low speed of the tanker due to the damage sustained and thanks to the calm weather conditions the S.S. Ohio encountered (Pearson, 2004), (Bogart, 1994), (Met Office, 1942). Synoptic charts for the 12th, 13th and 14th of August 1942, show high pressure areas forming over the Mediterranean Sea, with low wind speeds and low wave heights reminiscent to calm weather conditions. In fact from the synoptic charts, the average wave height for the 12th, 13th and 14th of August 1942 was equal to 1.28m (Met Office, 1942). Thus it was concluded that if heavy weather was encountered after the tanker was torpedoed, a different fate would have served the Maltese islands. However, the reduction in the ship's sagged condition and bending moments probably reduced the stresses acting on the remaining intact plating, minimising the risk of breaking in half. In fact, as history says, the S.S. Ohio entered Grand Harbour as a single ship (Pearson, 2004), (Bogart, 1994), (Shankland & Hunter, 1983), (Caruana, 1992), (Wyld, 1942), (Mason, 1942), (Gray, 1942).

10. CONCLUSION

The stability, floodable length and residual strength analyses provided an engineering perspective on how the S.S. Ohio survived her ordeal. Further insight on the tanker's stability, floodable length and residual strength characteristics was obtained after the results were compared to contemporary criteria. Finally the hypothesis put forward in historical literature were verified or disproved.

The stability analysis indicated that for the first two damage scenarios, stability was improved but was not the case for the remaining scenarios. Despite the stability reduction when severely damaged, the S.S. Ohio was not subjected to a capsizing risk and only suffered parallel immersion when damaged. Furthermore, the analysis indicated that the S.S. Ohio satisfied the intact stability criteria applicable to modern tankers.

The floodable length calculations confirmed that the auxiliary water pumps supplied by the escorting destroyers partially restored the tanker's buoyancy. The S.S. Ohio could be assumed lost when the engine room was flooded. Had it not been for the auxiliary water pumps, the tanker would have been lost and never reached Grand Harbour. Nonetheless, the calculations disproved the hypothesis that the S.S. Ohio kept afloat because of the cargo on-board being less dense than water. The results indicated that even though the majority of the cargo tanks remained intact, the flooded engine room could have rendered the tanker as lost. The calculations also showed that the tanker was efficiently subdivided as per today's requirements.

The hypothesis that a strong fully welded hull was able to withstand the sustained damage was disproved. Literature provided by Chevron Corporation (The Texas Company 1940(a)) showed that the S.S. Ohio was a combination of riveted and welded construction. However despite being of welded and riveted construction, the intact residual strength results met contemporary LR and ABS strength criteria applicable to single hull oil tankers. The damage residual strength assessment showed that when the S.S. Ohio was torpedoed (First Damage Scenario), the maximum bending moment was greater than the ultimate bending moment. At this instant, the S.S. Ohio was exposed to the greatest risk of collapse. However, as further damage was inflicted along the tanker's length, the bending moment decreased. Reason being, as the remaining buoyant sections were flooded, the sagged condition decreased, resulting in lower bending moments. Thus it was concluded that despite the initial risk of hull collapse, the damage itself prevented the ship from breaking in half.

The results presented here served as a means to fill the vacuum in the area of knowledge and determine how the S.S. Ohio survived her onslaught. In addition, the research shed light on stability, floodable length and residual strength of the S.S. Ohio. The information provided will answer some of the longstanding questions on how the S.S. Ohio saved Malta.

11. ACKNOWLEDGEMENTS

Acknowledgements go to:

- Allan Shaw - S.S. Ohio veteran
- Anne Cowne - LR
- Antonio Prestigiacomo - LR
- Bertin Rodolphe - STX Europe
- Emmanuel Magro Conti - Malta Maritime Museum Curator
- Gian Luca Mantegazza – RINA
- Howard Clayton - ABS

- Joep Bollerman - LR
- Joep Broekhuijsen - Damen Schelde Naval Shipbuilding
- Joerg Poettgen - Meyer Werft
- John Harper - Chevron Corporation
- Jörg Peschmann - DNVGL
- Joseph Stephen Bonnano - U-Boat Navigator
- Kim E. Demory - USCG
- Kurt Guttridge - Naval Architecture Services
- Leslie Schembri - ABS
- Marcus J. Akins - USCG
- Mark Beswick - UK Met Office National Meteorological Archive
- Michael Pearson - Author of *The Ohio and Malta – The Legendary Tanker that Refused to Die*
- Neville Galea Pirotta - Geography & Creative Art Teacher, St. Michael's School
- Patrick Camilleri - S.S. Ohio aesthetic model builder
- Patrick Chaurand - STX Europe
- Paul Caruana - Historian
- Rosalie van Egmond - Shell International B.V.
- Simon Cusens – Historian

12. REFERENCES

22. ADMIRALTY, "Ohio War Loss Cards," Guildhall Library, London, UK, 1942-1946.

36. AMERICAN BUREAU OF SHIPPING, *1938 ABS Rules for Building and Classing Steel Vessels*. 1938.

41. AMERICAN BUREAU OF SHIPPING, "Part 3 - Hull Construction and Equipment," in *Rules for Building and Classing Steel Vessels*, ABS, 2015, pp. 32-63.

15. BAILEY, D., *The NPL High Speed Round Bilge Displacement Hull Series: Resistance, Propulsion, Manoeuvring and Seakeeping Data.* Royal Institution of Naval Architects, 1976.

24. BARTON, D. E, "Operation Pedestal - M/011281/42," London National Archives - ADM1/15526, United Kingdom, 1942, August 20.

20. BENFORD, H. "The Practical Application of Economics to Merchant Ship Design," *Journal of Marine Technology*, 1967, January.

14. BENTLEY SYSTEMS MAXSURF 20.04 V8I SUITE SOFTWARE, (2014, January 6) "Maxsurf - Naval Architecture Software for all Types of Vessels", https://www.bentley.com/~/asset/14/2708.ashx [Accessed 2014, February 10]

3. BOGART, C. H. "Operation Pedestal," *Steamboat Bill*, vol. LI, No.3, pp. 173-185, 1994.

13. CARUANA, J., "Ohio Ordeal," *The Sunday Times*, 1992.

11. COOK, H. E. "Operation Pedestal and the Siege of Malta, August 1942," *Imperial War Museum*, vol. IWM GM 1480.

19. GANESAN, V. "A Model for Multidisciplinary Optimization of Containerships," Virginia Polytechnic Institute and State University, July, 1999.

39. GRAY, D. H. "Report by Chief Officer D. H. Gray," Shell Historical Archives, The Hague (SLA), SC 88/5 file 1. 1942.

10. HOLLAND, J. *Fortress Malta.* UK: Orion Books Ltd., 2003.

44. HORTE, T. SKJONG, R. FRIIS-HANSEN, P. TEIXEIRA, A.P. and VIEJO DE FRANCISO, F. "Probabilistic Methods Applied to Structural Design and Rule Development," *Developments in Classification and International Regulations*, 2007.

33. INTERNATIONAL COMMUNITY, "SOLAS Chapter II: Construction, Part B: Subdivision and Stability, Regulation 7 - Stability of Ships in Damaged Condition," in *SOLAS Convention*, Consolidated Edition, London, UK: International Maritime Organization, 1948, June 10.

35. INTERNATIONAL COMMUNITY, "SOLAS Annex I - Construction," in *International Convention for the Safety of Life at Sea* 1929, May 31.

27. INTERNATIONAL MARITIME ORGANIZATION (IMO), *International Code on Intact Stability, 2008, Chapter 2 – General Criteria*. London, UK: International Maritime Organization, 2009.

28. INTERNATIONAL MARITIME ORGANIZATION (IMO), "MARPOL Annex I: Regulations for the Prevention of Pollution by Oil, Regulation 27 - Intact Stability," in *MARPOL Convention*, Consolidated Edition ed. London, UK: International Maritime Organization, 2011.

34. INTERNATIONAL MARITIME ORGANIZATION (IMO), "SOLAS Chapter II-1: Construction - Structure, Subdivision and Stability, Machinery and Electrical Installations, Regulation 4 -General," in *SOLAS Convention*, Consolidated Edition, London, UK: International Maritime Organization, 2014a.

38. INTERNATIONAL MARITIME ORGANIZATION (IMO), "SOLAS Chapter II-1: Construction - Structure, Subdivision and Stability, Machinery and Electrical Installations, Part A-1 - Structure of Ships, Regulation 3-1 - Structural, Mechanical and Electrical Requirements for Ships," in *International Convention for the Safety of Life at Sea (SOLAS), 1974, as amended*, Consolidated Edition, London, UK: International Maritime Organization, 2014b.

26. JEROME, H. J. A. S. "Report on Operation "Statue" from the evening of Wednesday, 12th to 0800 of Saturday, 15th of August," London National Archives - ADM1/15526, United Kingdom, 1942, August 26.
37. LLOYD'S REGISTER, *Lloyd's Register of Shipping - Rules and Regulations 1938-1939*. UK: LR, 1938.
17. LLOYD'S REGISTER, *S.S. Ohio Scantlings and General Arrangement Plan*. Royal Museums Greenwich, London, UK. 1939.
7. LLOYD'S REGISTER, "S.S. OHIO - CLASS SURVEY REPORT," TECH. Rep. 7881, 1940, July 31.
8. LLOYD'S REGISTER MARINE, "Classification," in *Classification and Statutory Surveys*, London, UK: LR Marine Training Services, 2014a, pp. 1-12.
40. LLOYD'S REGISTER, "Part 4 - Ship Structures (Ship Types), Chapter 9 - Double Hull Oil Tankers, Section 3 - Longitudinal Strength," in *Rules and Regulations for the Classification of Ships*, LR, 2014b, January.
9. LUCAS, L. *Malta - The Thorn in Rommel's Side*. UK: Penguin Group, 1993.
25. MASON, D. W. "Report by Captain Dudley. W. Mason," Shell Historical Archives, The Hague (SLA), SC 88/5 file 1. 1942.
45. MET OFFICE NATIONAL METEOROLOGICAL ARCHIVE, *Climatological Return for Valletta for August 1942 and Northern Atlantic Charts which Cover the Mediterranean for 1st to 15th of August 1942*. Exeter, United Kingdom.
32. NICKUM, G. C. "Subdivision and Damage Stability," in *Stability and Strength*, 1st ed., E. V. Lewis, Ed. USA: The Society of Naval Architects and Marine Engineers, 1988, pp. 111-194.
42. PAIK, J. K. THAYAMBALLI, A. K. and HONG YANG, S. "Residual Strength Assessment of Ships After Collision and Grounding," *Mar. Technol. SNAME News*, vol. 35, pp. 38, Jan 1998.
1. PEARSON, M. *The Ohio and Malta: The Legendary Tanker that Refused to Die*. England: Pen and Sword Books, 2004.
29. RIDLEY, J. and PATTERSON, C. "Large Angle Stability - Just How Far Can She Roll?" in *Reeds Vol 13: Ship Stability, Powering and Resistance*, Bloomsbury Publishing, 2014.
18. SCHNEEKLUTH, H. and BERTRAM, V. "Chapter 5: Computation of Weights and Centres of Mass," in *Ship Design for Efficiency and Economy*, 2nd ed. Oxford, UK: Butterworth-Heinemann, 1998, pp. 149.
12. SHANKLAND, P. and HUNTER, A. *Malta Convoy*. UK: Fontana Press, 1983.
30. SHAW, A. "S.S. Ohio Related Queries - Personal Communication with Allan Shaw via E-mail," 2014, January 4.
31. SHIROKAUER, F. *A Simplified Method for Exact Arithmetical Determination of Bulkhead Curves*. 1928.
21. SMITH, P. *Pedestal - the Convoy that Saved Malta*. England: Crecy Publishing Limited, 1970.
43. TEIXEIRA, A. P. and GUEDES SOARES, C. "Reliability Assessment of Intact and Damaged Ship Structures," in *Advanced Ship Design for Pollution Prevention*, Split, Croatia, 2009, pp. 79-96.
2. THE TEXAS COMPANY, "1939-1940 S.S. Ohio Sun Shipbuilding Construction Reports," Chevron Corporation, California, USA, 1940a.
5. THE TEXAS COMPANY, "Trial Trip of a Texaco Tanker," *The Texaco Star*, vol. 27, pp. 14-17, 1940b.
4. UK MINISTRY OF WAR TRANSPORT, "Transcript of Register for Transmission to Registrar General of Shipping and Seamen," 1942, June 29.
6. UNITED STATES COAST GUARD, "Ohio Registration Card - ON: 239732," 1942, June 2.
16. US MARITIME ADMINISTRATION, "Historic American Engineering Record – USS Saugatuck T2-SE-A1," *HAER*, vol. HAER No. VA-128, 2006.
23. WYLD, J., "Report by Chief Engineer Mr. J. Wyld," Shell Historical Archives, The Hague (SLA), SC 88/5 file 1. 1942.

SAFE MOORING OF LARGE CONTAINER SHIPS AT QUAY WALLS SUBJECT TO PASSING SHIP EFFECTS

(DOI No: 10.3940/rina.ijme.2017.a4.441)

T Van Zwijnsvoorde and **M Vantorre**; Ghent University, Belgium.

SUMMARY

Container traffic and individual ships' sizes increased dramatically over the last decades, testing the existing harbour infrastructure to its limits. An important aspect regarding the safety of the berthed vessel is the quality of the mooring configuration. A case study is presented, where an 18000 TEU container vessel is moored at a quay. The motions of the moored vessel and the forces in its lines due to ship passages are simulated, using the potential software ROPES and the UGent in-house package Vlugmoor. Focus is on the mooring plan (operational parameter) and the characteristics of the individual lines (design parameter).

NOMENCLATURE

B	Beam (m)
C_B	Block coefficient (-)
D	Depth of the vessel (m)
F_{br}	Breaking load line (ton)
$F_{br,r}$	Maximum force in mooring line, relative to breaking load (-)
$F_{fen,br}$	Fender capacity (ton)
$F_{fen,r}$	Maximum load in fender, relative to fender capacity (-)
l	Length of the rope (m)
L_{pp}	Length between perpendiculars (m)
n	Number of lines (-)
$O_{x,y,z}$	Earth bound axis system (-)
T	Draft (m)
ukc	Under keel clearance (%)
x	Longitudinal position centre of gravity moored vessel in $O_{x,y,z}$ (m)
X_p	Passing ship force: longitudinal component (kN)
y	Transversal position centre of gravity moored vessel in $O_{x,y,z}$ (m)
y_a	Transversal position aft perpendicular in $O_{x,y,z}$ (m)
y_f	Transversal position fore perpendicular in $O_{x,y,z}$ (m)
Y_{pa}	Passing ship force: transversal component aft perpendicular (kN)
Y_{pf}	Passing ship force: transversal component fore perpendicular (kN)
Δ	Displacement vessel (ton)
Δx_{max}	Maximum longitudinal motion amplitude (m)
$\Delta y_{a,,max}$	Maximum transversal motion amplitude, at aft perpendicular (m)
$\Delta y_{f,max}$	Maximum transversal motion amplitude, at fore perpendicular (m)
$\Delta y_{m,max}$	Maximum transversal motion amplitude, at midship (m)
ε	Strain of the rope (%)
ε_{10}	Strain at 10% of the breaking load (%)
ε_{br}	Strain at breaking load (%)
ξ	Dimensionless x-position of the passing vessel in $O_{x,y,z}$
EN	Equipment number
HMPE	High Modulus PolyEthylene
IACS	International Association of Classification Societies
IMO	International Maritime Organisation
OCIMF	Oil Companies International Marine Forum
SIGTTO	Society of International Gas Tanker and Terminal Operators

1. INTRODUCTION

The container shipping industry has the biggest share in worldwide transport nowadays, combined with a substantial growth in container ship size (Lloyd's Register, QinetiQ, Strathclyde University, 2013), this leads to a congestion of existing channels and terminals. This paper addresses the safety of moored vessels in case of passing ship events, focussing on the mooring configuration itself, not on the parameters defining the passing event (ship speed, passing distance,…). The configuration consists of the mooring plan and the individual characteristics of lines and fenders. The discussion in this paper focusses on the properties of the lines (design parameter) and their spatial configuration (operational parameter).

Present regulatory bodies as IMO and the IACS, do not impose regulations with regard to the mooring plan and the stiffness of the individual lines. Only the required breaking strength and number of lines is imposed. This is in sheer contrast with the oil and gas industry, where OCIMF and SIGTTO implement requirements for mooring plans and characteristics of the individual lines. These requirements cannot be copied directly, as the force dynamics are different when vessels are moored at a quay. The bollard configuration also differs, as the bollard pattern must not interfere with the tracks of the gantry cranes.

For evaluation of the simulation results, criteria are required. For periodic loads (e.g. waves), maximum significant motions are defined by PIANC, as a result of a probabilistic study, demanding 95% efficiency of the terminal operations. As a passing event is limited in time, it hardly influences the overall efficiency over a larger time window. The attention shifts here to the safety of the (un)loading operation.

A case study is presented, considering 18000 TEU container vessels, based on experience on mooring studies in Flemish ports. Simulations are performed using the potential code ROPES to calculate the passing ship forces and the in-house tool Vlugmoor to evaluate the motions of the moored vessel and the forces in lines and fenders.

The case study is used to illustrate the shortcomings in international regulations, which were mentioned earlier. Having the reference case for comparison, the influence of design and operational aspects on the quality of the mooring operation is discussed. From a design perspective, different rope materials are investigated, focussing on main materials, rather than specialised (modified) brands of ropes. The importance of the elasticity of the lines is highlighted.

The mooring plan is discussed from an operational point of view, assuming that the positions of winches, fairleads and bollards are fixed. The reference mooring plan which is presented is a configuration which has been observed in practice. An optimisation of this configuration is discussed in this paper. The influence of an unbalanced pattern, resulting from a lack of available bollards due to reduced space in between two moored ships, is shown as well. The importance of providing pretension, and thus avoiding slack, is presented in a last discussion.

2. PRODUCTION OF MOORING LINES: A GLOBAL MARKET

The expertise in rope design and production is present worldwide and globalisation offers the possibility to ship-owners to seek the best ropes for their specific needs. IMO (IMO, 2005) and IACS (IACS, 2005) mention similar regulations with respect to the needed number of lines, their strength and the minimum length of each of the individual lines, based on the equipment number of the vessel (EN). This is discussed further in section 5.2. The elasticity of the lines is not regulated, which is a severe shortcoming, as the elasticity is a crucial aspect of the line as it defines the dynamic behaviour of the vessel.

The stiffness of the ropes is primarily a function of the main material which is used. Nylon lines are very flexible lines, whereas steel lines are extremely stiff. Production techniques offer possibilities to modify the specifications of these main materials (strength, elasticity, handling, UV and thermal resistance,…). Rope suppliers often dispose of their own certified ropes, which incorporate specialised production techniques. As the aim of the paper is to discuss the general behaviour of lines, without any commercial interference, the lines are subdivided based on the characteristics of the main materials. Table 1 shows the stress-strain behaviour of five main materials, based on the specifications obtained from six rope manufacturers.

Table 1: Stress-strain behaviour of mooring lines as a function of the main materials.

Base material	**ε_{10} [%]**	**ε_{br} [%]**
Steel	0.2	2
HMPE	0.5	5
Polyester	3	15
Polypropylene	4	20
Nylon	10	30

Table 1 shows the breaking strain (ε_{br}) of the lines and the strain of the rope at 10% of the breaking load (ε_{10}), which indicates the non-linearity in the lines. Steel and HMPE lines show a linear stress-strain curve, whereas the nylon ropes are denoted by a limited stress build-up for small loads.

3. SAFE MOORING OF CONTAINER VESSELS

The topic of ship safety involves two aspects. The safety of moored vessels can be increased by imposing regulations with regard to mooring configurations. In order to evaluate the safety of the moored vessel during (un)loading operations, safety criteria need to be defined. Both aspects are discussed from the perspective of passing ship events.

3.1 EXISTING REGULATIONS

For container vessels, there is general lack of clear regulations with an international significance, apart from the IMO and IACS cited earlier, which fail to incorporate regulations regarding the mooring plan and elasticity of the lines. For oil and gas tankers, OCIMF and SIGTTO, provide guidance on lines and mooring plans, which are in general practice translated into terminal guidelines. These rules do not cover container vessels, or more in general vessels moored at a quay wall. Not only are the force dynamics different, as is shown in section 5.3, the general layout of the terminal differs entirely, with regard to the bollard positioning. The case studies in this paper show that there is an urgent need to produce some sort of international recommendations or even regulations, in order to guarantee safe mooring conditions at quay walls, for ever increasing ship sizes.

3.2 DEFINING CRITERIA FOR SAFE MOORING

Defining criteria for safe mooring of large container vessels is a challenging matter, as it involves a good understanding of the parameters which are of interest (motions and forces). The forces in the ropes are limited by the breaking strength of the rope, but foremost by the holding capacity of the winches, which is usually around 60% of the breaking force of the lines. The forces which can develop in the fenders are a function of the properties of the individual fenders and fall outside of the scope of the current paper. In general, it is expected that the fenders start to show plastic deformation at around 90% of their maximum capacity.

Defining limits for ship motions is a more challenging field, as they are a function of the nature of the applied load, more specific of its periodicity and the evaluation procedure. PIANC WG 115 (PIANC, 2012) has published a dedicated report on this subject, focussing on a variety of environmental forces and determining criteria based on the results of a probabilistic study, demanding a 95% efficiency of the (un)loading operation. The focus on efficiency is understandable, when (mainly) periodic forces are acting on the moored vessel. An example here is a berthed vessel exposed to incoming swell. The result of the calculations is a significant motion. A passing event should however be seen as a stand-alone event, which only has limited influence on the long-term efficiency of the operation. The focus here is on the safety of the moored vessel, quay wall and shore-based equipment, passing vessel and not to forget the wellbeing of workers on board and on shore.

Regarding the safety aspect, the longitudinal ship motions, along the quay wall, are most critical. A catastrophic event would be a collision between a gantry crane (or its spreader) and the accommodation or funnel. As the shipping companies are forced to offer the lowest rates, due to international competition, they need to use each square metre of the vessel as efficient as possible. Often the distance between container and accommodation will be limited to 1.0 m, which means that this is a upper limit for longitudinal motions. Even at lower motions, dangerous situations may arise, thinking of accidents regarding gangways, damage to containers and injuries (or even casualties) amongst crew members.

4. SIMULATION OF PASSING EVENTS

Simulation studies are a fast and efficient method to execute a systematic mooring analysis, replacing expensive model testing. For this case study, the forces induced by the passing vessel are calculated using the potential code ROPES. The analysis of the motions and mooring line forces is performed using the in-house package Vlugmoor. As these models always incorporate a simplified representation of the real-life situation, the user needs to be aware of the opportunities and drawbacks of using a specific numerical tool.

4.1 ROPES

The ROPES software tool is a potential double body flow method, developed by PMH (Pinkster & Pinkster, 2014), which has been validated with model tests performed at several leading model test facilities (Van Wijhe & Pinkster, 2008), including Flanders Hydraulics Research in Antwerp, Belgium. The assumption of the flow being inviscid, irrotational and incompressible is valid, as long as no (large) flow separation zones are present. Flow separation typically occurs when ships pass with a non-zero drift angle (Talstra & Bliek, 2014) or in case of entering a narrow channel or lock (Toxopeus & Bhawsinka, 2016). The double body theory assumes a rigid surface, which means that no free surface effects are taken into account. This has two important consequences. Long waves, generated by the passing vessel, cannot be simulated (Pinkster, 2004). The passing ship's squat is also not incorporated in the model, which means that the effect on the under keel clearance (ukc) of the vessel is not taken into account. As a consequence the passing ship forces are under-predicted in shallow water at high passing speeds. A correction factor, based on the depth based Froude number, as proposed in (Talstra & Bliek, 2014), is included in Vlugmoor.

4.2 VLUGMOOR

Vlugmoor is the in-house tool, developed and used at the Maritime Technology Division of Ghent University to simulate the dynamic behaviour of a moored vessel. The calculations are performed in the time domain, evaluating the force equilibrium at each time step. The resulting motions are used as input for the next step. Vlugmoor has been validated in a non-published thesis work and is used frequently to perform mooring studies for Flemish ports.

5. CASE STUDY: MOORED 18000 TEU CONTAINER SHIP

Based on the experience gained by performing mooring studies for Flemish ports, a case study is presented in this paper. This chapter elaborates on the passing event and mooring parameters, which define the reference case.

5.1 PASSING EVENT

The passing event has been carefully selected, in order to represent a real-life case, without reaching the limitations of the software tools. Figure 1 shows the passing event at a busy container terminal, where the waterway section is restricted in width and depth, resulting in a limited passing distance and ukc value. The channel is modelled as a rectangular section with a width of 450 m and a uniform water depth of 18.24 m, which results in a 20% ukc. As the market share of ultra large container carriers increases, it is plausible that moored and passing vessel are 18000 TEU container vessels.

The quay wall is assumed to be a continuous structure, avoiding transitions in flow sections, which would call for the use of CFD or model tests. The passing distance, measured side-to-side is two and a half times the beam of the vessel. The ukc is 20%, which means that the correction factor for free surface effects needs to be applied. The 18000 TEU container ship passes at 6 knots, sailing both in- and outbound. The simulations of both passing events is necessary, because the mooring configuration is not symmetrical, due to the difference between the layout of fore and aft ship.

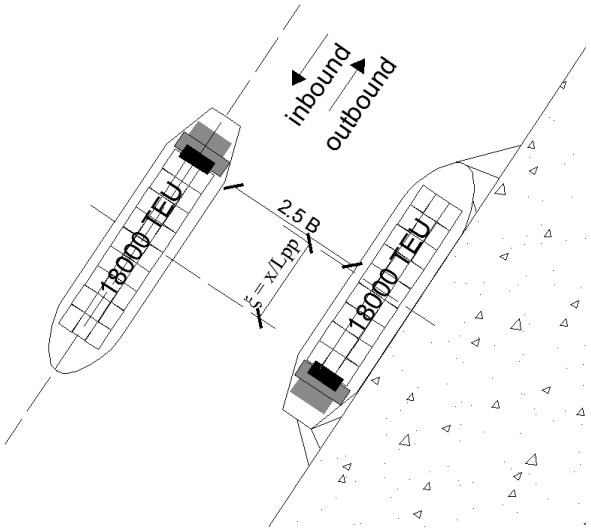

Figure 1: Case study: reference passing event at a congested container terminal. (inbound passing vessel is shown).

In Figure 1, the dimensionless parameter ξ expresses the relative position of the passing vessel with respect to the moored vessel during the passing event. Further insight regarding this parameter is given in section 5.3, where the forces acting on the moored vessel are given as a function of this parameter ξ.

5.2 MOORING LINES AND PLAN

The characteristics of the 18000 TEU container carriers are given in Table 2. The vessel is equipped with 16 polyester ropes, with a breaking strength of 140 tons. These values are chosen based on practical experience and exceed the demands of IMO and IACS. For the vessel defined in Table 2, the EN number is 9992, requiring 14 lines with a F_{br} of 75 tons. The total capacity of the lines, expressed as the product of the individual breaking strength and the number of lines is more than double the required value according to IMO.

The fenders, which are less of interest for this paper, have a capacity of 396 tons and a maximum compression of 0.24 m. It is assumed that the fenders deform in a linear way. A detailed study of the fender friction is outside of the scope of this paper, as there exists a variety in materials and coefficients. For this paper, a conservative approach is followed, limiting the friction to a constant value of 2% of the normal force on the fender. All bollards are aligned with the quay side, spaced 20 m apart and are designed as double bollards. Each individual bollard can support two lines with a F_{br} of 140 tons.

Table 2: Characteristics 18000 TEU container carrier.

L_{OA} [m]	399.00	**$F_{fen,br}$ [ton]**	396
L_{pp} [m]	376.00	**F_{br} [ton]**	140
B [m]	59.00	**ε_{br} [%]**	15
T [m]	15.20	**l [m]**	200
C_b [-]	0.73	**n [-]**	16
D [m]	30.20	**EN [-]**	9992
Δ [ton]	264343		

The lines pattern which is used is a function of design parameters (winch, fairlead and bollard positioning) and operational considerations (available space, influence of tide / changing draft, skill of the crew). In this paper, it is assumed that the design parameters are fixed, in order to focus on the operational parameters which affect the mooring plan. Figure 2 shows the mooring plan which is used as reference in this case study. This mooring plan has been defined based on plans of an existing ultra large container vessel. It is indicated as mooring plan A. The earth bound axis system $O_{x,y,z}$ is also defined, with as origin the initial centre of gravity of the moored vessel. The x-axis is defined parallel with the quay wall. A right-handed coordinate system is used. The lines are modelled between the bollard on the quay and the fairlead, considering an equivalent breaking strain to account for the line section between the winch and the fairlead.

The spatial configuration shown in Figure 2 is an example of a well-balanced mooring plan, which is able to cope well with passing ship forces, when the ship is moored at a quay wall.

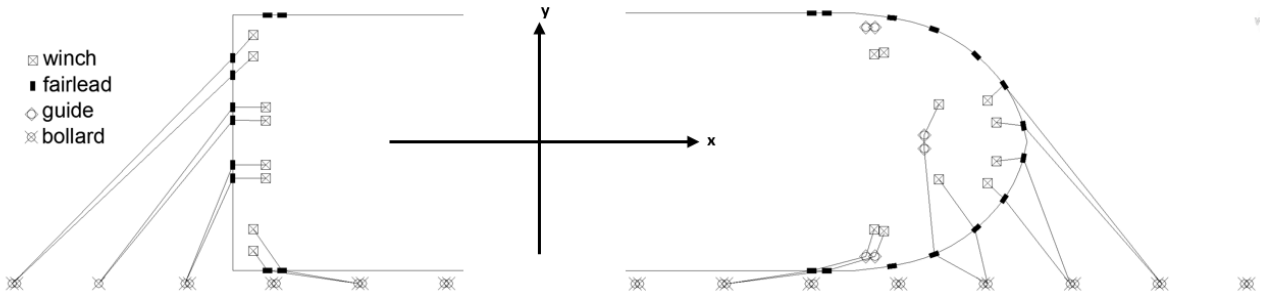

Figure 2: Mooring plan A, with indication of bollards, winches, guides and fairleads on the vessel and bollards on the quay. Definition of right-handed, earth-bound coordinate system $O_{x,y,z}$.

5.3 RESULTS REFERENCE MOORING SIMULATION (MOORING PLAN A)

Based on the defined case study parameters, the mooring simulation is performed, consisting of the ROPES and Vlugmoor calculations. The results of the ROPES simulation are given in Figure 3. The vertical axis shows the passing ship forces and the horizontal axis the relative position of passing and moored vessel, as defined in Figure 1 , with x (and thus ξ) according to the earth bound axis system $O_{x,y,z}$. (Figure 2). All the graphs shown in this paper have ξ as abscissa. The results are expressed as longitudinal forces (X_p) and a transversal force fore (Y_{pf}) and aft (Y_{pa}).

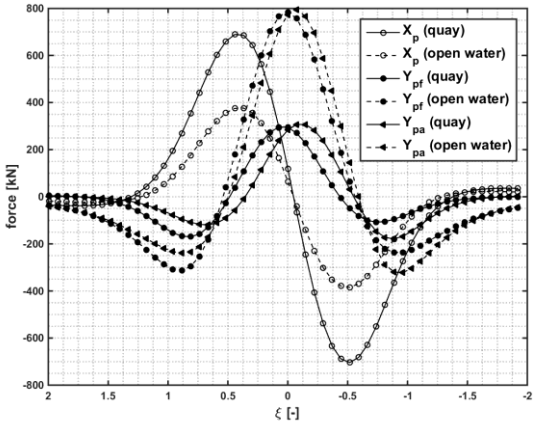

Figure 3: Passing ship forces (X_p, Y_{pf}, Y_{pa}): quay wall and open water case; inbound passing vessel.

In Figure 3, the starting position of the vessel is $\xi = 2.0$ and it sails towards the end location, given by $\xi = -2.0$. As the inbound sailing vessel approaches the moored vessel ($2.0 > \xi > 0.5$), the moored vessel is pushed towards the quay and rotates clockwise ($\xi = 1.0$) . This is confirmed by a Y_{pf} which is more negative than Y_{pa}, indicating a clockwise rotation. The moored vessel is pulled towards the approach direction of the passing vessel (positive X-force), reaching the maximum force around $\xi = 0.5$. When the vessels' midships are in the same (longitudinal) position ($\xi = 0$), there is no longitudinal force. There is however a strong suction force in the direction of the channel, indicated by a positive transversal force. For ($-2.0 < \xi < -0.5$), the moored vessel wants to follow the passing vessel (negative X-force, maximum at $\xi = -0.5$) and the vessel is pushed towards the quay ($\xi = 1.0$).

In figure 3, the forces acting on the moored ship with and without the presence of the quay wall are given, to emphasize the difference between the open water case and mooring a vessel at a quay wall. When a quay wall is present, the longitudinal force increases, whereas the transversal force decreases, compared to the open water case (Varyani, 2008).

Vlugmoor simulates the behaviour of the moored vessel during the ship passage, giving the forces in lines and fenders and the motions of the moored vessel, as functions of time. The pretension, which is equal to 10% of F_{br}, is applied at the start of the simulation in all lines. The forces are slightly redistributed to attain a reference equilibrium position. This equilibrium is reached before the passing ship forces affect the moored vessel.

Figure 4 shows the motions of the moored vessel during the passage. The vertical axis gives the longitudinal position of the moored vessel's centre of gravity, in the $O_{x,y,z}$ system and transversal position of the fore and aft perpendicular. It can be observed that the longitudinal motions (difference in x-positions) are significant, whereas the transversal motions (difference in y-positions) are limited.

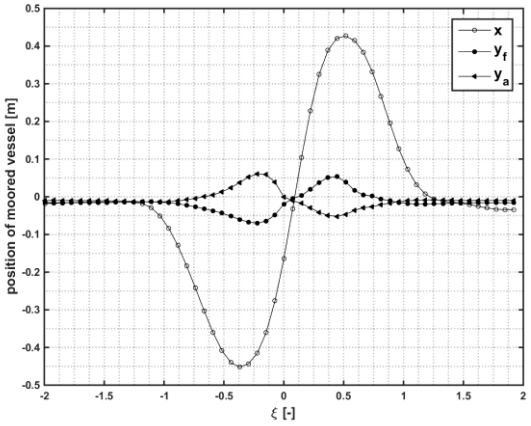

Figure 4: Position of the moored vessel (x, y_f, y_a) as a function of the position of the passing vessel relative to the moored vessel; outbound passage.

Table 3 : Results mooring analysis (mooring plan A).

$F_{br,r}$ [-]	0.23	Δx_{max} [m]	0.46	$\Delta y_{f,max}$ [m]	0.09
$F_{fen,r}$ [-]	0.11	$\Delta y_{m,max}$ [m]	0.02	$\Delta y_{a,max}$ [m]	0.07

Table 3 gives an overview of the simulation results, displaying the maximum forces and motions, resulting from either inbound or outbound passing events, depending on whichever is the highest. The maximum force in lines and fenders is expressed relative to the breaking strength of the lines and the capacity of the fenders, respectively. The motions are expressed as motion amplitudes, relative to the equilibrium position, which is reached after applying pretension in the lines. The maximum longitudinal motion amplitude is given by Δx_{max}. The transversal motions at the midship, the fore and aft perpendicular, are given by $\Delta y_{m,max}$, $\Delta y_{f,max}$ and $\Delta y_{a,max}$, respectively. The results show that the forces are limited, whereas the longitudinal motion reaches 0.46 m. The transversal motion is limited, which follows from the decrease in transversal forces when mooring at a quay wall, compared to the open water case (Figure 3).

6. INFLUENCE OF MOORING LINE CHARACTERISTICS (DESIGN PARAMETER)

Container ships are equipped with varying types of mooring ropes. All ropes within the range defined in Table 1 are found on large container vessels. A change in elasticity of lines, alters the behaviour of the moored vessel substantially, as is shown in Table 4. It is assumed that the breaking load of the lines is 140 tons for all lines, despite varying strengths (N/mm²) of the main materials. In practice, these lines will have different diameters. A nylon line with a diameter of 104 mm, with a weight of 6.66 kg/m has the same strength as a 48 mm HMPE line, with a weight of 1.27 kg/m. This will have consequences for the handling, but has no influence on the simulation results.

Table 4 shows that the longitudinal motions, which are the most critical motion because of safety reasons, vary between 0.17 m for very stiff HMPE lines, over 0.46 m for common polyester lines, to 0.84 m for highly elastic nylon lines. This means that whereas the ship hardly moves when using stiff lines, the motions become unacceptable when elastic lines are used. It is thus very important that ropes are not only categorised according to breaking strength, but that the stress-strain properties should be taken into account as well when imposing regulations.

We can conclude that for the specific case of a passing container vessel, the use of stiff lines is recommended. One must keep in mind that stiff lines lead to a high eigenfrequency of the system, which means that it is susceptible to (short) waves (Varyani, 2008). This can be solved by working with medium stiff lines (polyester), or by adding nylon tails to the stiff lines to increase the flexibility and lower the eigenfrequency.

Table 4: Results mooring analysis – influence of the elasticity of the mooring lines (mooring plan A).

Line	**HMPE**	**ε_{10} [%]**	**0.5**	**ε_{100} [%]**	**5**
$F_{br,r}$ [-]	0.23	Δx_{max} [m]	0.17	$\Delta y_{f,max}$ [m]	0.06
$F_{fen,r}$ [-]	0.09	$\Delta y_{m,max}$ [m]	0.02	$\Delta y_{a,max}$ [m]	0.03
Line	**Polyester**	**ε_{10} [%]**	**3**	**ε_{100} [%]**	**15**
$F_{br,r}$ [-]	0.23	Δx_{max} [m]	0.46	$\Delta y_{f,max}$ [m]	0.09
$F_{fen,r}$ [-]	0.11	$\Delta y_{m,max}$ [m]	0.02	$\Delta y_{a,max}$ [m]	0.07
Line	**Nylon**	**ε_{10} [%]**	**10**	**ε_{100} [%]**	**30**
$F_{br,r}$ [-]	0.24	Δx_{max} [m]	0.84	$\Delta y_{f,max}$ [m]	0.11
$F_{fen,r}$ [-]	0.13	$\Delta y_{m,max}$ [m]	0.03	$\Delta y_{a,max}$ [m]	0.11

7. INFLUENCE OF THE MOORING PLAN (OPERATIONAL PARAMETER)

In this section, we discuss the mooring arrangement from an operational point of view, which means that the position of bollards, winches and fairleads (design parameters) is assumed to be fixed. The aim is to show the importance of achieving, and most importantly maintaining an optimal mooring configuration. Providing terminal guidelines, combined with training and supervision of crew, are vital to ensure a safe mooring operation.

The following topics are addressed:

- Optimising the mooring plan (section 7.1);
- Consequences of an unbalanced mooring configuration (section 7.2);
- Importance of providing pretension (section 7.3).

7.1 OPTIMISING THE MOORING PLAN

The biggest drawback of using ropes to moor a vessel, is that they need to stretch before they can take up loads, which means that the ship must move to start generating reaction forces. Certainly for stiff lines, it is critical that the lines have similar lengths, so that they are all loaded simultaneously. In general, fore and aft lines are longer lines, which will thus build up less forces than spring and breast lines. They are also less suited to cope with pure longitudinal or transversal forces. These shortcomings are counteracted by allowing lines to cross each other, as is shown in Figure 5. This configuration leads to a more efficient use of all the lines. The simulation results are given in Table 5. The results for mooring plan A are repeated, to allow direct comparison between the results.

Table 5 : Results mooring analysis – crossing fore and aft lines (mooring plan B).

Mooring plan A					
$F_{br,r}$ [-]	0.23	Δx_{max} [m]	0.46	$\Delta y_{f,max}$ [m]	0.09
$F_{fen,r}$ [-]	0.11	$\Delta y_{m,max}$ [m]	0.02	$\Delta y_{a,max}$ [m]	0.07
Mooring plan B					
$F_{br,r}$ [-]	0.22	Δx_{max} [m]	0.40	$\Delta y_{f,max}$ [m]	0.03
$F_{fen,r}$ [-]	0.06	$\Delta y_{m,max}$ [m]	0.01	$\Delta y_{a,max}$ [m]	0.02

When the optimised mooring plan is considered, the transversal motion of the vessel becomes next to nothing. The longitudinal motion decreases with 13% with respect to mooring plan A (Figure 2). It is important to remark that the configuration shown in Figure 5 can only be obtained if the fairleads are positioned higher than the bollards at the quay at all times. This could be problematic at tidal terminals and with vessels having a smaller freeboard.

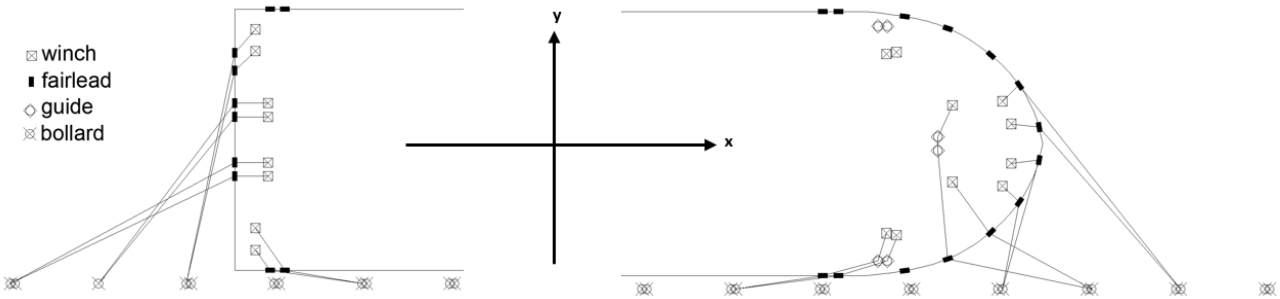

Figure 5: Mooring plan B: optimising plan A, by implementing crossing fore and aft lines.

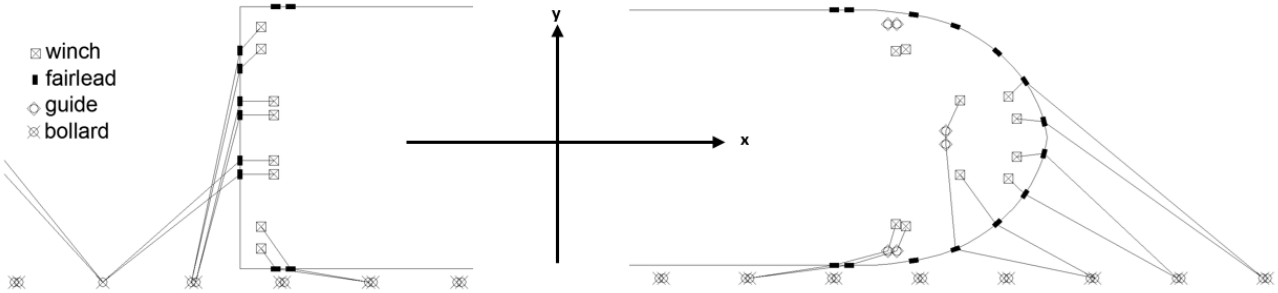

Figure 6: Mooring plan C: unbalanced mooring line configuration.

7.2 UNBALANCED CONFIGURATION

Existing container terminals accommodate as many container vessels as possible, in order to maximize the terminal occupation. As the main dimensions of these vessels have increased drastically in the last decades, existing terminals need to decrease the space in between moored container vessels, which leads to a shortage of bollards to moor the vessel adequately. An example of an unbalanced mooring configuration is given in Figure 6.

In Figure 6, the number of bollards which is available for the aft lines is restricted, due to the presence of another container vessel at the terminal. To make to situation even worse, the fore lines are almost parallel to the quay, resulting in a lack of fore breast lines. The simulation results are shown in Table 6, together with the results for plans A and B.

Table 6: Results mooring analysis – unbalanced mooring configuration (mooring plan C).

Mooring plan A					
$F_{br,r}$ [-]	0.23	Δx_{max} [m]	0.46	$\Delta y_{f,max}$ [m]	0.09
$F_{fen,r}$ [-]	0.11	$\Delta y_{m,max}$ [m]	0.02	$\Delta y_{a,max}$ [m]	0.07
Mooring plan B					
$F_{br,r}$ [-]	0.22	Δx_{max} [m]	0.40	$\Delta y_{f,max}$ [m]	0.03
$F_{fen,r}$ [-]	0.06	$\Delta y_{m,max}$ [m]	0.01	$\Delta y_{a,max}$ [m]	0.02
Mooring plan C					
$F_{br,r}$ [-]	0.26	Δx_{max} [m]	0.61	$\Delta y_{f,max}$ [m]	0.54
$F_{fen,r}$ [-]	0.23	$\Delta y_{m,max}$ [m]	0.19	$\Delta y_{a,max}$ [m]	0.16

Table 6 shows a hefty increase of the motions of the moored vessel. The imbalance of the configuration not only causes an increase in longitudinal motions, it also leads to a transversal motion which is six times higher than in the reference case, due to the yaw motion of the moored vessel. Figure 7 shows the longitudinal motion and the transversal motion of the fore perpendicular, with as abscissa the position of the passing vessel.

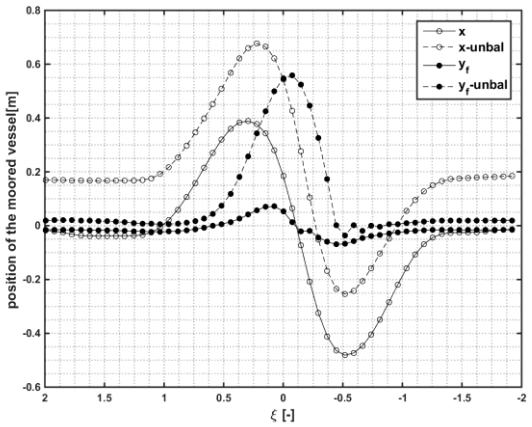

Figure 7: Comparison of x and y_f between the reference configuration (mooring plan A) and the unbalanced configuration (mooring plan C); inbound passage.

7.3 SLACK IN THE SPRING LINES

Even when a good mooring plan is delivered and executed in a satisfying way, maintaining this configuration, with emphasis on the pretension in the lines, is a demanding job. For a start, sufficient highly trained crew members are needed. Additionally, supervision by terminal operators or port authorities is recommended. The captain of the ship must be involved in this process.

As the longitudinal motions are the most critical, we assume in the following example that the pretension in the springs is absent. A possible cause is a change in draft during the (un)loading process and/or a change of water level due to tide. Table 7 shows the simulation results in case pretension is missing in the springs and in case a slack of 1.0 m is present.

Table 7: Results mooring analysis – no pretension and slack in spring lines (mooring plan A).

Pretension in all lines					
$F_{br,r}$ [-]	0.23	Δx_{max} [m]	0.46	$\Delta y_{f,max}$ [m]	0.09
$F_{fen,r}$ [-]	0.11	$\Delta y_{m,max}$ [m]	0.02	$\Delta y_{a,max}$ [m]	0.07
No pretension in the spring lines					
$F_{br,r}$ [-]	0.22	Δx_{max} [m]	0.87	$\Delta y_{f,max}$ [m]	0.27
$F_{fen,r}$ [-]	0.20	$\Delta y_{m,max}$ [m]	0.08	$\Delta y_{a,max}$ [m]	0.21
1.0 m slack present in the spring lines					
$F_{br,r}$ [-]	0.27	Δx_{max} [m]	1.47	$\Delta y_{f,max}$ [m]	0.58
$F_{fen,r}$ [-]	0.32	$\Delta y_{m,max}$ [m]	0.19	$\Delta y_{a,max}$ [m]	0.63

Table 7 shows that the performance of the mooring configuration, can be severely jeopardised by a lack of pretension and in worst case the presence of slack in the springs. Figure 8 shows a comparison of the forces in one of the fore spring lines. The vertical axis shows the force in the line.

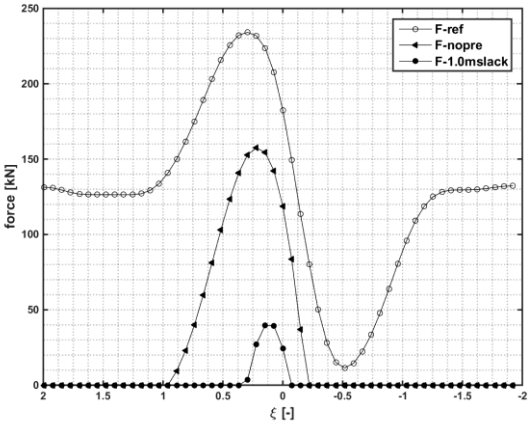

Figure 8: Force in one of the fore springs (mooring plan A): with pretension (F-ref), without pretension in the springs (F-nopre) and 1.0 m slack in the springs (F-1.0mslack); inbound passing vessel.

Figure 8 shows that in the absence of pretension, the spring line is activated in a later stage during the ship passage, which is even more clearly visible when slack is present in the line. The later reaction leads to a smaller total force in the spring. As the total force of the passing vessel on the moored vessel is of equal magnitude for the three cases, the fore and aft lines need to take up more load, when the springs show less response due to slack. As the fore and aft lines are less effective in taking up longitudinal forces, they show large elongations, resulting in substantial transversal motions as well, despite the slack only being present in the spring lines. This case yet again shows the importance of attaining a well-balanced mooring configuration, as slack in four lines, affects the entire configuration.

8. CONCLUSIONS

This paper focusses on the influence of passing vessels on large container vessels moored at quay walls. Simulations, using ROPES and the in-house tool Vlugmoor are performed, calculating the motions of the moored vessel and the forces in the lines and fenders. The paper focusses on the ship motions, as their presence can jeopardize the safety of the (un)loading process.

A reference passing event is presented, where an 18000 TEU container vessel passes a vessel of similar dimensions, in a restricted channel. The mooring plan and ship characterises, including mooring equipment, are given. The breaking strength of each individual line is 140 tons, which is almost twice the IMO/IACS requirement. The regulating bodies also only demand the use of 14 ropes, compared to the 16 lines used for the simulations.

The effect of the elasticity of the ropes, as a design parameter, is investigated, keeping the breaking strength constant. Simulations with very stiff lines (HMPE), elastic polyester lines and very flexible nylon lines, show that the motions of the moored vessel increase substantially with the use of more flexible materials. As motions of the moored ship endangers the safe (un)loading, there is a need to impose regulations by IMO and/or IACS, disallowing the use of very flexible lines for large container vessels.

The mooring plan is investigated from an operational point of view, assuming winches, fairleads and bollards have fixed positions. Ensuring a safe mooring situation comprises of implementing a well-balanced mooring configuration and maintaining it during the stay at the terminal. Crossing the fore and aft lines, leads to a decrease of the movement of the moored vessel, due to an increased efficiency of the lines. An imbalance in the configuration, due to limited bollard availability on the quay, leads to large longitudinal and transversal motions, even when the quality of the individual lines is assured. Again, there is a lack of international regulations, enforcing the use of well-balanced configurations. An approach similar to OCIMF/SIGTTO is

suggested, where clear rules are defined and translated into terminal manuals.

The simulation with no pretension in the springs, due to draft or water level changes, shows an increase in longitudinal motion, as can be expected. Because the springs react slower to the passing vessel, the fore and aft lines need to take up more longitudinal forces, causing them to elongate more and generating significant transversal motions as well. This shows that a lack of pretension, only in the spring lines, affects the balance of the entire configuration. A simulation with a one meter slack in the springs magnifies the described effect. Maintaining the mooring configuration must not be neglected, as it can nullify the efforts put into regulating the individual ropes and the mooring plan.

9. REFERENCES

1. LLOYD'S REGISTER; QINETIQ; STRATHCLYDE UNIVERSITY, 'Global marine trends 2030', 2013.
2. IMO, 'Anchoring, mooring and towing equipment (report of the drafting group)', *DE 48/WP.7*, 2005.
3. IACS, 'Requirements concerning mooring, anchoring and towing (A1.2)', 2005.
4. PIANC, 'Report n°115 – Criteria for the (un) loading of container vessels', *PIANC*, 2012.
5. PINKSTER J.A.; PINKSTER, H.J.M., 'A fast, user-friendly, 3-D potential flow program for the prediction of passing vessel forces, *PIANC world congress, San Francisco*, 2014.
6. VAN WIJHE, H.J.; PINKSTER, J.A., 'The effects of ships passing moored container vessels in the Yangtzehaven, Port of Rotterdam, *International Conference on Safety and Operations in Canals and Waterways*, 2008.
7. TALSTRA, H.; BLIEK, A.J., 'Loads on moored ships due to passing ships in a straight harbour channel, *PIANC world congress, San Francisco*, 2014.
8. TOXOPEUS, S.L.; BHAWSINKA, K., 'Calculation of hydrodynamic interaction forces on a ship entering a lock using CFD, *Proceedings of 4th MASHCON, BAW*, 2016.
9. PINKSTER, J.A., 'The influence of a free surface on passing ship effects', *int. shipbuild. Progr*, 2004.
10. VARYANI, K.S., 'Estimation of loads on mooring ropes of a moored ship due to a passing ship, *International conference on safety and operations in canals and waterways*, 2008.

THE SAFETY OF SHIP BERTHING OPERATIONS AT PORT DOCK – A GAP ASSESSMENT MODEL BASED ON FUZZY AHP

(DOI No: 10.3940/rina.ijme.2017.a4.442)

Wen-Kai K. Hsu, Department of Shipping & Transportation Management, National Kaohsiung Marine University, and **Jui-Chung Kao**, Graduate institute of Marine Affairs & Business Administration, National Kaohsiung Marine University, Taiwan, R.O.C.

SUMMARY

The purpose of this paper is to discuss the safety of ship berthing operations at port dock. Based on the features of ship's berthing operations and the relevant literature, the safety factors (SFs) of ship berthing at port docks are first investigated. A gap assessment model based on Fuzzy AHP is then proposed to assess the perceived differences on those SFs between port marine pilots and shipmasters. Finally, the ships' berthing operations at Kaohsiung Port in Taiwan were employed to illustrate the model's practical application. The result may provide practical information for both marine pilots and shipmasters to improve the safety performance of ship berthing operations at port docks.

NOMENCLATURE

SF	Safety factor
HF	Human factor
ME	Machinery and equipment
PM	Port management
PF	Port facility
CI	Consistency index
CR	Consistency rate
MW	Marine pilot's weight on SFs
SW	Shipmaster's weight on SFs
GAM	Gap assessment model
WGI	Weight gap index
RGI	Rank gap index

1. INTRODUCTION

Recently, the ships in the world are not only becoming faster and larger, but also rapidly increasing in quantity, leading to raising maritime accidents (Hsu, 2012). A historic statistic indicated that the frequency of ship accidents during 12-20th century significantly increased from 59% in the past decade to 83% in the last 20 years (Darbra and Casal, 2004).

Generally, the most common damages caused by ship accidents include ship crash, port facility destruction, cargo damage and human casualty. In practice, those damages may affect the reputations of shipping carriers and port companies, leading to diminish their businesses. Further, more seriously, a ship accident may cause fuel oil leakage, leading to port pollution. For example, a classical case is the oil spill accident of Hebei Spirt in 2007 in Korea. The government officials called it the South Korea's worst oil spill ever. At least 30 beaches have been affected and over half of the region's sea farms are believed to have lost their stocks due to the spill. The cost of cleanup has been estimated at $330 million (Wikipedia, 2017). Since the losses from a ship accident can be so enormous, many port authorities in worldwide have paid attention to reducing the ship accidents in port (Debnath *et al*., 2011).

In practice, collision is the most frequent maritime accident (Debnath and Chin, 2010; Hsu, 2012; Alyami, 2014), and is the most commonly occur when ship berths at port dock (Hsu, 2012). Thus, to reduce ship accidents, issues related to ship berthing safety at port dock should be considered (Hsu, 2015). Further, for ship berthing operations, marine pilot and shipmaster are both of the most important key men. In practice, their close cooperation may greatly contribute to the ship berthing safety. Thus, how to reduce their perceived difference in ship berthing operations is another important issue that should be concerned. Unfortunately, in the relevant literature, there are few studies on those topics.

The purpose of this paper is to discuss the determinants of ship berthing safety at port dock. Based on the relevant literature and the features of ship's berthing operations, the safety factors (SFs) of ship berthing at port docks are first investigated. Since ship berthing safety is a highly professional issue, a fuzzy AHP model is thus constructed to weights those SFs from both perspectives of marine pilots and shipmasters. Based on those weights, a gap assessment model is finally proposed to assess their perceived differences on the SFs. Finally, the ships' berthing operations at Kaohsiung Port in Taiwan were empirically investigated to explain how to apply the model in practice. The rest of this paper is organized as follows. Section 2 reviews the literature. Section 3 explains the research method in this paper. The results are then examined in Section 4. Finally, some general conclusions and limitations for further research are given.

2. LITERATURE REVIEWS

Based on the practical operations of ship berthing, this paper reviews the determinants of ship berthing safety from ship's internal and external operational environments. The former contains ship crews and ship machinery, and the latter includes: marine pilot, tugboat operation, dock operation and port management policy.

2.1 THE INTERNAL FACTORS

2.1(a) Ship crews

In practice, the ship crew factor for ship berthing safety includes the ship crews' operational skills and their work attitudes in cooperating with the mariner pilot. The relevant literature showed the ship crews' professional skills and work attitudes have significant effects on navigation safety (Hsu, 2012). Communication and interpersonal relationships among crews significantly influence the reporting performance of shipping accidents, and so do the feedbacks from crews to the shipmaster (Oltedal and McArthur, 2011). Further, in practice, the ship crews need to work in shifts. Therefore, their physical and mental health may influence ship navigation safety (Hsu, 2012). Previous studies showed there were potentially disastrous outcomes from fatigue in terms of poor health (Hetherington, 2006).

2.1(b) Ship machinery

The previous studies indicated machinery failure (Hsu 2012) and vessel performance (Liu et al., 2005) may increases marine disasters. The type, size, age and condition of a vessel at accidents significantly affect the ship loss (Kokotos and Smirlis, 2005). The performances of machinery for ship berthing operations, including steering gear, windlass on dock, bow thruster etc., may affect the ship berthing safety (Hsu, 2015).

2.2 THE EXTERNAL FACTORS

2.2 (a) Marine pilot

In practice, marine pilot is the main commander in ship berthing operations. Thus, their professional skills should be a significant determinant of ship berthing safety. Practically, during ship berthing operations, the marine pilot needs to give steering orders to the ship crews who may come from different areas and speak different languages. Thus, poor communication may lead to crews' misunderstanding and, as a result, increase ship's berthing accidents. Therefore, in addition to professional skills, the marine pilot's language and communication abilities may also be an important determinant of ship berthing safety. Relevant studies indicated that poor communications between crews and marine pilot significantly affect the safety of ship navigation in ports (Hetherington *et al*., 2006; Darbra *et al*., 2007; Hsu, 2012). The language and cultural differences of seafarers may affect the shipping safety (Hetherington. *et al*., 2006; Knudsen and Hassler, 2011).

2.2 (b) Tugboat operation

In practice, tugboats could assist a ship in berthing alongside and departing from docks by pushing and towing the ship. Relevant studies showed that tugboat failure is one of the determinants of marine accidents in ports (Darbra et al., 2007). Further, the factors affecting the tugboat performances include the number of tugboats, the horse powers of the tugboats, and the operating skills of the tugboat drivers (Hsu, 2012).

2.2 (c) Dock operational environment

For ship berthing operations, the dock operational environment includes two parts: the line handling operation and the dock facility. The former contains linemen, line handling boat and the windlass on the dock. Previous studies showed that the operating skills and work attitudes of linemen have significant effects on ship navigation safety in port (Hsu, 2012). The operating location of the line handling boat and the number of windlass on the dock may affect ship berthing safety (Paulauskas; 2006). As for the dock facility, the berth's length usually is the most important determinant of ship berthing safety. In practice, for providing enough space for ship mooring operations, the berth's length should be at least 1.2 times longer than the berthing vessel (Liu et al., 2006). However, due to the trend of large-sized ship development, the space may frequently be squeezed, leading to increase collisions between neighboring ships.

2.2 (d) Port regulations

To improve port safety, port authorities may develop rules to regulate the ships' operations in port. For example, in Kaohsiung port, the regulations for ship's berthing operations include: *Ship navigation regulations in port*, *Marine pilot laws*, *Tugboat operator regulations* and *Line handling operator regulations*. Relevant studies showed that safety management system in port is an important determinant of operational safety offshore (Wang, 2002). However, in practice, the operators may not comply with the regulations completely, and further those regulations may not be developed perfectly.

2.2 (e) Port policy

For improving businesses, port authorities may allow excessive ships to enter port simultaneously. This may lead to rush ship berthing operations, increasing ship collisions. Relevant studies showed that the risks of ship collision increase with the density of ships at a particular water area (Hsu, 2015). Further, another policy for improving port's businesses is to speed up the logistical operations of terminals. This may lead to haste the berthing operations, also increasing ship accidents (Hsu, 2012).

3. RESEARCH METHOD

3.1 RESEARCH FRAMEWORK

The research framework of this paper is shown in Figure 1. The safety factors (SFs) for ship's berthing operations are first investigated. A fuzzy AHP model is then

proposed to weight the SFs from both marine pilots and shipmasters. Based on those two weights, a gap assessment model is finally constructed. Finally, the ships berthed at Kaohsiung port in Taiwan were empirically investigated to illustrate the practical application of the model.

3.2 MEASUREMENT OF SAFETY FACTORS

3.2 (a) The definitions of safety factors

Based on the relevant literature and interviews with several practical marine pilots and shipments, we reorganized the determinants mentioned in Section 2 and identified the safety factors (SFs) as four dimensions, in which the weather and geography is not considered for it is a natural factor,

(1) Human factor (HF)

For ship berthing operations, the operators include marine pilot, ship crews, turbot drivers and linemen on dock. Thus, the human factor is defined as those operators' capabilities, such as professional skill, communication, emergency handling and working concentration, etc. (Hetherington *et al*., 2006; Darbra *et al*., 2007; Knudsen and Hassler, 2011; Hsu, 2012; Ding and Tseng, 2013; Hsu 2015).

(2) Machinery and equipment (ME)

This factor is defined as the conditions of machines and equipment onboard ship and on dock for the ship's berthing operations, such as the main engine, steering engine and deck machines (windlasses) onboard ship, and the turbots and mooring lines on dock. (Paulauskas; 2006; Darbra *et al*., 2007; Liu *et al*., 2006; Hsu, 2012; Hsu, 2015).

(3) Port management (PM)

This factor contains both port regulation and pot policy. It is defined as the completeness and performance of the regulations about ship's berthing operations in port, and the policy for improving the port's businesses, such as speeding up the logistical operations of the port, allowing excessive ships to stay in port, etc. (Paulauskas; 2006; Debnath *et al*., 2011; Hsu, 2012; Hsu 2015).

(4) Port facility (PF)

This factor is defined as the infrastructures and equipment of the dock for ship's berthing operations, such as the berth length, the situation of bollard and pads on dock, etc. (Paulauskas ; 2006; Liu *et al*., 2006; Tai and Yang, 2016).

Based on the above definitions, a two-layer hierarchy structure of SFs for ship berthing safety was first created. For improving the practical validity of the SFs, two experts (one marine pilot and one shipmaster) were then asked to revise those SFs and check if any important SFs were missed. Further, they also were asked to check the independences among the SFs. After several rounds of discussions and modifications, the final hierarchy structure of the SFs, shown in Table 1, contains four dimensions of SFs for the first layer and 14 SFs for the second layer.

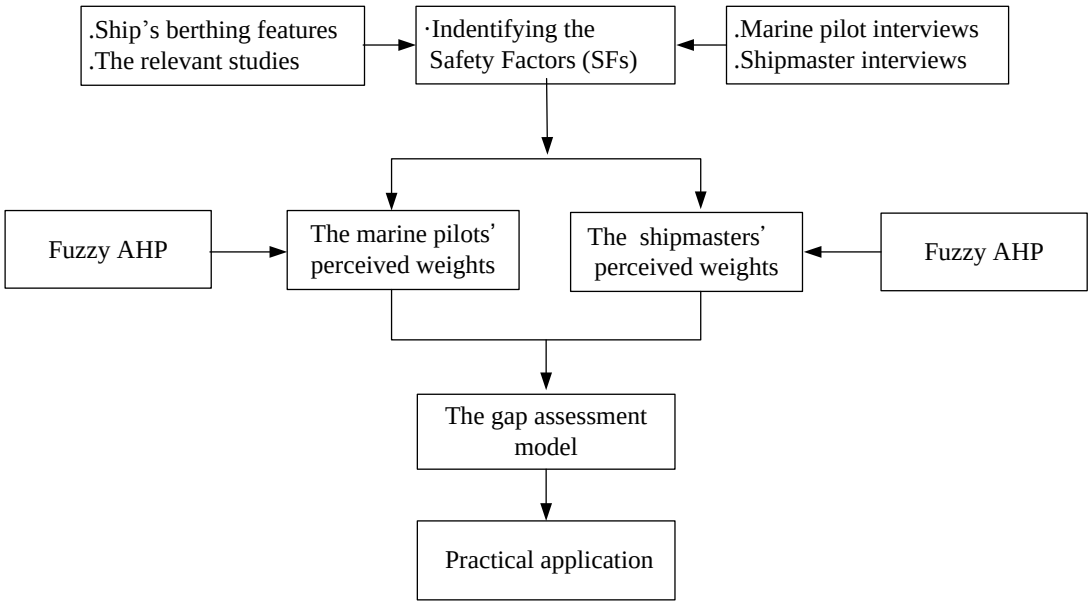

Figure 1. Research framework.

Table 1. Hierarchical structure of safety factors (SFs) for ship berthing operations

Layer 1: Construct		Layer 2: Safety factors (SFs)
Human factors (HF)	HF1	Professional skills.
	HF2	Communications.
	HF3	Emergency response.
	HF4	Working concentration.
Machinery (ME)	ME1	The conditions of the main engine and steering engine.
	ME2	The number and condition of the tugboats.
	ME3	The number and condition of the windlasses.
	ME4	The condition of the mooring lines.
Port management (PM)	PM1	The completeness of the port's rule and regulations.
	PM2	The performance of the port's rule and regulations.
	PM3	The port policy for improving business.
Port facility (PF)	PF1	The width and depth of the main channel.
	PF2	The berth's length
	PF3	The shore equipment, such as bollard and pads.

Table 2: Profile of the respondents

Characteristics	Range	Marin pilot		Shipmaster	
		Frequency	%	Frequency	%
Experience	5-10	2	14.29	5	26.32
	10-15	2	14.29	3	15.78
	16-20	3	21.42	5	26.32
	Above 20	7	50.00	6	31.58
Age (years)	40-50	1	7.14	5	26.32
	51-55	4	28.57	6	31.58
	56-60	5	35.72	6	31.58
	Above 60	4	28.57	2	10.52
Education level	Master	1	7.14	2	10.52
	University	5	35.72	15	78.95
	College	8	57.14	2	10.53

3.2 (b) Questionnaire design

In this paper, an AHP survey with a nine point rating scale was designed to measure subject's perceived importance on SFs. Based on the hierarchical structure of SFs in Table 1, an AHP survey, shown in Appendix, with five criteria and 14 sub-criteria was created. To validate the scale, the survey was then pre-tested by two experts, who revised the SFs previously, to check if the statements in the survey were understandable.

3.2 (c) Research sample

Since both of marine pilot and shipmaster are the main characters in ship's berthing operations, the marine pilots of Kaohsiung Port and the shipmasters berthing ships at Kaohsiung Port were surveyed in this paper. To enhance the validity of the survey, an assistant was dispatched to help each subject fill out the survey. In this paper, the research sample contains 20 marine pilots and 20 shipmasters.

For each of the sample, the consistency index (CI) was first calculated to test the consistency of its pairwise comparison matrix. The results indicated seven samples with CI > 0.1 were highly inconsistent (Saaty, 1980), including 6 marine pilot samples and 1 shipmaster sample. Therefore, those questionnaires were discarded, and thus only 33 valid surveys were remained in this paper. The profiles of the validated respondents' characteristics are shown in Table 2. It shows that, for marine pilot samples, all of the subjects have at least 10 years of experience with over 80% respondents having over 20 years. For shipmasters, all of the respondents have at least 10 years of experience with over 40% respondents having over 20 years. Note, the remarkable qualifications of the respondents could endorse the reliability of the survey.

3.3 THE WEIGHTS OF SAFETY FACTORS

From the sample data, 33 pairwise comparison matrices (14 marine pilot and 19 shipmasters) were obtained. In the traditional AHP, an arithmetic mean is used to integrate the multiple subjects' opinions. However, the arithmetic mean is usually sensitive to extreme values. Thus, we adopt fuzzy AHP to integrate the subjects' perceptions. In this paper, we first used the geometric mean to measure the consensus of the subjects (Buckley 1985; Saaty 1980). Then, a triangular fuzzy number characterized by minimum, geometric mean and maximum of the measuring scores was constructed to

integrate the 33 pairwise comparison matrices into two fuzzy positive reciprocal matrix, one for marine pilot samples and one for shipmaster samples. Finally, based on those fuzzy reciprocal matrices, a fuzzy AHP approach was conducted to weight the SFs, including both of the measurements of marine pilots and shipmasters (Hsu *et al*., 2015).

3.3 (a) The fuzzy positive reciprocal matrix

Suppose $\tilde{A}=[\tilde{a}_{ij}]_{n\times n}$ be a fuzzy positive reciprocal matrix with n SFs, where $\tilde{a}_{ij}=[l_{ij},\ m_{ij},\ u_{ij}]$ is a triangular fuzzy number with

$$[l_{ij},\ m_{ij},\ u_{ij}]=\begin{cases}[1,\ 1,\ 1], & \text{if } i=j\\ [1/u_{ji},\ 1/m_{ji},\ 1/l_{ji}], & \text{if } i\neq j\end{cases}.$$

Let $A^{(k)}=\left[a_{ij}^{(k)}\right]_{n\times n}$, $k=1,2,...,m$, denote the pair-wise comparison matrix of m subjects. Then, according to the abovementioned integration procedure, those m matrices can be integrated into the following fuzzy matrix:

$$\tilde{A}=\left[\tilde{a}_{ij}\right]_{n\times n} \tag{1}$$

where $\tilde{a}_{ij}=\left[\min_{1\le k\le m}\left\{a_{ij}^{(k)}\right\},\left(\prod_{k=1}^{m}a_{ij}^{(k)}\right)^{1/m},\max_{1\le k\le m}\left\{a_{ij}^{(k)}\right\}\right]$ is a triangular fuzzy number, $i=1,2,...,n$, $j=1,2,...,n$ and $k=1,2,...,m$.

3.3 (b) The consistency tests

Since the $\tilde{A}$ is a fuzzy numbers, its consistency cannot be tested directly as traditional AHP. In this paper, the geometric means is first employed to defuzzify the criteria in $\tilde{A}$ (i.e. the $\tilde{a}_{ij}$ $i=1,2,...,n$, $j=1,2,...,n$) by the form of trapezoid fuzzy number, and thus convert the $\tilde{A}$ into a crisp matrix. Then, the consistency test is undertaken to the test the crisp matrix as traditional AHP (Buckley, 1985). Since $\tilde{A}$ is a triangular fuzzy number with parameter $\tilde{a}_{ij}=[l_{ij},\ m_{ij},\ u_{ij}]$, its trapezoid fuzzy number form is $a_{ij}=[l_{ij},\ m_{ij},\ m_{ij},\ u_{ij}]$. Thus, those a_{ij} can be defuzzified as:

$$a_{ij}=(l_{ij}\cdot m_{ij}\cdot m_{ij}\cdot u_{ij})^{1/4},\ i=1,2,...,n,\ j=1,2,...,n \tag{2}$$

In traditional AHP, both of indexes CI (Consistency Index) and CR (Consistency Ratio) are usually used to test the consistency of its positive reciprocal matrix:

$$\mathrm{CI}=\frac{\lambda_{\max}-n}{n-1} \tag{3}$$

and

$$\mathrm{CR}=\frac{\mathrm{CI}}{\mathrm{RI}} \tag{4}$$

where $\lambda_{\max}$ is the maximum eigenvalue of the positive reciprocal matrix and n is the number of criteria in the matrix. The RI represents a randomized index, whose values are shown in Table 3 (Hsu *et al*, 2015). Saaty (1980) suggested that a value for $\mathrm{CR}\le 0.1$ is an acceptable range for the consistency test of the matrix.

The results of consistency tests for both the pairwise comparison matrices, marine pilot sample and shipmaster sample, are listed in Table 4. Since all of the C.R. indexes in Table 4 are less than 0.1, all of the positive reciprocal matrixes in the sample data are consistent.

Table 3. The randomized index (RI)

n	3	4	5	6	7	8	9	10	11	12
R.I.	0.58	0.90	1.12	1.24	1.32	1.41	1.45	1.49	1.52	1.54

Table 4. The results of the consistency tests.

pairwise comparison matrices	Layer	C.I.	R.I.	C.R. (C.I./R.I.)
Marine pilot	Layer 1	0.076	1.115	0.068
	Layer2: HF	0.085	0.882	0.096
	Layer2: ME	0.071	0.882	0.080
	Layer2: PM	0.028	0.525	0.053
	Layer2: PF	0.053	0.882	0.060
Shipmaster	Layer 1	0.034	1.115	0.030
	Layer2: HF	0.074	0.882	0.084
	Layer2: ME	0.031	0.882	0.035
	Layer2: PM	0.075	0.882	0.085
	Layer2: PF	0.049	0.882	0.056

3.3 (c) The local weights of SFs

For determining the weights of the SFs in fuzzy positive reciprocal matrix $\tilde{A}$, we need to find the eigenvectors of the $\tilde{A}$. Due to the special structure of $\tilde{A}$ (positive reciprocal matrix), Saaty (1980) suggested four methods to find the eigenvectors: Average of Normalized Columns (ANC), Normalization of the Row Average (NRA), Normalization of the Reciprocal of Columns Sum (NRCS) and Normalization of the Geometric Mean of the Rows (NGMR). Since the NGMR method was applied most popularly in previous studies, this paper adopts it to determine the local weights of the SFs $\tilde{A}$.

For the $\tilde{A}$, the geometric means of the triangular fuzzy numbers for the *i*th SF ($i = 1, 2, ..., n$) can be found as:

$$\tilde{w}_i = \left(\prod_{j=1}^{n} \tilde{a}_{ij}\right)^{1/n} = \left[\left(\prod_{j=1}^{n} l_{ij}\right)^{1/n}, \left(\prod_{j=1}^{n} m_{ij}\right)^{1/n}, \left(\prod_{j=1}^{n} u_{ij}\right)^{1/n}\right], \quad i = 1, 2, ..., n \tag{5}$$

Based on Equation (5), we have:

$$\sum_{i=1}^{n} \tilde{w}_i = \left[\sum_{i=1}^{n}\left(\prod_{j=1}^{n} l_{ij}\right)^{1/n}, \quad \sum_{i=1}^{n}\left(\prod_{j=1}^{n} m_{ij}\right)^{1/n}, \quad \sum_{i=1}^{n}\left(\prod_{j=1}^{n} u_{ij}\right)^{1/n}\right] \tag{6}$$

Also, based on Equations (5)-(6), the fuzzy weight of the *i*th SF ($i = 1, 2, ..., n$) can then be obtained as:

$$\tilde{W}_i = \frac{\tilde{w}_i}{\sum_{i=1}^{n} \tilde{w}_i} = \left[\frac{\left(\prod_{j=1}^{n} l_{ij}\right)^{1/n}}{\sum_{i=1}^{n}\left(\prod_{j=1}^{n} u_{ij}\right)^{1/n}}, \frac{\left(\prod_{j=1}^{n} m_{ij}\right)^{1/n}}{\sum_{i=1}^{n}\left(\prod_{j=1}^{n} m_{ij}\right)^{1/n}}, \frac{\left(\prod_{j=1}^{n} u_{ij}\right)^{1/n}}{\sum_{i=1}^{n}\left(\prod_{j=1}^{n} l_{ij}\right)^{1/n}}\right], \quad i = 1, 2, ..., n \tag{7}$$

3.3 (d) The defuzzification process

Since the local weight, $\tilde{W}_i$, of the *i*th SF ($i = 1, 2, ..., n$) is fuzzy, this paper uses Yager's index (1981) to defuzzify the $\tilde{W}_i$ into a crisp number W_i, $i = 1, 2, ..., n$ (Hsu *et al*, 2016). For convenience of explanation, let $\tilde{W}_i = [l_i^W, m_i^W, u_i^W]$, where

$$[l_i^W, m_i^W, u_i^W] = \left[\frac{\left(\prod_{j=1}^{n} l_{ij}\right)^{1/n}}{\sum_{i=1}^{n}\left(\prod_{j=1}^{n} u_{ij}\right)^{1/n}}, \frac{\left(\prod_{j=1}^{n} m_{ij}\right)^{1/n}}{\sum_{i=1}^{n}\left(\prod_{j=1}^{n} m_{ij}\right)^{1/n}}, \frac{\left(\prod_{j=1}^{n} u_{ij}\right)^{1/n}}{\sum_{i=1}^{n}\left(\prod_{j=1}^{n} l_{ij}\right)^{1/n}}\right], \quad i = 1, 2, ..., n$$

Then, the $\tilde{W}_i$, $i = 1, 2, ..., n$ can be defuzzified as:

$$W_i = (l_i^W + 2\, m_i^W + u_i^W)/4, \quad i = 1, 2, ..., n. \tag{8}$$

Finally, normalizing the W_i ($i = 1, 2.., n$), the crisp local weight of the *i*th SFs can be obtained as:

$$\omega_i = W_i / \sum_{i=1}^{n} W_i, \quad i = 1, 2, ..., n \tag{9}$$

3.3 (e) The global weights of the SFs

By the above steps in Sections 3.3.1~3.3.4, all the local weights of the SFs in Table 1 can be found. The global weights of the SFs can then be found by multiplying their low level of local weights by their corresponding high level of global weights. Table 5 shows the results of all global weights of the SFs for the marine pilot sample. The global weights (and ranks) of the SFs in layer 1 are shown in the second field, and the ones of the SFs in layer 2 are shown in the fifth and last fields. Likewise, the global weights of SFs for the shipmaster sample are shown in Table 6.

Table 5. The marine pilot weights (MWs) of safety factors.

Layer1 SFs	The global weights of Layer 1 SFs (%)	Layer2SFs	The local weights of Layer 2 SFs (%)	The global weights of Layer 2 SFs (%)	Rank
HF	38.55 (1)	HF1	45.934	17.71	1
		HF2	13.607	5.25	9
		HF3	24.565	9.47	3
		HF4	15.895	6.13	6
ME	28.55 (2)	ME1	42.94	12.26	2
		ME2	29.182	8.33	5
		ME3	17.414	4.97	10
		ME4	10.465	2.99	14
PM	20.03 (3)	PM1	45.016	9.02	4
		PM2	24.755	4.96	11
		PM3	30.23	6.06	7
PF	12.87 (4)	PF1	45.331	5.83	8
		PF2	29.482	3.79	12
		PF3	25.187	3.24	13

Table 6. The shipmaster weights (SWs) of safety factors.

Layer1 SFs	The global weights of Layer 1 SFs (%)	Layer2S Fs	The local weights of Layer 2 SFs (%)	The global weights of Layer 2 SFs (%)	Rank
HF	39.62 (1)	HF1	36.53	14.47	1
		HF2	12.62	5.00	10
		HF3	31.59	12.52	3
		HF4	19.27	7.63	5
ME	27.29 (2)	ME1	46.1	12.58	2
		ME2	24.27	6.62	7
		ME3	20.67	5.64	8
		ME4	8.96	2.45	14
PM	11.2 (4)	PM1	47.94	5.37	9
		PM2	25.48	2.85	13
		PM3	26.57	2.98	12
PF	21.9 (3)	PF1	46.44	10.17	4
		PF2	32.67	7.15	6
		PF3	20.89	4.57	11

3.4. THE GAP ASSESSMENT MODEL

For assessing the subjects' perceived differences on SFs, a Gap Assessment Model (GAM) is proposed in this paper. The GAM contains two steps: indentifying the SFs' gaps and determining the degrees of the SFs' gaps.

3.4 (a) The identification of the SFs' gaps

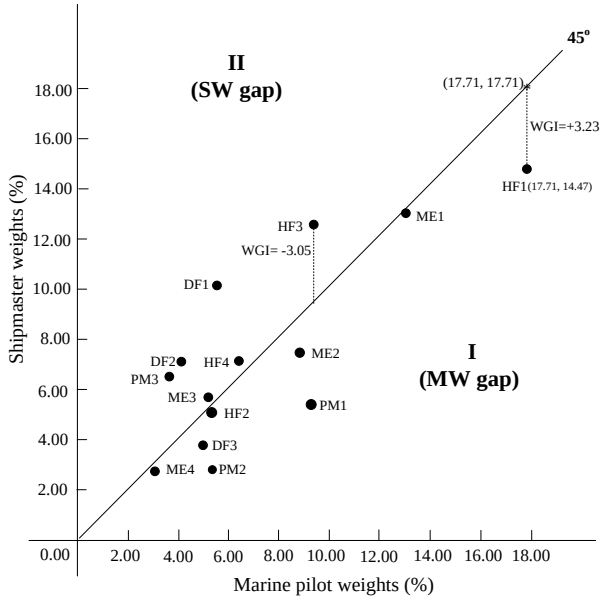

Figure 2. The identification matrix for SFs' gaps

The basic concept of GAM is that an SF with higher (or lower) marine pilots' perceived importance (marine pilot weight, MW) and lower (or higher) shipmasters' perceived importance (shipmaster weight, SW) should be a gap. Based on the above concept, a two-dimensional of identification matrix with both weights (MWs and SWs) is constructed to assess the gaps of SFs. The matrix is shown as Figure 2, in which the MW is depicted on the x-axis, the SW on the y-axes, and a 45° line divides the matrix into two quadrants. The SFs in Quadrant I imply that their MWs are higher than their SWs. In this paper, those SFs are termed as MW gaps. Likewise, the SFs in Quadrant II imply that their SWs weights are higher than their MWs. Thus, those SFs are named as SWs gaps. Further, the SFs on the 45° line is called NO gap for their MWs being equal to their SWs. The results of Figure 2 indicate there are 8 SFs locate in the Quadrant I zone (i.e. MW gaps) and 6 SFs located in the Quadrant II zone (i.e. SW gap).

3.4 (b) The degree of the SFs' gaps

Although the identification matrix can verified the SFs' gaps (MW gap , SW gap or NO gap), it does not show the degree for those gaps. Two gap index, Rank Gap Index (RGI) and Weight Gap Index (WGI), were proposed to determine the degrees of the SFs' gaps in each Quadrant.

(1) Weight Gap Index (WGI)

Let ω_i^M and ω_i^S denote the MW and the SW of the *i*th SF ($i = 1, 2, ..., n$), which can be obtained from the fifth fields of Table 5 and Table 6, respectively. Then, the WGI is defined by the difference of ω_i^M and ω_i^S:

$$WGI_i = \omega_i^M - \omega_i^S, \quad i = 1, 2, ..., n \tag{10}$$

(2) Rank Gap Index (RGI)

Let r_i^M and r_i^S denote the ranks of MW and SW of the *i*th SF ($i = 1, 2, ..., n$), Then, the RGI is defined by the difference of r_i^M and r_i^S:

$$RGI_i = r_i^M - r_i^S, \quad i = 1, 2, ..., n \tag{11}$$

Table 7. The safety factor' RGI (Rank Gap Index) and WGI (Weight Gap Index)

Layer 1 RFs	Layer 1 RFs RGI (%)	Layer 1 RFs WGI (%)	Layer 2 RFs	Layer 2 RFs RGI (%)	Layer 2 RFs WGI (%)
HF	0	-1.07	HF1	0	**3.23**
			HF2	-1	0.25
			HF3	0	**-3.05**
			HF4	1	-1.51
ME	0	+1.26	ME1	0	-0.32
			ME2	-2	1.71
			ME3	2	-0.67
			ME4	0	0.54
PM	**-1**	**+8.83**	PM1	**-5**	**3.65**
			PM2	-2	2.11
			PM3	**-5**	**3.08**
PF	**+1**	**-9.03**	PF1	**4**	**-4.34**
			PF2	**6**	**-3.36**
			PF3	2	-1.33

Note: The boldfaced numbers represent the SFs with higher gaps.

Equation (9) and (10) implies that a SF with a positive WGI or a negative RGI has a MW gap, and a SF with a negative WGI or a negative RGI has a SW gap. The results of the SFs' WGIs and RGIs for the empirical study are listed in Table 7.

4. RESULTS AND IMPLICATIONS

4.1 THE IMPORTANCE WEIGHYS OF SFs

The results of Table 5 and Table 6 indicate, in the first layer of SF constructs, both of the marine pilots and shipmasters consider the HF (MW = 38.551% and SW = 39.62%) is the most important construct to affect ship berthing safety, and followed by ME (MW = 28.55% and SW = 27.29%). Further, in the second layer of SFs, for marine pilots, the SFs with higher weights are: HF1 (17.71%), ME1(12.26%), HF3(9.47%) and PM1(9.02%); for shipmasters, the SFs with higher weights are: HF1 (14.47%), ME1(12.58%), HF3(12.52%) and PF1(10.17%). These results imply that the most important SFs to affect ship berthing safety should be HF1(*Professional skills*), and followed by ME1 (*The conditions of main engine and steering engine* and HF3 (*Emergency response*). Further, from Figure 2, we can also have a result that the larger the distance from SFs to the origin O, the higher the SFs' weights. In Figure 2, it is clear the largest distance from SFs to O is HF1, and followed by ME1 and HF3.

The above results conclude that human factor is the most important determinant of ship berthing safety, especially the capabilities of staffs' professional skills and emergency response. Practically, the main operators in ship's berthing operations include marine pilot, shipmaster, ship crews, tugboat drivers and linemen. Thus, for improving ship's berthing safety, port authority may focus on strengthening those operators' professional literacy. Further, in practice, most ship accidents occur in an instant. Thus, the response capability for emergencies is particularly important for those staffs. For enhancing those staffs' capabilities, this paper suggests the port authority may make policy to encourage or even mandatory require staffs to attend related training activities regularly, such as experience sharing, computer simulation for berthing operations, analysis of the causes of collisions, and how to prevent accidents etc. Further, the port authority may also make a license system to force the staffs to participate in those trainings.

4.2. THE RESULTS OF GAP ASSESSMENTS

Both of the RGI (Rank Gap Index) and WGI (Weight Gap Index) in Table 7 indicate that the main diverged viewpoints on the SF constructs between marine pilots and shipmasters are: PM (Port management) (RGI=-1 and WGI= +8.83%) and PF (Port facility) (RGI=+1 and WGI=-9.03%). The marine pilots pays more attention to port management (PM), especially to PM1 (port's rules and regulations) and PM3 (port policy for improving business). Whereas, the shipmasters perceive more importance on port facility (PF), especial on PF1(main channel's width and depth) and PF3 (shore equipment). Furthermore, the results of Table 7 also indicate that the other two constructs, HF and ME, have no gap in RGI and lower gap WGI (-1.07 and +1.26). However, for the SFs in the layer 2, even if both HF1 and HF3 have no gap in RGI, but have significant gap in WGI (+3.23 and -3.05). This result implies that the marine pilots perceive more importance on professional skills (HF1), whereas, shipmasters pay more attention on emergency response (HF3). The above results may provide information for both marine pilots and shipmasters to improve their cooperation in ship berthing operations.

In practice, the marine pilot and shipmaster are the most important roles in ship's berthing operations. The former

realizes the port environments, such as tide, dock facility, tugboats etc. The later knows the ship conditions, including main engine, steering engine, operating crews etc. Their close cooperation is the best guarantee for ship berthing operations. In practice, both the key men understand their diverged opinions is helpful to improve the cooperation.

5. CONCLUSION

The purpose of this paper is to assess the determinants of ship berthing safety at port dock. Specifically, this paper investigates the differences of perspectives between marine pilots and shipmasters who are the key men in ship berthing operations. In this paper, a gap assessment model based on a fuzzy AHP was proposed to assess the their perceived difference on the determinants of ship berthing safety. The proposed model is easy to use that can extend its practical applications. Further it can also provide theoretical references for relevant research on methodology and ship navigation safety.

For demonstrating the practical application of the proposed model, the ship berthing operations at Kaohsiung Port in Taiwan were empirically investigated. The results indicated operating human factor is the most important determinant of ship berthing safety. In practice, the main operating staffs in ship berthing operations include the marine pilot, ship crews, turbot drivers and linemen. Thus, those staffs' personal literacy should be enhanced, especially in professional skills and emergency response. Further, the main diverged viewpoints between marine pilots and shipmasters are the SFs of port management and port facility. The former emphasizes more the port management; and the latter cares more about the port facility. This result may provide practical information for both marine pilots and shipmasters to improve their cooperation, enhancing the safety performance of ship berthing operations.

For AHP approach, one of the main assumptions is the independences among the safety factors. In this paper, the assumption is only verified by practical experts. In theoretically, this is not rigorous enough. Thus, it should be further confirmed in future research. Furthermore, in this paper, 14 marine pilots and 19 shipmasters at Kaohsiung Port in Taiwan were empirically surveyed to validate the proposed model. For enhancing the validity of the questionnaire investigation, this paper adopted an interview survey instead of a mailed survey. Thus, the validity and reliability of the findings in this paper could be endorsed. However, for better confirming the empirical results, more representative samples may be necessary in future research.

6. REFERENCES

1. ALYAMI, H, LEE, PTW, YANG, Z, RIAHI, R, BONSALL, S, and WANG, J. An advanced risk analysis approach for container port safety evaluation. *Maritime Policy and Management* 2014, 41, 634-650.
2. BUCKLEY, JJ. Fuzzy hierarchical analysis. *Fuzzy Sets and Systems* 1985, 17, 233-247.
3. DARBRA, RM and CASAL, J. Historical analysis of accidents in seaports. *Safety Sciences* 2004, 42, 85-98.
4. DARBRA, RM, CRAWFORD, JFE., HALEY, CW and MORRISON, RJ. Safety culture and hazard risk perception of Australian and New Zealand maritime pilots. *Marine Policy* 2007, 31, 736-745.
5. DEBNATH, AK, CHIN, HC. Navigational traffic conflict technique: A proactive approach to quantitative measurement of collision risks in port waters. *Journal of Navigation* 2010, 63, 137-152.
6. DEBNATH, AK, CHIN, HC and HAQUE, MM. Modelling port water collision risk using traffic conflicts. *Journal of Navigation* 2011, 64, 645-655.
7. DING, JF. Partner selection of strategic alliance for a liner shipping company using extent analysis method of fuzzy AHP. *Journal of Marine Science and Technology* 2009, 17, 97-105.
8. DING, JF AND JI-FENG DING, See all articles by this author
9. Search Google Scholar for this author, TSENG, WJ. WEN-JUI TSENG
10. Fuzzy risk assessment on safety operations for exclusive container terminals at Kaohsiung port in Taiwan. Proceedings of the Institution of Mechanical Engineers, *Part M: Journal of Engineering for the Maritime Environment 2013*, 227, 208-220.
11. HETHERINGTON, C, FLIN, R and MEARNS K. Safety in shipping: The human element. Journal of Safety Research 2006, 37, 401-411.
12. HSU, WK. Ports' service attributes for ship navigation safety. *Safety Science* 2012, 50, 244-252.
13. HSU, WK. Assessing the safety factors of ship berthing operations. *Journal of Navigation* 2015, 68(3), 568-588.
14. HSU, WK, YU, HF and HUANG, SH. Evaluating the service requirements of dedicated container terminals: A revised IPA model with fuzzy AHP. *Maritime Policy and Management* 2015, 42(8), 789-805.
15. KNUDSEN, OF, HASSLER, B. IMO legislation and its implementation: Accident risk, vessel deficiencies and national administrative practices. *Marine Policy* 2011, 35, 201-207.
16. KOKOTOS, DX and SMIRLIS GY. A classification tree application to predict total ship loss. *Journal of Transportations and Statistics* 2005, 8, 31-42.

17. LIU, CP, LIANG, GS. SU, Y. and CHU, CW. Navigation safety Analysis in Taiwanese ports. *Journal of Navigation* 2006, 59, 201-211.
18. OLTEDAL, HA and MCARTHUR, DP. Reporting practices in merchant shipping, and the identification of influencing factors. *Safety Sciences* 2011, 49, 331-338.
19. PAULAUSKAS, V.. Navigational risk assessment of ships. *Transport* 2006, 21, 12-18.
20. SAATY, TL. The Analytic Hierarchy Process. *McGraw-Hill Companies, Inc* 1980, New York.
21. TAI, H. H. and YANG, C. C. A policy-making framework for enhancing Kaohsiung port's economic resilience. *International Journal of Maritime Engineering* 2016, 158(A4), 347-358.
22. WANG, J. Offshore safety case approach and formal safety assessment of ships. *Journal of Safety Research* 2002, 33, 81-115.
23. Wikipedia. 2007 South Korea oil spill. Retrieved June 7, 2017, from https://en.wikipedia.org/wiki/2007_South_Korea_oil_spill.
24. YAGER, RR. A Procedure for ordering fuzzy subsets of the unit interval. *Information Sciences* 1981, 24, 143-161.

APPENDICES

The AHP questionnaire

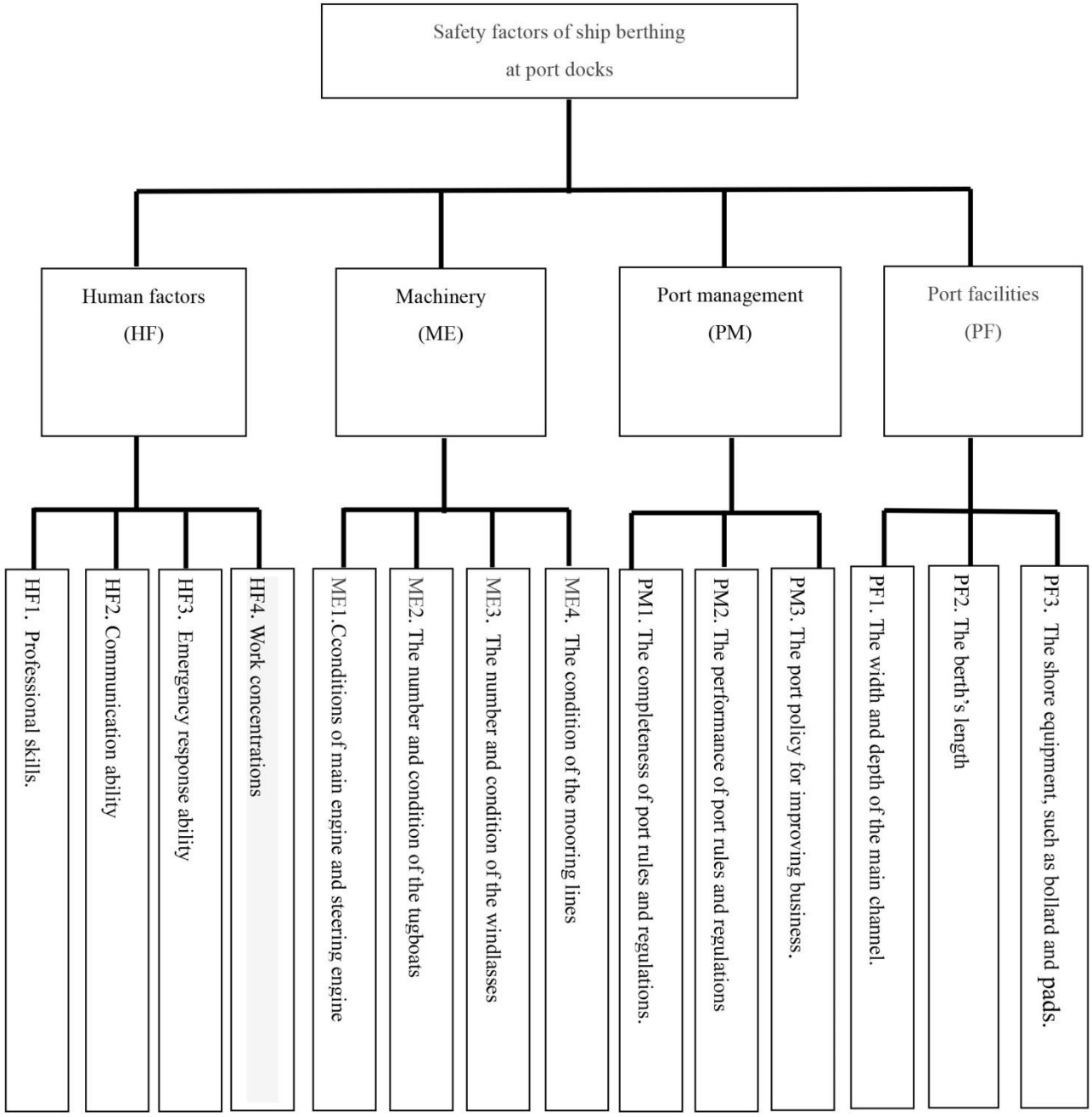

Continue to next page

※Please make ranking for 4 safety factors (HF, ME, PM and PF) to help following respondents in consistency:

≧___≧___≧

	Most important								Equally								Most important	
HF Human factors	9	8	7	6	5	4	3	2	1	2	3	4	5	6	7	8	9	**ME** Machinery
HF Human factors	9	8	7	6	5	4	3	2	1	2	3	4	5	6	7	8	9	**PM** Port management
HF Human factors	9	8	7	6	5	4	3	2	1	2	3	4	5	6	7	8	9	**PF** Port facilities
ME Machinery	9	8	7	6	5	4	3	2	1	2	3	4	5	6	7	8	9	**PM** Port management
ME Machinery	9	8	7	6	5	4	3	2	1	2	3	4	5	6	7	8	9	**PF** Port facilities
PM Port facilities	9	8	7	6	5	4	3	2	1	2	3	4	5	6	7	8	9	**PF** Port facilities

Continue to next page

Safety factors：Human factors; HF

※Please make ranking for safety factors to help following respondents in consistency, please ranking with the code (HF1, HF2, HF3 and HF4)：

____≧____≧____≧____

	Most important								Equally								Most important	
HF1. Professional skill	9	8	7	6	5	4	3	2	1	2	3	4	5	6	7	8	9	**HF2.** Conmunication
HF1. Professional skill	9	8	7	6	5	4	3	2	1	2	3	4	5	6	7	8	9	**HF3.** Emergency response
HF1. Professional skill	9	8	7	6	5	4	3	2	1	2	3	4	5	6	7	8	9	**HF4.** Work concentration
HF2. Conmunication	9	8	7	6	5	4	3	2	1	2	3	4	5	6	7	8	9	**HF3.** Emergency response
HF2. Conmunication	9	8	7	6	5	4	3	2	1	2	3	4	5	6	7	8	9	**HF4.** Work concentration
HF3. Emergency response	9	8	7	6	5	4	3	2	1	2	3	4	5	6	7	8	9	**HF4.** Work concentration

Continue to next page

Safety factors：Machinery and equipment; ME

※Please make ranking for safety factors to help following respondents in consistency, please ranking with the code(ME1, ME2, ME3 and ME4)：

_____≧_____≧_____≧_____

	Most important								Equally								Most important	
ME1. Situation of marine engines	9	8	7	6	5	4	3	2	1	2	3	4	5	6	7	8	9	**ME2.** Situation of tug-boats
ME1. Situation of marine engine	9	8	7	6	5	4	3	2	1	2	3	4	5	6	7	8	9	**ME3.** Situation of windlasses
ME1. Situation of marine engine	9	8	7	6	5	4	3	2	1	2	3	4	5	6	7	8	9	**ME4.** Situation of mooring lines
ME2. Situation of tug-boats	9	8	7	6	5	4	3	2	1	2	3	4	5	6	7	8	9	**ME3.** Situation of windlasses
ME2. Situation of tug-boats	9	8	7	6	5	4	3	2	1	2	3	4	5	6	7	8	9	**ME4.** Situation of mooring lines
ME3. Situation of windlasses	9	8	7	6	5	4	3	2	1	2	3	4	5	6	7	8	9	**ME4.** Situation of mooring lines

Continue to next page

Safety factors：Port management policies: PM

※Please make ranking for safety factors to help following respondents in consistency, please ranking with the code(PM1, PM2 and PM3)：

_____≧_____≧_____

	Most important								Equally								Most important	
PM1. Completeness of rule regulations	9	8	7	6	5	4	3	2	1	2	3	4	5	6	7	8	9	**PM2.** Performance of rule regulations
PM1. Completeness of rule regulations	9	8	7	6	5	4	3	2	1	2	3	4	5	6	7	8	9	**PM3.** Port policy for business
PM2. Performance of rule regulations	9	8	7	6	5	4	3	2	1	2	3	4	5	6	7	8	9	**PM3.** Port policy for business

Safety factors**:** Port facilities; PF

※Please make ranking for safety factors to help following respondents in consistency, please ranking with the code(PF1, PF2 and PF3)：

_____≧_____≧_____

	Most important								Equally								Most important	
PF1. Depth/width of main channel	9	8	7	6	5	4	3	2	1	2	3	4	5	6	7	8	9	**PF2.** Berth lengths
PF1. Depth/width of main channel	9	8	7	6	5	4	3	2	1	2	3	4	5	6	7	8	9	**PF3.** Situations of shore equipments
PF2. Berth lengths	9	8	7	6	5	4	3	2	1	2	3	4	5	6	7	8	9	**PF3.** Situations of shore equipments

NUMERICAL PREDICTION OF VERTICAL SHIP MOTIONS AND ADDED RESISTANCE

(DOI No: 10.3940/rina.ijme.2017.a4.450)

F Cakici, **E Kahramanoglu**, and **A D Alkan**, Yildiz Technical University, Turkey

SUMMARY

Along with the development of computer technology, the capability of Computational Fluid Dynamics (CFD) to conduct 'virtual computer experiments' has increased. CFD tools have become the most important tools for researchers to deal with several complex problems. In this study, the viscous approach called URANS (Unsteady Reynolds Averaged Navier-Stokes) which has a fully non-linear base has been used to solve the vertical ship motions and added resistance problems in head waves. In the solution strategy, the FVM (Finite Volume Method) is used that enables numerical discretization. The ship model DTMB 5512 has been chosen for a series of computational studies at Fn=0.41 representing a high speed case. Firstly, by using CFD tools the TF (Transfer Function) graphs for the coupled heave-pitch motions in deep water have been generated and then comparisons have been made with IIHR (Iowa Institute of Hydraulic Research) experimental results and ordinary strip theory outputs. In the latter step, TF graphs of added resistance for deep water have been generated by using CFD and comparisons have been made only with strip theory.

NOMENCLATURE

A	Wave amplitude (m)
B_{WL}	Waterline breadth (m)
C_{AW}	Added resistance coefficient (-)
Cb	Block coefficient (-)
Cm	Midship section coefficient (-)
f	Wave frequency (s^{-1})
fe	Encounter wave frequency (s^{-1})
Fn	Froude number (-)
g	Gravitational acceleration (m s^{-2})
Iy	Inertia moment of mass (kg m^2)
k	Wave number (m^{-1})
LCG	Longitudinal position of center of gravity (m)
L_{PP}	Length between perpendiculars (m)
L_{WL}	Waterline length (m)
M	Mass (kg)
N	Number of elements (-)
r	Refinement factor (-)
R	Convergence coefficient (-)
R_{AW}	Added resistance (N)
R_F	Frictional resistance (N)
R_R	Residuary resistance (N)
R_T	Total resistance (N)
Re	Reynolds number (-)
S	Wetted surface area (m^2)
T	Draught (m)
T_e	Wave encounter period (s)
V	Ship speed (m/s)
VCG	Vertical position of center of gravity (m)
λ	Wave length (m)
CFD	Computational fluid dynamics
DFBI	Dynamic fluid body interaction
EEDI	Energy efficiency design index
GCI	Grid convergence index
IMO	Intergovernmental Maritime Organization
N-S	Navier-Stokes
FS	Fourier series
FVM	Finite volume method
TF	Transfer function
URANS	Unsteady Reynolds averaged Navier-Stokes
SMP	Ship Motion Program

1. INTRODUCTION

Ship motion computations even in regular waves are still one of the leading and challenging working areas for researchers. Difficulties mainly stem from the sources listed below:

- The second order velocity term when calculating the pressure acting on the hull surface.
- Flows are highly nonlinear around the ship and the Reynolds numbers covered in ship motions are usually high.
- In reality, waves are not in a simple sinusoidal form due to gravitational force.
- The complex ship geometries majorly affect the restoring terms in the equations of ship motions.
- Kelvin wave pattern of the ship in given advancing velocity may affect the ship motions in waves especially at high Froude numbers.

In addition to these, performing seakeeping tests are difficult and costly compared with experiments dealing with the resistance characteristics for displacement types of models. The primary reason is that measured forces and moments are strongly time-dependent in seakeeping tests compared with a fixed hull in resistance experiments. Some additional difficulties include:

- Measuring the amplitude of the waves reaching the ship. Also, the amplitudes of the generated waves tend to change until the ship encounters them.
- Determination of the radius of inertia of the ship with a sufficient level of accuracy is difficult.

Therefore, developing numerical methods may support experiments by using their flow visualization abilities or in some cases they may even be used as a substitute for experiments due to the above-mentioned difficulties in ship motion experiments. In fact, ship motion experiments are generally used to validate numerical approaches in the academic world (Bertram, 2000).

As a numerical approach, URANS and the additional turbulence equations, which are discretized by using FVM, have recently been implemented to obtain vertical ship motions and added resistance in waves. However, some potential methods for vertical ship motions and added resistance calculations in deep water have been used, as mentioned in a comprehensive study of Tezdogan et al. (2015) and related references reported therein.

In this section, pioneering studies associated with URANS are given. Sato et al. (1999) studied the coupled vertical motions for Wigley and Series 60 hull forms at head waves. They compared their results with experimental data and concluded that CFD analyses are in good accordance with experiments for the Wigley hull but not for the Series 60 hull form. Beck and Reed (2001) advised that the best options to solve maritime problems are 3D URANS methods. Carrica et al. (2006) studied the forward speed diffraction problem for the DTMB 5512 model under head seas at two speeds and two wavelengths. They discovered that relatively short wavelength waves show non-linear characteristics on heave forces and pitch moments with a remarkable second harmonic component. In their following study, for the same ship model, Carrica et al. (2007) performed URANS analyses to compute the heave and pitch motions in small and large amplitude regular head waves for near-resonant cases. They observed transom wave breaks and extreme motions in large amplitude cases. They only dealt with the encounter frequency near the resonance region. Irvine et al. (2008) carried out seakeeping towing tank experiments of coupled pitch and heave motions and presented a very large database for vertical motions for DTMB 5512. Weymouth et al. (2005) also carried out seakeeping simulations by implementing CFD. Their results were compatible with experiments and they advised possible methods to be implemented in a wide Froude number range. However, in this study the motions were investigated only for a low wave slope range. High wave slope ranges were investigated by Deng et al. (2009) and they studied the vertical motions of a benchmark container ship form. However, in their study, differences for added resistance calculations were quite high compared with experiments. Wilson et al. (2008) performed CFD analyses to obtain TF's of vertical responses of the S-175 ship in regular head waves. The nonlinear URANS approach was used by many researchers to find the hydrodynamic coefficients regarding the added mass as well as the damping. One of these studies was the work of Querard et al. (2009) and they dealt with the computations of added mass and damping of 2D sections. Calculations were done for a very wide range of frequency spectrum. The main focus of their work was to make a comparison with the results obtained by the potential theory; therefore, the motions of the sections that they selected were rather low. For this reason, Querard's method is more accurate compared with potential methods but still deficient due to low motion amplitude. Bhushan et al. (2009) carried out vertical ship motion analyses for both the model and the full scale of the Athena hull form. Simonsen et al. (2010 and 2013) prepared a comprehensive study by using CFD for many different types of ships for seakeeping calculations. Guo et al. (2012) investigated the vertical motions for head waves of the KVLCC2 hull model by using URANS and made added resistance predictions. They showed that CFD can be used for vertical motions and added resistance calculations by comparing the results with experimental data. Tezdogan et al. (2015) investigated the behaviour of vertical motions and added resistance in waves for the full scale KRISO Container model. Their predictions were quite satisfactory. Ozdemir and Barlas (2017) focused on resistance in calm water, ship motions and added resistance calculations for the KVLCC2 model. They claimed that their numerical prediction was in good agreement for resistance, pitch and heave motions. However, an accurate prediction was not achieved for added resistance calculations.

In this study, the TF graphs for the coupled pitch and heave motions in regular head waves were obtained by using CFD for regular frequencies which were the same as those in the experiments conducted in IIHR (Irvine et al., 2008). Added resistance calculations were also performed for the same scenario. Both calculations were carried out in the deep water case for Fn=0.41. While CFD vertical motion TF graphs were compared with experiment and strip theory, CFD added resistance TF graphs were only compared with strip theory. The papers of Salvesen et al. (1970) and Salvesen (1978) was used for comparison of vertical ship motions and added resistance in waves with CFD. The resistance characteristics of the ship in calm water were also calculated for the purpose of validation as shown in Section 5. The commercial CFD software Star-CCM+ was used to discretize the URANS equations by implementing FVM.

This study has two main aims:

1. To compare two numerical techniques and take advantage of their benefits when obtaining vertical motions in head waves for a high speed case. In addition to Carrica's work (2006 and 2007), in the present study, the performed analysis covers the whole frequency range for validation with the experiment.
2. To compare the CFD added resistance TF graph in regular waves against strip theory for a high speed case.

This paper is organised as follows. In Section 2, the main dimensions and physical conditions are presented. In Section 3, the governing equations with computational domain, time step selection, mesh generation and Fourier Series formulation for the problem are given. CFD verification and validation studies are presented in Section 4. Finally, results and discussions are given in Section 5.

The reader should be reminded that experimental results are not available for the second purpose.

2. MAIN PARTICULARS AND PHYSICAL CONDITIONS

A 1/46.588 scaled model of the DTMB 5512 hull given in Figure 1 was used. The experimental results are given in the paper of Irvine et al. (2008). The geometric feature of the model hull is given in Table 1. The numerical simulations were carried out for the bare hull only.

Table 1: Geometric feature of the model

Main Parameters	Value
L_{PP}	3.048 m
L_{WL}	3.052 m
B_{WL}	0.409 m
T	0.132 m
M	84.2 kg
LCG (from aft)	1.536 m
VCG (from base line)	0.152 m
C_m	0.821
C_b	0.507
I_y	48.90 kg-m^2
V	2.2419 m/s
Fn	0.41

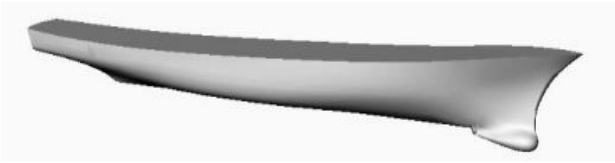

Figure 1**:** 3D representation of the DTMB 5512 model

An Earth-fixed Cartesian coordinate system xyz was selected for the solution domain. The xy plane represented the calm free water surface and z was defined as the vertical axis. The model was allowed to advance in the positive x direction with 2DOF vertical pitch and heave motions. A new local coordinate system was created for the ship to obtain 2DOF motion. The CFD and strip theory calculations were performed at seven different encounter frequencies for Fn=0.41 as shown in Table 2. All calculations were performed in deep water at regular head waves.

Wave encounter frequency can be defined as:

$$f_e = f + \left(\frac{2\pi f^2 V}{g}\right) \tag{1}$$

for the ship advancing in head seas. In Equation (1), g denotes the gravity, f denotes the frequency of the wave and V denotes the velocity of the ship. Small amplitude waves (Ak=0.025) were chosen for CFD simulations to be consistent with performed experiments by Irvine et al. (2008) where A denotes the wave amplitude and k denotes the wave number.

Table 2: Definition of cases for strip theory and CFD calculations

Case No	Method	Ak (-)	f_e (1/s)	A (m)	λ/L_{PP} (-)
1	CFD and Strip Theory	0.025	1.9918	0.0080	0.66
2			1.7388	0.0096	0.79
3			1.4572	0.0121	1.00
4			1.3032	0.0141	1.16
5			1.1448	0.0167	1.38
6			1.0766	0.0182	1.50
7			0.7972	0.0279	2.30

3. URANS EQUATIONS AND MODELLING

The averaged continuity and momentum equations can be written for incompressible flow in Cartesian coordinates and tensor form as indicated in Equations (2) and (3):

$$\frac{\delta U_i}{\delta x_i} = 0 \tag{2}$$

$$\rho\left(\frac{\delta U_i}{\delta t} + U_j \frac{\delta U_i}{\delta x_i}\right) = -\frac{\delta P}{\delta x_i} + \frac{\delta \tau}{\delta x_j} - \frac{\delta(\rho \overline{u_i' u_j'})}{\delta x_j} + F_i \tag{3}$$

where τ_{ij} are the mean viscous stress tensor components as shown in Equation (4).

$$\tau = \tau_{ij} = \mu\left(\frac{\delta U_i}{\delta x_j} + \frac{\delta U_i}{\delta x_i}\right) \tag{4}$$

In this paper, the two equation *k-ε* turbulence model was used to include the effects of the viscosity, as it is considered to be one of the most commonly used turbulence models for industrial applications (Querard, 2008). It is also cheaper in terms of computer memory compared to the k-*ω* SST model which requires higher CPU time (Tezdogan, 2016 and Querard, 2008). The employed solver uses a finite volume method which discretizes the Navier–Stokes (N-S) equations for the numerical model of fluid flow. Segregated flow model was used in the URANS solver, and convection terms in the URANS equations were discretized by applying a second order upwind scheme. In the analyses, the URANS solver runs a predictor–corrector SIMPLE-type algorithm between the continuity and momentum equations. A first-order temporal scheme was applied to discretize the unsteady term in the N-S equations. Volume of Fluid (VOF) model was used to represent the free surface. In this model, computations were performed

for water and air phases. Due to the mesh structure and the number of elements having great importance in capturing the free surface deformations, some refinements were defined close to the free surface to accurately predict VOF wave profiles. A second order convection scheme was used to present the results calculated by VOF more precisely. Summary of the numerical discretization is given in Table 3.

Table 3: Numerical modelling properties

Temporal Discretization	First Order
Convection Term	Second Order
Pressure Link	SIMPLE
Turbulence Model	k- ε
VOF Wave	Second Order

The flow within the boundary layer has to be solved correctly for accurate calculation of the boundary layer dynamics. Therefore, y^+ values on the hull surface should remain within the limits for the *k-ε* turbulence model. The y^+ values on the hull surface were around 45 and this value is considered to be suitable since it remains between the recommended ranges 30-300 for the selected turbulence model (CD-Adapco, 2014). Two layer all y+ wall treatment was used.

The DFBI (Dynamic Fluid Body Interaction) module in the software STAR CCM+ was used for the motion of the body, and the vessel is set free to pitch and heave motions. The 2DOF motion of the body was obtained by calculating the velocity and pressure field in the fluid domain.

3.1 TIME STEP SIZE DETERMINATION

An explicit method generally requires a higher computer memory because of the relatively larger computational domain. In the explicit method, the CFL condition has to be satisfied for the stability of the method. In the present study, an implicit method was used due to computational limitations. In unsteady implicit problems, the restriction imposed by the CFL condition is not a strict issue anymore which frees up the computer in terms of required memory.

Time step size was selected to be $1/2^8$ of T_e for seakeeping analyses which is considered to be more accurate than the value recommended by ITTC (2011). Here T_e denotes the encounter period. The variation of time step size and the obtained results are given in the CFD verification and validation section.

3.2 COMPUTATIONAL DOMAIN AND BOUNDARY CONDITIONS

The given boundary and initial conditions must be proper for all analytical and numerical solutions to have a well-posed problem. These conditions must be determined according to the flow characteristics. In this study, the computational domain was created in order to simulate the seakeeping and added resistance behaviour of DTMB 5512 in regular waves for deep water.

Only half of the body was modelled in order to reduce the domain size and computational time. The boundary conditions for deep water cases are shown in Figure 2.

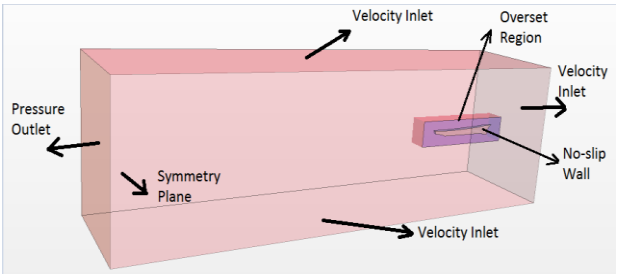

Figure 2: Boundary conditions of computational domain

The top, bottom and side boundaries were modeled as velocity inlet to avoid formation of boundary layers that would form near these boundaries as can be seen in Figure 2. By doing this, numerical simulation is accelerated. 5th-order Stokes waves were used to represent the regular wave for all CFD cases. This wave profile was selected because it is more similar to real waves than the one generated by the first order method (Fenton, 1985). The waves generated by advancing ship were dealt by implementing a numerical damping, which length is 0.50xLPP from the boundaries. A damping function was applied according to the study of Choi and Sung (2009).

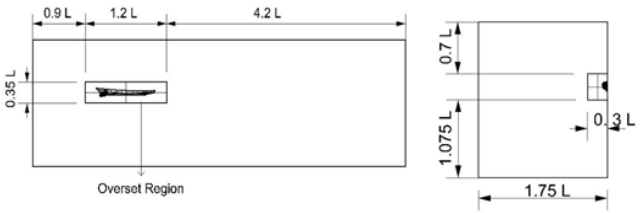

Figure 3: Sizes of the computational domain

As can be seen in Figure 3, the computational domain for deep water cases extended 0.9L in front of the overset region, 4.2L behind the overset region, and 1.75L to the side of the boundaries of the overset region and 1.075L under the boundaries of the overset region. The air region was 0.7L above the overset region.

3.3 MESH GENERATION

Overset mesh, which is considered to have great flexibility for bodies moving inside a fluid, was used for all calculations. This grid system, which is embedded in the background mesh enclosing a certain zone of domain, was used to represent the motion of the hull and there is an "overlap" zone that encompasses the overset region. The information is passed through the overlap block between the

overset and background regions by using linear interpolation method. With the overset grid system, any mesh modification or deformation is not necessary which provides greater flexibility over other standard meshing techniques. In related references, overset mesh technique was used to represent vertical motions of the ships (Tezdogan et al., 2015), (Carrica et al., 2007).

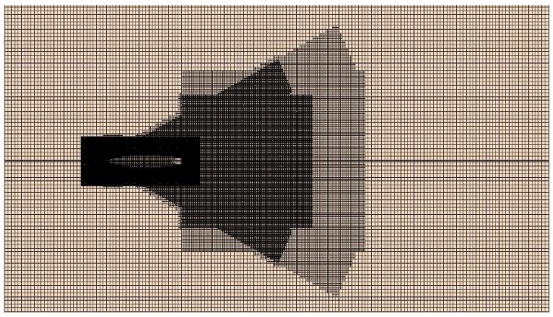

Figure 4: Mesh structure in free surface plane

The mesh was then refined at five regions; overset region, overlap region, vicinity of the hull, around free surface and Kelvin wake region where wave deformation is significant. Refinement blocks were also added near the ship's bow and stern regions in order to capture the pitch motion accurately. Figure 4 and Figure 5 show the mesh system in the computational domain for the deep water cases.

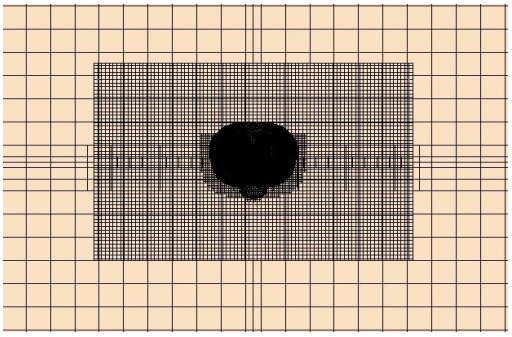

Figure 5a: Overset and overlap mesh structures around the ship

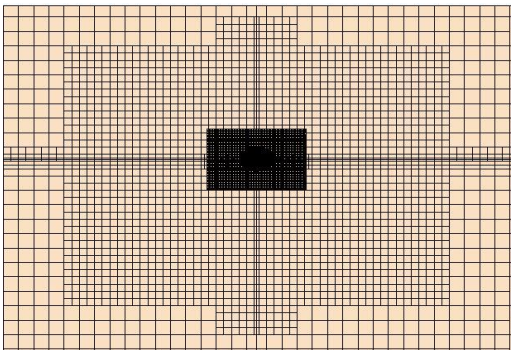

Figure 5b: Overall mesh structure in computational domain

Three different unstructured hexahedral mesh systems were used to calculate the numerical uncertainties which are coarse, medium and fine. The number of elements is given in Table 4. It has to be noted that the reference mesh is fine mesh.

Table 4: Number of elements

	Coarse Mesh	Medium Mesh	Fine Mesh
Background	2.24×10^5	2.24×10^5	2.24×10^5
Overset	3.40×10^5	4.83×10^5	7.25×10^5
Total	5.64×10^5	7.07×10^5	9.49×10^5

3.4 FOURIER SERIES (FS) EXPANSION

The FS formulation part is probably the most cumbersome part of the process because of the number of analyses. Unsteady time histories of the analyzed motions, $\eta(t)$ can be represented by using FS as indicated in Equation (5).

$$\eta(t) = \eta_0 + \sum_{n=1}^{N} \eta_n \cos(\omega_e t + \beta_n) \quad n = 1,2,3... \tag{5}$$

In Equations (8) and (9), η_n and β_n denote the η_{th} harmonic amplitude and phase angle, respectively. These values can be calculated by using a_n and b_n in Equations (11) and (12) as follows.

η_0 is the zeroth harmonic of the unsteady signal which means the averaged value of the signal and it can be found by solving the integral given in Equation (8). η_0 can be used to obtain the added resistance in waves or resistance in calm water.

$$\eta_0 = \frac{1}{T_e}\int_0^{T_e} \eta(t)dt \tag{6}$$

$$\eta_n = \sqrt{a_n{}^2 + b_n{}^2} \tag{7}$$

$$\beta_n = \arctan\left(\frac{b_n}{a_n}\right) \tag{8}$$

$$a_n = \frac{2}{T_e}\int_0^{T_e} \eta(t)\cos(2\pi f_e n t)dt \tag{9}$$

$$b_n = \frac{2}{T_e}\int_0^{T_e} \eta(t)\sin(2\pi f_e n t)dt \tag{10}$$

In these equations, T_e refers to the sampling time and is the encounter period of the given signal. Vertical ship motions, pitch and heave in regular waves can be expressed in terms of transfer functions by the following first harmonic statements given in Equations (11) and (12):

$$TF_{Heave} = \frac{\eta_{1Heave}}{A} \tag{11}$$

$$TF_{Pitch} = \frac{\eta_{1Pitch}}{Ak} \tag{12}$$

where A denotes the wave amplitude and k denotes the wave number.

4. CFD VERIFICATION AND VALIDATION

In the present study, uncertainty analysis was made by using the Grid Convergence Method. This method was first proposed by Roache (1998) and then applied in several studies with some improvements. Out of these refinements, in the present study, the procedure of Celik et al. (2008) has been implemented and is explained in this section.

The following method can be generally considered for unstructured mesh. The refinement factors r_{21} and r_{32} have been calculated according to Equation (13) by taking into account the number of cells.

$$r_{21} = \left(\frac{N_1}{N_2}\right)^{1/3} \qquad r_{32} = \left(\frac{N_2}{N_3}\right)^{1/3} \tag{13}$$

Heave motion numerical uncertainties have been investigated for Case no. 6 as outlined below. The difference between the solutions of the two different meshes can be calculated by Equation (14):

$$\varepsilon_{21} = \varphi_2 - \varphi_1 \qquad \varepsilon_{32} = \varphi_3 - \varphi_2 \tag{14}$$

In this equations φ_1 denotes the solution of fine mesh or time step size, φ_2 denotes the solution of medium mesh or time step size and lastly φ_3 denotes the solution of coarse mesh or time step size. At this point, the convergence condition R can be calculated by Equation (15):

$$R = \frac{\varepsilon_{21}}{\varepsilon_{32}} \tag{15}$$

-1 < R < 0 Oscillatory convergence
0 < R < 1 Monotonic convergence
R < 1 Oscillatory divergence
R > 1 Monotonic divergence

The apparent order of p can be calculated by Equation (16):

$$p = \frac{\ln\left|\varepsilon_{32}/\varepsilon_{21}\right| + q|}{\ln(r_{21})} \tag{16}$$

Here,

$$q = \ln\left(\frac{r_{21} - s}{r_{32} - s}\right) \tag{17}$$

$$s = \mathrm{sgn}(\varepsilon_{32}/\varepsilon_{21}) \tag{18}$$

are given as Equation (17) and Equation (18).

If the refinement factors (r_{21} and r_{32}) are the same, q is equal to zero. The extrapolated values are:

$$\varphi_{ext}^{21} = (r^p\varphi_1 - \varphi_2)/(r^p - 1) \tag{19}$$

The approximate relative error and extrapolated relative error are:

$$e_a^{21} = \left|\frac{\varphi_1 - \varphi_2}{\varphi_1}\right| \qquad e_{ext}^{21} = \left|\frac{\varphi_{ext}^{12} - \varphi_1}{\varphi_{ext}^{12}}\right| \tag{20}$$

At last, the GCI index can be calculated by:

$$GCI_{fine}^{21} = \frac{1.25e_a^{21}}{r_{21}^p - 1} \tag{21}$$

Numerical uncertainty originated from grid and time step size in the present study. Iteration uncertainty was neglected. The procedure states that when obtaining the uncertainty of one, the other must be kept constant. When grid uncertainty was performed, time step size was taken medium. On the other hand, for time step convergences, fine grid was used because grid convergence was reached. The numerical uncertainty for heave motion was given in Table 5a.

Table 5a: Numerical uncertainity for heave motion

	Grid Convergence	Time Step Convergence
φ_1	1.304	**1.360**
φ_2	1.286	1.297
φ_3	1.311	1.158
R	-0.720	0.450
GCI_{FINE}	4.89 %	4.72 %

Validation of Case no 6 was listed in Table 5b. In this table, CFD value was found for fine grid and fine time step size and experiment value was taken from the study of Irvine et al. (2008).

Table 5b: Validation of Case no 6.

Heave Motion TF	**CFD**	**Experiment**	**Difference**
	1.360	1.366	% 0.439

5. RESULTS AND DISCUSSIONS

CFD calculations lasted approximately twelve hours on a 32-core processor with 128 GB RAM for thirty-second simulations for each case. This corresponds to a very short time period because the element number for the fine mesh was less than one million.

5.1 SHIP MOTIONS IN WAVES

The presented results and discussion on vertical motion calculations in regular head waves of DTMB 5512 in deep water are presented with figures and tables in this section. Ship motions in deep water were compared with experimental data of the same model (Irvine et al., 2008). Pitch and heave TF graphs for Fn=0.41 which were obtained by implementing CFD, strip theory and experiments are demonstrated in the figures.

In CFD simulations, time histories of the coupled pitch and heave motions were obtained using the fine grid φ_3 for all cases. As the first harmonics dominate the system for vertical motions of the whole frequency range, they were derived by implementing FS for each case. Then the TF's for vertical motions were generated and compared with the experimental data.

Figure 6 and Figure 7 reveal the non-dimensional pitch and heave amplitudes obtained by CFD, SMP and experimentally. The pitch response of the hull calculated by CFD is in excellent agreement with experiments over the entire frequency range as given in Figure 6. It may be said that the agreement of the strip theory results are comparatively poor. Over almost the entire frequency range, except for fe=1.4572, heave response CFD solutions were in very good accordance with experiments as can be seen from Figure 7. Generally, it can be said that CFD predictions were closer to the experiments. The results which are presented in Figure 6 and Figure 7 are tabulated in Table 6. Although the SMP result is also quite satisfactory, there are some differences when Table 6 is considered.

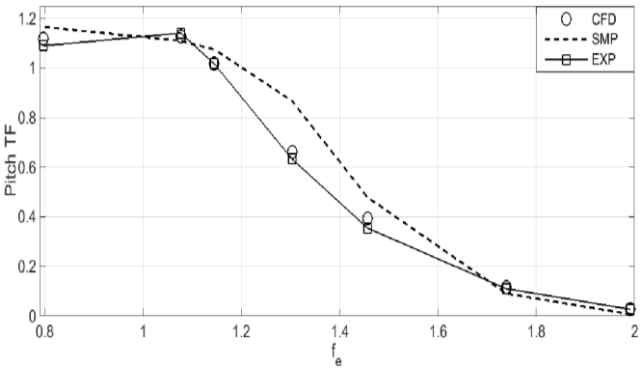

Figure 6: Pitch TF for Fn=0.41 in regular head waves

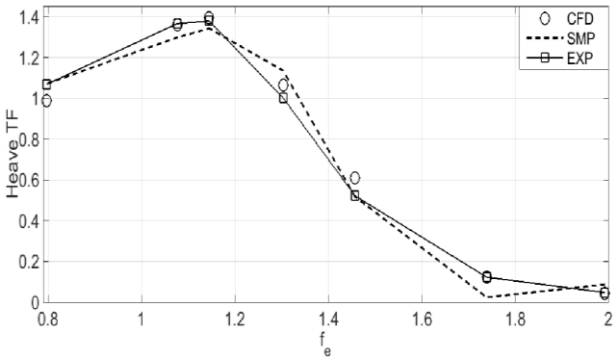

Figure 7: Heave TF for Fn=0.41 in regular head waves

Table 6: TF's for vertical motions

Case No.	Heave TF			Pitch TF		
	CFD	SMP	EXP.	CFD	SMP	EXP.
1	0.0436	0.087	0.0472	0.0276	0.007	0.0266
2	0.1250	0.024	0.1229	0.1166	0.091	0.1103
3	0.6108	0.517	0.5219	0.3923	0.478	0.3541
4	1.0631	1.136	1.0019	0.6619	0.867	0.6330
5	1.3958	1.343	1.3792	1.0196	1.075	1.0171
6	1.3601	1.298	1.3662	1.1287	1.110	1.1412
7	0.9890	1.072	1.0687	1.1172	1.166	1.0898

As mentioned earlier, the Fn=0.41 case is assumed to represent the high speed regime for a displacement vessel. In this case, the motions in waves flowing around the ship are highly turbulent and viscous effects are playing an important role. It is the main reason that at this speed nonlinear modelling returns better results compared to the linear strip theory. Besides, the complexity of the bulbous bow form and transom stern leads to generation of the flow separation phenomena which can only be calculated by a viscous solver. At the same time, in strip theory, hydrodynamic pressure is calculated by the first order velocity potential component. The second order velocity component is neglected. This assumption may lose its validity for relatively high speeds and should be reconsidered. In addition to these, excitation wave force is associated with simple sinusoidal form in potential strip theory. In real seaway, no wave has sinusoidal form due to gravitational force. However, in CFD analyses, a fifth order Stokes wave which is assumed to be more similar to the one generated from a wave generator is used. Finally, the Kelvin wave system of the ship at Fn=0.41 affects the ship motions in waves because the radiated waves from the ship have high amplitudes for transverse and divergent waves. This effect is included in CFD analyses. Therefore, it is strongly recommended that the reliable non-linear CFD tool should be used for high speed cases.

5.2 SHIP RESISTANCE IN WAVES

Before calculating added resistance in waves, the total resistance R_T must be obtained in calm water. R_T can be decomposed into two essential components - R_R (residuary resistance) and R_F (frictional resistance) as given in Equation (22):

$$R_T = R_R + R_F \tag{22}$$

Resistance is usually given in non-dimensional form as in Equation (23):

$$C_X = \frac{R_X}{\frac{1}{2}\rho S V^2} \tag{23}$$

where x in the subscript represents any resistance component. Here, ρ denotes the water density, S the wetted surface area and V the ship velocity. R_R and R_F are functions of Froude (Fn) and Reynolds (Re) numbers. The following statement can be expressed in Equation (24):

$$C_T = C_R(Fn) + C_F(Re) \tag{24}$$

Here, C_T denotes the total resistance coefficient, C_R the residuary resistance coefficient and C_F the frictional resistance coefficient. In the CFD calculation, the zeroth harmonic of the total resistance signal gives the averaged value of the predicted total resistance. Hence, the C_T of DTMB 5512 in calm water is achieved by implementing FS to the time series of the total resistance signal. The wave pattern of the ship at Fn=0.41 for the calm water case is given in Figure 8.

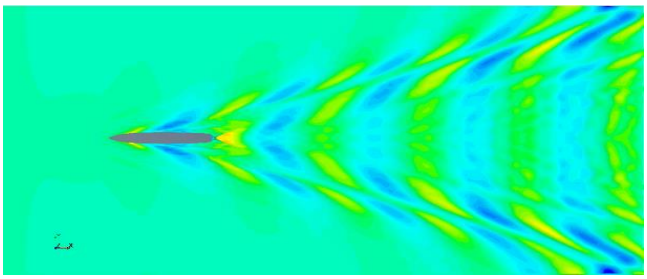

Figure 8: Presentation of the correctly captured Kelvin wave pattern behind the ship

As shown in Table 8, C_T is predicted with a high level of accuracy. The present study under-predicts C_T less than 0.5% as compared with the experimental data (Gui, 2001).

Table 8: Experimentally and numerically calculated total resistance coefficients

Calm Water Resistance	CFD	Experiment
	6.725 E-03	6.732 E-03

The added resistance in regular waves is calculated by using Equation (25):

$$C_{AW} = \frac{R_{AW}}{A^2 \rho g B^2 / L_{WL}} \tag{25}$$

Here, C_{AW} denotes the added resistance coefficient, A denotes the regular wave amplitude. B denotes the beam of the ship and L_{WL} denotes the water line length of the ship. In this equation, R_{AW} represents the added resistance value and it can be found by subtracting the calm water resistance R_T from the total resistance value for all cases. TF added resistance graphs are generated for all encountered frequencies except for Cases no. 1 and 2 as can be seen from Figure 9 because these two cases have two essential harmonic components when Fourier transform is applied to the total resistance signal as can be understood from Figure 10.

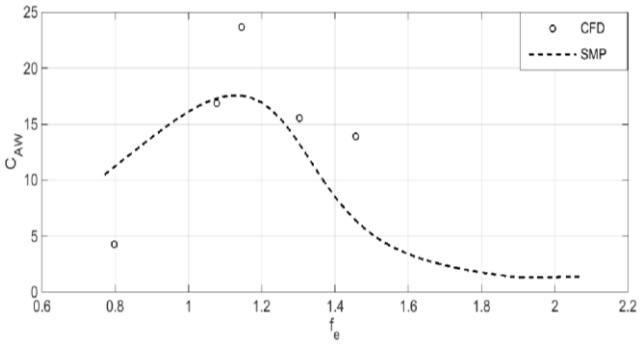

Figure 9: Added resistance TF for Fn=0.41

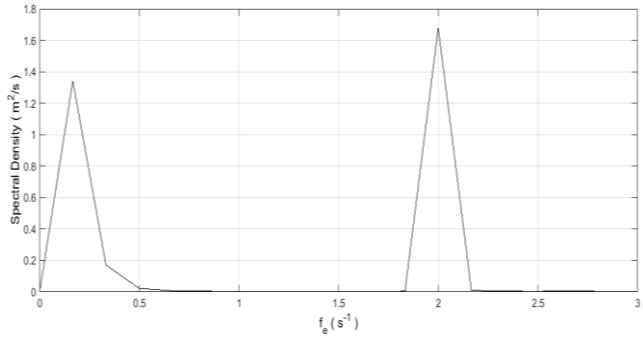

Figure 10: FFT analysis of total resistance signal for Case No. 1

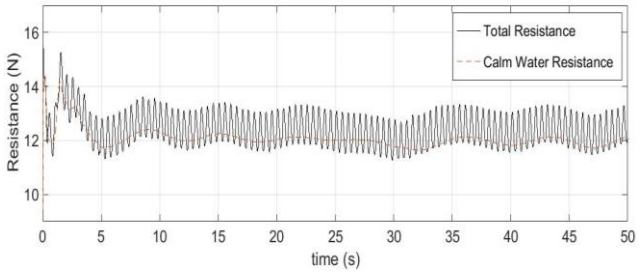

Figure 11: Computed time history of total resistance for Case No. 1 and calm water case

As shown in Figure 11, the total resistance signal in waves does not oscillate around a fixed line which means the zeroth harmonic of the oscillation is time-dependent. This is the reason the average of the signal is not constant. Thus, the TF approach does not make any sense for these two frequencies and is excluded.

As commonly known, added resistance computation is second order with respect to the wave amplitude of incident waves based on computed motions. Referring to the study of Salvesen (1978), if one evaluates the vertical motions with an accuracy of around 10–15% then the resulting added resistance computations will likely to have an accuracy of around 20–30%. Due to this fact, the discrepancy of the computed vertical motions by utilizing CFD and SMP will cause a remarkable deviation on the added resistance outputs to appear. Moreover, it is known that Salvesen's method is based on calculating the second-order longitudinal wave force acting on the constant wetted surface of the vessel which has no viscosity effect at all. However, CFD tools enable fully non-linear governing equations to be solved by taking into consideration both the viscous effects and the draught change due to ship motions.

Added resistance in waves has become more insightful due to its direct relation with the EEDI (Energy Efficiency Design Index) which is mandatory for the construction of new ships, which significantly influences the CO2 amount emitted (IMO 2011, Seong-Oh Kim et al., 2014). Therefore, accurate calculation of the added resistance is needed to save the environment and to mitigate global warming to some level.

6. CONCLUSIONS

In the present paper, a promising approach to the problem of a fast displacement ship form, DTMB 5512, free to pitch and heave motions and added resistance in regular head waves was presented based on the numerical analyses using the URANS approach. The verification and validation studies were performed for the heave motion near-resonant case. The obtained results were compared with the corresponding outputs offered by the experiment and strip theory calculations where very good agreement was achieved for vertical motions in waves by using URANS. Added resistance calculations were only compared with respect to the strip theory because of the lack of experimental data. Remarkable differences between strip theory and URANS were observed on generated added resistance TF graphs. Therefore, the authors suggest that the URANS computed added resistance results reported here need a validation study.

7. ACKNOWLEDGMENT

This research was supported by Yildiz Technical University Scientific Research Projects Coordination Department. Project No: 2015-10-01-KAP01. The first author was supported by ASELSAN Graduate Scholarship for Turkish Academicians.

8. REFERENCES

1. BERTRAM V. *Practical Ship Hydrodynamics.* Butterworth-Heinemann. 2000
2. TEZDOGAN T., DEMIREL Y.K., KELLETT P., KHORASANCHI M., INCECIK A. and TURAN O. *Full-scale unsteady RANS CFD simulations of ship behavior and performance in head seas due to slow steaming*. Ocean Engineering, 186-206. 2015
3. SATO, Y., MIYATA, H. and SATO, T. *CFD simulation of 3-dimensional motion of a ship in waves: application to an advancing ship in regular heading waves*. Journal of Marine Science and Technology, 4: 108-116. 1999.
4. BECK, R.F. and REED, A.M. *Modern computational methods for ships in a seaway*. Transactions of the Society of Naval Architects and Marine Engineers, 109 pp.1-51.2001.
5. CARRICA, P.M,. WILSON, R. V. and STERN, F. *Unsteady RANS simulation of the ship forward speed diffraction problem*. Computers & Fluids 35 545–570. 2006.
6. CARRICA, P.M,. WILSON, R. V, NOACK, R. W., and STERN, F. *Ship motions using single-phase level set with dynamic overset grids.* Computers & Fluids 36 1415–1433. 2007
7. IRVINE, M., LONGO, J. and STERN, F., *Pitch and Heave Tests and Uncertainty Assessment for a Surface Combatant in Regular Head Waves*. Journal Ship Research, Vol. 52, No. 2, pp. 146-163. 2008.
8. WEYMOUTH, G.D., WILSON, R.V. and STERN, F. *RANS Computational fluid dynamics predictions of pitch and heave motion in head seas.* Journal of Ship Research. 49 (2): 80-97. 2005.
9. DENG, G.B., QUEUTEY, P. and VISONNEAU, M. *Seakeeping prediction for a container ship with RANS computation*. 22nd Chinese conference in hydrodynamics. 2009.
10. WILSON, R.V., JI, L., KARMAN, S.L., HYAMS, D.G., SREENIVAS, K., TAYLOR, L.K. and WHITFIELD, D.L. *Simulation of large amplitude ship motions for prediction of fluid-structure interaction*. 27th Symposium on Naval Hydrodynamics. Seoul. 2008.
11. QUERARD, A.B.G., TEMAREL, P. and TURNOCK, S.R. *The hydrodynamics of ship-like sections in heave, sway and roll motions predicted using an unsteady Reynolds averaged Navier-Stokes method*. Engineering for the Maritime Environment, 233. 2009.
12. BHUSHAN, S., XING, T., CARRICA, P. and STERN, F. Model and full-scale URANS simulations of Athena resistance, powering,

seakeeping, and 5415 manoeuvring. Journal of Ship Research, 53 (4), pp.179-198. 2009.

13. SIMONSEN, C.D., OTZEN, J.F., JONCQUEZ, S. and STERN, F. *EFD and CFD for KCS heaving and pitching in regular head waves*. Journal of Marine Science and Technology, 18 (4), pp.435-459. 2013.
14. SIMONSEN, C.D. and STERN, F. *CFD simulation of KCS sailing in regular head waves*. Gothenburg 2010-A Workshop on Numerical Ship Hydrodynamics. Gothenburg. 2010.
15. GUO, B.J., STEEN, S. and DENG, G.B. *Seakeeping prediction of KVLCC2 in head waves with RANS*. Applied Ocean Research, 35: 56-57. (4), pp.179-198. 2012.
16. OZDEMIR, Y.H. and BARLAS, B. *Numerical study of ship motions and added resistance in regular incident waves of KVLCC2 model*. International Journal of Naval Architecture and Ocean Engineering, 9:2, pp 149-159. 2017.
17. QUERARD, A.B.G., TEMAREL, P. and TURNOCK, S.R. *Influence of viscous effects on the hydrodynamics of ship-like sections undergoing symmetric and anti- symmetric motions, using RANS*. In: Proceedings of the ASME27th International Conference on Offshore Mechanics and Arctic Engineering (OMAE), Estoril, Portugal, pp.1–10. 2008.
18. CD-ADAPCO. *User guide STAR-CCM Version 9.0.2*. 2014.
19. INTERNATIONAL TOWING TANK CONFERENCE (ITTC), (2011b). *Practical guidelines for ship CFD applications*. In Proceedings of the 26th ITTC. 2011.
20. ROACHE, P. J., *Verification of Codes and Calculations*. AIAA J., vol. 36, no. 5, pp. 696–702, 1998.
21. CELIK, I., GHIA, U., ROACHE, P., FRETIAS, C.J. , COLEMAN, H., RAAD, P.E., *Procedure for estimation and reporting of uncertainty due to discretization in CFD applications*. J. Fluids Eng.-Trans. ASME, vol. 130, no. 7, Jul. 2008.
22. GUI, L., LONGO, J., and STERN, F. *Towing Tank PIV Measurement System, Data and Uncertainty Assessment for DTMB Model 5512*. Experiments in Fluids, Vol. 31, pp. 336-346. 2001.
23. FENTON, J. D. *A fifth-order Stokes theory for steady waves*, J. Waterw. Port. Coast. Ocean Engineering, 111 (2), 216-234. 1985.
24. KIM, S.O., OCK, Y.B., HEO, J.K., PARK, J.C., SHIN, H.S., LEE, S.K, *CFD simulation of added resistance of ships in head sea for estimating energy efficiency design index*, https://doi.org/10.1109/ Oceans-Taipei. 2014. 6964578, 07-10.04.2014.
25. SALVESEN, N., *Added Resistance of Ships in Waves*, Journal of Hydronautics, Vol. 12, No.1 (1978), pp. 24-34. http://dx.doi.org/10.2514/3.63110
26. CHOI, J., and SUNG, B. Y., *Numerical simulations using momentum source wave-maker applied to RANS equation model*, Coastal Engineering, 56 (10), pp. 1043 - 1060. 2009

REGULATORY APPROACHES LEADING TO HOLISTIC IMPLEMENTATION IN A FISHING VESSEL FLEET LESS THAN 24 M IN LENGTH

(DOI No: 10.3940/rina.ijme.2017.a4.452)

M J Núñez Sánchez, Ministry of Transport and Public Works, Spain, and **L Pérez Rojas**, Escuela Técnica Superior de Ingenieros Navales, Universidad Politécnica de Madrid (UPM), Spain

SUMMARY

Fishing is a very dangerous sea activity with a high rate of fatalities that is difficult to deal with by Maritime and Fisheries Administrations around the world. Meanwhile the Ocean Governance requires a global approach to sustainability and safety, with overarching principles governing both of them. This paper deals for the first time with the implementation of a complete methodology to assess the safety at sea, by means of a bottom-up goal based standards with safety level approach, encompassing the national regulations and using formal safety assessment as the driver in a fishing vessel fleet below 24 m in length (L). It is concluded that such methodologies are applicable, goal based regulations can be established, flexibility in the design can be provided and have the potential to be later extrapolated to holistic approaches.

NOMENCLATURE

L	Length between perpendiculars
FSA	Formal Safety Assessment.
GBS	Goal Based Standards
SLA	Safety Level Approach
GBS-SLA	Goal Based Safety Level Approach
ALARP	As Low As Reasonably Practicable
VPF	Value of Preventing a Fatality
GCAF	Gross Cost of Averting a Fatality
NCAF	Net Cost of Averting a Fatality

1. INTRODUCTION

Fishing has been traditionally considered one of the most dangerous activities, with more than 4.5 million vessels below 24 m in length and millions of fishermen operating them worldwide.

The rates of fatalities per 100,000 fishermen in developed countries show a decline in the last 15 years, however the figures are still high. In the UK the rate of fatalities varies between 80 (highest) and 30 (lowest), in Norway between 50 and 40 and in Canada between 30 and 20, in a context of a declining number of fishermen and fish stocks. Meanwhile in Spain the rate is between 45 and 22, with a soft decline in frequencies in the last eight years. However in the national context, the Spanish rate is between 6 to 9 times above average and 3 times higher than popular sectors such as house building, as it can be seen in figure 1.

In some cases health and labor accidents in fishing vessels are mixed with safety at sea related accidents thus making difficult to separate incidents and isolate those strictly related to the lack of safety. In general, accidents in vessels below 12 m in length tend to be more related to safety whereas for the range from 15 m to 24 m in length are more related to occupational health.

It is not easy to find literature that can quantify the casualty risk of fishing vessels. The available data refer to the fatality rates or number of fatalities, but never in very detailed manner and even less taking into account the impact of these accidents in the national economies. This issue, among others, diverts the attention in maritime safety towards the more global international shipping in merchant ships.

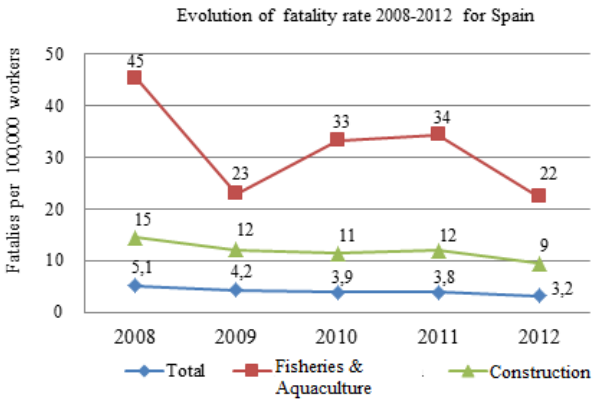

Figure 1. Rates of fatalities in Spain. Total working force, fisheries and aquaculture and construction

The achievement of high level goals in the fishing vessel industry is more cumbersome than in international shipping, due to the complexities of an activity that is mainly carried out at regional level and, in addition, the low level of commitment at international level to deal with these vessels.

This complexity requires a collaborative approach between the agencies involved and also a holistic approach. However, in order to be holistic, it is necessary to carry out an exercise to assess how safety at sea can be considered in isolation in such a broad manner that it later allows to combine it with other elements such as the management of the resource, pollution and labor conditions.

With all of the above challenges, fishing vessels below 24 m in length between perpendiculars (L) were chosen as a case study due to the following:

- the higher incidence in safety at sea versus. occupational safety in comparison to larger vessels;
- the frequency of fatalities that seems difficult to be further reduced;
- availability of statistical data in a single fishing vessel fleet;
- the need to be able to find a systematic approach to decide on the most adequate technical solutions to reduce the high fatality rates; and
- the future challenges, in particular related to Ocean Governance and life below the water management;

2. OBJECTIVES

To assess safety at sea in fishing vessels of less than 24 m in length in a quantifiable manner in order to be able to move to a more holistic approach that can be later connected with sustainability.

In this regard a research was carried out in the Spanish fishing vessel fleet with the following objectives.

- Quantify risk and find the safety level of the national fishing vessel fleet (excluding aquaculture) by analyzing its impact on the national economy, the regulatory framework and analyzing the accidents in a fleet that has changed in the last 17 year due to the pressure on the fishing stocks.
- Generate a structure and methodology to be able to change the reactive approach to accidents.
- Provide a certain degree of freedom in the design in a very heterogeneous fleet that can be later extrapolated to the worldwide fleet.

3. TOOLS FOR QUANTITATIVE ASSESSMENT, DECISION AND RULE MAKING

In order to identify and apply tools for a change towards a more quantifiable and holistic regime in maritime safety this research it is necessary to explain several IMO methodologies, some of which are still under development (Núñez, 2016).

3.1 FORMAL SAFETY ASSESSMENT

Formal safety assessment (FSA) (IMO, 2015), as outlined in figure 2 is a tool that evaluates new regulations in steps and helps to compare proposed changes with existing standards, enabling a balance to be drawn between the various technical and operational issues, including the human element, and between safety and costs. FSA uses risk models (step 2) that help to evaluate recommendations (step 3), known as risk control options, which should be presented to the decision-makers in an auditable and traceable manner (steps 4 and 5).

These recommendations are based upon:

- the comparison and ranking of all hazards and their underlying causes;
- the comparison and ranking of risk control options as a function of associated costs and benefits; and
- the identification of those risk control options which keep risks as low as reasonably practicable.

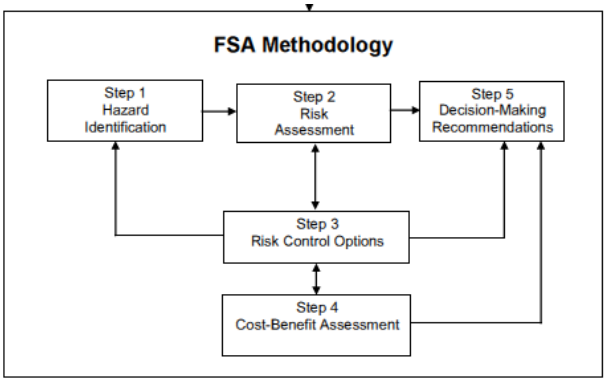

Figure 2. FSA step approach (IMO, 2015)

However, this risk-based approach technique has some challenges, such as:

- the quality and quantity of the data collected in order to support monitoring and development of safety regulations;
- the integration of risk-based methodologies and the latest analysis techniques into the safety regulatory framework to provide a sound scientific and practicable basis for the development of future safety regulations; and
- the know-how required to use these tools versus the traditional approach to propose new rules or amend existing rules, with justifications that do not require detailed documented rational, basis for assumptions, description of uncertainties or sensitivity analysis.

3.2 SAFETY LEVEL APPROACH (SLA)

SLA is the structured application of risk based methodologies to reach an explicit safety level or to verify compliance of rules. The aim is to have quantitative and rational safety levels to be able to be used and provide a way to measure safety in the ship concept and the human element in the IMO rule making process.

This approach needs the development of quantitative or qualitative safety levels and processes to be used for achieving a practicable safety level, or an implicit safety

level such as that in the ALARP principle (IMO, 2000) with F-N curves (societal risk). By doing this the safety level may be revised and adjusted as needed when this is not sufficient or it is exceeded.

3.3 GOAL BASED STANDARDS (GBS)

GBS is a "top-bottom" concept that offers a tiered approach, "rules to develop rules", working with the following principles (IMO, 2015), also indicated in figure 3:

- Tier I- Goal, which is a high level objective to be met that should address an issue of concern;
- Tier II- Functional Requirements, which provide the criteria to be complied in order to meet the goals and are developed after the goals and considering the relevant hazards;
- Tier III- Verification of Conformity, which provides a transparent instrument necessary for monitoring and verifying that the associated rules and regulation for vessels conform the goals and functional requirements.
- Tier IV- Rules and regulations for vessels, which are the detailed requirements (developed by IMO, a National Administration, a Recognized Organization or a Classification Society) that need to meet the goals and functional requirements
- Tier V- Industry practices and standards, developed as a consequence that may be referenced in the rules and regulations.

These have the aim to provide more clarity and flexibility to comply with the functional requirements by means of risk management tools without a pre-established agreed criteria in their definition.

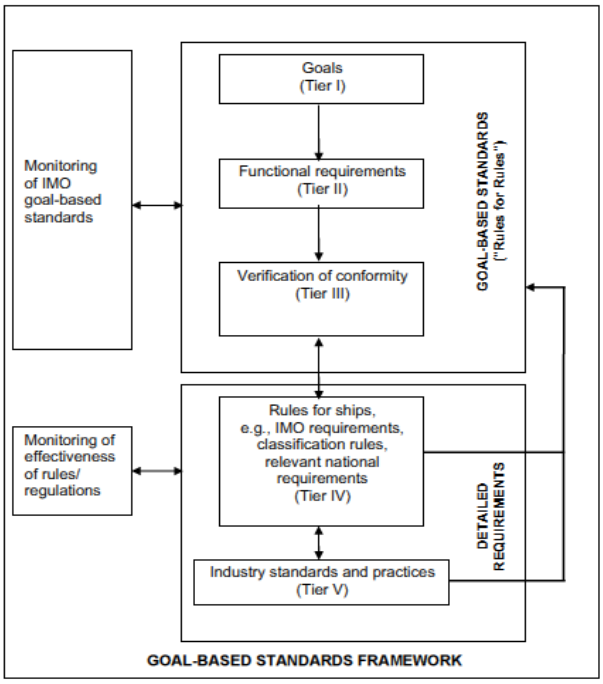

Figure 3. Goal Based Standard tiered structure (Data source: (IMO, 2015)

With the proper use of these tools there is a possibility to structure the rule development when interconnected as indicated in Figure 4, and therefore it was decided to proceed accordingly.

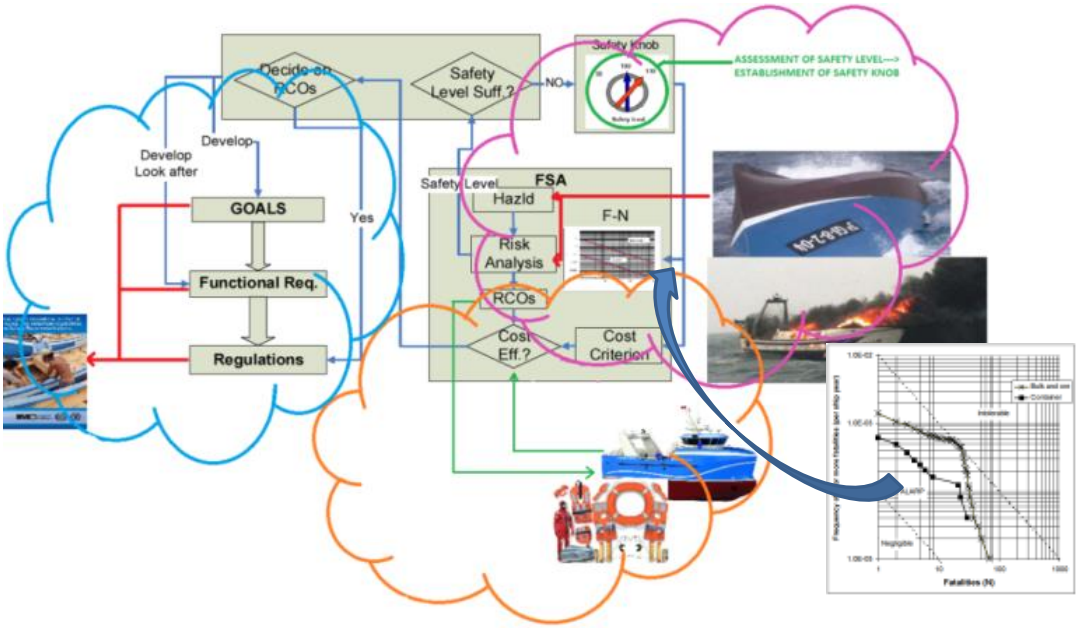

Figure 4. The combination of risk analysis, hazard identification, FSA, GBS and SLA (Núñez, 2016)

In this regard the following steps were taken:

- Analyze the fishing vessel fleet and the industry in terms of revenues, benefit and impact on the GDP;
- Analyze the fishing vessel fleet in terms of regulatory regime, fatalities and develop suitable high risk level models that can turn the frequencies into probabilities, to be able to analyze the impact of risk control measures. This is carried out in steps 1 and 2 of the FSA;
- Identify a safety level of the fishing vessel fleet using the previous two items based on cost analysis, considering some of the elements of step 3 of the FSA;
- Carry out a detailed formal safety assessment (FSA) of the fleet to determine the risk control options that can be implemented, taking into account the safety level as calculated; and
- Determine goals and quantifiable functional requirements for the national safety at sea regulations that can incorporate a safety level and be used as high level principles, to develop rules in a GBS-SLA environment inserting them in the high level risk models.

4. ANALYSIS OF THE FISHERIES ECONOMY

In order to be able to later consider in the national economy the costs and benefits of fishing vessel accidents an analysis was carried out.

Spain is traditionally considered one of the most important players in the world of fishing and one of the top 3 consumers in the world, with an important fishing vessel fleet below 24 m in length. The impact in the GDP by small scale fisheries with vessels less than 24 m in length constitutes approximately, 2,000 million € per year, approximately 0,1 % of the national economy, as indicated in figure 5.

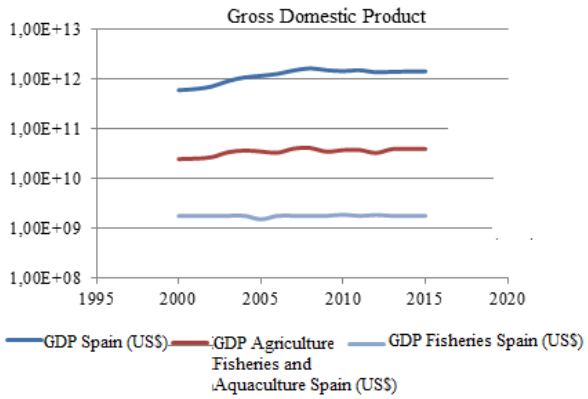

Figure 5. Evolution of the Spanish fisheries GDP

These revenues are heavily influenced by the size of the fleet that has been progressively decreasing due to the lack of stocks, but has been balanced with the increase in value of the captures. In order to assess how the fleet will evolve a forecast was carried out by means of a multi-regressive ARIMA (1,1,1) (Rodríguez-Aragón, 2015). The results are shown in figure 6, that indicated a continuous decline that will probably continue in the future.

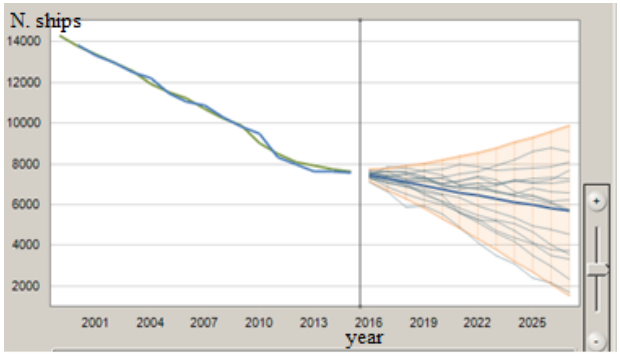

Figure 6. Evolution of the Spanish FV fleet below 24 m L and future forecasts by means of ARIMA (1,1,1)

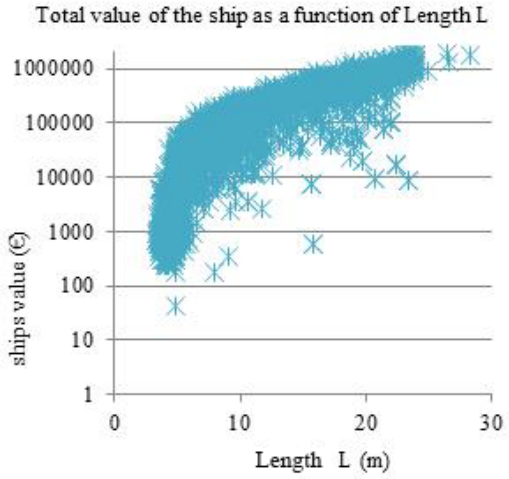

Figure 7. Vessels value (€) against length

The fisheries economy and the value of ships were quantitatively analyzed from 2000 to 2015, taking into account the evolution of the fleet, the economic value of the ship indicated in national certificates and the loss of the asset as the fishing vessel increases its age. Figure 7, shows the value of the fleet below 24 m in the year 2015.

The daily income per fishing vessel is heavily dependent upon its size and the type of fisheries. Taking into account the captures and its value, the revenue was calculated as indicated in figure 8. This data was then used to assess the loss of income per day in case of accident of a fishing vessel.

Finally the costs of repairs in case of accident were assessed taking into consideration the necessary hull and machinery repairs in the reported accidents, after consultations with shipyards and manufacturers. Due to the limited data, the values provided were adjusted to statistical distributions, such as the one indicated in figure 9, by means of Montecarlo simulations.

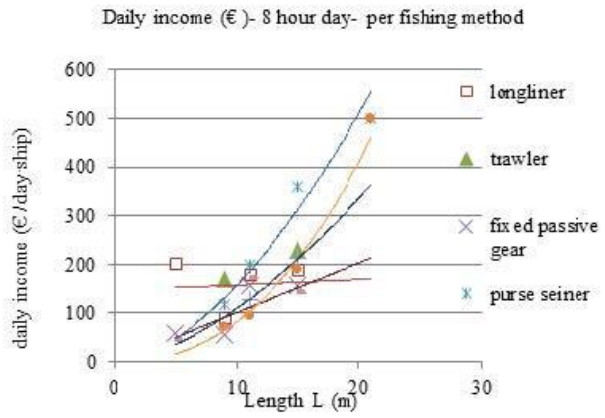

Figure 8. Daily income, fishing vessels below 24 m L depending on the ship´s method

The above three elements constitute the basic costs and loss of benefits of accidents in monetary terms, in case of accident.

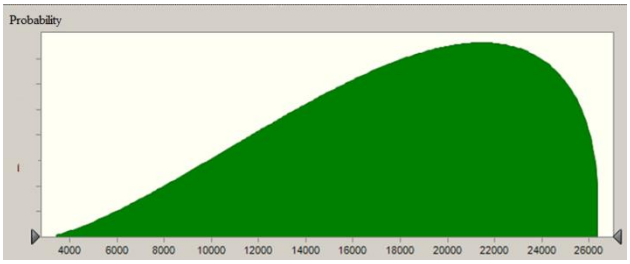

Figure 9. Beta distribution with costs of repairs to the structure for accidents in vessels between 15 and 24 m L

5. ANALYSIS OF THE SAFETY AT SEA REGIME TAKING INTO ACCOUNT ACCIDENTS

The fishing vessel safety regime depends on the ship size. The use of tonnage as per the International Convention on the Measurement of Ships, 1969 is well established in Europe, however the use of length in the 1930 or 1966 Load lines Convention (as transposed to fishing vessels) and the 1993 Torremolinos Protocol turns length (L) into the main parameter, whose main threshold is set at 24 m. For vessels below 24 m key figures such as 12 m, 15 m or 18 m are normally used. In the case of Spain the regulatory regime below 24 m sets a limit of 12 m, which is approximately 15 m length over all (LOA). This creates a division in the regulation which is similar to other countries like the UK (MCA, 2002).

A database of 975 accidents was analyzed in order to get valuable information, such as the monthly percentages, that remained approximately constant irrespective of the season, as indicated in figure 10. With these data, the individual risks (taking into account the exposure) and the potential loss of life per ship per year (PLL) per type of accident were also calculated.

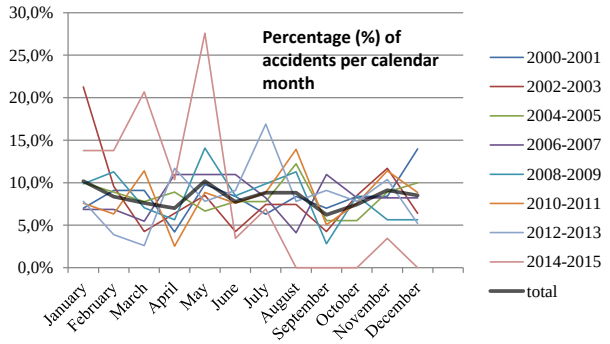

Figure 10. Percentage of bi-annual accidents in the fishing vessels fleet below 24 m L per calendar month

The rate of fatalities in Spain in the period 2000-2013 provide acceptable values of the potential loss of lives (PLL) in terms of fatalities per ship per year except for some types of incidents, such as foundering and shows a decline when comparing the periods 2000-2007 versus 2008-2013.

The societal risks by means of FN curves (Svein, 2005) were also calculated. These curves show the frequency of accidents with N or more fatalities in vessels of less than 12 m, as indicated in figure 11 and for vessels on or over 12 m in figure 12.

These FN curves were limited by an as low as reasonable possible "ALARP" region that allowed to assess the status of the fleet in terms of societal risk, whether unacceptable (above ALARP) and negligible (below ALARP), that is built taking into consideration the Potential loss of life of the activity (PLL_A), which refers to the potential number of fatalities in the fisheries activity by comparison to the economic value of the activity and the national GDP. Figures 11 and 12 show different bands for comparison of merchant vessels: IMO standard for general cargo ships as chain line, the 2000-2007 region as a dotted line and the 2000-2013 region as a dashed line.

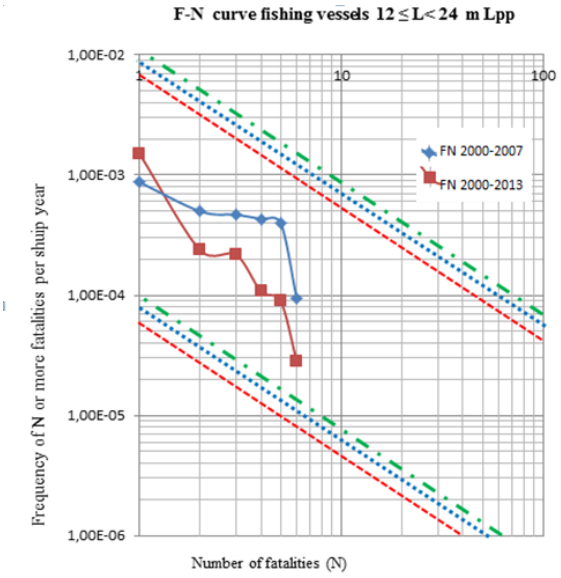

Figure 11. F-N curves fishing vessels from 12m to 24 m L

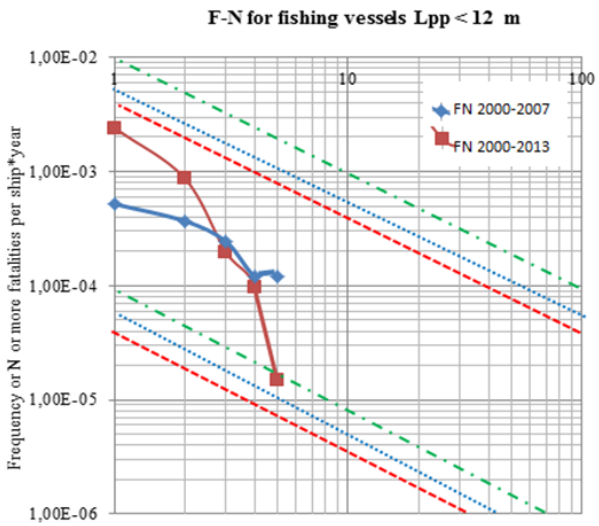

Figure 12. F-N curves fishing vessels of less than 12 m L

Taking the above into consideration, it was found that this fishing vessel fleet was performing within the ALARP zone and relatively well, if compared to the global merchant ship fleet in terms of individual risks and the value of the activity (Svein, 2005).

Finally, after considering the PLLs and the F-N curves it was decided to develop "bow- tie" high level risk models (Papanikolau *et al*, 2009), that would consider fault and event trees with the aim to capture the reasons why an accident was triggered and its consequences. These trees were made for the following types of accidents: collision, fire-explosion, grounding, foundering and list, as the example shown in figure 13. These models would take also into account*; inter alia*, the area of operation of the ship, the loading conditions and the consequences.

Not all the accidents could be included in the models, but only those with sufficient information. In order to compare the data in the model with historic data, the PLLs were benchmarked in the FN curves with satisfactory results. However, in terms of loss of benefits, a deviation of 15% was obtained. This error will be accumulated in the whole research whenever benefits had to be considered.

6. IDENTIFICATION OF THE SAFETY LEVEL

Taking into consideration the costs calculated above, it was decided to calculate a safety level for the Spanish vessel fleet by means of costs criterion for the years 2000 to 2013. In order to achieve it and considering the decline in frequencies, as indicated before, it was benchmarked how the implementations of new safety regulations in 2006 and 2007 had helped to reduce the fatalities taking into consideration the evolution of the fleet.

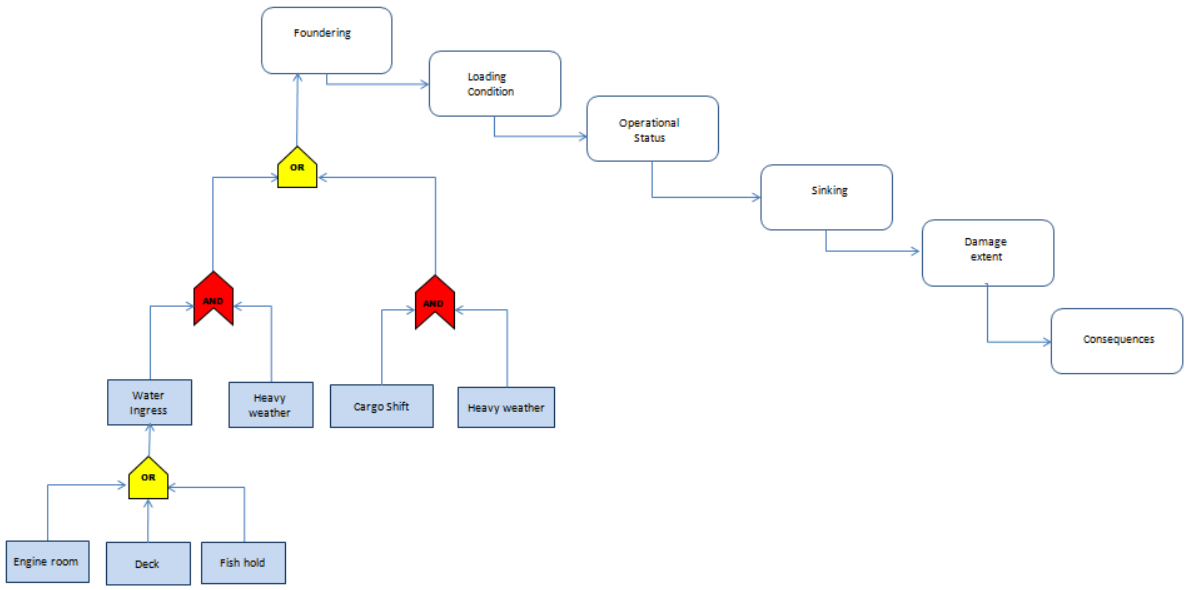

Figure 13. Foundering High level risk model

These measures included the implementation of the Code of Safety for fishing vessel below 24 m L (Ministry of Transport, 2007) that required additional safety and navigation equipment for all vessels, together with measures for new ships, such as new load-line assignment (see figure 14) and other measures implemented , such as GMDSS regulations and concentrated inspections.

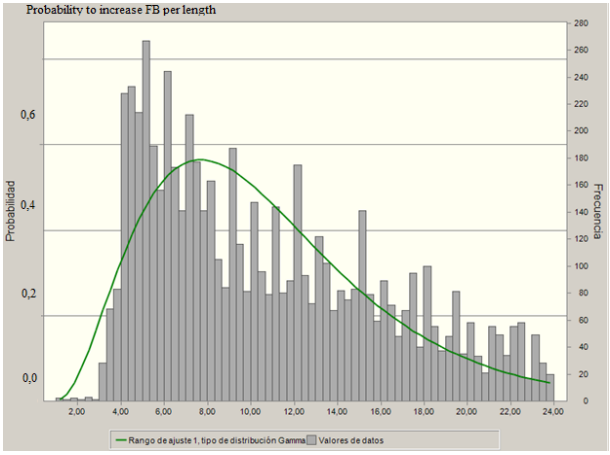

Figure 14. Probability (1/10) of necessity to increase freeboards depending on the ship length

In order to calculate this level the value of preventing a fatality (VPF) was also determined for Spain (4.5 M €) and this value compared with the Gross cost of averting a fatality (GCAF) and Net cost of averting a fatalities (NCAF) of the combined implemented measures as indicated in formulas 1 and 2.

$$GCAF = \frac{\Delta Cost}{\Delta Risk} \quad (1)$$

$$NCAF = \frac{\Delta Cost - \Delta Benefit}{\Delta Risk} = GCAF - \frac{\Delta Benefit}{\Delta Risk} \quad (2)$$

The costs of implementation of these new regulations (ΔCost) were determined in consultation with manufacturers and designers. The benefits (ΔBenefit) were taken from the historic data, and the calculations carried out as shown in section 4 of this paper. The risk reduction (ΔRisk), in terms of fatalities, were determined with the statistical values as shown in section 5. All of the above was calculated taking into consideration the forecasts of the fleet in the next 15 years.

The ratios obtained when dividing the parameters GCAF or NCAF by the VPF indicates the percentage of VPF to be used to determine safety measures. Therefore, considering the impact of the implemented regulations, this ratio is assumed to be the safety level of the current regime and the "lever" indicating, in terms of costs, which potential new regulations can be developed depending on the risk reduction, costs and benefits.

Using GCAF only and taking into account the fatalities in the years 2014 and 2015 the factor needed further readjustments as indicated in figure 15, showing how sensitive the parameter is to the change in frequencies. In terms of safety the calculation shows that vessels from 12 m to 24 m L have performed well and also shows that special attention is needed on those vessels below 12 m, which is coincident with the initial consideration that vessels below 12 m L are more prone to have safety at sea related incidents and the FN curve shown in figure 12.

It also shows that during the period 2014 and 2015 the reduction in the risk of fatalities was not sufficient and therefore the increase in costs triggered an increase in the safety level factor.

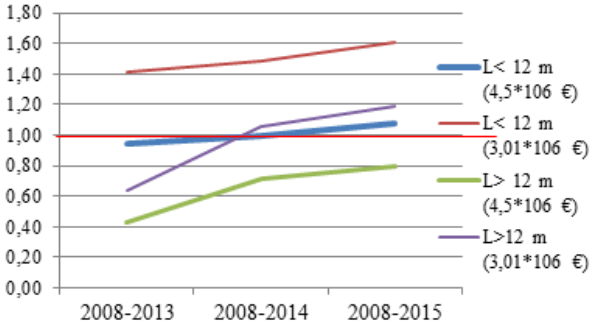

Figure 15. Safety level adjustment incorporating the accidents on the year 2014 and 2015

7. COMPLETION OF A FORMAL SAFETY ASSESSMENT

Once the safety level was determined, this was assessed by means of a complete FSA to determine potential risk control measures to be implemented. Twenty two (22) risk control options were proposed, as indicated in table 1. These were quantified in terms of costs and its effectiveness was assessed by a group of experts.

Taking into account the effectiveness of these risk control measures, as indicated in figure 16, and the reduction of risks provided by them, these risk control options were ranked by means of a cost and benefit analysis using the GCAF and NCAF formulation indicated above.

Due to the instability in the safety level as indicated in section 6 a cautious approach for rule development is recommended, with a safety level of 1,0 (100%).

A sensitivity analysis was carried out, taking into consideration different possible scenarios in terms of VPF value (the Spanish value of 4.50 M€ and the IMO standard value of 3.01 M€), the most extreme forecasts in the evolution of the fleet and the highest and lowest values of effectiveness. With all of these, some risk control measures have a solid potential to be implemented.

Table 1. Risk Control Options proposed to be implemented by a group of experts. (N means "new vessel" and E means "existing vessel")

RCO 1	Improvement of safety culture with promotion campaigns (N&E)
RCO 2	Concentrated campaigns of inspection (N&E)
RCO 3	Improvement of Stability Training for skippers (N&E)
RCO 4	Improvement in Stability booklets (L≥15 m)
RCO 5	Lightweight control (N&E) (L≥15 m)/ Stability test (N&E) (L<15 m)
RCO 6	Marking and control of fishing gear (N&E) (7,5<L≤12 m and L≥12 m)
RCO 7	Allow for fish stowage on deck N&E (7,5<L≤12 m)
RCO 8	Draught marks (E) (L≥15 m)
RCO 9	General Arrangement and hull forms enhanced control (N) (7,5<L≤12 m and L≥12 m)
RCO 10	Increase door sills height (E)(L≥12 m)
RCO 11	Improved design of shipside valves (N) (L≥12 m)
RCO 12	Stability Software installation (N&E) (L≥15 m)
RCO 13	Shipyard Quality Control (N)
RCO 14	Engine room ventilation calculation with engine compartment (N)
RCO 15	Improvement of ventilation systems for existing ships(N&E) (L≥12 m)
RCO 16	Engine room machinery controls automated (E) (L≥12 m)
RCO 17	Smoke detectors in accommodation, fire detectors in engine room (N&E)
RCO 18	GMDSS radio communication information available on the bridge (N&E)
RCO 19	Safety Management System implementation (N&E)
RCO 20	Enhance monitoring of vessels (N&E) (L≥15 m)
RCO 21	Plan Approval by Classification Society (N)
RCO 22	Improvement of freeing ports (E)

The most relevant measures to be implemented are the development of a safety culture by means of a structured program, the need to consider fish on deck during stability calculations for decked vessels below 12 m in length, and the need to have available draught marks for vessels between 12 m and 24 m in length. Other measures such as the implementation of ISM or the approval of new constructions under the rules of a classification society did not pass the cost benefit analysis (FSA step 4) and therefore shouldn´t be considered as risk control measures to be made applicable (FSA step 5).

Taking into consideration the parallelisms with other fishing vessel fleets in Europe, the use of VPF values (both the Spanish and the OMI values) and the evolution of the fleets in other parts of the world these risk control options could be applied globally, although necessary studies should be carried out, including the model adjustments and the use of the fishing vessel accidents in the region of concern.

8. DEVELOPMENT OF GOALS AND FUNCTIONAL REQUIREMENTS

The FSA methodology had helped to develop the risk models and the safety level nevertheless, in order to further progress in a holistic approach; a GBS-SLA was decided at the next step. This could help to develop long lasting regulations in the future (IMO, 2015).

In this regard overarching goals and functional requirements for the safety of fishing vessels following tiers I and II of GBS as indicated in figure 17 could be developed. These could be quantifiable and able to incorporated the safety level approach.

Hence, it was necessary to develop text that would avoid the prescriptive nature of the current regulations encompassing the current applicable national safety regulations, in particular the above mentioned Code of Safety for fishing vessels adopted in 2007 (Ministry of Transport, 2007), therefore a bottom-up approach was decided.

The current works in IMO (IMO, 2017) and NATO (NATO, 2014) were used to develop functional requirements with the three following elements: a description, performance requirements/rationale and justification following the example indicated in table 2.

The rationale and description were based on the analysis of the current regulations that could also address the hazards. The justification was developed to address the risks and risk factors, thus making the functional requirements quantifiable.

The 50 functional requirements developed were connected to the high level models developed during the risk assessment in step 2 of the FSA as shown in figure 18. Quantitative/qualitative goals were subsequently developed, but the quantification rests in the functional requirements themselves.

These functional requirements are not only the basis to develop new regulations and therefore considered "rules for rules", applicable to a very heterogeneous fleet, but also the means to start developing risk based design (Papanikolau *et al*, 2009). In order to do so the high level models developed could be used by the sector (mainly shipyards and designers in this particular world of fisheries) combined with low level risk models.

Following this approach safety would not only be in the hands of the regulatory bodies but also in the hands of the whole sector and would allow consistency and alternative design (IMO, 2006), providing flexibility and allowing the whole sector to build and use the methodology.

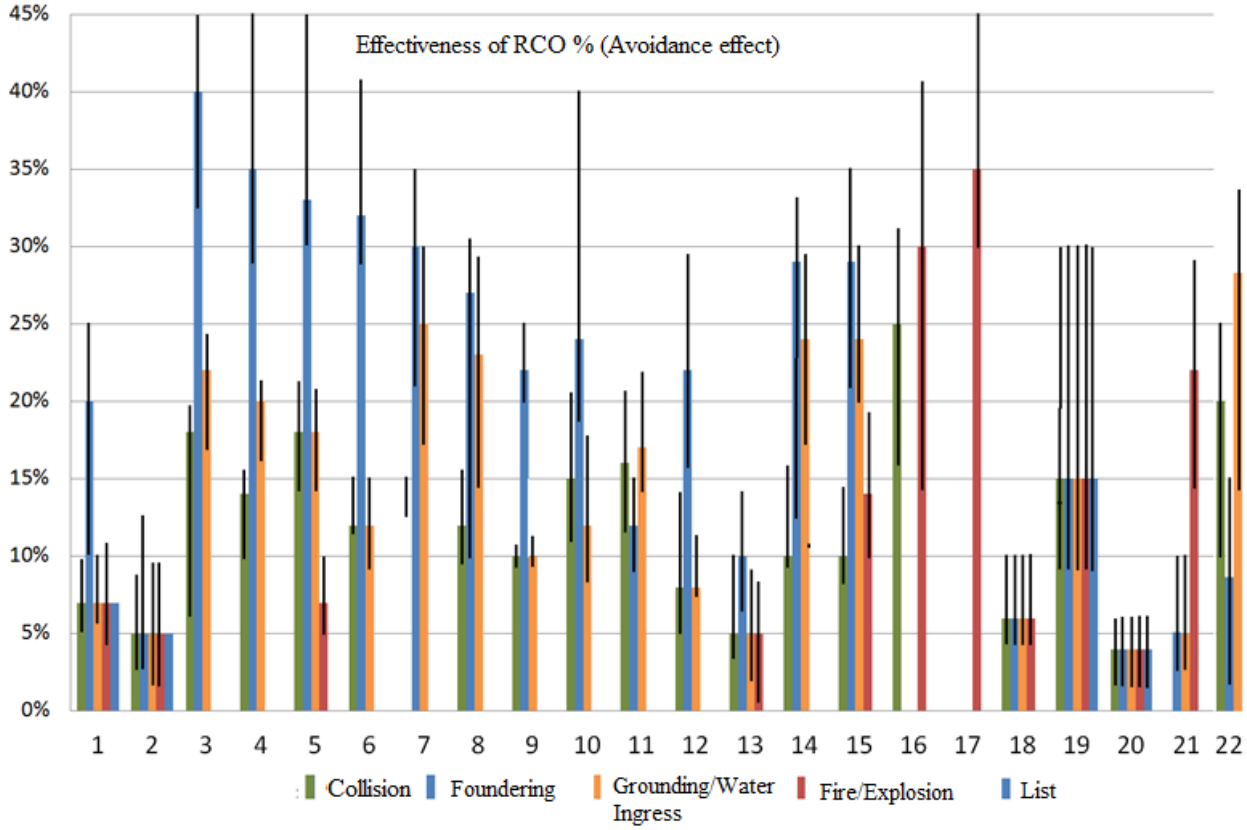

Figure 16. Effectiveness of proposed risk control options for each type of accidents and bands showing maximum and minimum values

Table 2. Example of functional requirement as developed

	Description	Performance requirement/Rationale	Justification
What it is	a specific and short explanation of the required function.	description of the necessary function in quantitative terms. this description should cover all aspect necessary for verifying compliance and the conditions under which these have to be reached	assignment of hazards to be mitigated by the function under consideration
What was developed (example)	Provide ready access to survival systems for all persons	• quantity, distribution and arrangement of life saving appliances on board • spare capacity • signage for life-saving appliances • reflect the physical characteristics and capabilities of the embarked persons	Collision, grounding, fire/explosion, foundering, list in case of total loss of the ship and abandonment.

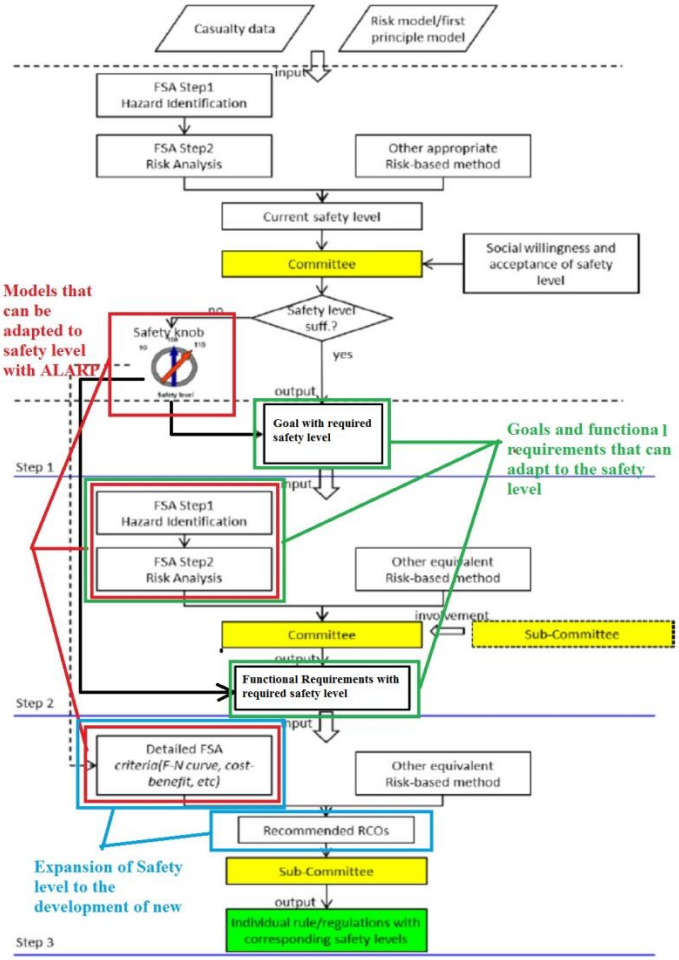

Figure 17. Development of Goals and functional requirements in a GBS-SLA approach (IMO, 2015)

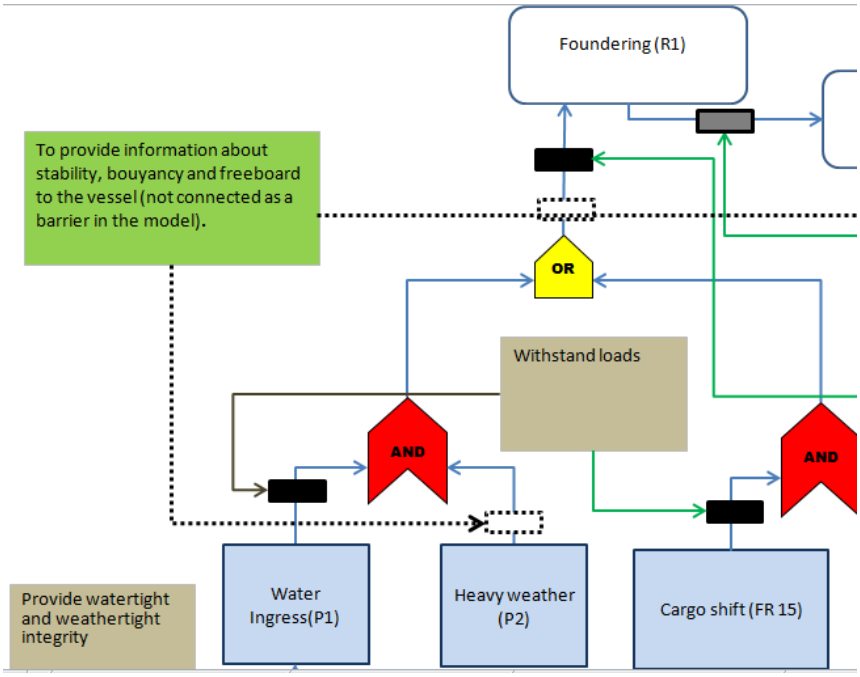

Figure 18. One Section of the foundering high level model incorporating functional requirements

The developed GBS-SLA goals and functional requirements allow to develop rules and also to go into a holistic approach, introducing later matters of pollution, responsible fisheries, sustainable development and others. In this regard a fishing vessel owner with high safety standards would be more likely to be involved in responsible fisheries.

All this process constitutes an application of the GBS-SLA approach using FSA techniques, that will assist to develop holistic regulations and also to address very heterogeneous fishing vessel fleets. A further refinement by the Administration would remain pending.

The developed goals and functional requirements could also be considered by Maritime Administrations, provided suitable models were adjusted and populated with accidents.

9. CONCLUSIONS

The above research in combination with the assessment of the current situation leads to the following conclusions:

- Fishing activity is dangerous due to its complexity and the substantial risks involved. It is difficult to quantify its risk and therefore to legislate.
- The implementation of overarching principles such as sustainability requires the regulations to be more holistic. In order to do this it is necessary to put the safety legislation into context to be able to move into the future.
- The safety level can be measured and applied taking into consideration the needs of reduction of risk in terms of fatalities, taking into consideration cost and benefits.
- Suitable measures for fishing vessels and small craft can be analysed taking into consideration costs, benefits and risks reduction with sensitivity analysis in an FSA environment that has been restricted for the moment to merchant vessels.
- Safety culture is an issue in this activity. Fishermen assume certain risks even consciously while these can be avoided by means of cost-effective measures. In order to improve this it is necessary to raise awareness by means of training courses, enhance knowledge of stability and create safety culture by means of explanatory concentrated campaigns of inspection.
- Safety of fishing vessels is seen as a regional activity but requires overarching policies. A GBS-SLA approach may help to develop consistent Maritime Policies at national, regional and international levels
- The GBS-SLA approach will help to develop risk based design regulations for fishing vessels in the future and overcome the difficult exemption regime.

10. REFERENCES

1. NÚÑEZ, M. (2016) Towards a new SOLAS Convention: a transformation of the ship safety regulatory framework Transactions RINA, Intl J Maritime Eng Vol 158, Part A2, Apr-Jun 2016 (ISSN 1479-8751) (pages A139-A146)
2. IMO, (2015) *Revised guidelines for Formal Safety Assessment (FSA) for use in the IMO rule-making process*,,MSC-MEPC.2/Circ.12/Rev. 1
3. IMO (2000). *Decision parameters including risk acceptance criteria for safety*, MSC 72/16
4. IMO (2015).*Generic guidelines for developing IMO Goal-Based standards*, MSC.1/Circ. 1394/Rev 1.
5. RODRÍGUEZ-ARAGÓN L (2015), Statistical Quantitative Methods in Industrial. [Consulted 10/05/2015]. Available at https://www.uclm.es/profesorado/licesio/Docencia/mcoi/Tema4_guion.pdf.
6. MCA MSC 1770 (F) (2002) Code of Safe Working Practice for the Construction and Use of 15 Metre (LOA) to less than 24 Metre (L) Fishing Vessels.
7. SVEIN KRISTIANSEN, (2005) *Maritime Transportation Safety Management and Risk Analysis*, Elsevier.
8. APOSTOLOS D.PAPANIKOLAU et al (2009). *Risk-Based ship design, methods, tools and applications*, Springer
9. MINISTRY FOR TRANSPORT AND PUBLIC WORKS, SPAIN Royal Decree 543/2007, 27th April to determine the safety and pollution prevention regulations for fishing vessels below 24 m in length L «BOE» 131, 1 June 2007.
10. IMO (2015) *Goal-Based new ship construction standards report of the GBS working group*, MSC 95/WP.9
11. IMO (2017) SSE 4/WP.3 Safety objectives and functional requirements of the guidelines on alternative design and arrangements for SOLAS chapters II-1 and III.
12. NATO (2014) Standardization Office (NSO) © NATO/OTAN *NATO Standard, ANEP-77, Naval Ship Code Edition F* Version 1, August 2014
13. IMO (2006), Guidelines on alternative design and arrangements for SOLAS Chapters II-1 and III, MSC.1/Circ.1212

11. ACKNOWLEDGEMENTS

Thanks to Dr. Rainer Hamman for his patience with me when discussing these issues.

A SIMULATION-BASED METHODOLOGY FOR EVALUATING THE FACTORS ON SHIP EMERGENCY EVACUATION

(DOI No: 10.3940/rina.ijme.a4.2017.453)

P A Sarvari and **E Cevikcan**, Istanbul Technical University, Turkey

SUMMARY

There are many hazards on a ship that makes an emergency evacuation process inevitable. Providing safe and effective evacuation of passengers from ships in an emergency situation becomes critical. Handling a real ship evacuation practice is often unaffordable as modelling such an environment is very expensive and may cause severe distress to participants. As an alternative, simulation models have been used to overwhelm the issue above in recent years. Therefore, this paper proposes a novel simulation-based methodology for evaluating the effect of factors including physical as well as psychological passenger characteristics and routeing systematic on emergency evacuation process for public marine transportation. A detailed questionnaire has been conducted in this work to reflect passenger characteristics on simulation model in a more realistic manner. Also, a new routeing systematic is developed to provide an efficient evacuation procedure. As another contribution, a novel grid-based approach where the meshed discretized nodes can contain more than one passenger is proposed in simulation model for the first time. Then, a statistical analysis is included within the methodology to assess the importance level of each factor on evacuation time. The proposed methodology is applied to a real life Ro-Ro ferry. A validation protocol based on IMO regulations is conducted and confirmed the effectiveness of the suggested simulation model. The simulation of different scenario types have indicated the influencing factors in a ship emergency evacuation. According to results, passenger characteristics has been identified as the most dominant factor on evacuation performance. The highest evacuation time difference has been observed for different levels of weight attribute. Moreover, it is concluded that the consideration of load utilization balancing among evacuation systems for routeing decreases evacuation time significantly. Finally, significant evacuation time difference between grid approaches have been demonstrated.

NOMENCLATURE

[Symbol]	[Definition] [(unit)]
a_{ij}	Distance order between the j^{th} MES and the i^{th} hall
AS	Set of halls that are partially or completely assigned to an MES
AUR	Average load factor of the MES
α_{lm}	Passengers' ratio for factor l and category m
β_w	Capacity ratio of MES_w
CAP_w	Total capacity of MES_w
cap_j	The capacity of the MES that is placed at the j^{th} MES
C_j:	Number of passengers who have been assigned to the j^{th} MES
d_{ij}	Distance from saloon i to the j^{th} MES
d_{oj}	Distance from seat group o to the j^{th} MES
IMO	International Maritime Organisation
IDO	Istanbul Sea Buses Industry and Trade
RGBS	Rigid Grid-Based Simulation
FBGBS	Flexible-Board Grid-Based Simulation
SIC	Safety Information Card
SDA	Shortest Distance Algorithm
SDA+EPLRBA	Shortest Distance Algorithm is integrated with Evacuation Points Load Rate Balancing Algorithm
MES	Marine Evacuation System
N	Number of evacuation points
M	Number of saloons
ESI	Smoothing index of the evacuation
ts_j	Total number of passengers directed to the j^{th} MES
LSA_j	Set of MESs that passengers can be transferred from
P	Number of seat groups
SE	Hall-MES matrix
pas_o	Total number of seats for the seat group o
$tpas_i$	Total number of seats of the i^{th} hall
SG	Seat group-evacuation point matrix
POP	Population (number of respondents) for questionnaire
PAS_{wlm}	Number of passengers with factor l and category m who are locating on the nearest seats to the MES_w
RAS_{jq}	Alternative exit point
S_{lm}	Number of passengers with factor l and category m
T_{cap}	The total number of passengers
URj	Load factor of the j^{th} MES

1. INTRODUCTION

The investigation of the National Transportation Safety Board (NTSB) revealed that 78% of all casualties happened post-impact, of 95.4% were resulted from the hazards like smoke inhalation and burns resulted from delayed and inefficient evacuations. They also mentioned that if the passengers who are survived after crash can be evacuated quickly, the survival rate would be raised by

98.3% as claimed by NTSB (Coalition for Airport and Airplane Passenger Safety, 1999). Afterwards, because of marine accidents all over the world between 2002 and 2015, 10899 fatalities has occurred, and 1982 ships were sunk or lost (European Maritime Safety Agency, 2015 and (EMSA) 2014).

Maritime safety is one of the core topics discussed in global platforms, especially to enhance design and operation of safe systems at sea (Akyuz, Akgun, and Celik 2016; Njumo, 2017; Akyuz, 2017). Every company/institution that is performing public marine transportation activities must consider the security of its passengers and crew. In case of an emergency, ensuring safe and prompt evacuation of passengers from ship is critical. Understanding how people behave during emergency within maritime transportation are vital if one is to design and develop efficient evacuation vessels and evacuation procedures (Galea *et al*. 2011). A series of tests must be conducted during ship design to meet domestic and international regulations, service permissions. The International Maritime Organization (IMO, C 105/3(a)/1) requires that the passenger ships must be provided with appropriate emergency procedures and sufficient exits to help fast and smooth evacuation within a reasonable time.

On February 2nd, 1987 the engine of the tanker O.T. Garth exploded and the ship ran aground in the Bay of Seine. The evacuation of the victims was made in debatable conditions and based on this unfortunate event, the first research paper on maritime emergency evacuation was released by Bigo *et al*. (1989). They tried to analyse the problems of coordination among crisis schemes according to SECMAR (Sauvetage maritime) directions, ministerial instructions of 1983 and the reality of operational obligations. There have been numerous accidents of passenger vessels at sea, and they have caused massive losses of human lives, so the need of improving the evacuation procedures considering guiding, directing, mustering, and controlling of passenger movements was firmly vital. The 1995 International Conference on the Safety of Life at Sea (SOLAS 1995) addressed this issue particularly by the adoption of a new regulation (SOLAS II-2/28.3), where it is declared that a proper evacuation analysis shall evaluate onboard escape routes of Ro-Ro ferries.

Simulation is a fast and cost-effective tool for modelling marine emergency evacuation in complex ship environment including different hazards such as heel/trim and fire. In this context, cell-based and, in a privileged way the grid-based simulation techniques are considered to apply. The cell-based simulation model divides the space into a uniform grid called a cell. This leads naturally to the concept of "grid-based simulation", in which simulations are performed at various points comprising a grid. In Klupfel *et al*. (2001), the importance of simulation in maritime emergency evacuation (MEE) is highlighted. They mentioned that it is possible to perform evacuation under ideal conditions if the parameters are chosen correctly. Therefore, an important part of MEE studies has employed simulation methods. A distance based passenger routeing methodology utilized by the code EVDEMON (EVacuation DEmonstration & MOdeliNg) as described by Boulougouris and Papanikolaou (Boulougouris and Papanikolaou, 2002). A crowd simulation for improving the design of the built environment and guidelines was conducted by Sagun *et al*. (Sagun, Bouchlaghem, and Anumba, 2011). The purpose of their Simulation Case Studies (SCS) was to investigate how the factors identified in the Observation Case Studies (OCS) affect evacuations using crowd modelling techniques. Thus, they defined three different scenarios based on predefined procedures and their observations. They simulated an emergency evacuation process in case of fire on board to assess the time of evacuation and number of casualties. They used EXODUS simulation program to perform different scenario types. Ha *et al*. (2012) presented a simulation of advanced evacuation analysis using a cell-based simulation model for human behaviour that consists of individual, crowd, and counter flow-avoiding behaviours, in a passenger ship. In term of validation, they compared simulation results of their proposed evacuation model with the passenger behaviour model through IMO tests and confirmed that the proposed model realizes the evacuation process with only the difference of 5%.

Roh and Ha (2013) presented an advanced ship evacuation analysis as a stochastic method in which the total evacuation time was calculated via computer-based simulations, by considering each passenger's characteristics. They tried to model the individual behaviour, the crowd reaction, the counter flow-avoiding behaviour and then tried to verify the passenger behaviour model through IMO tests on a Ro-Ro passenger ship. They compared their results with those of EVi simulation program and concluded that despite the 4% difference, the total evacuation time met the requirements. A multi-agent based congestion evacuation model incorporating panic behaviour is proposed in the paper of Wang *et al*. (2015) to simulate pedestrian evacuation in public places. In Fang *et al*. (2016), the impact of seating area and pedestrian's ''hesitation'' before leaving exits are considered on escape process of Airbus A380 to optimize the rule of exit choice. They reproduced typical characteristics of aircraft evacuation such as the movement synchronisation by simulation technique. A velocity-based egress model, which took into account different aspects of human behaviour in an emergency situation, for the evacuation analysis on passenger ships was presented by Cho *et al*. (2016). They assumed that the escape model consists of three behaviours; individual, crowd, and emergency behaviour. The personal behaviour was represented by the body shape, walking speed, walking direction, and rotation of each passenger. The basic walking direction of each passenger was obtained as a solution to the shortest distance route to a destination using a visibility graph. The crowd behaviour of the passengers was composed of two elements; one was a crowd behaviour, a form of

collective behaviour of a vast number of interacting passengers with a common group objective, and the other was a leader following behaviour, which caused one or more passengers to follow another moving passenger who was designated as the leader. The emergency behaviour of the passengers in their work was represented by a counter flow-avoiding behaviour to evade collision with other passengers walking in the opposite direction. They conducted eleven necessary tests and two detailed examples in IMO Maritime Safety Committee/Circulation 1238 and confirmed the validity of such trials. They used EVi commercial program to simulate and compare the results.

To address the issues mentioned above, this study contributes to the relevant literature by developing a novel simulation based methodology that considers physical and psychological characteristics of passengers for emergency evacuation process in public marine transportation. Moreover, a Flexible-Board Grid-Based Simulation (FBGBS) approach in conjunction with a multi-level network representation is proposed for the first time within the methodology. In addition, three different passenger routeing algorithms are used in this work to emulate the emergency evacuation process.

The rest of this paper is organised as follows: Section 2 describes the emergency evacuation process. Section 3 explains grid-based simulation approaches. Section 4 presents different passenger routeing approaches. Section 5 introduces the proposed methodology for marine emergency evacuation. An application together with the comparative analysis, results and analyses are discussed in details in Section 6 and a brief closure is presented at the last section.

2. THE EMERGENCY EVACUATION PROCESS

In recent years, the research of crowd evacuation in emergency has greatly been enhanced more deeply (Shao and Yang, 2015). Evacuation of people can be defined as mustering, directing or taking many people away from an area under the existing or potential hazard to a relatively safe place in a planned manner. There are many hazards on a ship like fire or sinking that makes an emergency evacuation process inevitable. Structure for evacuation process in marine transportation systems is given in Figure 1.

While accruing an emergency condition on board, the ship authorities make a decision regarding the IMO regulations for commencing the evacuation or not. The process starts by striking up the alarm by the skipper and ends by evacuating the last passenger to a safe place. Through this process, all the ship passengers are following the directions coming from crew and safety information card (SIC). It should be noted that physical and psychological factors affect the movement of passengers. In the panic mode of evacuation, in which the density of walkers is relatively large, the distances between the passengers are small (Li *et al*, 2017).

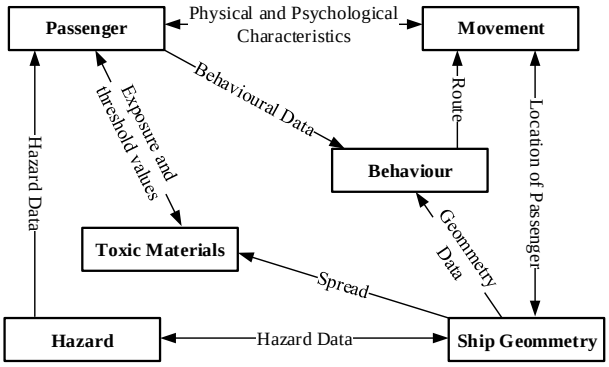

Figure 1: Marine Emergency Evacuation Process

The most realistic closed area simulators are mostly grid based. They can cover the geometry of construction by discretizing all spaces into dimensioned shapes. Consequently, grid-based marine evacuation simulation programs have the halls of a ship meshed into a set of square nodes with an identical size equal to the space occupied by a passenger in a dense crowd. Thereby, all movements of passengers are subjected to the restriction that a node can only be occupied by at most one passenger at the same time. If another passenger occupies the target node, at this moment a passenger has to wait for moving into the target node until the node is unoccupied. By this way, passengers' movement can be dramatically simplified and coded readily. (Kirchner *et al*., 2003). However, this simplified treatment will cause a "gap" between passengers in the process of moving, because a node will be in an occupied status until the occupant is completely moved out. It can be observed that the passengers are tended to stay very closely next to each other and cause different conflicts in a real emergency evacuation (Guan, Wang, and Chen, 2016).

Regarding the next dimension of our proposed evaluation, to overcome the issue above, artificial passengers are permitted to move towards their target node with small steps according to their speed of movement. Any node may contain more than one passenger at a time simultaneously, but passengers are not allowed to overlap with each other. The rules of movement for each passenger are as follows:

(1) Passengers moving along the same direction can enter the same node with no "gap" between two passengers.

(2) Passengers are supposed to move towards the targets based on the defined routeing method for each scenario type.

(3) In any time unit (i.e. the minimum simulation step), all passengers have opportunities to move. All passengers are sorted by the distance from their current positions to their target exit. Those who have a smaller distance to exit will move first within the same time unit.

3. GRID APPROACHES FOR EMERGENCY EVACUATION SIMULATION

Compared to other simulation environments, like buildings, aircraft, parks, and public squares, a passenger ship has several unique features, such as complex structure, numerous obstructions and stairs on evacuation paths, and narrow aisles. In most marine evacuation simulation models, the internal structure of a ship can be represented by a set of interconnected two-dimensional "nodes", each of which can be either empty or occupied by passenger(s).

One of the planned simulation models is RGBS model while one node can contain at most one person despite the possible space of the node to have more persons as it is illustrated in Figure 2. In order to study the evacuation process in more detail, researchers have paid more attention to finer discrete model, in which a pedestrian occupies more than one lattice site (Cao *et al*., 2015). Based on this, the need for a more flexible grid-based simulation approach seems to be inevitable.

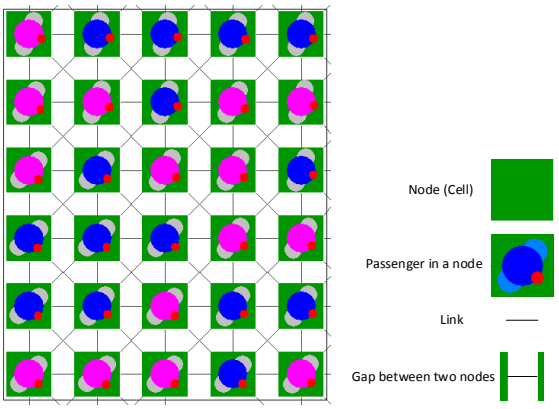

Figure 2: Illustration for Rigid Grid-Based Simulation model geometry

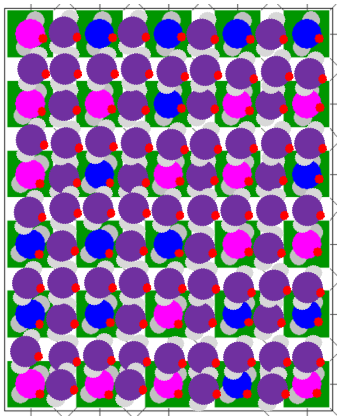

Figure 3: Illustration for Flexible-Board Grid-Based Simulation model geometry

The second grid approach is the FBGBS model providing that one node can contain more than one person at the same time if it is possible based on the size of the passenger and node. At this moment, each cell and gaps between cells can be permissible to the agents as it is illustrated in Figure 3.

4. PASSENGER ROUTEING METHODS

Although a significant amount of studies have already been performed on how to control the pedestrian outflow and to maximize the escape velocity in hazardous situations, there is no very simple but effective approach to obtain the optimal geometrical parameters of obstacles, including the optimal size of obstacle, the optimal obstacle–door gap and asymmetric offset distance of obstacle to the centre of the exit (Zhao *et al*., 2017). Therefore, the best way is to work on the passenger routeing methods for better evacuation procedures. Recently, two methods have been proposed in shape of a passenger routeing systematic that has been developed for the sake of ensuring the efficient evacuation of passengers regarding the evacuation time. As mentioned in Appendix A, the Shortest Distance Algorithm (SDA), one of the passenger routeing techniques, has been composed of first, second and third modules of the routeing systematic. The Shortest Distance Algorithm is integrated with Evacuation Points Load Rate Balancing Algorithm (Module 4) and this integration has been considered as a different routeing technique has been abbreviated as SDA+EPLRBA. The related definitions, parameters and formulations are given as follows.

Definitions

Seat group: Contiguous seats that any corridor, way or the main horizontal axis of the ship is not passing through.

Hall: Seat groups that are separated on the floor by a separator or a wall (providing the main horizontal axis of the ship passes through a hall so that the hall is considered as two independent halls).

Parameters

C_j: Number of passengers who have been assigned to the j^{th} MES
AS: Set of halls that are partially or completely assigned to an MES
N: Number of evacuation points
M: Number of saloons
P: Number of seat groups
SE: Hall-MES matrix

$$SE = \begin{bmatrix} (d_{11}, a_{11}, b_{11}) & \cdots & (d_{1N}, a_{1N}, b_{1N}) \\ \vdots & \cdots & \vdots \\ (d_{M1}, a_{M1}, b_{M1}) & \cdots & (d_{MN}, a_{MN}, b_{MN}) \end{bmatrix} \quad (1)$$

In this matrix, each cell consists of three components (d_{ij}, a_{ij}, b_{ij}).

d_{ij}: Distance from saloon i to the j^{th} MES; i=1… M, j=1… N.

$$d_{ij} = \frac{\sum_{i \in T_i} d_{oj} \times pas_o}{tpas_i} \quad (2)$$

d_{oj}: Distance from seat group o to the j^{th} MES; o= 1… P, j= 1… N.

pas_o: Total number of seats for the seat group o; o= 1… P.

$tpas_i$: Total number of seats of the i^{th} hall; i= 1… M.

a_{ij}: Distance order between the j^{th} MES and the i^{th} hall (the closest=1, and the furthest=N); i= 1… M, j= 1… N.

b_{ij}: 1, On condition that the j^{th} MES is in (or in the borders of) the i^{th} hall; 2, Provided that the j^{th} MES and the i^{th} hall are on the same floor; ,. As long as the i^{th} hall is on an upper floor than the j^{th} MES; 4, Providing the i^{th} hall is on a lower floor than the j^{th} MES; i=1… M, j=1… N.

SG= Seat group-evacuation point matrix.

$$SG = \begin{bmatrix} (d_{11}, a_{11}, b_{11}) & \cdots & (d_{1N}, a_{1N}, b_{1N}) \\ \vdots & & \vdots \\ (d_{P1}, a_{P1}, b_{P1}) & \cdots & (d_{PN}, a_{PN}, b_{PN}) \end{bmatrix} \quad (3)$$

The three components (d_{oj}, a_{oj}, b_{oj}) are indicated in this matrix as well as SE matrix.

d_{oj}: Distance from seat group o to the j^{th} MES; o= 1… P, j= 1… N.

a_{oj}: Distance order between the j^{th} MES and the i^{th} hall (the closest=1, the furthest=N); i= 1…M j= 1…N.

b_{ij}: 1. On condition that the seat group o is in (or in the borders of) the j^{th} MES; 2. Provided that the seat group o and the j^{th} MES are on the same floor; 3. As long as the seat group o is on an upper floor than the j^{th} MES; 4. Providing the seat group o is on a lower floor than the j^{th} MES.

RAS_{jq}: Alternative exit point that passengers have been transferred during an emergency q, where the j^{th} MES is unavailable; J= 1… N, q= sinking, fire, sinking+fire.

ESI: Smoothing index of the evacuation

$$ESI = \sum_{j=1}^{N} \left| UR_j - AUR \right| \quad (4)$$

URj: Load factor of the j^{th} MES; j: 1…N.

$$UR_j = \frac{ts_j}{cap_j} \quad (5)$$

ts_j: Total number of passengers directed to the j^{th} MES; j= 1…N.

cap_j: The capacity of the MES that is placed at the j^{th} MES

LSA_j: Set of MESs that passengers can be transferred from the j^{th} MES (while using occupancy rate balancing of the MESs module); j=1… N.

AUR: Average load factor of the MES

$$AUR = \frac{\sum_{j=1}^{N} UR_j}{N} \quad (6)$$

The developed routeing systematic is presented in Appendix A. Within the first module, parameters for the evacuation points, halls and seat groups are determined. Then, passenger halls (Module 2) and seat groups (Module 3) are assigned to evacuation points with the aim of matching them with MESs with respect to "closest distance" principle so that partial or complete assignment of each hall is possible under the MES capacity restrictions. Consecutively, a balancing algorithm has been presented in the fourth module that decreases the evacuation time by balancing the density difference between evacuation points (Appendix B). The algorithm performs calculations through capacity load factor as the capacities of evacuation systems at the several points differ from each other. Based on load factor balancing algorithm for evacuation points, transfers from the evacuation points with a higher load factor (more than average) to the ones that have a lower load factor (less than average) under the capacity and flow restrictions. Finally, the fifth module determines the other available evacuation exits, in the presence of any unavailable MES related to the emergency scenarios.

5. THE PROPOSED EVACUATION METHODOLOGY

Recently, some attention was drawn upon the fact that a full description and analysis of aspects involved in an evacuation process. This issue needs to consider the disposition of the individuals as internal states which may influence the reactions of the pedestrians and, ultimately, their motions (Dossetti, Bouzat, and Kuperman, 2017). Aiming this, the steps of experimental research are going to

be fulfilled via the proposed methodology which includes five phases, namely survey, experimental design, simulation, validation and statistical analysis (Figure 4). A reliable research methodology should be designed and performed based on a well-defined research question to obtain desired results. Therefore, the methodology starts with defining the research question(s) that is a liable inquiry into a particular matter or subject.

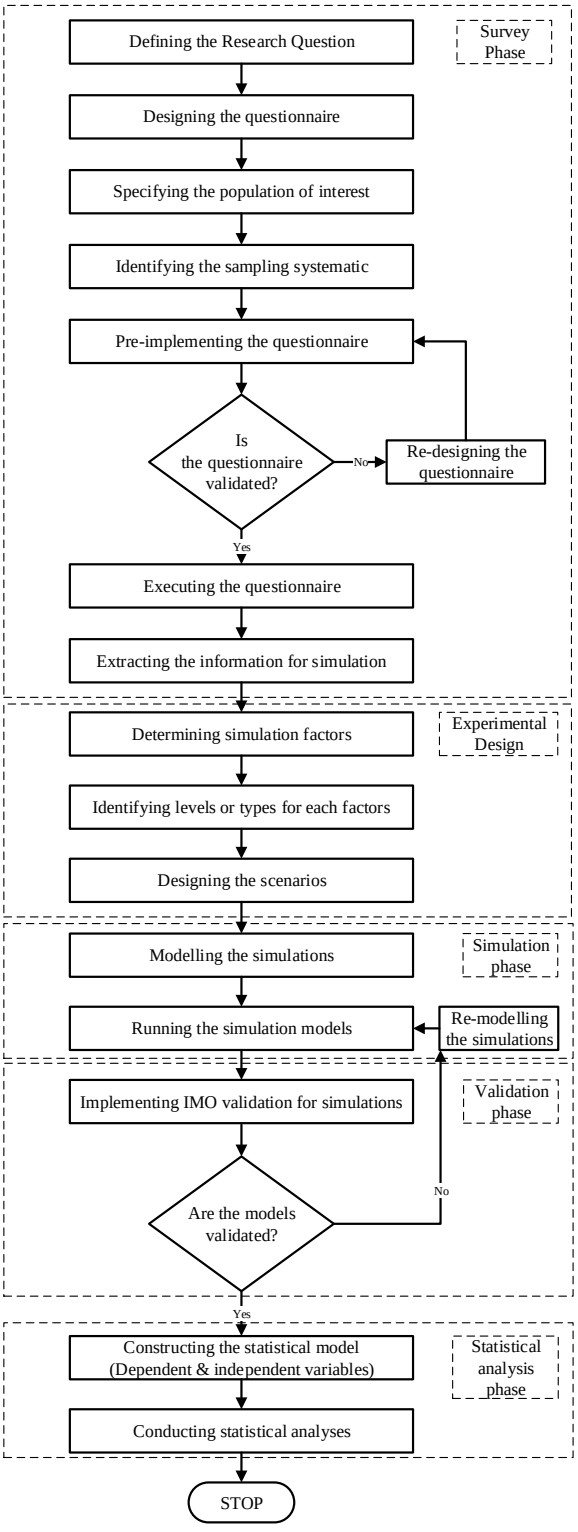

Figure 4: Research methodology

After defining research question(s), a comprehensive questionnaire must be designed to obtain the characteristics of passengers. Then an appropriate sampling technique for the specified population of interest should be determined so as to provide effectiveness in conducting the questionnaire. Survey phase ends with compiling the data about passenger characteristics which will be used for simulation.

The experimental design phase is a crucial stage to catch required factors for simulation models with respect to reliability and reality. Through this phase, demographic (e.g. gender and age) and physical characteristics (height and weight) of passengers and also behaviour types of passengers (panic levels while emergency) are gathered. The factors mentioned above need to be categorised into sub-factors and levels to catch the precise specifications of the passengers by the simulation program. Generally, the categorisation process for human demographic and characteristics have been based on "Height and Weight Charts" (2017). After categorisation of the passenger factors, the simulation scenarios are designed taking passenger routeing and grid approaches into account. This stage combines the physical-psychological characteristics of the passengers with routeing and grid approaches to model various scenario types for examining the effects of different factors on evacuation time.

An emergency evacuation simulator handles the designed scenarios at the simulation phase. As the developed simulation models are unique, their results from the fulfilling of the simulations are meant to be validated regarding verification. Thus, a systematic verification is still essential to evaluate the simulation results. The next phase of the proposed methodology is to verify the simulation results comparing based on the International Maritime Organization-IMO, MSC/Circ.1033 (Galea *et al*., 2012) validation formula and guidelines.

After collecting the characteristic data of passengers and the evacuation data resulted from performing the simulations, statistical analysis has to be conducted to capture the significant relations between the evacuation factors. A statistical analysis technique that assesses potential differences has been adopted.

6. APPLICATION

The logical approach is based on three research questions which have been listed as below;

1. Is there any effect of locating a particular group of the passengers with certain characteristics nearer to the exits during an emergency on the evacuation time?
2. Does the FBGBS approach yield a significant difference on the evacuation time compared to the RGBS approach for emergency evacuation simulation?

3. Is there any difference among passenger routeing methods regarding emergency evacuation time.

In this section, to apply the proposed evaluation methodology, we focus on an application that is involving a real Ro-Ro ferryboat. Therefore, the fleet of Istanbul Sea Buses Industry and Trade (IDO) has been considered to apply each methodological step. Hereby, Osman Gazi ferry commuting between Istanbul (Yenikapi) and Bursa (the ship carried 1.154.088 passengers in 2016) is selected as the case. The ferry has the capacity of 1184 passengers and 225 cars. This feature makes the ship the highest passenger capacitated vessel among the other ships in the fleet of IDO. Besides, there are six marine evacuation systems (MES) on the ferry which are designed to evacuate, in the event of an emergency, passengers from high freeboard fast ferries directly into inflatable liferafts. The slide/liferaft units are installed in or adjacent to the passenger accommodation area, from where direct access is gained. The link liferaft units are located adjacent to each MES and are linked to the associated MES by permanently rigged lines so that the effective capacity of each MES is doubled or tripled depending on the number of link rafts associated with the MES in question. The inflation cycle of the slide and liferaft takes approximately sixty seconds (Liferaft Systems Australia, 2006).

Information about the capacity and location of each MES is presented in Table 1, and technical drawing of Osman Gazi 1 ferry is given in Appendix C.

Table 1: The location and capacity information for MESs

MES	**Location**	Capacity
1	Mezzanine Deck-Starboard	200
2	Mezzanine Deck-Port	200
3	Upper Deck-Starboard	250
4	Upper Deck-Port	300
5	Main Deck-Starboard	200
6	Main Deck-Port	200

The principles and the methodology suggested by (Sekaran, 1992) were taken into account for designing of the questionnaire. Categorical scaling was used in the response parts due to its consistency with the current survey questions. The survey designed is illustrated in Appendix D. In addition to passenger characteristics, the survey obtained the information like passengers' travel frequencies, the status of their accompaniment, passenger's experiences in any emergency case or practice, their knowledge levels about ship layout and emergency assemblies or evacuation points during emergencies.

Systematic sampling technique was used as the sampling method. Within the scope of the method, the participant selection process was conducted in order with eight seats intervals. If someone sitting on the determined place rejected to answer or was unavailable to fill a survey, or the place was free, then the next seat was focused. Before executing the survey on board the pre-testing of the questionnaire, the survey was conducted for a group of 30 persons as a pilot practice, and then it was modified to the final version. The questionnaire was addressed to 1563 passengers during the survey, and 594 individuals responded (participation rate: 38%); therefore, the sample size was 594. Based on the survey results, we categorised the factors based on the classification of "Height and Weight Charts" (2017). In addition, we considered the first and second quartile of passengers' age as young, the third quartile as middle age and the fourth quartile as old. In order to catch the effects of locating a certain group of passengers with predefined physical and panic level categories we need to have the passengers groups located on the nearest seats to the MESs. Therefore, the exact numbers of passengers to be located near each MES are calculated through the formulation (9).

T_{cap} = The total number of passengers

α_{lm} = Passengers' ratio for factor l and category m

R_{lm} = Number of passengers for factor l and category m

POP = Population (number of respondents) for questionnaire

$$\alpha_{lm} = \frac{R_{lm}}{POP}$$

S_{lm} = Number of passengers with factor l and category m

β_w = Capacity ratio of MES_w

CAP_w = Total capacity of MES_w

PAS_{wlm} = Number of passengers with factor l and category m who are locating on the nearest seats to the MES_w

$$S_{lm} = T_{cap} \times \alpha_{lm} \tag{7}$$

$$\beta_w = \frac{CAP_w}{\sum_w CAP_w} \tag{8}$$

$$PAS_{wlm} = \beta_w \times S_{lm} \tag{9}$$

Table 2 illustrates the factors and their levels, the categorisation orders and the calculation steps of the number of passengers to be located near the MESs.

Table 2: Survey results and the table of simulation factors

	Factor (l)	Level	Frq.	Category (m)	α_{lm}	S_{lm}	PAS_{1lm}	PAS_{2lm}	PAS_{3lm}	PAS_{4lm}	PAS_{5lm}	PAS_{6lm}
Physical Characteristics	**Age**	-17	0.04	Young	0.26	334	49	49	62	75	49	49
		18-25	0.22									
		26-35	0.235	Middle Age	0.62	796	117	117	148	175	117	117
		36-45	0.23									
		46-55	0.155									
		56+	0.12	Old	0.12	154	23	23	28	41	23	23
	Gender	-	0.52	Male	0.52	666	99	99	123	152	99	99
		-	0.48	Female	0.48	618	91	91	114	140	91	91
	Weight	-50	0.03	Lightweight	0.06	79	12	12	15	20	12	12
		51-60	0.03									
		61-70	0.265	Moderate	0.82	1051	156	156	194	236	156	156
		71-80	0.29									
		81-90	0.265									
		91-100	0.105	Heavyweight	0.12	154	23	23	28	36	23	23
		101+	0.015									
	Height	-150	0.04	Short	0.175	225	33	33	42	52	33	33
		151-160	0.135									
		161-170	0.305	Moderate	0.655	841	124	124	156	190	124	124
		171-180	0.35									
		181-190	0.15	Tall	0.17	218	32	32	40	51	32	32
		191+	0.02									
Psychological Characteristics	**Panic**	I would follow the warning signs to the nearest evacuation point.	0.15	Low	0.2	256	38	38	47	59	38	38
		I would wait for the crew directions.	0.05									
		I would orient to the point I entered.	0.35	Moderate	0.5	642	95	95	119	145	95	95
		I would orient to the evacuation point that I know.	0.15									
		I would follow the crowd.	0.17									
		I would jump into the water at the first opportunity.	0.13	High	0.13	166	25	25	31	39	25	25
	Grid			RGBS FBGBS								
	Routeing			MER SDA SDA+EPLRBA								

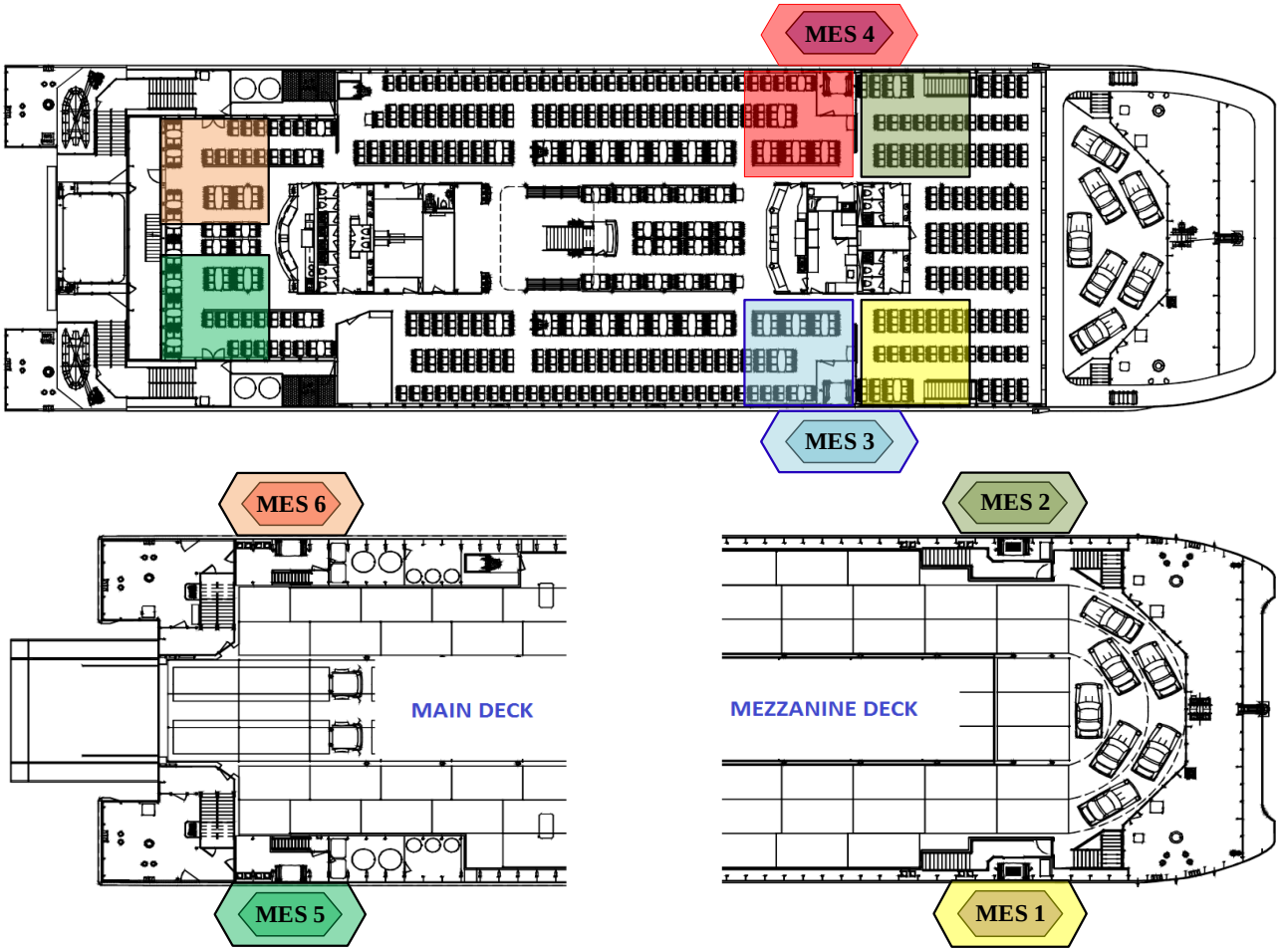

Figure 5: The closest seats to MESs

Table 3: Scenario generation table

Passenger characteristics					**Grid**	**Routeing**
Age	**Gender**	**Weight**	**Height**	**Panic Level**		
Young_closest	Male_closest	Lightweight_closest	Short_closest	Low level_closest	RGBS	MER
Middle age_closest	Female_closest	Moderate weight_closest	Moderate_closest	Moderate_closest	FBGBS	SDA
Old_closest		Heavyweight_closest	Tall_closest	Highlevel_closest		SDA+EPLRBA

Based on the calculation of distances between seat groups and MESs, the nearer seats are illustrated in Figure 5.

As for FBGBS aspect, the pseudocodes for each grid approach is given in Appendix E. One of the passenger routeing methods considered in this paper is the grid-based simulation software, named MER (Maritime EXODUS Routeing), is an autonomous passenger routeing. The others are SDA and SDA+EPLRBA which are thoroughly described in Section 4.

In the light of the information above and based on Table 3, eighty-four different combinations of scenarios (fourteen levels of passenger characteristics (three for age, two for gender, three for weight, three for height and three for the panic level)× two different grid approaches× three different routeing methods) occur. It should be noted that, "category m_closest" indicates that PAS_{wlm} passengers (in category m for factor l) located on the nearest seats to MES_w.

Scenarios for emergency evacuation were simulated via Maritime EXODUS V5.1. Simulation of each scenario was run for 250 times in an interior environment of the simulator and the average evacuation time was recorded. Figures 6 and 7 illustrate the visualisations of the simulations while running.

Figure 6: A cross section of halls using Maritime EXODUS V5.1

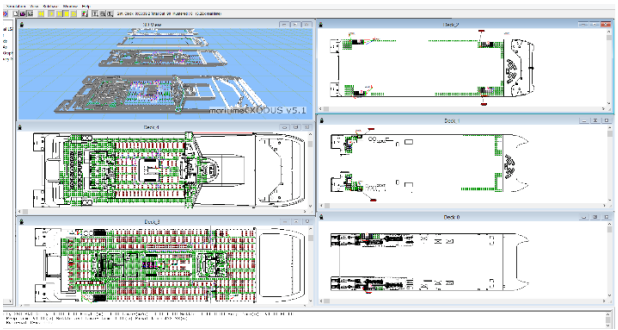

Figure 7: Simultaneous display of evacuation simulation on different layers

The simulator tests all scenario types while each one contains one of the two distinct conditions. The first condition is when one node can contain at most one person despite the possible space of the node to have more agents (RGBS), and the other test condition is when one node can include more than one person simultaneously if it is possible based on the size of the agent and the node (FBGBS). The second simulation state is possible if the modifications are installed with producing a command file as Script Control File to control basic simulation program's functionality. The changes in the script provide the expert user higher and easier control over the setting up of a model as well as the conditions present during the simulation.

The validity of the simulations was examined based on the guideline of International Maritime Organization-IMO with number MSC/Circ.1033 (IMO, 2002). In this guideline, the evacuation time for the ship was computed by the formulation using door-to-hallway dimensions, the number of passengers on the floor and passenger movement parameters.

Based on the simulation results, the average evacuation time in an emergency for the considered ship is 947 seconds. This value deviated almost 3.3% from the IMO validation result that is 917 seconds for the mentioned ship. Considering this research's results, the average egress time while each node contains more than one person is 922 seconds and it is more realistic and very close to the IMO validation results with 0.5% error.

After the simulation of the generated scenarios, Analysis of Variance (ANOVA) is conducted via SPSS 23.0 software to analyse the effects of the independent variables of physical characteristics of travellers, grid approaches, and routeing methods on the dependent variables of total evacuation time. The significance level was set to be 5%.

The effects of passenger characteristics, grid approach and routeing method are all found to be statistically significant (Table 4). What's more, the effect of two-way and three-way interactions are not significant.

Table 4. Test between-subject effects.

Source	**F**	**Sig. (*p*)**	**Partial Eta Squared**
Passenger Characteristics	65.407	0.000*	0.970
Grid Approach	11.152	0.003*	0.300
Routeing Method	6.615	0.005*	0.337
Passenger Characteristics *Grid Approach	1.665	0.130	0.454
Grid Approach *Routeing Method	0.507	0.608	0.038
Passenger Characteristics *Routeing Method	1.212	0.314	0.548
R Squared = 0.973 (Adjusted R Squared = 0.913)			
(*) significant at 0.05 level.			

Table 5. Mean evacuation time for factor

Factor	**Level**	**Mean Evacuation Time (sec.)**
Gender	Female	980.167
	Male	949.457
Weight	Heavy	1028.667
	Moderate	880.833
	Light	810.000
Height	Tall	980.467
	Moderate	965.247
	Short	960.112
Age	Young	881.716
	Middle Age	963.839
	Old	1008.660
Panic Level	Low	874.646
	Moderate	981.063
	High	1057.136
Grid Approach	RGBS	980.500
	FBGBS	882.310
Routeing Method	MER	936.002
	SDA	912.860
	SDA+EPLRBA	843.329

According to Table 5, evacuation time differs among factors and their levels. Mean evacuation time for men is observed to be less than that of women. Similarly, mean evacuation time for heavy weighted and old passengers are proportionally high. As an important finding, average evacuation time dramatically increases with increasing level of panic factor. The results clearly present the effects of FBGBS and SDA+EPLRBA routeing method on the average evacuation time.

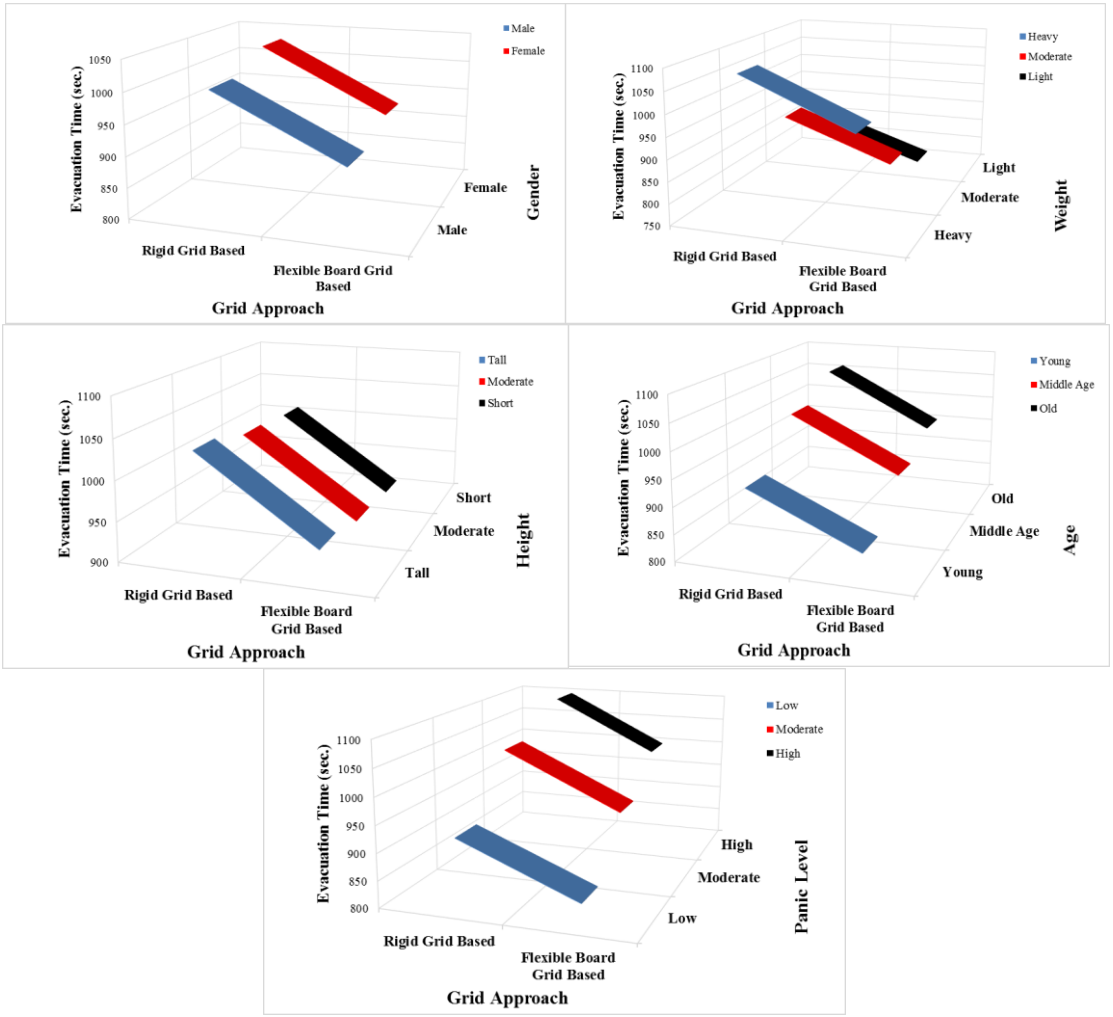

Figure 8: The effect of passenger physical-psychological characteristics with different grid approaches

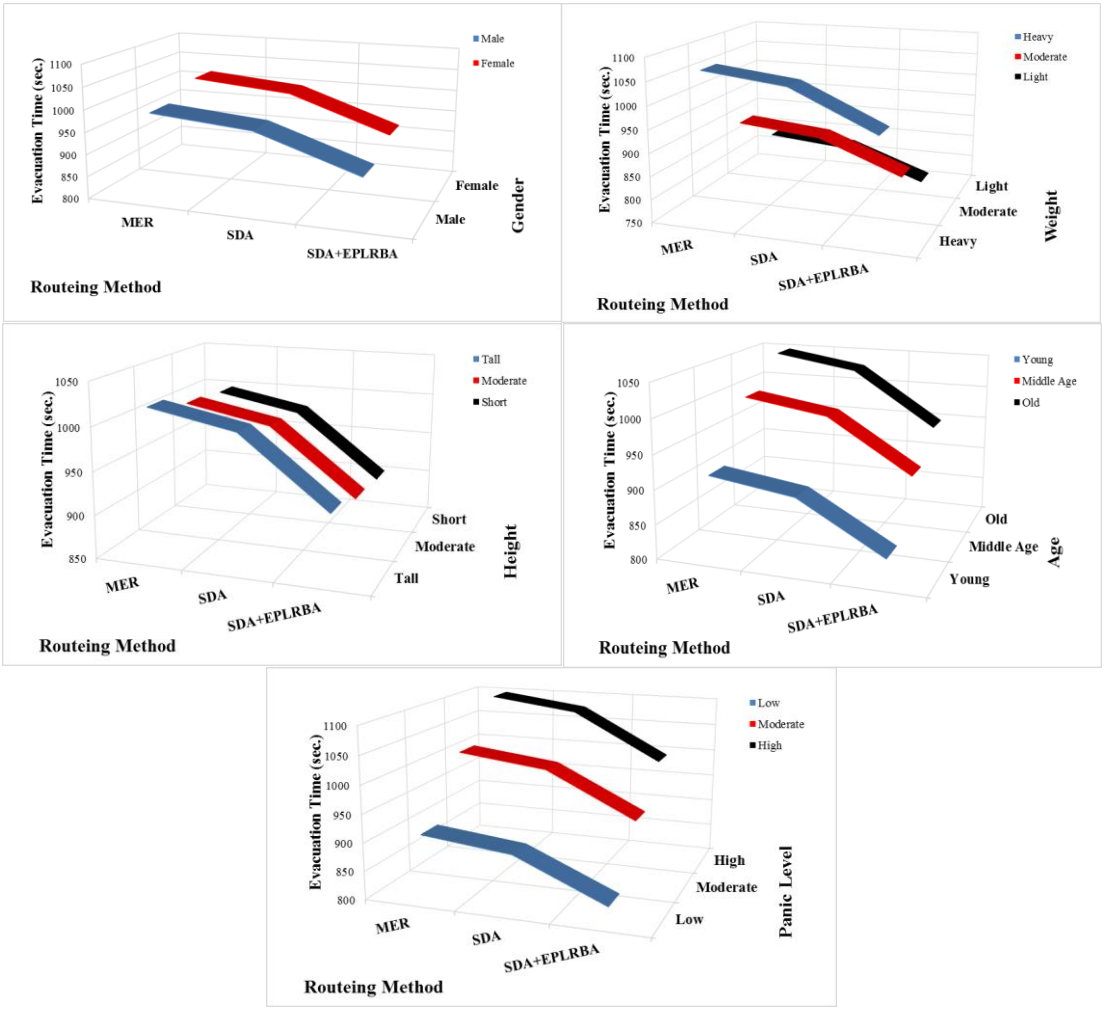

Figure 9: The effect of passenger physical-psychological characteristics with different routeing methods

7. CONCLUSIONS

Issues regarding the marine evacuation of passengers have received increasing attention due to significant losses caused by major maritime disasters and the boost in the number of large capacity cruise ships. Therefore, we propose a methodology for maritime emergency evacuation which contributes to the relevant literature which considers different passenger characteristics by developing a novel routeing systematic and a flexible-board grid-based approach for the first time.

The methodology was applied to a real life ferry-boat and the results from the constructed simulation model match well with the IMO regulation based validations. Besides, a series of elaborations and adjustments is scripted into the coded background of the default commercial simulation program to subdivide the ship's grid spaces into the nodes with the capability to take more than one person in case of possibility. Therefore, the limitation that each node could be only occupied by one passenger has been overcome in the new model to make the simulation closer to the reality.

The paper is believed to improve planning and control capability of administrators who are related to evacuation management. Moreover, results and conclusions, achieved by this article, could provide guidelines for ship design and on-line check-in systems. Consequently, it should also be emphasized that the proposed methodology is expandable to other passenger ships.

It will be meaningful to state some insights which are inferred from obtained results.

- Significant effect of routeing on evacuation has been demonstrated in this study. Evacuation convenience of ships should be addressed especially since design phase and should be supported by training during their operating.
- Keeping load utilization balance among evacuation systems decreases evacuation time significantly due to the fact that smoothness among evacuation systems leads to less waiting time for passengers. This issue may also be adapted to on-line check-in systems in such a way that seat assignment/suggestion may be performed with respect to real time utilization rate of evacuation systems.

- In an emergency scenario, the physical characteristics of a passenger, like body weight, gender, age yield a significant impact on evacuation time performance. This point can be considered in online check-in systems. For instance, when information about such attributes is obtained, some seats may be suggested for the passenger.
- Determining the number and position of guiding crew appropriately is thought to increase evacuation performance. As for position aspect, stairways and large halls are critical crew positions.
- Because of complex nature of ship structure, the level of passenger knowledge about layout has a vital importance on MEE with respect to panic level of passengers. Therefore, this aspect should be improved via instructor monitors, guidance arrows on floors, visual lightening.
- Having the knowledge about the exact location of passengers is a critical point for emergency evacuation. That being the case, passenger traceability can be enhanced using technological applications (RFID, Augmented reality, sensors, embedded systems, etc.).

However, there are several research directions to be pursued for future work. First, sensitivity analysis can be performed for specifying the dimensions of the nodes respecting to more accurate evacuation time for commercial simulation programs. What is more, the time effect of group behaviour which makes evacuation behaviours more complicated may be analysed.

8. ACKNOWLEDGMENTS

This research was carried out as a research project at Istanbul Sea Buses Co. Inc.(IDO).

9. FUNDING

This work was supported by the Scientific and Technological Research Council of Turkey (TUBITAK) under project grant number 215M246.

10. REFERENCES

1. AKYUZ E, AKGUN I, CELIK M. A fuzzy failure mode and effects approach to analyse concentrated inspection campaigns on board ships. *Marit Policy Manag*. 2016;43(7):887-908. doi:10.1080/03088839.2016.1173737.
2. AKYUZ, E, Application of Fuzzy FMEA to Perform an Extensive Risk Analysis in Maritime Transportation Engineering, Transactions RINA, Vol 159, Part A1, International Journal Maritime Engineering, 2017, doi: 10.3940/rina.ijme.2017.a1.400
3. Applications SM. Simulation of pedestrian dynamics using a two-dimensional cellular automaton . Physica A two-dimensional cellular automaton. 2016;295(February):507-525. doi:10.1016/S0378-4371(01)00141-8.
4. BIGO M, ROSE D, GUILLOU P, ROTH AJ, VIVIES A, DRIEU C. Place du SAMU dans les plans de catastrophes maritimes. *Urgences médicales*. 1989;8(2):128-131. http://cat.inist.fr/?aModele=afficheN&cpsidt=6672393. Accessed April 13, 2016.
5. BOULOUGOURIS EK, PAPANIKOLAOU A. Modeling and Simulation of the Evacuation Process of Passenger Ships. *Proc 10th Int Congr Int Marit Assoc Mediterr IMAM 2002*. 2002;757(18):1-5. http://www.naval.ntua.gr/~sdl/Publications/Proceedings/IMAM2002_Proceed57.pdf.
6. CAO S, SONG W, LV W, FANG Z. A multi-grid model for pedestrian evacuation in a room without visibility. *Phys A Stat Mech its Appl*. 2015;436:45-61. doi:10.1016/j.physa.2015.05.019.
7. CHO YO, HA S, PARK KP. Velocity-based egress model for the analysis of evacuation process on passenger ships. *J Mar Sci Technol*. 2016;24(3):466-483. doi:10.6119/JMST-015-1012-1.
8. Coalition for Airport and Airplane Passenger Safety. *Surviving the Crash*. iaff; 1999.
9. DOSSETTI V, BOUZAT S, KUPERMAN MN. Behavioral effects in room evacuation models. *Phys A Stat Mech its Appl*. 2017;479:193-202. doi:10.1016/j.physa.2017.03.021.
10. European Maritime Safety Agency 2015, (EMSA). *Annual Overview of Marine Casualties and Incidents 2014*. Lisboa Portugal; 2014. http://www.emsa.europa.eu/news-a-press-centre/external-news/item/2303-annual-overview-of-marine-casualties-and-incidents-2014.html.
11. FANG ZM, LV W, JIANG LX, XU QF, SONG WG. Modeling and assessment of civil aircraft evacuation based on finer-grid. *Phys A Stat Mech its Appl*. 2016;448:102-112. doi:10.1016/j.physa.2015.12.092.
12. GALEA ER, BROWN RC, FILIPPIDIS L, DEERE S. Collection of Evacuation Data for Large Passenger Vessels at Sea. In: *PED 2010*. NIST, Maryland USA; 2011. doi:10.1007/978-1-4419-9725-8.
13. GALEA ER, FILIPPIDIS L, DEERE S, *et al*. IMO Information Paper-The SAFEGUARD validation data-set and recommendations to IMO to update MSC/Circ. 1238. In: *Safeguard Passenger Evacuation Seminar*. London, UK.; 2012.
14. GUAN J, WANG K, CHEN F. A cellular automaton model for evacuation flow using

game theory. *Phys A Stat Mech its Appl*. 2016;461:655-661. doi:10.1016/j.physa.2016.05.062.

15. HA S, KU NK, ROH M IL, LEE KY. Cell-based evacuation simulation considering human behavior in a passenger ship. *Ocean Eng*. 2012;53:138-152. doi:10.1016/j.oceaneng.2012.05.019.
16. Height and Weight Charts. www.healthchecksystems.com/heightweightchart.htm. Published 2017.
17. IMO. *Interim Guidelines for Evacuation Analyses for New and Existing Passenger Ships*. London, UK.; 2002.
18. KIRCHNER A, KLÜPFEL H, NISHINARI K, SCHADSCHNEIDER A, SCHRECKENBERG M. Simulation of competitive egress behavior: Comparison with aircraft evacuation data. *Phys A Stat Mech its Appl*. 2003;324(3-4):689-697. doi:10.1016/S0378-4371(03)00076-1.
19. KLUPFEL H, MEYER-KONIG T, WAHLE J, SCHRECKENBERG M. Microscopic simulation of evacuation processes on passenger ships. *Theor Pract Issues Cell Autom*. 2001:63-71.
20. LI Y, LIU H, LIU G PENG, LI L, MOORE P, HU B. A grouping method based on grid density and relationship for crowd evacuation simulation. *Phys A Stat Mech its Appl*. 2017;473(88):319-336. doi:10.1016/j.physa.2017.01.008.
21. Liferaft Systems Australia. Marine Evacuation System Operations Manual for Austal Hull 294. 2006.
22. NJUMO, DA, Stability Failure Analysis in the Operations of Floating Dry Docks, Transactions RINA, Vol 159, Part A1, International Journal Maritime Engineering, 2017, doi: 10.3940/rina.ijme.2017.a1.386
23. ROH M IL, HA S. Advanced ship evacuation analysis using a cell-based simulation model. *Comput Ind*. 2013;64(1):80-89. doi:10.1016/j.compind.2012.10.004.
24. SAGUN A, BOUCHLAGHEM D, ANUMBA CJ. Computer simulations vs. building guidance to enhance evacuation performance of buildings during emergency events. *Simul Model Pract Theory*. 2011;19(3):1007-1019. doi:10.1016/j.simpat.2010.12.001.
25. SEKARAN U. *Research Methods for Business*. New york, New York: John Wiley & Sons; 1992.
26. SHAO ZG, YANG YY. Effective strategies of collective evacuation from an enclosed space. *Phys A Stat Mech its Appl*. 2015;427:34-39. doi:10.1016/j.physa.2015.01.080.
27. SOLAS. *Passenger Vessels*. London, UK.; 1995.
28. WANG J, ZHANG L, SHI Q, YANG P, HU X. Modeling and simulating for congestion pedestrian evacuation with panic. *Phys A Stat Mech its Appl*. 2015;428:396-409. doi:10.1016/j.physa.2015.01.057.
29. ZHAO Y, LI M, LU X, *et al*. Optimal layout design of obstacles for panic evacuation using differential evolution. *Phys A Stat Mech its Appl*. 2017;465:175-194. doi:10.1016/j.physa.2016.08.021.

APPENDIX A: The Developed Routeing Systematic

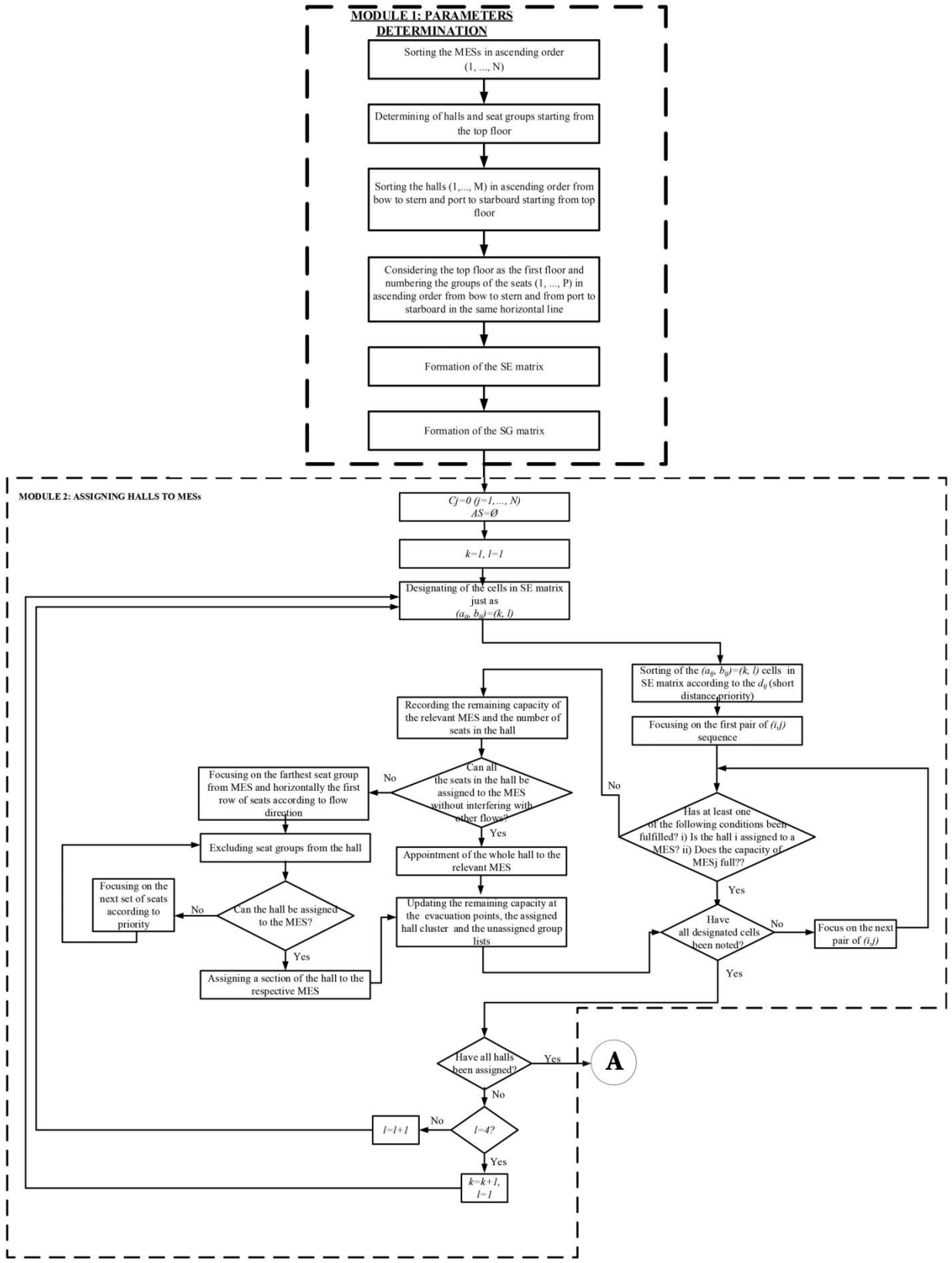

Figure. A1. Flowchart of the proposed systematic illustrating the routeing modules

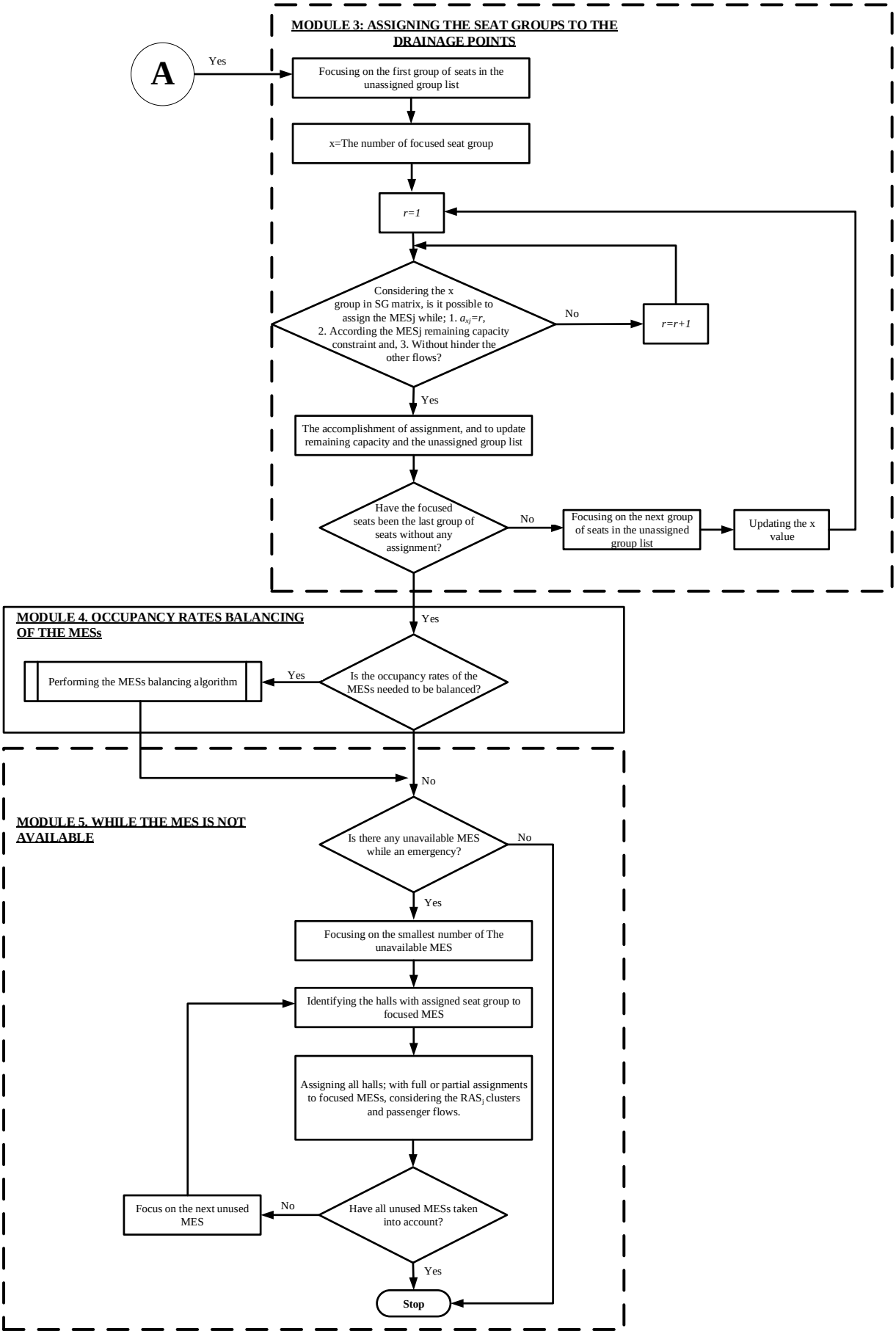

Figure. A1. Flowchart of the proposed systematic illustrating the routeing modules (Continued).

APPENDIX B: The Balancing Algorithm for the Proposed Routeing Systematic

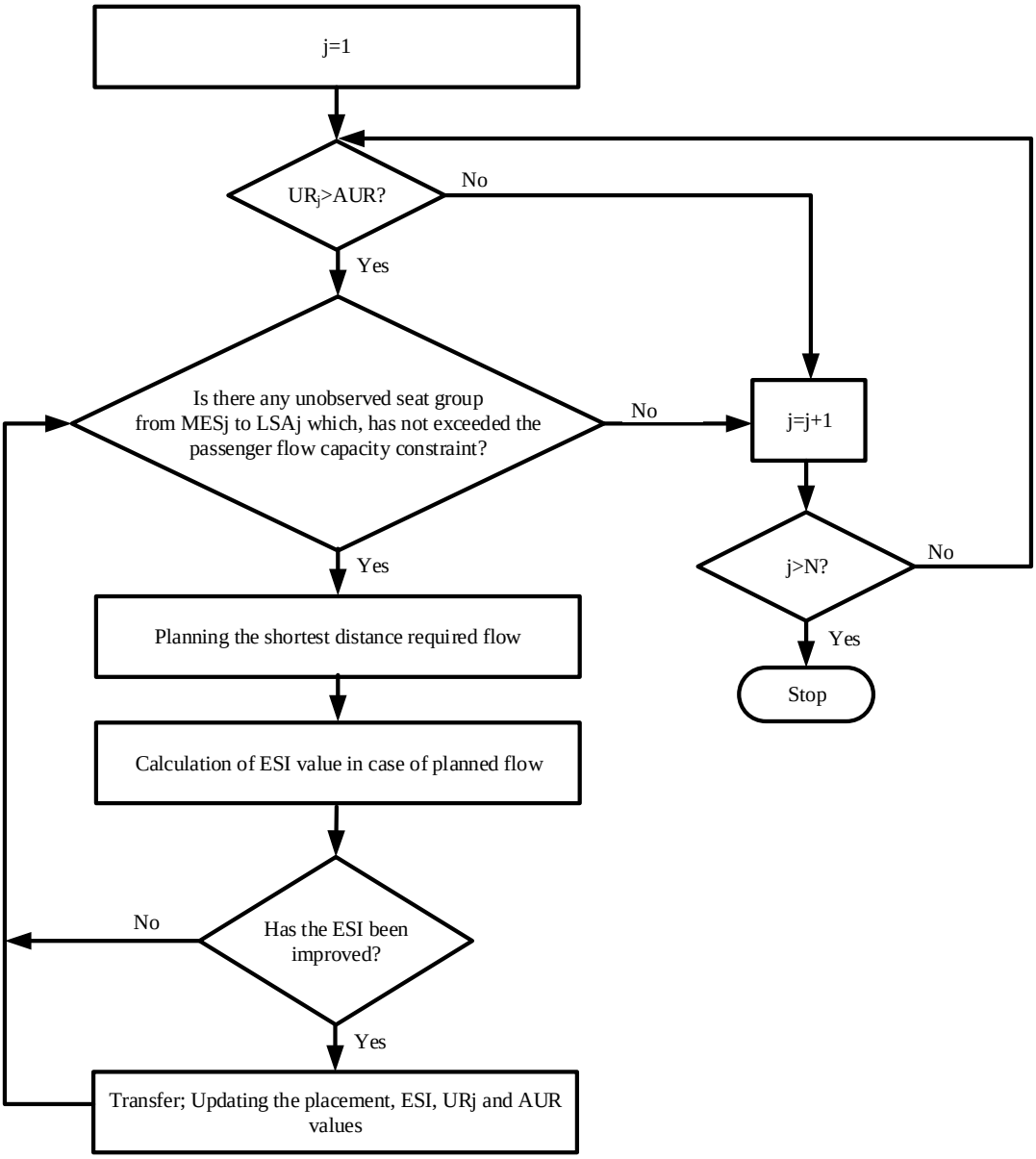

Figure. B1. Flowchart of the balancing algorithm

APPENDIX C:

Ship Layout

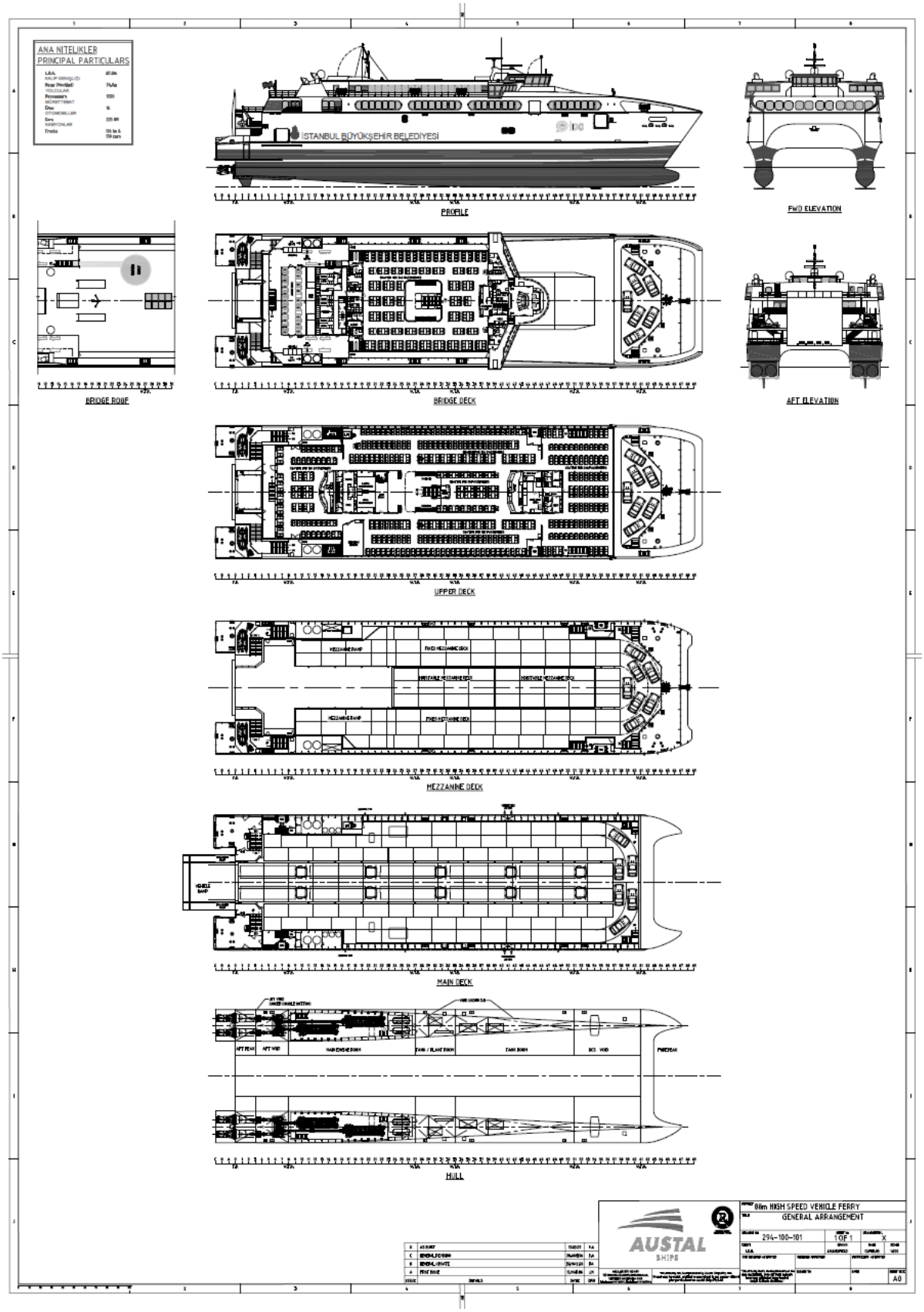

Figure. C1. Layout of the Focused Ship

APPENDIX D:

Questionnaire

PERSONAL INFORMATION

Gender:
Female ☐ Male ☐

Age
☐ under 18 years old ☐ 18-25 ☐ 26-35 ☐ 36-45 ☐ 46-55 ☐ Over 56 years

Education Status
☐ Primary school ☐ Middle School ☐ High school ☐ Associate Degree ☐ 4 years Degree ☐ Post graduate

PHYSICAL PROPERTIES AND SWIMMING

Length
☐ Under 150 cm ☐ 151-160 cm ☐ 161-170 cm ☐ 171-180 cm ☐ 181-190 cm ☐ Over 190 cm
Weight
☐ Under 50 kg ☐ 51-60 kg ☐ 61-70 kg ☐ 71-80 kg ☐ 81-90 kg ☐ 91-100 kg ☐ Over 100 kg
Do you have any disability?
☐ Yes ☐ No (Please specify if your answer is Yes)
Do you know swimming?
☐ Yes ☐ No

COMMUTING and ACCOMPANIMENT STATUS

Please specify your frequency use of the current/ prospect sea journey
☐ One or two times per day
☐ Every 2-3 days
☐ Once a week
☐ Every 2-3 weeks9
☐ Once a month
☐ Every 2-3 months
☐ Once a year
☐ Less than once a year

Are there any passengers you are currently escorting?
☐ Yes ☐ No (Please specify if your answer is Yes)

Are there any companions at the moment?
☐ Yes ☐ No

BEHAVIOUR WHILE EMERGENCIES

Do you have any emergency condition or practice experience on the sea journey?
☐ Yes ☐ No

Please indicate your level of knowledge regarding the ship layout and evacuation assemblies/exits.
☐ None ☐ Low ☐ intermediate ☐ High ☐ Very high

Indicate the behaviour you will show when you encounter an emergency in a sea voyage.
☐ I would orient to the point I entered.
☐ I would follow the warning signs to the nearest evacuation point.
☐ I would orient to the evacuation point that I know
☐ I would follow the crowd
☐ I would wait for the crew directions
☐ I would jump into the water at the first opportunity.
☐ Other (Please specify)

OTHER OPINIONS AND COMMENTS ABOUT THE SURVEY:

APPENDIX E:

Pseudocodes for FBGBS and Simulation Iterations

```
# Load geometry
LoadGeom Durum1_Exodus.exo
# instructions
LoadGeomFlexibleNods.exo
LoadPopPermisedAgents.epb
IOLocation C:\TubitakProject\SettingsFile
# Additional commands appended below
# Redirect people in Node1 and Node1
# Identify previously created zone
AssignNode Node1
AssignAgent Agent1
AssignAgent Agent2
# Delete existingBoundary
ClearItinerary
AssignZone Zone1
# Delete Population itineraries
ClearItinerary
# Assign Populationto Zone 1 population
ContinueSimulation
# Load geometry
LoadGeom Durum1_Exodus.exo
# Link data with existing zones
AutoLinkHazards
# Load scenario file setting behavioural response
LoadESO PassengerBehaviour.eso
# Run simulation for 250 times
RunSimulation 250
# Save each iteration
SaveSimulationResultsAndReturn
ContinueSimulation
Shutdown
```

DISCUSSION

HULLFORM & HYDRODYNAMIC CONSIDERATIONS IN THE DESIGN OF THE UK FUTURE AIRCRAFT CARRIER (CVF)

M E Campbell-Roddis, British Aerospace & BAE Systems, Glasgow & Filton (Bristol), UK
(Vol 159, A4, 2017)

COMMENT

Prof D Andrews, **FREng**, **PhD**, **FRINA**, **RCNC**, Vice President

The author is to be congratulated in producing a paper for the journal on an important aspect (hydrodynamics) of a design, which was taken to a considerable level of definition before not being proceeded with. The fact that we so rarely get visibility of the thinking and effort behind "abortive" designs – so very little was allowed to be preserved of the cancelled CVA01 of the 1960s – and that this can be compared to the separately evolved, subsequently fully design and, now in 2017, about to go into service QUEEN ELIZABETH (QEC) carrier, makes this a very worthwhile document for the Transactions.

Not only can the various detailed conclusions on the hydrodynamically related design choices be read for their input to the BAE Systems alternative to the Thales design, that was finally developed into the QEC (see S Knight's 2009 RINA Conference paper), the paper also provides general insights into the interaction of one specific topic (hydrodynamics) with wider design developments. This can be instructive to future designers of complex ships – not just aircraft carriers. It could be argued that despite the growing capabilities of CFD tools, that there still appears to be a need for substantial model testing of discrete elements of the hydrodynamic design, as described. Would the author like to comment as to whether he sees this dual need for CFD and physical model testing likely to continue whenever new designs "are just that little bit too different" and how one might judge the latter?

Given this discusser set up the procedure for the extensive UK Ministry of Defence (MoD) concept work on the Future Carrier, when Head of Concept Design in DFP(N) in the early 1990s (Andrews, 1994), it is surprising that the author does not refer to the paper that reported that extensive in-house design exploration work undertaken before the "competitive MoD funded feasibility level work that this paper covers. Eddison and Groom's (1997) paper lists the five ship option types (notably the four STOVL options with 15 to 40 aircraft and two CTOL options with 26 and 40 aircraft). These authors also list some 16 design investigations, ranging from side lifts and flight deck arrangements to shock and vulnerability measures as well as hull form and propulsion fits, directly relevant to the current paper. It is presumed all this work informed not just the Staff Target in 1998 but was also provided to the two industry design teams? What is of interest is not just that these discrete topics go well beyond the hydrodynamic but how much they all have a bearing on the seemingly hydrodynamic specific issues, showing so much of the design process is so clearly interrelated.

It would also be insightful if the author could add a further comment addressing, beyond the timescale of the paper as it stands with the 2003 decision to proceed with the Thales design, how the hydrodynamic conclusions of this work matched the subsequent design development. It is noted that there has been a subsequent paper on the QEC's hydrodynamics (Harris *et al* of BMT DSL, Thales Naval Ltd. & QinetiQ (2009)), which can be seen to have taken up many of the choices made by the author's early team's efforts. Could the author comment as to both the commonality and difference between these two sequential hydrodynamic efforts?

On the hydrodynamic aspects of the carrier design, it is interesting to observe that in our earlier paper on the very novel INVINCIBLE design (Honnor & Andrews, 1982) the only aspect of hydrodynamics that we thought necessary to flag up was that of the seakeeping analysis undertaken to assess the wetness implications regarding the location of the foremost ship side openings outboard of the hangar. This was probably not seen as a concern for the much larger and, specifically, considerably longer, QEC but I would like to ask if this one (significant) hydrodynamic issue in the INVINCIBLE design was also investigated in the BAE Systems CVF design? When design comparisons are drawn, too many just compare design displacements – however a much better comparison of size, for these essentially space driven vessels, is that of gross enclosed volume. Thus that for INVINCIBLE is 80,000m^3 which is directly comparable with HERMES, its companion carrier in the Falklands' campaign although the latter was some 50% heavier.

In Section 7.2 in the first of the set of five bullet points on "key discriminators" the author invokes a structural issue when adopting the "highly flared midsection" (Figure. 4) in preference to the traditional "sponson" style (Figure. 3). This non-hydrodynamic issue is said to simplify the structural arrangement ("by eliminating the need for continuous longitudinal bulkheads"). Could the author say how this "elimination" was confirmed? Thus without continuous longitudinal bulkheads, was there sufficient stiffness in the hull girder? This aspect of strength was a concern in the INVINCIBLE design (see Honnor & Andrews, 1982), which had two sets of longitudinal

bulkheads port and also starboard to ensure the longitudinal stiffness of the tall (three decks) and (amidships) narrow hangar was transmitted efficiently into the hull girder. It was only when the SESAM FEM analysis finally delivered (after the structure was built due to the novelty of the modelling of a whole ship's structure in the 1970s) its results that the assurance of the maintenance of the hull girder's structural stiffness was shown to be sufficient. In fact, despite the current author's comment in Section 2 of the "relatively light structural scantlings" of INVINCIBLE, the high D/L hull ratio meant that the midships longitudinal strength was actually massively adequate. This was due to the scantlings of the flight deck and hanger deck being (like the aircraft lifts) primarily designed for future aircraft loadings.

In repeating my thanks for this paper on an unfulfilled design, I would like to re-iterate its value in showing how just one element of the naval architect's concern in working up anew ship design (that of hydrodynamics) is both sophisticated and largely interactive with the other elements of the design (e.g. strength, stability, configuration and fighting (aircraft) effectiveness). It would be good to have the aspects of producibility and, eventually, aircraft operability presented alongside this presentation and its companion paper (Harris et al, 2009) and indeed the 2005 general aircraft carrier configurational paper by this discusser (Andrews, 2005).

AUTHOR'S RESPONSE

The author would like to thank **Professor Andrews** for his comments and for his input and guidance as one of the referees for this paper. The primary aim of the author in seeking to get this paper published, 14 years after it was originally withheld from publication by the UK MoD, was to provide some form of lasting record of the efforts of the unsuccessful 'Team BAe' carrier design team from 1996 to 2003, and also to provide additional background on the early days of the carrier project and some of the more interesting ideas and options that we considered. The author hopes that it will serve these purposes well.

The first point raised by Professor Andrews in his comments relates to Computational Fluid Dynamics (CFD).

The January 2003 aircraft carrier downselect decision ended the author's direct involvement in both warship design and hydrodynamics, so he can no longer claim to be fully up to date on this. Notwithstanding this caveat, the overall guiding principles on the applicability and use of CFD have not changed over the past 30 years, in spite of improvements in hardware, software and methodology. Too many in our industry wrongly regard Computational Fluid Dynamics (CFD) as being a mature and reliable field, akin to structural Finite Element Analysis (FEA), which it is not. Whilst it is perfectly reasonable for an engineer with limited training and experience to generate reliable and trustworthy structural analysis results with an off-the-shelf FEA package, without the need for experimental validation, this is still not the case with CFD, at least not for marine hydrodynamics use. CFD without experimental validation remains unreliable and potentially grossly misleading. Allied to this, CFD (unlike structural FEA) tends to be a limited and intermittent activity in ship design, and therefore a difficult (and expensive) capability to sustain in times when demand for it is low. As such it is the author's firmly held view that CFD in ship design should remain the specialist preserve of towing tank institutions and specialist university-based consultancies, who have the specialist knowledge, volume of work, experience, time and experimental facilities to generate reliable and properly validated CFD results. Shipyard design departments, warship project teams and ship consultancies themselves (as non-specialists) should overcome the temptation to acquire their own CFD tools and dabble in CFD, as the costs of building and maintaining the capability to generate reliable (validated) CFD results is generally not worth the expense, and the consequences of getting things wrong are generally too great. Shipyards and project teams that acquire their own CFD tools soon tend to find that they soon fall into disuse, or that they cannot place any degree of reliance on the results. This applies to both CFD tools for resistance & powering prediction, CFD tools for detailed flow modelling, as well as advanced 3D diffraction tools for seakeeping assessment - all are best left to specialists!

If one accepts this (i.e. that one has to go to a reputable towing tank institution for reliable CFD modelling), then it follows that one should listen to their specialist advice on whether it is best to proceed with CFD or model tests (or a combined package of both) for a given hydrodynamic task. Cost also plays a factor in this though, and in the author's experience detailed CFD studies can be almost as expensive and time-consuming as model tests, with CFD results commonly regarded as less trustworthy or robust. In the author's experience, end-customers and ship-owners generally also still prefer experimental model tests over the vagaries of CFD. Indeed, cost is (in many ways) the biggest barrier to more widespread use of CFD. In the author's view, CFD is best reserved for initial broad order comparison of hullform options, modelling of detailed flow areas that are difficult to assess in detail through experiment (e.g. around shaft 'A'-brackets) and for hullform optimisation and refinement (e.g. bow shape and bulbous bow optimisation) prior to tank testing.

Our team found that use of much-simpler regression-based (empirical) powering prediction tools, when calibrated against sea trials data for a similar hull type, and accompanied by sensible input assumptions and margins for uncertainty, gave an excellent first prediction

of speed-power characteristics that aligned very well with subsequent tank test results, without having to resort to CFD. For new "slightly similar" designs of the type referred to by Professor Andrews, the author would recommend use of such a regression-based (rather than CFD-based) approach in the first instance. The author would then recommend approaching a towing tank institution and take their advice on whether CFD or model testing were appropriate for more detailed powering assessment.

In terms of Professor Andrews' paper (Andrews, 1994), this depicts very well the high level MoD preliminary design framework that we (on the industry side) operated within in the early carrier project, and the approach that MoD in-house studies followed. As industry / consultancy participants we had very little control over this framework, and even during the competitive stage were rarely given more than three or four months of 'loose rein' to work up an initial design and progress our studies, without having then to report back to the MoD with our findings and be redirected onto a re-baselined design variant or new set of cost-reduction studies. The reality was that, for all the cost-capability studies, the MoD knew pretty much what size of ship it wanted from the 1998 SDSR onwards, and steered us toward this ship size with a good degree of certainty that the allocated budget would be blown. In this regard, it would have been better for the MoD to have allowed the industry teams a longer run working up a single design variant to a greater degree of design and cost maturity, prior to downselect based on firm and fixed price bid for design and build. Alternatively, it would have been fairer and more transparent for the MoD simply to form a 'rainbow' team from the outset of the funded carrier design studies in 1999, with industry partners promoted to it (and demoted from it) according to the stage of design and their individual performance. The situation that came to pass in early 2003, whereby the winning contractor was selected through a carrier design 'beauty contest', based on preliminary cost estimates, and a design that subsequently needed to be fundamentally re-worked, without having to commit to a firm price for design and build, was both unfair to the 'losing' contractor and paved the way for the significant cost overruns that have now had to be shouldered by the UK taxpayer. Rather than delve too far into the politics on this here, please see the author's 6th November 2013 letter in 'The Financial Times' outlining his views on how things could have been done better on the both the carrier and the associated FCBA aircraft projects.

Swiftly moving on, Professor Andrews rightly highlights Eddison and Groom's (1997) paper as a key record of the early stages of the carrier project. This paper is essentially a high level (and 'sanitised') summary of the MoD's May 1997 CVF aircraft carrier concepts report, which summarised the findings and final outcome of the MoD's in-house aircraft carrier studies (as input to the 1998 Strategic Defence Review). The industry teams were provided with a copy of this MoD concepts report as 'GFI' (Government Furnished Information) at the commencement of the MoD-funded industry studies in December 1999. This formed an incredibly useful starting point for our studies, and all concerned from the MoD can be justifiably proud of this report.

As we progressed our studies, we found that emergent assumptions and constraints regarding aircraft stowage and operation, increased steelweights and scantlings associated with adoption of Lloyds Naval Ship Rules (in place of the MoD's previous 'SSCP 23' structural standard), movement to more generous accommodation standards (4-berth vs 6-berth cabins), and over-zealous interpretation of requirements by specialists and former-Royal Navy personnel on our team resulted in ship designs that were somewhat larger and more costly (for a given aircraft capacity) than the MoD concepts. To some extent this 'requirements creep' and over-specification could (and should) have been pushed back on and resisted more firmly, as it undoubtedly resulted in carrier designs that were larger, more costly and carried higher risk than should have been the case. The fact that we were in a design competition, and that MoD requirements for the ship were high level, comparatively loose and open to interpretation, did not help this any. On reflection it would have been better for the MoD to be firmer from the outset on requirements and budget for the ships, rather than leaving it to the industry teams themselves to adjudicate on the interpretation of requirements.

As regards similarity of the final Queen Elizabeth Class (QEC) carrier design and our 'losing' design, the first thing the author must stress that he has not had any detailed visibility of the final QEC design, nor indeed any of the preceding Thales designs, other than what has been openly published. Whilst the papers by Harris *et al* (2009) and Knight (2009) provide some background on the Thales designs, they are limited in the level of detail to which they go, making it difficult for the author to comment in detail on differences between the two teams.

Notwithstanding this, in early March 2003, in the immediate aftermath of the downselect decision, the author (acting on direct instruction from BAE SYSTEMS) attended at the Thales carrier design offices in Bristol and handed over all our team's hydrodynamic work, requirements decomposition and design information onto Mr. Harris of the 'winning' Thales team (lead author of Harris *et al* (2009)). Allied to this, two of the author's hydrodynamics team transferred to the Thales team, as did the marine engineer who had been heading up detailed design of our twin shaftline arrangement (Mr Sears, co-author of Harris *et al* (2009)), also our team's two most senior platform design managers. The author would therefore like to think that there was some cross-pollination from our 'losing' design (including our requirements decomposition work and our approach to key issues, as well as design features) onto the 'winning' Thales design.

It is clear (Knight, 2009) that the 'winning' Thales design went through several design iterations in the years after the 2003 downselect decision, in an attempt to contain cost and reduce risk. Although the overall visual style and appearance of the BMT/Thales design did not change, features and detail of it most certainly did (see Knight (2009) and Harris et al (2009)), which seem to have brought it closer (in content, if not visual appearance) to our 'losing' carrier design.

During our post-downselect discussions senior members of the Thales / BMT team flatly refused to entertain any notion of moving to our highly flared above water hullform; perhaps understandably, as this would have fundamentally changed the style and appearance of the 'winning' design to something approaching our 'losing' design !

Whilst the underwater form of our team's carrier design was based on a refined derivative of the 'Invincible' class hullform, Harris et al (2009) indicate that the hullform of the Thales QEC design was based on past ocean liners. Unlike the modern cruise ship underwater form that our team considered (and rejected), which was designed for a comparatively low ship speed and appeared to be significantly optimised toward maximising space for standardised cabins, the traditional ocean liner-type forms considered by the Thales team would have been optimised for higher ship speeds (traditional liners being a form of transport rather than a means of recreation). The author's understanding (based more on anecdote than hard evidence) is that such liner-type forms (typified by the RMS Queen Mary of the 1930s and the Queen Elizabeth II of the 1960s) share a common ancestry with the aircraft carrier underwater form that we adopted (whose ancestry could be traced back via the 'Invincible' class and HMS Hermes to the battlecruiser and carrier forms of the 1920s and 1930s). As such, the author doesn't believe that the rival Thales and BAE SYSTEMS designs were that far apart in terms of underwater form design.

Both team's designs featured a bulbous bow, which at the time our studies was something of an innovation for a front line Royal Navy warship and aircraft carrier. Ultimately the Thales design evolved from a 'swan neck bulb' (similar to ours) to a cylindrical bulb design (see Harris *et al*, 2009). However, the author suspects that the real life hull resistance benefits of a cylindrical build over an equivalent (fully optimised) 'swan neck' bulb are marginal – the main benefit is ease of fabrication (less double curvature plate).

In terms of other hydrodynamic features, it is evident (Harris et al, 2009) that the twin shaft element of our hybrid shaftline arrangement was carried through into the Thales design in place of their all-podded arrangement, albeit with separate motor rooms for each shaft. Had our team's design been successful, the author believes that we too would have come under pressure to eliminate the single pod of our design. In that event, the author's preference would have been to substitute a third conventional shaftline in its place. The resulting triple 'conventional' shaft arrangement (with motors for the two outboard shaftlines located in the same longitudinal compartment, so as to achieve shaftline symmetry (for produceability reasons), and a separate motor room for the centreline shaft for survivability reasons), would have avoided the high propeller loading of the twin shaft arrangement finally selected for the Queen Elizabeth carrier, mitigating noise and vibration risk. Contrary to what our team's survivability specialists indicated back in 2001 / 2002, the author doesn't believe that a triple shaftline arrangement would have been that unacceptable from an underwater signatures point of view (noting that aircraft carriers have a pretty unique infrared signature anyway during aircraft operation, are pretty horrendous from a radar cross section standpoint, and a carrier flotilla is arguably pretty easy to spot by satellite or through passive electronic warfare). Had it been the author's call, the carrier design presented in this paper (and indeed QEC) would have had a triple conventional shaftline arrangement. Or (had we wanted to be innovative) twin conventional shaftlines for cruise and one or two waterjets for boost up to maximum speed, noting that high carrier speeds are generally only required in calmer conditions where waterjet performance would be reasonable. However, the author's view is that a triple shaft arrangement is the best all-round solution for this size and speed of warship. The modest cost 'delta' of a triple shaft arrangement compared to a twin shaftline arrangement was (in the author's view) more than offset by the reduction in technical risk (re: reduced propeller loading), produceability and survivability benefits.

Early on in our studies we firmly concluded that two pairs of retractable fin stabilisers were the most appropriate solution for the carrier, as a motions-critical vessel, in spite of concerns regarding their shock survivability and cost pressure to move to a single pair. Harris et al (2009) noted that the MoD imposed such a solution onto the Thales design, possibly based on our team's work.

In terms of ship speed, the author understands (from open source data) that the design speed for the final Queen Elizabeth carrier aligns with that derived by our team back in 2002 for CTOL operations (which in turn was just one knot higher than what we concluded was necessary for STOVL operations). At the outset of the industry studies the presumption was that the carrier would have a significantly higher maximum ship speed, comparable to the 'Invincible' class. However, the 'Invincible' class were in many ways Marine Engineers' ships, with a high maximum speed, once-novel gas turbine propulsion system, huge amounts of space given over to gas turbine uptakes and downtakes, and dedicated machinery removal lifts that compromised hangar stowage space for aircraft. Our team recognised early on

that the high speed of the 'Invincible' class was only achieved at some compromise to the ship's core aviation function, and that challenging the presumption of high maximum ship speed was key to minimising cost and risk of the new carriers, and maximising space available for the ship's primary (aviation) role. We therefore played a key role in challenging this presumption and bringing ship speed down to more modest levels. The author was a keen advocate of progressing with a maximum ship speed as low as 23 knots, as a way of saving cost (long, slow ship vs short, fast ship). However, this proposal was considered too challenging of expectation by our team's management, and so (for our carrier designs) we settled on a maximum ship speed somewhere in the middle (between these extremes). This modest (but nonetheless reasonable) maximum ship speed seems to have been carried forward into the final Queen Elizabeth carrier design.

The author's involvement on the BAE SYSTEMS team carrier design studies extended beyond hullform and hydrodynamics, and he would therefore also like to comment on some of the broader similarities and differences between the BAE SYSTEMS and Thales design offerings:

For our final 2002 carrier designs, our team switched from the WR-21 based gas turbine propulsion plant of our earlier carrier designs, to a Marine Trent-based gas turbine propulsion plant (with supplementary diesel generators). A similar arrangement seems to have been adopted on the final Queen Elizabeth carrier design. The author's view, having been involved on the periphery of our team's marine engineering studies from 1996 to 2003, was that the WR-21 based solution, with its smaller power units, was a neater fit for the carrier, that would have provided a well-distributed and redundant propulsion plant, beneficial commonality with the Type 45 Destroyer fleet, and allowed greater effort to be devoted to dealing with the 'teething troubles' of the WR-21 engines.

From the earliest days of the British Aerospace PV-funded studies (1997 onwards, well before the involvement of Thales in the project), our team recognised the potential of modern shoreside warehouse stores handling systems for automating handling and stowage of the large quantities of air weapons onboard the new carriers, and the significant reduction in crewing levels that this might achieve. Cdr Kevin Donnelly (RN, rtd.) of our team opened up the early dialogue with equipment vendors on this, and over the course of the next six years progressed things into a baseline automated air weapons handling proposal that is now a feature of the final Queen Elizabeth carrier design. Similarly, other aviation design features of the final QEC design, such as the 'Flyco' (Flying Control Room) configuration, bear uncanny similarity to our team's proposal. Less obvious, our aviation team also played a key role in progressing and resolving a number of key design issues relevant to the new carriers and clarifying thinking on key areas of design policy. In his January 2003 speech to UK Parliament announcing the carrier downselect decision in favour of Thales / BMT, then Secretary of State for Defence Geoff Hoon indicated that aviation design was an area of weakness on our team's design. He was wrong and did the members of our aviation team a grave injustice in suggesting this.

To conclude the discussion on similarities and differences between the Thales and BAE SYSTEMS designs, the author would like to touch on the important issue of island superstructure design. In general, the island superstructure represents an obstruction and impediment to aviation operations and there is therefore a tendency to favour the smallest possible island footprint and size. In the case of a nuclear powered carrier (where there are no main engine uptakes), or a conventional steam or diesel-powered carrier (where uptakes are of comparatively low diameter, low allowable bend radii, and consequently easy to route), this means that the optimum island arrangement is a single island superstructure, as typified by USS Enterprise (CVN-65), HMS Hermes (1959) and HMS Ocean (1998). However, for carriers with gas turbine main propulsion, the uptakes are of much larger diameter, restrictions on uptake bend radii are more onerous, and the space consumed in trying to route gas turbine uptakes together from the separated machinery spaces (required for survivability) is huge. Thus it is difficult to route the uptakes into a single superstructure with gas turbine main propulsion. The end result, if one tries to do this (unless one resorts to cascade bends, as we did on our earlier designs), tends to be a very long superstructure, as typified by HMS Invincible (1980). Consequently, our team concluded that the optimum solution for the new carriers (as gas turbine powered ships) was:

- a comparatively short main island superstructure up forward, fitted with a single funnel for the forward machinery spaces;
- a standalone and minimally-sized broad-based 'mack' (i.e. a combined mast and funnel stack) sited further aft, just big enough to accommodate the uptakes for the after machinery spaces and provide an access stairway beneath deck.

This solution, shown in Figure 15, was somewhat different to the two larger island superstructures of the Thales and final QEC designs. For our final 2002 design iterations, our aviation team proposed a 'bridge' between our main island and the 'mack', in order to generate extra superstructure space without compromising flight deck parking, resulting in the arrangement shown in Figure 1 of this paper. The author never really liked this arrangement, and remains of the view that the optimum arrangement for the new carriers would have been a short fwd main island supplemented by a standalone broad-based 'mack' further aft, as shown in Figure 15.

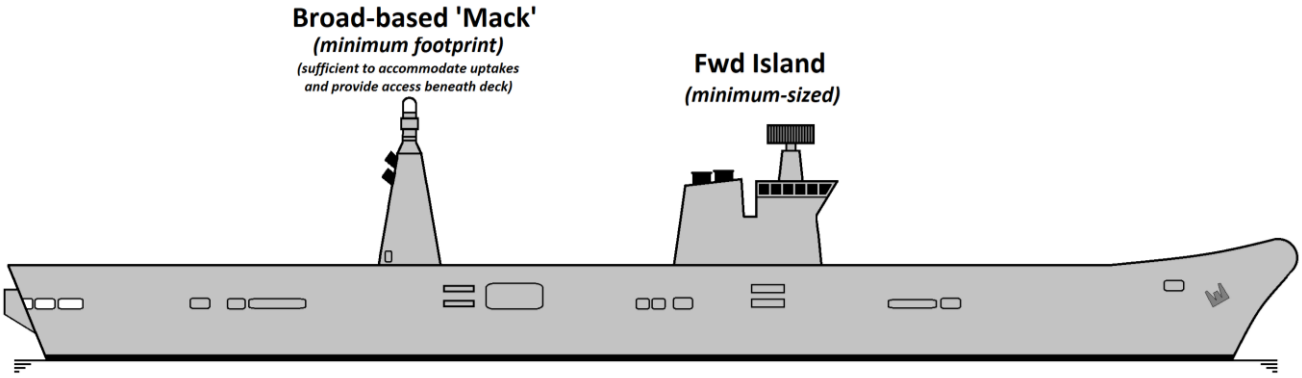

Figure 15: Optimum island Arrangement for a Gas Turbine-Propeller Aircraft Carrier (Author's opinion)

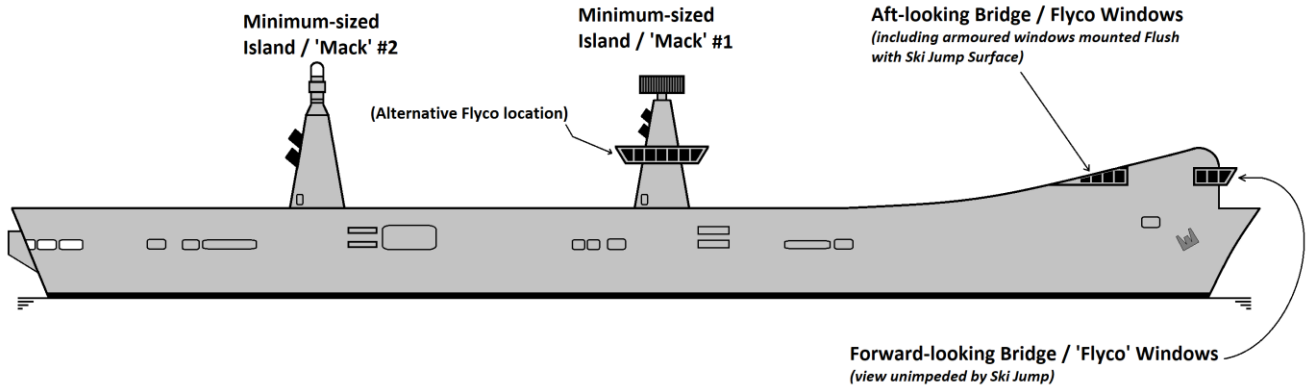

Figure 16: Large Exit Angle Ski Jump Concept for STOVL and STOBAR Carriers (Bridge and 'Flyco' located beneath Ski Jump)

The author also observes that our team's carrier designs all had 'tumblehome' island superstructures (i.e. sides tapering inwards with height above the flight deck), whereas the Thales island design flares outwards with height above deck. Whilst the Thales approach provides additional space in the island for a given flight deck footprint, our inward-flared island avoided re-entrant angles at the flight deck and is therefore better for radar cross-section (RCS). That said, side lift openings and flight deck activity ensure that the RCS characteristics of an aircraft carrier are less than ideal, in any case.

Input from our colleagues at BAe (Warton) during our early PV-funded carrier studies indicated that (for STOVL and STOBAR carrier variants) there might be significant benefit (in terms of aircraft performance) of proceeding with a large exit angle ski jump (around 20° exit angle rather than the 12°- 14° exit angle typical of existing carriers). However, the problem with such a high exit angle is that the ski jump becomes very tall (around three or four decks tall, as the author recalls), which limits view from the ship's bridge. As a potential solution to this, the author proposed relocating the ships bridge from the island superstructure to a position beneath the ski jump. Under this concept (Figure 16 below), 'Flyco' (the Flying Control Room) would also have been relocated alongside or beneath the ski jump (with aft-facing armoured glass / protective grilles for rear visibility), the main island would have been reduced to a 'mack', and the after machinery spaces would have exhausted either through a second 'mack' or directly overboard through the ships stern. An innovative proposal that was too adventurous to be considered in any detail!

In terms of the side openings that Professor Andrews refers to on the 'Invincible' class, the author's understanding is that the openings that he is referring to are the large air intake plenums (extending over two deck levels sited comparatively low in the hull, immediately abreast the hangar). Ingress of green seas through these openings would have represented a down-flooding risk, and (in spite of the separation arrangements in the plenum) could also have interfered with the operation of the gas turbines. We were aware of this issue and did attempt to assess the risk of this in our early studies. However, the reality was that our intakes were sited much higher in the hull (immediately below the flight deck or in the island, depending on ship design) and closer to midships. As such, they were sited as high as practicable above the waterline in a location where the risk of green seas ingress was minimised. Although (as ever) it is possible to conceive of 'extreme weather survival' scenarios where green seas could have entered

these openings, the onus under these scenarios fell on the marine engineers to ensure that the engines could continue to operate (e.g. through appropriate filtration / water separation arrangements) and on those undertaking the stability analysis to model them as unprotected (down-flooding) points. There were (of course) other openings in the hull sides of our carrier design, in particular boat and mooring recesses. However, it was accepted that these would be out of bounds in extreme weather, and they (and their fittings - doors, tank vents, etc) would have been in full compliance with civilian freeboard and UK naval / load line requirements.

Professor Andrews makes an interesting point regarding the similar internal space but significantly different displacements of HM ships Invincible and Hermes. Steel weight typically represents something approaching 40% - 50% of the displacement of an aircraft carrier. Much of this weight difference is therefore likely to be down to Invincible having more optimised (lighter) scantlings than Hermes (whose build originally commenced in World War II where heavier scantlings and some armour was the norm). Additionally:

- Hermes' flight deck was strengthened for the more challenging loads of CTOL (vs STOVL) aircraft operation;
- Invincible (with its clean sides) lacked the hull sponsons fitted to Hermes, which would have significantly added to steel weight;
- Hermes had a much larger air group capacity than Invincible, meaning much denser outfit (2,100 vs 1,540 crew) and greater variable load (air weapons, aviation fuel, etc);
- Hermes' steam propulsion plant would have been significantly heavier than the aero-derived gas turbine propulsion plant of Invincible;
- Invincible had a shorter hull (but a much larger island superstructure) than Hermes.

In the author's view, waterline length is a more reliable baseline comparator than displacement for aircraft carrier designs. As part of our team's early studies, the author undertook a detailed trendline (scattergram) analysis of aircraft carrier design characteristics (dimensions, aircraft capacity, crew and payload) for existing and past aircraft carrier designs, and this amply demonstrated this point. Such trendline analysis is easy to do using tools such as MS EXCEL and open source warship data, and so long as one ensures that they are informed (rather than constrained) by the trends indicated, and accepts that unreliable data and scarcity of data can skew the analysis, then this is an extremely valuable tool for validating and estimating required design dimensions and parameters. Potentially the basis for another paper !

The author tends to leave the hocus-pocus of structural design and analysis to others, whilst keeping an interested and watchful eye on the overall outcome and any high level issues that it unearths. In the case of the carrier designs presented in this paper, the preliminary structural design and analysis was undertaken by structural engineers from BAE SYSTEM's Barrow-in-Furness shipyard. The results of this quite extensive assessment did not (as the author recalls) highlight any concerns (as raised by Professor Andrews) regarding stiffness of the hull girder; the hull (by virtue of its depth, many decks and very wide, thick, flight deck) was found to have more than adequate longitudinal bending stiffness. Instead, the key structural concerns were:

- The comparatively high location of the neutral axis in the hull, due to the disparity in width between the above water form and below water form (74m flight deck width vs 40m Waterline Beam) and the comparatively heavy flight deck scantlings in comparison to the keel plating. The result was high keel stresses in hull bending scenarios, with a particular concern being the risk of buckling of the hull bottom plating in hull girder hogging scenarios;
- The structural discontinuity caused by the large hull side lift openings. As with most modern large carriers, these side lift openings were situated close to the points of maximum hull girder shear force and bending moment (Figure 17). In particular, the location of the after side lift openings being close to the point of maximum hull shear force was a key concern, as the sideshell and hangar side longitudinal bulkheads are key contributors to the shear strength of the hull girder.

Our team's advisor, the late Professor Louis Rydill, played a key role in highlighting these concerns to us at an early stage, based on his experience with the cancelled Royal Navy CVA01 aircraft carrier of the 1960s. As with most structural issues, there was nothing insurmountable in these two issues, nothing that couldn't be resolved through routine structural design and judicious reinforcement / compensation details, but they were nonetheless key issues that were best addressed from the earliest stages of design.

In terms of the author's comment regarding the "relatively light structural scantlings" of the 'Invincible' class, this is based on the following:

- Steelweight estimates for our team's earliest carrier designs were based on extrapolation of scantlings of the 'Invincible' class to our hull, using the MoD 'Shipstruct' software. A short time later we commissioned QinetiQ to perform a comparison of our estimated steelweights against data that they held for other aircraft carriers, which highlighted that our steelweights were well below norm (by several thousand tonnes). This lead to a fundamental re-evaluation and upward increase in our steelweight estimates. The conclusion from this work was that 'Invincible' class had scantlings significantly lighter than other aircraft carriers;

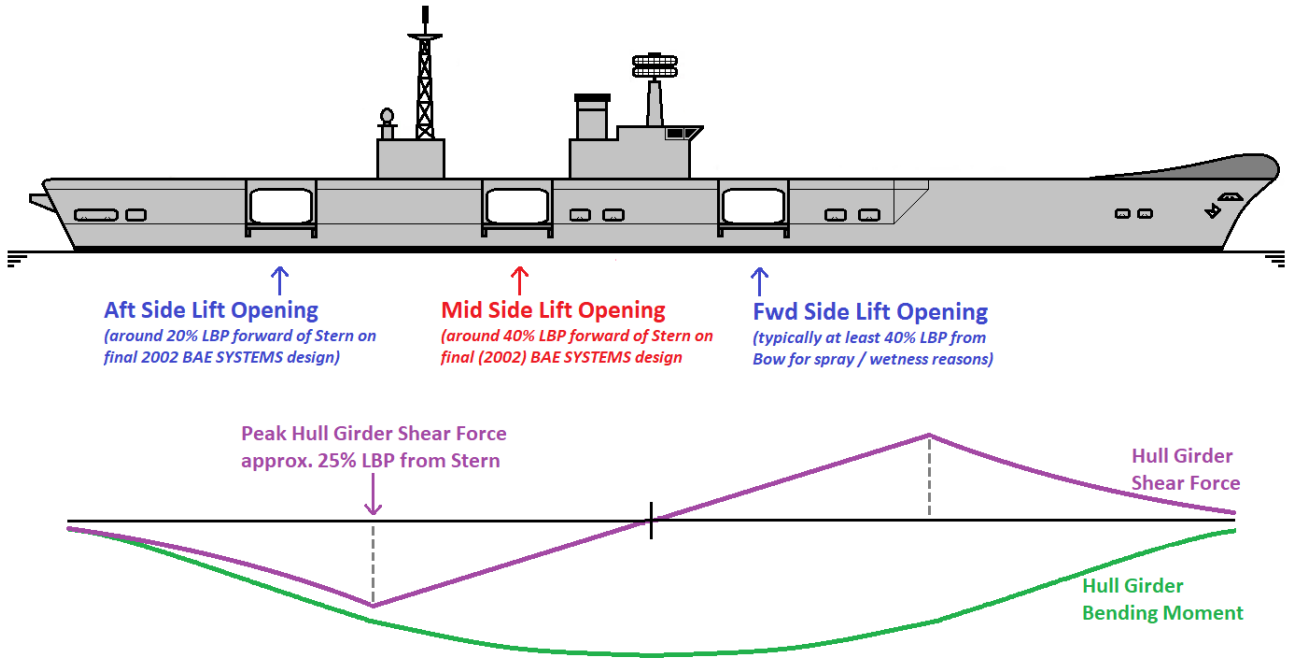

Figure 17: Generic Aircraft Carrier Profile, showing the Location of Aircraft Lift Sideshell Openings relative to Positions of Maximum Hull Girder Shear Force and Bending Moment

- When we re-baselined our steelweights based on the (then newly issued) Lloyd's naval ship rules, we found that minimum allowable steel thicknesses (specifically deck thicknesses) were in excess of the thicknesses of the 'Invincible' class. Due to the size and internal volume of our design, the resulting (modest) increase in required deck thickness had a significant effect on steelweight;
- During a visit to a large US Navy aircraft carrier in April 2000, it became apparent that the subdivision and thickness of the steel was far in excess of comparable structure and subdivision of the 'Invincible' class;
- During a visit to one of the 'Invincible' ships at sea in the late 1990s, a senior officer attributed the vibration experienced when the ship accelerated to the hull being design to light "cruiser scantlings", optimised for higher ship speed, as opposed the heavier scantlings of previous carriers.

This is not to say that the scantlings of the 'Invincible' class were in any way inadequate – just that they were lighter and more optimised for higher speed.

Professor Andrews requested further justification of the author's assertion that our highly flared above water form simplified internal structural arrangement 'by eliminating of the need for a longitudinal bulkhead'. To clarify this, the author refers to Figure 18. With the traditional (sponson) style of above water form (Figure 18(a)) the sponsons typically extend vertically over the entire depth of the Hangar. Moreover, the junction of the sponsons with the hull (Points C & D of Figure 18(a)) represent a fundamental discontinuity in shape. Consequently, to maintain structural continuity:

- Longitudinal bulkheads (effectively the vertical continuation of the main hull sideshell) are required as indicated by 'A' and 'B' of Figure 18(a), extending over the full depth of the hangar. Without this, load transmittal paths become complicated.
- Structural compensation is required at locations 'C' and 'D' of Figure 18(a).
- Any opening in bulkheads 'A' and 'B' (or removal of them) requires significant compensating detail to ensure adequate load transmittal to (and within) the main hull.

With the highly flared style of above water form, the transitions indicated by points 'G' and 'H' of Figure 18(b) are gentle, avoiding the need for excessive reinforcement at this location. Although small (shallow) sponsons are required on the upper part of the hull to adjust the post-flare upper reaches of the hull to match the local flight deck width, these sponsons are far smaller than with the traditional style of above water form. Thus, although small longitudinal bulkheads (or other form of support, such as pillars) are required at 'E' and 'F', as indicted in Figure 18(b), these are far smaller and lighter than the corresponding full depth bulkheads ('A' and 'B') required by the traditional style of above water form. As such, the author stands by his comment that the highly flared style of above water form is simpler and neater structurally. As ever, there is more than one structural arrangement possible with either option, but (hopefully) looking at Figure 18 the reader will see that the highly flared above water form is more elegant (both structurally and aesthetically) than the traditional (sponson) style of above water form.

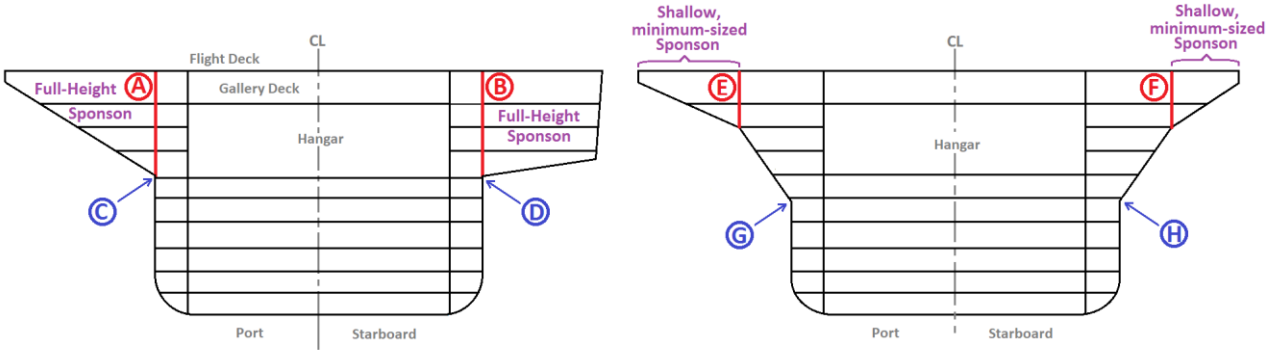

(a) Traditional (Sponson) Style of Above Water Form (b) Highly Flared Above Water Form

Figure 18: Differing Structural Layout of the Traditional (Sponson) and Highly Flared Styles of Above Water Form

From our team's earliest carrier concept design (our May 1998 PV-funded 40 STOBAR carrier design) onwards, our team employed a highly flared above water form, and no formal structural comparison was undertaken between the highly flared and conventional 'sponsoned' styles of carrier above water form. There was no need, it was a top level decision regarding the style of our design. To us the highly flared approach (i.e. using flare to accommodate as much of the disparity between waterline beam and overall (flight deck) beam as possible, and then using small (shallow) sponsons to accommodate the remaining disparity), was by far the most elegant solution. Our team's structural design work demonstrated that an efficient hull structure compliant with Lloyds Naval Ship rules could be achieved with the highly flared above water form, and data provided by Qinetiq indicated that our resulting hull steelweights were not excessive. Our team's considered view, based on based on 4 years of assessment, was that the Highly Flared Form was better spatially, for structural simplicity, from a build perspective and less likely to experience structural problems through-life (re: structural continuity). In the author's view, the sponsons of the Thales design and US aircraft carriers are a throwback to the major upgrade and retrofit of angled runways to axial deck carriers in the 1950s, rather than an elegant solution for a newbuild 21st century carrier. Aside from the move to nuclear propulsion, the US Navy has followed a largely evolutionary approach to carrier design since the first 'Forrestal' supercarrier of the 1950's and are pretty much tied to continuing with the sponson-based approach of the 'Nimitz' class, due to the prohibitive cost of moving away from this existing legacy design – not the case for our totally new carrier design. In terms of infrastructure, fundamentally re-worked / all-new infrastructure has been required for our new carriers in any event (including re-working of existing drydocks and construction of extra-wide harbourside pontoons), even with a sponson-style of above water form, so this is not a fair discriminator between the two styles of above water form.

Our team's highly flared above water form was part of a broader strategy of attempting to minimise the need for ad hoc (local) sponsons extending beyond the basic envelope of the main hull. In the case of STOBAR carrier variants, a novel proposal from the author during our team's early studies, similarly intended to minimise the need for sponsons, is as shown in Figures 19 & 20 (never progressed beyond initial concept). This would have eliminated the large Port-side sponsons more traditionally associated with STOBAR carriers (Figure 21), by obviating the need for an angled runway. Instead, under this novel proposal, a hinged / retractable ski jump would have been fitted to the ship, to allow use of the ship's axial launch runway for STOBAR aircraft recovery. As this concept remains a potential means for facilitating STOBAR operation of conventional carrier aircraft (e.g. F/A-18 E/F Super Hornet) from the new carriers, with only relatively modest modification to the ships, the author encloses the sketches of Figures 19 & 20 as a record of this concept.

One further point that the author would like to make, concerns hangar and side lift configuration:

All carrier designs produced by the BAE SYSTEMS team aligned with established US carrier practice, in having a single level (tall) hangar. The hangar height, as driven by Merlin helicopter maintenance (rotor head removal) requirements, resulted in a hangar far in excess of that required to simply stow F-35 fixed wing aircraft. Significantly increased F-35 aircraft stowage would have resulted had a twin level hangar been adopted (see Figure 22). This could have been achieved without significantly increasing hull depth, had it been accepted that helicopters could only be stowed and maintained in one (taller) part of the hangar, or had movable / removable decks been considered, or had the gallery deck (above the hangar) been deleted from the design. The post-war 'Audacious' class carriers of the 1950s and some preceding World War II Royal Navy carriers featured such a twin level (or partial twin level) hangar. With each F-35 aircraft for the new carriers costing in excess of £75M, and equipped with specialist stealth coatings and sensitive electronics, the scope that such a twin-level hangar would offer for stowing the entire air group below decks during lengthy, low-risk transits (rather than around 30% - 50% of the air group having to be stowed in the open on the flight deck, exposed to the elements) is attractive. Clearly a second Hangar deck could also have served a useful secondary purpose as a

stores / equipment stowage area when acting in humanitarian relief and amphibious roles. Also, as demonstrated by HMS Ark Royal IV (1955), whose lower hangar was successively converted to other purposes during the life of the ship (leaving just a partial-length lower hangar later in the vessels life), a twin hangar configuration provides a useful space margin for future conversion. Unfortunately, although highlighted as a possibility in the MoD's in-house studies for the new carrier (Eddison & Groom, 1997), there was no appetite to explore this option during our industry studies. In many ways, this lack of due consideration of a twin-level hangar option was a missed opportunity. Yes, the increased hull depth would likely have increased draught, but the base porting and infrastructure issues around this were not insurmountable.

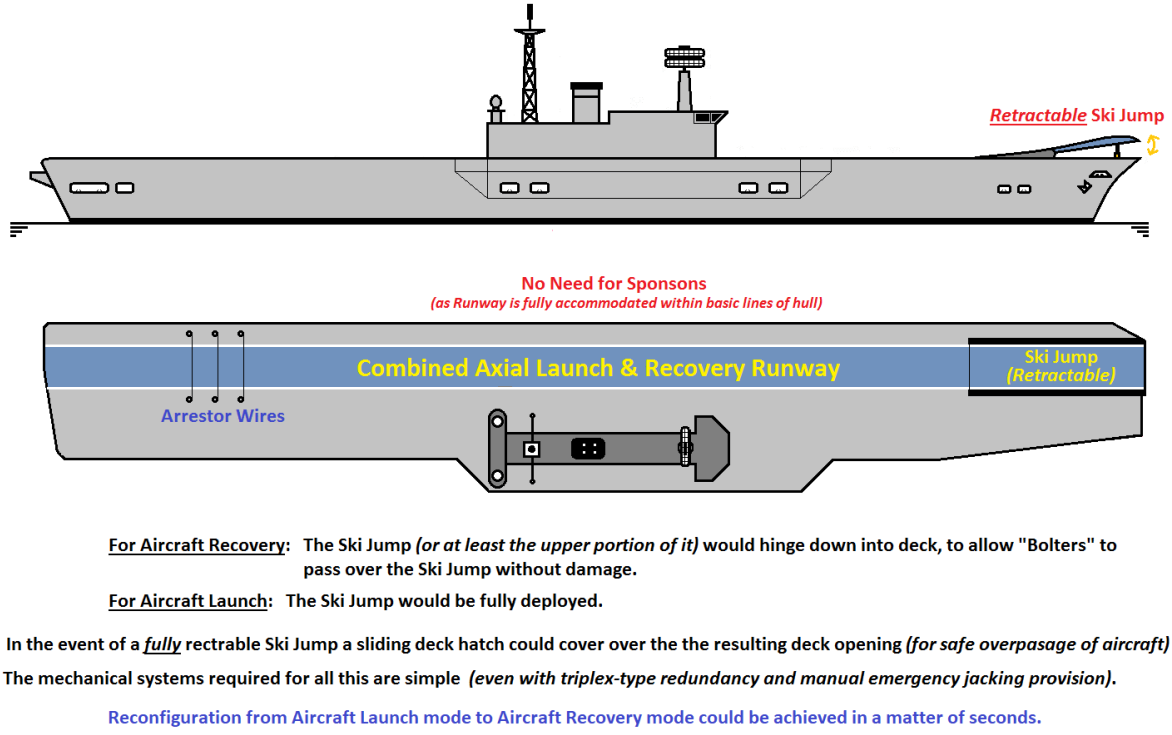

Figure 19: Author's Proposed Novel STOBAR Aircraft Carrier Configuration (based on a Combined Axial Launch & Recovery Runway and a Hinged / Retractable 'Ski Jump' Launch Ramp as per Figure 20 below)

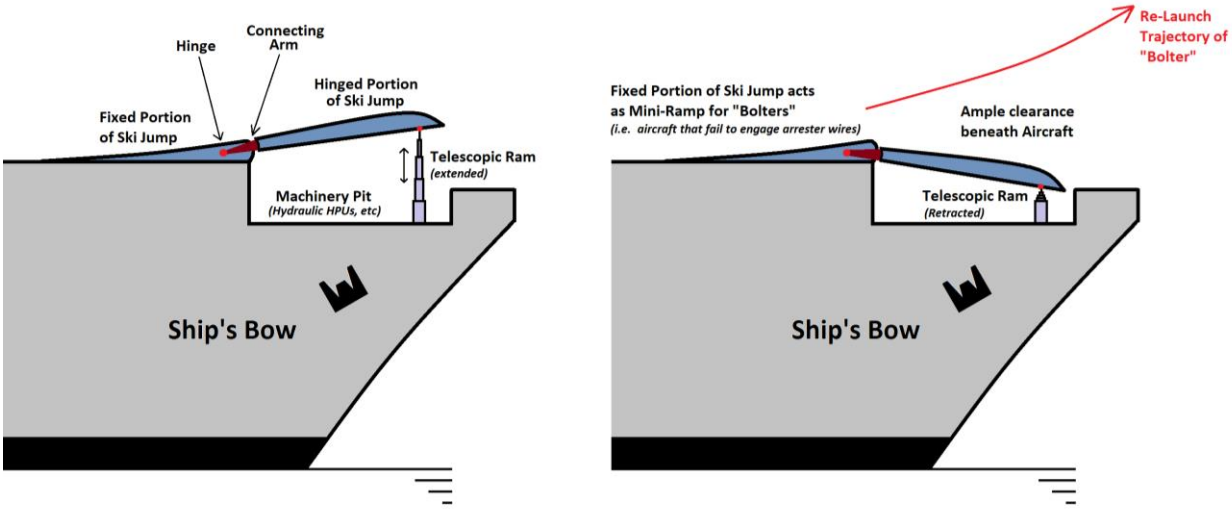

(a) Ramp Fully Deployed (for normal Aircraft Launch Operations)

(b) Ramp Retracted (during Aircraft Recovery when there is a Risk of "Bolters")

NOTE: The relative lengths of the fixed vs retractable portions of the Ski Jump would be determined by allowable undercarriage loads. The entire ramp could be made retractable if needs be.

Figure 20: The Author's Proposed Concept of a Retractable Ski Jump for STOBAR Aircraft Carriers

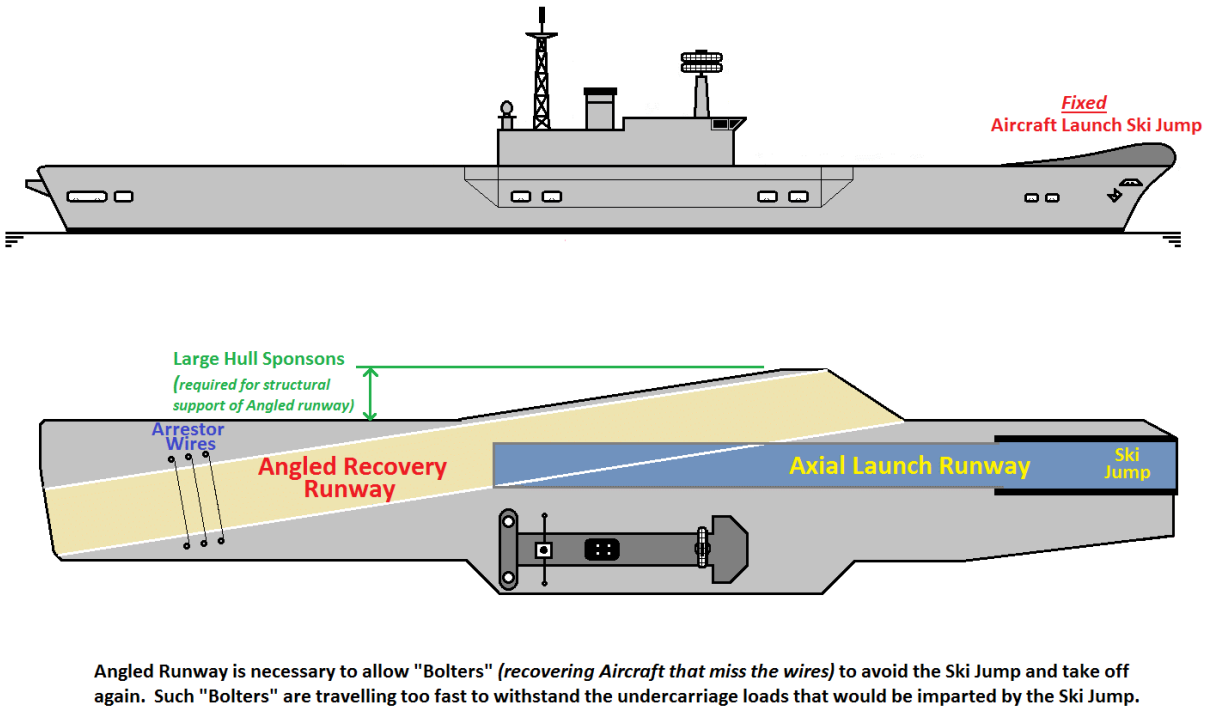

Figure 21: More Traditional Configuration of STOBAR Aircraft Carriers (as per current Russian, Indian & Chinese Aircraft Carrier practice)

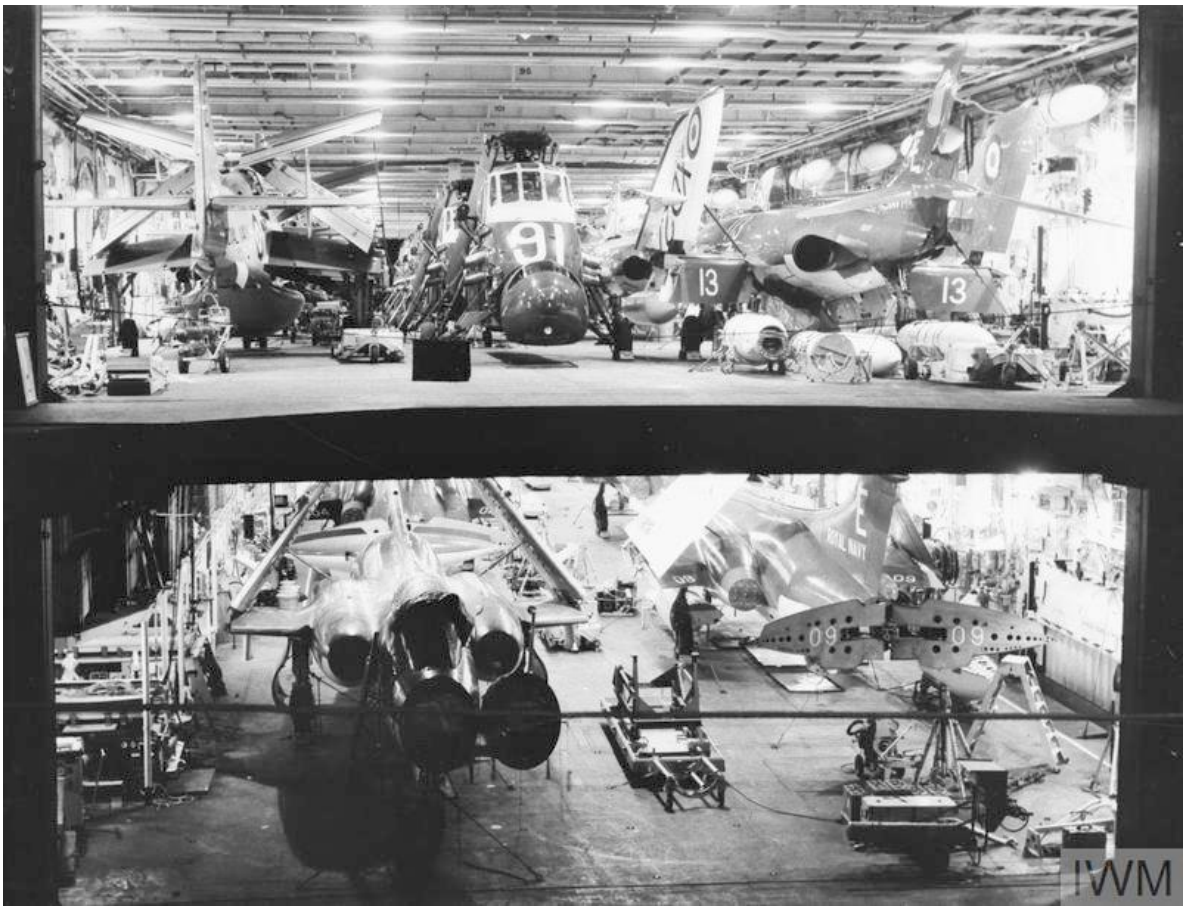

Figure 22: The Twin Level Hangar Arrangement onboard Royal Navy 'Audacious' Class Carrier HMS Eagle (1965)
© UK Imperial War Museum / UK Crown Copyright, Source: www.iwm.org.uk/collections/item/object/205164866

From the start of the MoD-funded studies, our designs mirrored US practice by employing side lifts (rather than inboard lifts) for transferring aircraft between the hangar and the flight deck. The use of such open (exposed to the elements) side lifts dates from the immediate post-war years where naval aircraft were much lower cost and where occasional aircraft loss / damage was tolerated. Whilst the likelihood of lift platform immersion and spray were minimised in our design, the reality is that ship motions and sea states are random in nature. In the modern era, where naval aircraft cost in excess of $100M a piece, it is arguable that aircraft deserve greater protection from the green seas and spray during lift transfer to and from the flight deck. Although inboard lifts offer such protection from the elements, they are undesirable due to the impediment they impose on flight deck operations. One novel solution therefore proposed by our team was to 'plate-in' the side lifts, as shown in Figure 23, so that they become fully enclosed and protected from the elements (i.e. effectively become an inboard lift located hard-up against the sideshell). With the highly flared hullform, such an 'enclosed' side lift would be canted so as to follow the sideshell flare, resulting in some headroom restrictions on the inboard side of the lift platform. In the author's view the increased hull steel weight of this approach was justified both in terms of increased protection of aircraft, reduced vulnerability of the hangar to weapons entry, and a beneficial reduction in radar cross-section (RCS) due to the elimination of large lift openings in the sideshell. Unfortunately, as with many novel suggestions on a project of this scale, this option of enclosing the side lifts (although outwardly promising) was never progressed beyond initial suggestion.

One other noteworthy potential innovation, highlighted by the author, but never progressed by our team, was the potential use of electrically-powered boilers (in place of conventional fuel-powered boilers) to generate steam for the steam catapults of CTOL aircraft carrier variants. The marine engineers were clear that thermodynamics were not on the side of this concept, as using fuel to generate electricity via a gas turbine alternator, only to then use that electricity to generate steam is not an efficient process. Nonetheless, to the author, the idea seemed to offer potential on 'all electric' ships such as ours, in that it would avoid the need for a totally standalone fuel-based steam raising plant to be fitted for the catapults. This electric boiler concept would have integrated neatly with the ships' all-electric propulsion system, could have offered some maintenance benefits over conventional boilers, and could have been readily retrofitted to the ship part-way through the vessels life (as part of a then-proposed through-life upgrade from STOVL to CTOL operation). Developing an electric boiler for the catapults was (in the author's view) preferable to dusting off a 1950s or 1960s naval boiler design. It is easy to see how four of six of these electrically-powered boilers dotted around the ship would have been considerably easier to implement and been spatially less-demanding than a steam-raising plant based (for redundancy reasons) on two large fuel-powered boilers sited necessarily (for survivability reasons) in separate boiler rooms. In the author's view this electrically-powered boiler concept was a potentially good compromise between proceeding with a technologically immature (and consequently high risk) electromagnetic aircraft catapult launch system and the unpalatable alternative of going back to a 1960's-style catapult steam-raising plant. The American and French would not have been able to help us very much on a steam-raising plant, as their carrier fleets are now nuclear-propelled and are readily able to raise large amounts of steam (albeit 'wet' steam) from the reactor plant, without the need for fuel-powered boilers.

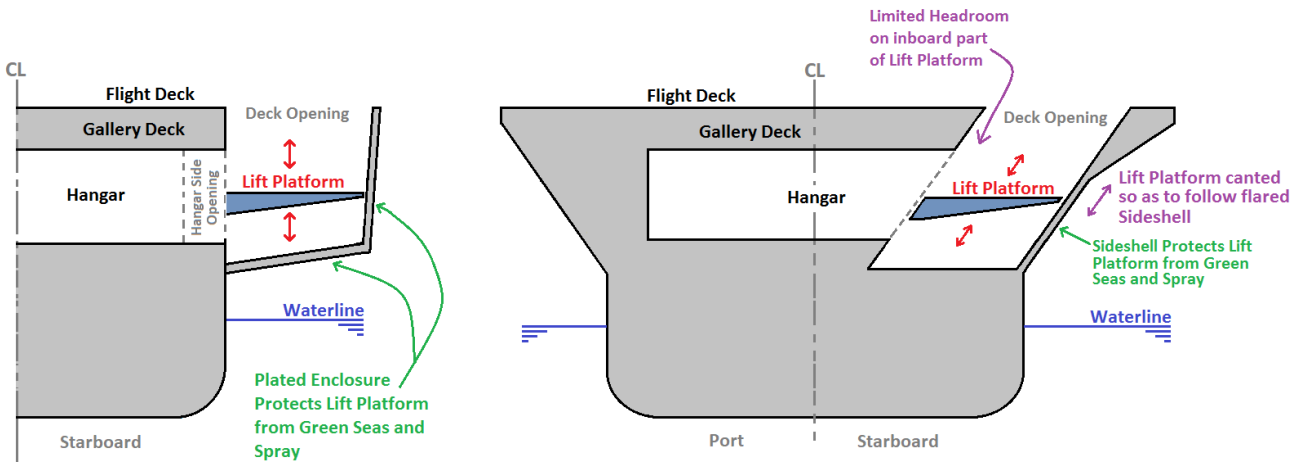

(a) Applied to a Traditional (Sponson) Style of Above Water Form

(b) Applied to Highly Flared Style of Above Water Form

Figure 23: Enclosed Side Lift Concept

One final point, that the author feels almost duty bound to mention, concerns the limited self-defence provision on the Queen Elizabeth class carriers. Whilst our early carrier designs incorporated a whole plethora of survivability features, and dare say all are replicated (or surpassed) on the final ship design entering service now, the best bet is not to get hit by weaponry in the first place. In this regard it is unfortunate that the self-defence capability of the new carriers seem to have been so limited by funding considerations. Our early designs allowed for 'Navalised ASRAAM' (which has since evolved into Sea Ceptor) or Sea RAM, both of which were promising and affordable defensive missile systems significantly more capable than the 'entry-level' Phalanx guns now being fitted. The author always hoped that 'hard kill' Anti-Torpedo Torpedo (shelved in the late 1990s) would be revived for the carriers, given the crew size, high value of the ships / aircraft as strategic assets, and their vulnerability to submarines. All of which could be funded by foregoing the cost of a couple of F-35 aircraft. One only has to look at the cases of Atlantic Conveyor, General Belgrano and HMS Coventry to see what fate faces large naval ships without the wherewithal to properly defend themselves against close-in threats, and over-reliant on other vessels for defence.

Finally, in closing, on a more savoury note, the author shares Professor Andrews' view that it would be worthwhile (while minds are still fresh) for there to be a paper on construction and shipbuilding strategy for the aircraft carriers, and can suggest some potential contacts who may be able to assist on this.

REFERENCES

Please also refer to References listed in the Paper on pages A-440-A441 of this edition.

10. EDDISON, J and GROOM, J: "*Innovation in the CV(F) – An Aircraft Carrier for the 21st Century*" WARSHIP '97 Air Power at Sea, London, June 1997.
41. KNIGHT, S: "*Design of the QUEEN ELIZABETH Class Aircraft Carriers*", RINA Airpower at Sea Conference, London, June 2009.
42. ANDREWS, D J: "*Preliminary Warship Design*", Trans RINA 1994 (Reprinted in Journal of Naval Engineering 1995)
43. HARRIS *ET AL*.: "*Hydrodynamic design of the QE Class aircraft carriers*", RINA Airpower at Sea Conference, London, June 2009.

The Transactions of The Royal Institution of Naval Architects – Part A

International Journal of Maritime Engineering

GUIDANCE NOTES FOR AUTHORS

All papers, technical notes and discussions should be submitted in electronic form, normally in MSWord format. Authors wishing to submit in other formats should first contact RINA Headquarters. Submissions should be forwarded on PC compatible disks or CD-ROM, containing the full text, including inserted figures. Submissions less than 5Mb may be forwarded by email or online.

Authors are responsible for obtaining security clearance as required. If they so wish, authors may add a disclaimer stating that the opinions expressed are solely those of the author.

In submitting papers or technical notes for publication, authors implicitly assign copyright to the Royal Institution of Naval Architects if the paper or technical note is published. Where copyright is held elsewhere, authors must present evidence of approval to re-publish.

When submitting contributions for publication, authors must state if the paper or technical note has been published before and where, or whether it is being considered for publication by some other publisher

Papers: Papers should not normally exceed 6000 words (with up to 10 illustrations). Longer papers where the content justifies the extra length may be published at the Editor's discretion. The required format of papers submitted for publication may be obtained from the RINA website or from RINA Headquarters

Technical Notes: Technical notes should not normally exceed 1500 words (and up to 5 illustrations). The required format of technical notes submitted for publication may be obtained from the RINA website or from RINA Headquarters

Discussion: Discussion of published papers, or comment on published discussion, should not normally exceed 500 words (with up to 2 illustrations).

All submissions for publication should be forwarded to:

The Editor (IJME)
The Royal Institution of Naval Architects
8-9 Northumberland Street
London WC2N 5DA, UK
Tel: +44 (0)20 7235 4622 Fax: +44 (0)20 7259 5912
Email: ijme@rina.org.uk Online: www.rina.org.uk

THE ROYAL INSTITUTION OF NAVAL ARCHITECTS

The Royal Institution of Naval Architects is an internationally renowned professional institution and learned society, whose members are involved at all levels in the design, construction and repair of ships, boats and maritime structures, in over 80 countries. RINA is widely represented in the marine industry, universities and colleges, and maritime organisations worldwide.

Membership is open to those who are professionally qualified in naval architecture or a related subject, or who are involved or interested in the maritime industry. RINA members enjoy a wide range of benefits and services, including advice on education, training and professional development. The RINA also publishes a range of technical journals, books and papers, and organises an extensive programme of international conferences and training courses covering all aspects of naval architecture and maritime technology, available to members free or at reduced rates

The Transactions of The Royal Institution of Naval Architects

Vol 159 Part A4 2017 ISSN 1471-8751

International Journal of Maritime Engineering

CONTENTS

PAPERS

TECHNICAL NOTES

There are no Technical Notes published in this issue of IJME

DISCUSSION